Understanding the regulatory basis of defense signaling in plants:

The role of Argonautes in modulating defense responses in *Nicotiana attenuata*

Dissertation

Zur Erlangung des akademischen Grades

doctor rerum naturalium (Dr. rer. nat.)

vorgelegt dem Rat der Biologisch-Pharmazeutischen Fakultät

der Friedrich-Schiller- Universität Jena

von Master of Science in Biotechnology

Maitree Pradhan

geboren am 15.07.1988 in Angul, India

Gutachter:

1. Prof. Dr. Ian Thomas Baldwin

   Max Planck Institute for Chemical Ecology, Jena, Germany

2. Prof. Dr. Ralf Oelmüller

   Institute of General Botany and Plant Physiology, Jena, Germany

3. Prof. Dr. Eva Holtgrewe Stukenbrock

   Environmental Genomics Botanical Institute

   Christian-Albrechts University of Kiel, Germany

Beginn der Promotion: 01.04.2016

Tag der Doktoprüfung: 27.06.2019

Tag der öffentlichen verteidigung: 18.10.2019

I want to dedicate this work to Dr. Shree P. Pandey

Table of Contents

Table of Contents

1. INTRODUCTION

1.1 Overview

Plants function in complex environments where they face constant challenges from their habitats to adapt, grow, reproduce, disperse and evolve. These challenges are now further confounded due to threats associated with climate change and global warming. For instance, there have been a significant change in number of summer days above 30 ^{0}C and precipitation patterns across the globe; such conditions favoring pathogens and pests, and negatively impacting plant productivity (Dresselhaus and Hückelhoven, 2018). Environmentally-driven, sudden changes in migration and evolution new races of pathogens and insect pests produce confounding threats for locally adapted genotypes in their agro-ecological habitats.

Plants are thus encountering a paradigm shift in the biotic and abiotic stresses they are encountering in their habitats. Under such circumstances, discovery of new traits for plant improvement further necessarily requires deeper understanding of mechanisms governing host responses to changes in their biotic and abiotic environments in wild species growing in their native habitats. However, most of the knowledge regarding molecular mechanisms associated with stress response have been elucidated in the developmental model plant, *Arabidopsis thaliana*. Whether such mechanisms operate in nature and in other plant species remains tested to very limited extent. Elucidation of mechanisms dictating organismal response to stress adaptation involve understanding of several components of signaling transduction network and how such networks are regulated to deliver outcomes that are functionally relevant in nature.

1.2 *Nicotiana attenuata:* a perfect model system to study ecological challenges and adaptive responses

Nicotiana attenuata, due to its unique ecology, offers a perfect model system to study adaptive plant responses and the underlying mechanisms in native habitats. *N. attenuata*, commonly known as Coyote tobacco, is an annual, wild herb species, native of south-western North America that grows in a variety of habitats. It gemmates from long-lived seed banks in post-fire environments, utilizing stimulants in wood-smoke (Baldwin et al., 1994). In the post-

fire burns, where soils have high nitrogen content, these plants form a pioneering species as the seeds of *N. attenuata* germinate in a highly synchronized manner, often forming populations of mono-cultures that resemble in primordial agricultural niches (Figure 1).

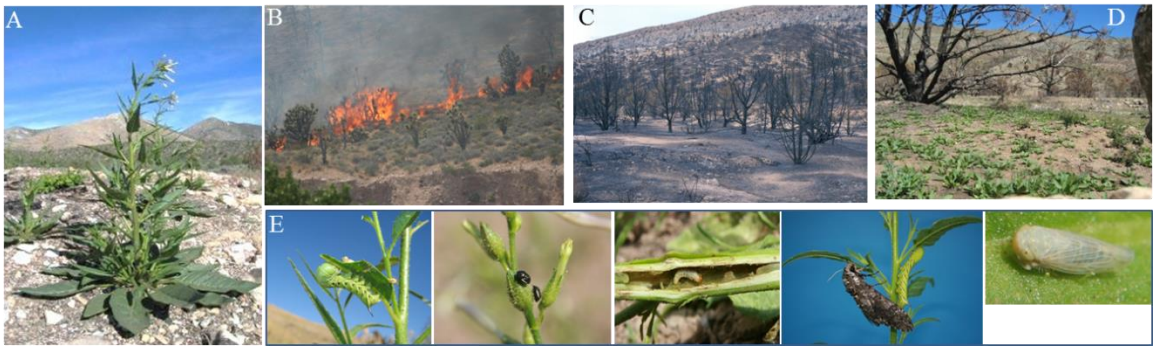

Figure 1. *N. attenuata* is the founding member of ecological interactions in post-fire environments in its native habitats.

Communities of unpredictable insect herbivores follow the synchronized germination and growth on *N. attenuata*. It is estimated that herbivores from more than 20 taxa attack these plants as specificity of herbivore populations vary from year-to-year as these herbivores also recolonize the host every year after the fire. *Manduca* is one of the crucial insects that colonize these plants. Whereas the *Manduca* larvae are a crucial insect herbivore of this plants, adults often act as pollinators. The monoculture-like population structure of *N. attenuata* has also resulted in evolution of several pathogenic microbes. Since 2005, *N. attenuata*, suffers from sudden wilt-like disease. *Fusarium* and *Alternaria* species from the central components of the highly dynamic fungal pathogen-system associated with *N. attenuata* (Schuck et al., 2014; Santhanam et al., 2015). In their native habitats, *N. attenuata* also interacts with the arbuscular mycorrhizal fungi (AMF). Colonization by AMF alters the root morphology and increases its surface area for absorption of water and facilitates the uptake of soil nutrients that are limiting for plant growth, especially inorganic phosphorus. AMF colonization may also help plants to defend against

pathogens and pests as well as help in reducing drought stress. The nearly ubiquitously root-colonizing AMF belong to the phylum Glomeromycota (Schüβler et al., 2001; Hibbett et al., 2007). As they form extensively complex hyphal networks that extend deep into the soil, AMF is thought to dictate plant-community structures as plants growing in the surrounding are connected via AMF-networks (Groten et al., 2015).

Due to such dynamic interactions of *N. attenuata* with its biotic environment that are highly complex and largely unpredictable makes it a perfect model system to study ecological events and the molecular mechanisms that underlie.

1.3 Molecular host responses to ecological challenges

Ecological challenges, such as attack of herbivores or interactions with the microbes, inflict a large-scale reprograming in plant metabolism. Such reprograming are tailored by plants to avoid, tolerate and induce defenses against the imposed stress. For instance, attack of insect herbivores elicit responses that include activation of direct induced defenses such as toxins and anti-feeders as well as indirect defenses by recruitment of natural enemies. Perception of herbivore attack results in reprograming of a significant portion of the transcriptome; hundreds to thousands of genes are differentially regulated (for instance as shown in studies by (Schmidt et al., 2005; Ralph et al., 2006). The transcription of ~2.5 Gb *N. attenuata* genome (Xu et al., 2017) is rapidly reconfigured after herbivore attack in manner that is highly specific for the attacking species (Voelckel and Baldwin, 2004; Schmidt et al., 2005). Attack of herbivores down-regulate the photosynthetic apparatus of the plant and funnels substrates to enhance secondary metabolites related to signaling and defense that are synthesized from an array of biological pathways (Figure 2) related to biosynthesis and metabolism of shikimic acid, malonic acid, mevalonic acid, DXP/MEP, oxylipins, nitrogen-containing secondary products, phenolics, terpenes and other classes (Schmidt et al., 2005).

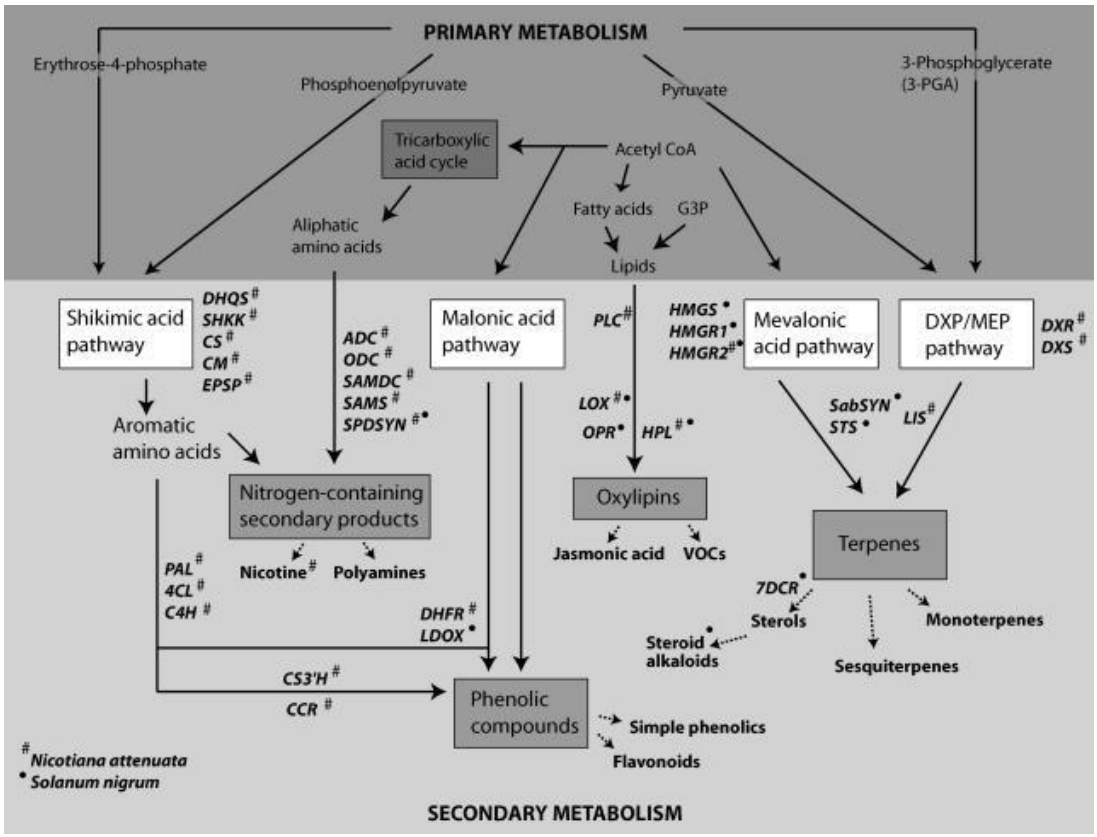

Figure 2. An overview of major pathways/metabolite groups reprogrammed during stress adaptation (adapted from (Schmidt et al., 2005)).

Infections by phytopathogens also induce large-scale reprograming of the host transcriptome in a tissue and pathogen-dependent manner. Infection by *Fusarium* species inculcates change of expression of 2000-7000 host genes that vary between the resistant and the susceptible genotypes (Lanubile et al., 2014; Huang et al., 2016). Functional classification of differentially expressed genes during *F. verticillioides* suggest enrichment of pathogen perception, transcription factors such as WRKY, phytohormone signaling such as of jasmonic acid (JA)/ethylene-mediated defense response, and secondary metabolism (Lanubile et al., 2014). Indeed, JA has appeared as a key signaling regulator during the infection of *N. attenuata* and *F. brachygibbosum* (Luu et al., 2015; Luu et al., 2017). Yet, due to its recent identification, knowledge of the infection as well as the molecular components regulating defense signaling responses of *N. attenuata* against *F. brachygibbosum* remains in its infancy.

Interaction of *N. attenuata* with AMF is governed by calcium- and calmodulin dependent protein kinase (CCaMK). Infection of roots by AMF have systemic effects on transcriptional reprograming of genes of P-starvation and -transport in leaves in a highly CCaMK-dependent manner (Wang et al., 2018). AMF colonization also regulates amino acid and phenolic metabolism in the roots. Impairment of AMF-interactions seem to have fitness disadvantages to the plants (Wang et al., 2018).

It is clearly evident that successful adaptation of plants to biotic challenges requires an ability to vary the expression of traits as a consequence of change in biotic environment. Adaptive plasticity allows a genotype to grow successfully in variable environments and plays a major role in ecological distribution, maximizing fitness and in maintaining the evolutionary variability. As elaborated above, such phenotypic plasticity encompasses large-scale reprograming of expression of genes of the host's genome but the information on the regulatory mechanism that provides this plasticity is still in its infancy.

1.4 Regulatory basis of induced defenses and the role of small-RNAs

It is now established that adaptive responses to biotic stress is construed by reprograming of metabolomics space of the plant, which is in turn executed by changing the expression of a large proportion of genes of the genome in a rapid and time-dependent manner. The next challenge is to uncover the identity and understand the mechanism of action of molecular regulators of phenotypic plasticity during biotic interactions. A large variety of non-coding, small-RNA (smRNA) pathways, which are involved in plant development, reproduction and genome stability, qualify as suitable candidates for regulating phenotypic plasticity (Borges and Martienssen, 2015). Thought to have originated for defending against RNA viruses and transposable elements, and later adapted to regulate endogenous gene expression (Borges and Martienssen, 2015), smRNA pathways offer ideal candidates for molecular regulators of

plasticity as specific components are rapidly elicited in stress dependent manner. They can amplify the signal as a consequence of stress and systemically transport them, their action is not masked by environment, and can coordinate regulation of various defense-signaling pathways.

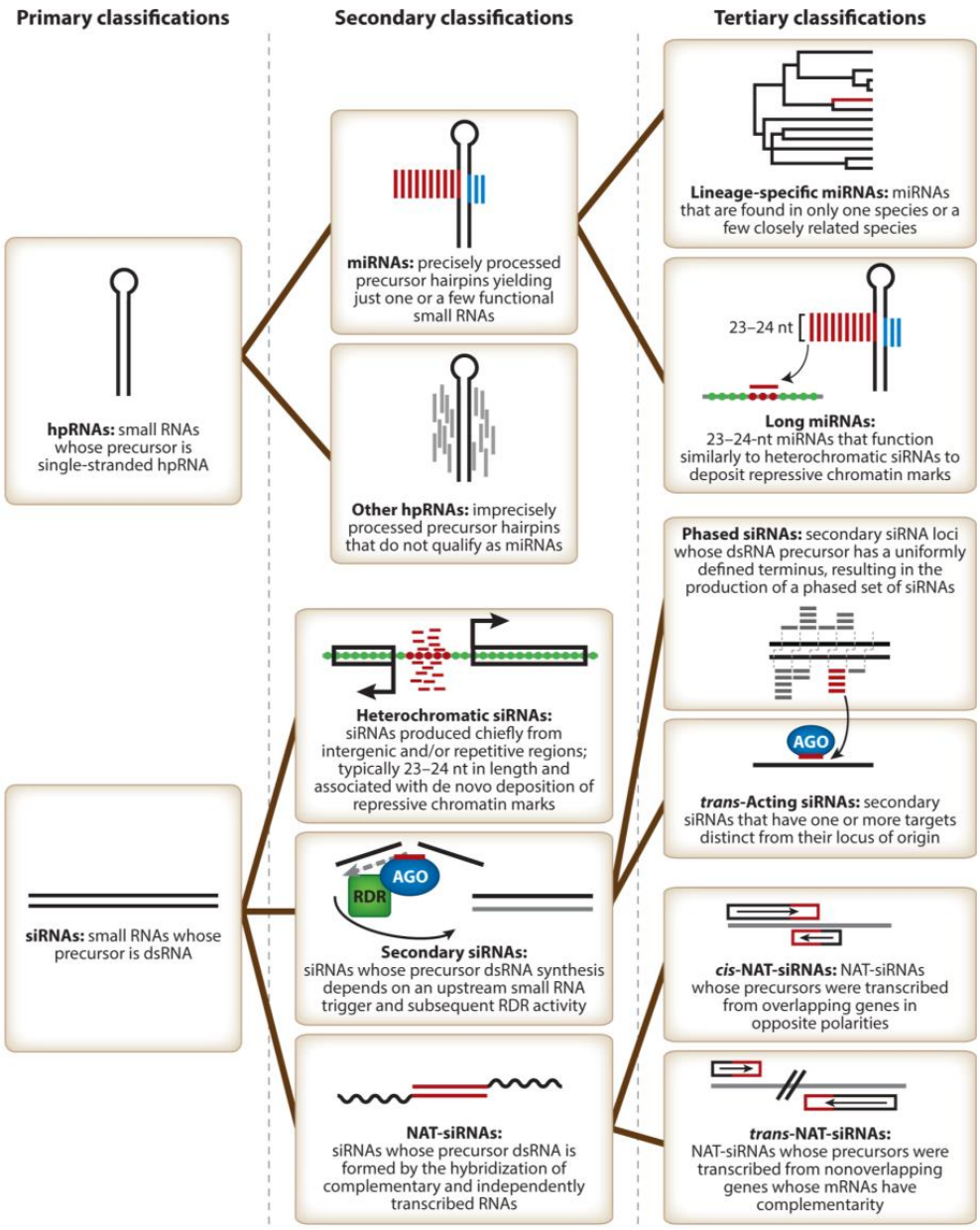

Figure 3. Classification of endogenous smRNAs in plant cells (modified from (Axtell, 2013))

Plant cell produces a variety of smRNAs in the size range of 18-30 nucleotides by processing of helical RNA precursors and could be categorized into several classes; the two broadest groups being the microRNAs (miRNAs) and the small-interfering RNAs (siRNAs; as example of detailed classification is summarized in Figure 3). miRNAs are synthesized from the

endogenous miRNA genes, transcribed into long primary miRNAs (pri-miRNA) in RNA-Pol II dependent manner. Other smRNAs are derived from the synthesis of double stranded RNA (dsRNA) precursors from single stranded RNAs by the action of RNA-directed RNA polymerases (RdRs; Figure 4). These dsRNA-intermediates (including the hair-pin precursors of miRNAs) are acted upon by the Dicer like protein (DCLs; Figure 4) to the processed smRNA duplexes. These are then loaded on to the Argonaute (AGO; Figure 4) proteins that act like effectors to help smRNAs to recognize their targets with the help of sequence complementarity. Dictated by the nature of the AGO and the loaded transcripts, the process of RNA-interference results in transcript cleavage and degradation, translational inhibition or recruitment of other cofactors for transcriptional gene silencing and DNA methylation (Borges and Martienssen, 2015). RdRs, DCLs and AGOs are coded by multiple genes. For instance, in *A. thaliana*, 6 RdRs, 4 DCLs and 10 AGOs are known, whereas in *N. attenuata*, 3 RdRs and 4 DCLs have been functionally characterized, whereas 11 AGOs have been estimated in *N. attenuata* genome (Singh et al., 2015).

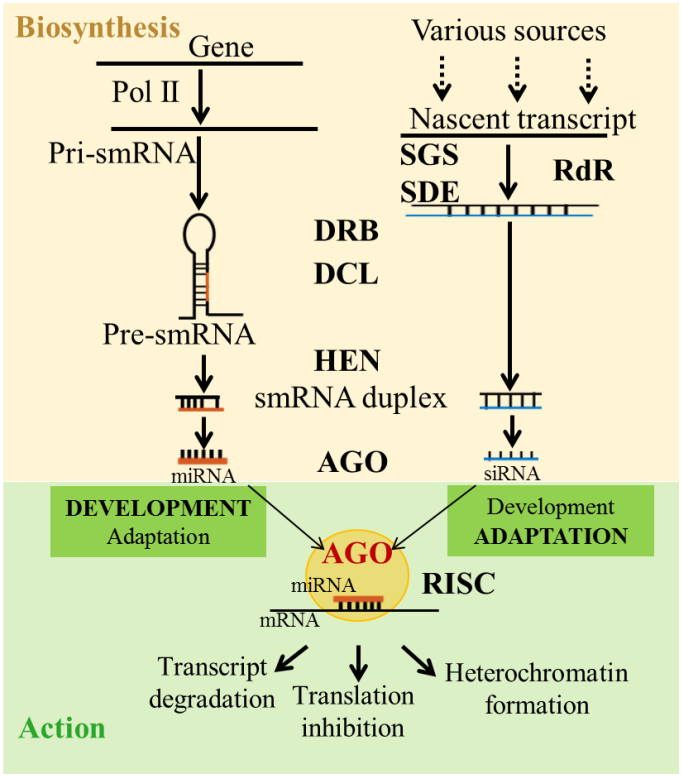

Figure 4. An overview of the major steps in biogenesis of smRNAs and the components involved.

1.5 The 'ARGONAUTEs' of the smRNA pathways

Despite diversity in their biogenesis and functions, all the characterized smRNAs are known to associate with AGO proteins (Fang and Qi 2016) during the formation of RNA-induced silencing complex (RISC). The smRNA component of the RISC as only as a guide to direct the complex to the target RNA (post transcriptional gene silencing, PTGS) or DNA (transcriptional gene silencing TGS) with the help of complementary base pairing. In plants, the role of AGOs are now well established during the PTGS and TGS processes. AGOs are multi-member gene family. All the eukaryotic AGOs share common structural and biochemical properties and function through conserved core mechanisms (Singh et al., 2015; Fang and Qi, 2016): The eukaryotic AGOs are comprised of four domains (Figure 5), the variable N-, PAZ, MID and the PIWI domains. While the biochemical function of N-domain is still poorly understood, it is believed that it blocks the pairing of guide smRNA and the target beyond 16th position and in humans, it might be required for duplex unwinding. PAZ domains helps in recognizing 3'-end of smRNA, binding single-stranded nucleic acids, anchors smRNAs and contributes to slicer-independent unwinding of the duplex. The MID domain recognizes the 5'-end of the smRNAs and accounts for binding preference of the smRNAs to the AGOs. PIWI-domains have RNaseH-fold and often have slicer activity, helping in target cleavage. Yet, the AGO family of genes have constantly expanded in plant genomes: They comprise 3-6 genes in species such as *Chlamadomonas* and *Physcomitrella*, whereas in flowering plants their numbers are as high as 10-19 in *A. thaliana* and rice. The expansion of AGO family suggest functional diversification of their genes and the associated endogenous smRNA pathway in plants.

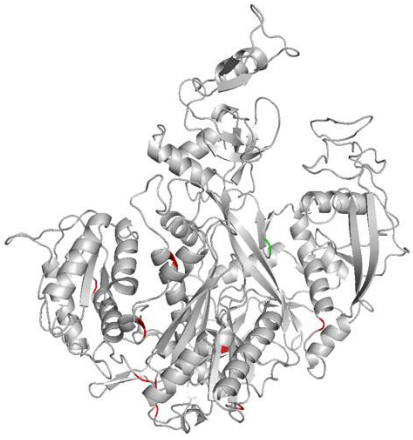

Figure 5. A model of AtAGO4 (Singh and Pandey, 2015) showing the overall structure of plant AGOs.

Introduction

In *N. attenuata*, 11 AGOs, encoded from 8 unique genes, are reported but their functions remained untested (Singh et al., 2015). Therefore, AGOs offer a perfect model for a gene family to investigate the role of smRNA pathways in modulating phenotypic plasticity and stress responses in *N. attenuata*. The overarching objective of this work was to test the hypothesis that AGOs (and thus the smRNA pathways) offer functional specificity in modulating plant defense response in stimulus-dependent manner. This hypothesis has been tested by determined by characterizing AGOs against various ecologically relevant biotic stresses and by performing loss-of-function analysis in controlled conditions and natural habitats.

References

Axtell MJ (2013) Classification and comparison of small RNAs from plants. Annu Rev Plant Biol **64:** 137-159

Baldwin IT, Staszak-Kozinski L, Davidson R (1994) Up in smoke: I. Smoke-derived germination cues for postfire annual,Nicotiana attenuata torr. Ex. Watson. Journal of Chemical Ecology **20:** 2345-2371

Borges F, Martienssen RA (2015) The expanding world of small RNAs in plants. Nat Rev Mol Cell Biol **16:** 727-741

Dresselhaus T, Hückelhoven R (2018) Biotic and Abiotic Stress Responses in Crop Plants. Agronomy **8:** 267

Fang X, Qi Y (2016) RNAi in Plants: An Argonaute-Centered View. Plant Cell **28:** 272-285

Groten K, Nawaz A, Nguyen NHT, Santhanam R, Baldwin IT (2015) Silencing a key gene of the common symbiosis pathway in Nicotiana attenuata specifically impairs arbuscular mycorrhizal infection without influencing the root-associated microbiome or plant growth. Plant Cell Environ **38:** 2398-2416

Hibbett DS, Binder M, Bischoff JF, Blackwell M, Cannon PF, Eriksson OE, Huhndorf S, James T, Kirk PM, Lücking R, Thorsten Lumbsch H, Lutzoni F, Matheny PB, McLaughlin DJ, Powell MJ, Redhead S, Schoch CL, Spatafora JW, Stalpers JA, Vilgalys R, Aime MC, Aptroot A, Bauer R, Begerow D, Benny GL, Castlebury LA, Crous PW, Dai Y-C, Gams W, Geiser DM, Griffith GW, Gueidan C, Hawksworth DL, Hestmark G, Hosaka K, Humber RA, Hyde KD, Ironside JE, Kõljalg U, Kurtzman CP, Larsson K-H, Lichtwardt R, Longcore J, Miądlikowska J, Miller A, Moncalvo J-M, Mozley-Standridge S, Oberwinkler F, Parmasto E, Reeb V, Rogers JD, Roux C, Ryvarden L, Sampaio JP, Schüßler A, Sugiyama J, Thorn RG, Tibell L, Untereiner WA, Walker C, Wang Z, Weir A, Weiss M, White MM, Winka K, Yao Y-J, Zhang N (2007) A higher-level phylogenetic classification of the Fungi. Mycological Research **111:** 509-547

Huang Y, Li L, Smith KP, Muehlbauer GJ (2016) Differential transcriptomic responses to Fusarium graminearum infection in two barley quantitative trait loci associated with Fusarium head blight resistance. BMC Genomics **17:** 387-387

Lanubile A, Ferrarini A, Maschietto V, Delledonne M, Marocco A, Bellin D (2014) Functional genomic analysis of constitutive and inducible defense responses to Fusarium verticillioides infection in maize genotypes with contrasting ear rot resistance. BMC Genomics **15:** 710-710

Luu VT, Schuck S, Kim SG, Weinhold A, Baldwin IT (2015) Jasmonic acid signalling mediates resistance of the wild tobacco *Nicotiana attenuata* to its native Fusarium, but not Alternaria, fungal pathogens. Plant Cell Environ **38:** 572-584

Luu VT, Weinhold A, Ullah C, Dressel S, Schoettner M, Gase K, Gaquerel E, Xu S, Baldwin IT (2017) O-Acyl Sugars Protect a Wild Tobacco from Both Native Fungal Pathogens and a Specialist Herbivore. Plant Physiol **174:** 370-386

Ralph S, Oddy C, Cooper D, Yueh H, Jancsik S, Kolosova N, Philippe RN, Aeschliman D, White R, Huber D, Ritland CE, Benoit F, Rigby T, Nantel A, Butterfield YSN, Kirkpatrick R, Chun E, Liu J, Palmquist D, Wynhoven B, Stott J, Yang G, Barber S, Holt RA, Siddiqui A, Jones

References

SJM, Marra MA, Ellis BE, Douglas CJ, Ritland K, Bohlmann J (2006) Genomics of hybrid poplar (Populus trichocarpa× deltoides) interacting with forest tent caterpillars (Malacosoma disstria): normalized and full-length cDNA libraries, expressed sequence tags, and a cDNA microarray for the study of insect-induced defences in poplar. Molecular Ecology **15:** 1275-1297

Santhanam R, Luu VT, Weinhold A, Goldberg J, Oh Y, Baldwin IT (2015) Native root-associated bacteria rescue a plant from a sudden-wilt disease that emerged during continuous cropping. Proc Natl Acad Sci USA **112:** E5013-5020

Schmidt DD, Voelckel C, Hartl M, Schmidt S, Baldwin IT (2005) Specificity in Ecological Interactions. Attack from the Same Lepidopteran Herbivore Results in Species-Specific Transcriptional Responses in Two Solanaceous Host Plants. Plant Physiol **138:** 1763-1773

Schuck S, Weinhold A, Luu VT, Baldwin IT (2014) Isolating fungal pathogens from a dynamic disease outbreak in a native plant population to establish plant-pathogen bioassays for the ecological model plant Nicotiana attenuata. PLoS ONE **9:** e102915

Schüßler A, Schwarzott D, Walker C (2001) A new fungal phylum, the Glomeromycota: phylogeny and evolution**Dedicated to Manfred Kluge (Technische Universität Darmstadt) on the occasion of his retirement. Mycological Research **105:** 1413-1421

Singh RK, Gase K, Baldwin IT, Pandey SP (2015) Molecular evolution and diversification of the Argonaute family of proteins in plants. BMC Plant Biol **15:** 23

Singh RK, Pandey SP (2015) Evolution of structural and functional diversification among plant Argonautes. Plant Signal Behav **10:** e1069455

Voelckel C, Baldwin IT (2004) Generalist and specialist lepidopteran larvae elicit different transcriptional responses in Nicotiana attenuata, which correlate with larval FAC profiles. Ecology Letters **7:** 770-775

Wang M, Wilde J, Baldwin IT, Groten K (2018) Nicotiana attenuata's capacity to interact with arbuscular mycorrhiza alters its competitive ability and elicits major changes in the leaf transcriptome. J Integr Plant Biol **60:** 242-261

Xu S, Brockmöller T, Navarro-Quezada A, Kuhl H, Gase K, Ling Z, Zhou W, Kreitzer C, Stanke M, Tang H, Lyons E, Pandey P, Pandey SP, Timmermann B, Gaquerel E, Baldwin IT (2017) Wild tobacco genomes reveal the evolution of nicotine biosynthesis. Proc Natl Acad Sci USA **114:** 6133-6138

OVERVIEW OF MANUSCRIPTS

Manuscript I

Argonaute 8 (AGO8) mediates the elicitation of direct defenses against herbivory

Maitree Pradhan, Priyanka Pandey, Klaus Gase, Murali Sharaff, Ravi K Singh, Avinash Sethi, Ian T. Baldwin, Shree P. Pandey*

Plant Physiology (2017) 175:927-946, doi: 10.1104/pp.17.00702

In this manuscript, we have investigated the role of Argonautes (AGOs) in modulating defense against insect herbivory. *Nicotiana attenuata* genome codes for 11 AGOs (corresponding to 8 unique genes) and these were characterized here. Expression of AGOs was knocked-down with the help of inverted repeat strategy and loss-of-function characterization demonstrated that Na*AGO8* was necessary for herbivore defense. Gene-expression studies suggested the further involvement of AGO5 in herbivore defense. Deep sequencing revealed the composition and temporal dynamics of herbivore-responsive miRNome. Further, comparative analysis of domains revealed the plausible structural diversity of AGO conformations while interacting with the substrates, particularly in the smRNA binding pocket, which may influence substrate recognition or binding and functional specificity.

M.P., I.T.B. and S.P.P. designed the study, M.P., K.G., M.S., R.K.S, and S. P.P. carried out experiments, P.P., R.K.S, A.S, and S.P.P. carried out NGS data analysis and other computational experiments, M.P., I.T.B., and S.P.P. wrote the manuscript with contribution of all the authors. I.T.B. and S.P.P. provided resources.

Manuscript II

Argonaute 4 modulates resistance against hemibiotrophic fungal infection by regulating jasmonic acid signaling in *Nicotiana attenuata* plants

Maitree Pradhan, Priyanka Pandey, Ian T. Baldwin* and Shree P. Pandey*

(Plant Physiology (2019) under revision)

* Co-corresponding authors

In this manuscript, we have investigated the biological function of AGOs in modulating resistance response during interaction of *Nicotiana attenuata* with a naturally-occurring hemibiotrophic pathogen, *Fusarium brachygibbosum*. We found that AGO4 specifically responds to the fungal infection. The plants silenced in AGO4 (and not other AGO's) were highly susceptible to the disease. Kinetic studies revealed that irAGO4 plants were severely abrogated in accumulation of 24 nucleotide smRNA. The composition, dynamics of accumulation and AGO4-dependency of miRNAs during pathgenesis was also revealed. We also determined that DCL3 and RdR2/1 were the other components of the core machinery involved in resistance against hemibiotrophic pathogen infection. The hyper-susceptibility of plants silenced in smRNA-mechinary was due to abrogated jasmonate biogenesis and signaling. These findings were validated in the real world when plants silenced in expression of AGO4, RdR1, RdR2 and DCL3 and their binary combinations were introduced in natural habitats in fields harboring complex native fungal communities.

S.P.P. conceived the original research plan, M.P., I.T.B., and S.P.P. designed study, M.P., and S.P.P. carried out experiments, M.P. and I.T.B. carried out field work with inputs from S.P.P., P.P. carried out NGS analyses with inputs from S.P.P., M.P., I.T.B. and S.P.P. wrote the manuscript with contributions of P.P., I.T.B. provided several resources.

Manuscript III

Argonaute7 (AGO7) moderates plant fitness and arbuscular mycorrhizal fungal associations under competitive and resource limited conditions in *Nicotiana attenuata*

Maitree Pradhan, Klaus Gase[+], Ling Chuang[+], Ian T. Baldwin[*], Karin Groten[*], Shree P. Pandey[*]

(Manuscript under preparation-Plant Physiology)

Plant AGOs have diversified in their biological functions due to the expansion of the number of genes in this family due to duplication and loss events. The genome of the ecological model plant, *Nicotiana attenuata* contains 8 unique AGO genes, where biological functions have only been described for a few. *N. attenuata* interacts with arbuscular mycorrhizal fungi entailing reprograming of miRNAs and their target genes. We demonstrate that Na*AGO7* moderates such reprograming of miRNAs and mRNAs during host-AMF interaction under competitive resource-limited conditions. Silencing of AGO7 (and no other AGO) significantly reduced the competitive fitness of *N. attenuata* under resource limited conditions, while we could not observe any change in leaf development or juvenile to adult phase transition as described in other species. In these competitively growing plants, ir*AGO7* roots were over-colonized with AMF as ir*AGO7* plants had >3-fold higher numbers of arbuscules. AMF-induced miRNA expressions were altered in ir*AGO7* plants, consequently, the expression of the target genes was also inversely regulated. The results indicate that hypercolonization has a negative impact on plant competitiveness, probably due to P starvation and changes in auxin signaling. The biological function of NaAGO7 was validated in nature, confirming that the roles for NaAGO7 have diverged. The next step is to evaluate the function of individual miRNAs that are reprogramed in an AGO7-dependent manner during the progress of AMF-colonization of roots.

S.P.P. conceived the original research plan, M.P., K.G, and S.P.P. designed study, M.P.,K.G., carried out most of the experiments, M.P, and S.P.P. analyzed data, Kl.Ga. made transgenic constructs, L.G. and S.P.P and I.T.B carried out field work, M.P. with inputs from M.P., M.P., K.G., I.T.B. and S.P.P. wrote the MS, I.T.B. provided several resources.

2. MANUSCRIPTS

Manuscript I

Argonaute 8 (AGO8) mediates the elicitation of direct defenses against herbivory

Maitree Pradhan, Priyanka Pandey, Klaus Gase, Murali Sharaff, Ravi K Singh, Avinash Sethi, Ian T. Baldwin, Shree P. Pandey*

Plant Physiology (2017) 175:927-946, doi: 10.1104/pp.17.00702

Argonaute 8 (AGO8) Mediates the Elicitation of Direct Defenses against Herbivory[1]

Maitree Pradhan,[a,b] Priyanka Pandey,[c] Klaus Gase,[b] Murali Sharaff,[a] Ravi K. Singh,[a] Avinash Sethi,[a] Ian T. Baldwin,[b] and Shree P. Pandey[a,2]

[a]Department of Biological Sciences, Indian Institute of Science Education and Research Kolkata, Mohanpur 741246, Nadia, West Bengal, India
[b]Department of Molecular Ecology, Max Planck Institute for Chemical Ecology, 07745 Jena, Germany
[c]National Institute of Biomedical Genomics, Kalyani, 741251 West Bengal, India

ORCID IDs: 0000-0002-9279-640X (M.P.); 0000-0001-5371-2974 (I.T.B.); 0000-0002-4546-9123 (S.P.P.).

In *Nicotiana attenuata*, specific RNA-directed RNA polymerase (RdR1) and the Dicer-like (DCL3 and DCL4) proteins are recruited during herbivore attack to mediate the regulation of defense responses. However, the identity and role(s) of Argonautes (AGOs) involved in herbivory remain unknown. Of the 11 AGOs in the *N. attenuata* genome, we silenced the expression of 10. Plants silenced in *NaAGO8* expression grew normally but were highly susceptible to herbivore attack. Larvae of *Manduca sexta* grew faster when consuming inverted-repeat stable transformants (ir*AGO8*) plants but did not differ from the wild type when consuming plants silenced in *AGO1* (*a*, *b*, and *c*), *AGO2*, *AGO4* (*a* and *b*), *AGO7*, or *AGO10* expression. ir*AGO8* plants were significantly compromised in herbivore-induced levels of defense metabolites such as nicotine, phenolamides, and diterpenoid glycosides. Time-course analyses revealed extensively altered microRNA profiles and the reduced accumulation of *MYB8* transcripts and of the associated genes of the phenolamide and phenylpropanoid pathways as well as the nicotine biosynthetic pathway. A possible AGO8-modulated microRNA-messenger RNA target network was inferred. Furthermore, comparative analysis of domains revealed the diversity of AGO conformations, particularly in the small RNA-binding pocket, which may influence substrate recognition/binding and functional specificity. We infer that AGO8 plays a central role in the induction of direct defenses by modulating several regulatory nodes in the defense signaling network during herbivore response. Thus, our study identifies the effector AGO of the herbivore-induced small RNA machinery, which in *N. attenuata* now comprises RdR1, DCL3/4, and AGO8.

When plants are attacked by herbivores, they elicit a complex defense response, which includes direct or indirect defenses. Direct defenses often consist of chemicals that function as antifeedants, antinutrients, or toxins for herbivores (Howe and Jander, 2008; War et al., 2012). In *Nicotiana attenuata*, nicotine, polyamines (Kaur et al., 2010), and diterpenoid glycosides (DTGs; Heiling et al., 2010) often function as direct defenses, as they have been known to be antinutritive and toxic. Attacked plants also emit volatile organic compounds or provide nectar rewards that recruit predators and natural enemies of the attacking insects, and these function as indirect defenses (Howe and Jander, 2008). To elicit these defenses, plants reconfigure their signaling and metabolic networks, and this reconfiguration comprises a complex chain of events involving cell membrane depolarization, calcium flux, and MAPK activation (Maffei et al., 2007; Wu and Baldwin, 2010), increases in reactive oxygen and nitrogen species (Liu et al., 2010; Wu and Baldwin, 2010), and, finally, an intricate interplay of phytohormone signaling involving jasmonic acid (JA; Halitschke and Baldwin, 2003; Howe and Jander, 2008), ethylene (von Dahl et al., 2007), and salicylic acid (SA; Rayapuram and Baldwin, 2007) signaling networks. These complex signaling responses may, in turn, be modulated by small RNAs (smRNAs; Pandey et al., 2008b; Rasmann et al., 2012). However, our understanding of the herbivore-induced smRNA machinery remains incomplete, and the Argonautes (AGOs) involved in this pathway remain unidentified.

In plants, several classes of smRNAs exist (Axtell, 2013). Broadly, smRNAs modulate gene expression either post-transcriptionally (via mRNA degradation or translational blockage) or transcriptionally (such as by heterochromatin formation, paramutation, and other epigenetic mechanisms; Jones-Rhoades et al., 2006; Hutvagner and Simard, 2008; Axtell, 2013; Ma et al., 2013; Rogers and Chen, 2013).

[1] This work was funded by the MPG-India partner group program of the Max Planck Society (Germany) and the Indo-German Center for Science and Technology/Department of Science and Technology, Ministry of Science and Technology (India) and by the Collaborative Research Centre ChemBioSys (CRC1127 ChemBioSys) of the Deutche Forschungsgemeinschaft (DFG).

[2] Address correspondence to sppandey@iiserkol.ac.in.

The author responsible for distribution of materials integral to the findings presented in this article in accordance with the policy described in the Instructions for Authors (www.plantphysiol.org) is: Shree P. Pandey (sppandey@iiserkol.ac.in).

M.P., I.T.B., and S.P.P. designed the study; M.P., K.G., M.S., R.K.S., and S.P.P. carried out experiments; P.P., R.K.S., A.S., and S.P.P. carried out NGS data analysis and other computational experiments; M.P., I.T.B., and S.P.P. wrote the article with contributions of all the authors; I.T.B. and S.P.P. provided resources.

www.plantphysiol.org/cgi/doi/10.1104/pp.17.00702

Three important components of the pathways for the biogenesis and action of smRNAs in plants are the RNA-directed RNA polymerases (RdRs), the Dicer-like proteins (DCLs), and the AGOs (Brodersen and Voinnet, 2006; Axtell, 2013; Borges and Martienssen, 2015). RdRs use RNA templates to generate double-stranded smRNA precursors by synthesizing the second RNA strand. DCLs have endonuclease activity and process the double-stranded smRNA precursors (or stem-loop single RNAs) into 20- to 24-nucleotide duplexes with two-nucleotide overhangs. These are loaded onto the AGOs that retain one of the strands to form the RNA-induced silencing complex (RISC), thus determining the specificity of target selection based on smRNA-mRNA complementarities. In this way, AGOs are regarded as the effectors of the regulatory smRNA machinery (Axtell, 2013). All three central components of the machinery are coded in multigene families in plants; for instance, in Arabidopsis (*Arabidopsis thaliana*), six *RdRs*, four *DCLs*, and 10 *AGOs* have been identified (Höck and Meister, 2008; Mallory and Vaucheret, 2010).

Under different physiological conditions, specific members of these three components of the smRNA machinery are recruited to produce a particular functional class of smRNAs. For instance, during the regulation of developmental events of plants, specific microRNAs (miRNAs) are diced by DCL1 and DCL4 and loaded onto AGO1 or AGO10 to form the RISC that mediates the expression of developmentally important genes (Borges and Martienssen, 2015). RdR6 (along with RdR1) are implicated in producing and amplifying exogenous virus-induced small interfering RNAs (siRNAs; Axtell, 2013). During virus defense, the siRNA precursors are diced by DCL2, DCL3, or DCL4 and loaded onto AGO1 or AGO2 to form the RISC, which mediates resistance (Mi et al., 2008; Takeda et al., 2008). The concerted activity of RdR2 and DCL3 help to generate the 24-nucleotide heterochromatin-derived siRNAs that direct the RNA-dependent DNA methylation pathways (Vrbsky et al., 2010). Heterochromatin-derived siRNAs are loaded onto AGO4 and AGO6 to execute transcriptional silencing (Havecker et al., 2010), while AGO1 and AGO7 participate in the trans-acting siRNA-mediated silencing (Baumberger and Baulcombe, 2005; Qi et al., 2005; Brodersen et al., 2008; Montgomery et al., 2008; Mallory et al., 2009). DCL2 participates in the production of 22-nucleotide virus- and transgene-derived siRNAs and 24-nucleotide siRNAs derived from the natural antisense transcripts that help to mediate tolerance to salt stress in Arabidopsis (Xie et al., 2004; Borsani et al., 2005; Bouché et al., 2006).

Nicotiana attenuata is an ecological model plant, native of the southwestern United States, in which the role of smRNAs in herbivore defense is best studied, in part because the mechanisms of herbivore resistance are well known in this plant. *N. attenuata*'s genome harbors three functionally distinct *RdRs* (Pandey and Baldwin, 2007, 2008; Pandey et al., 2008a), four *DCLs* (Bozorov et al., 2012), and 11 *AGOs* (Singh et al., 2015). Silencing only *RdR1* makes *N. attenuata* plants highly susceptible to herbivory (Pandey and Baldwin, 2007). Furthermore, sequential loss-of-function analysis of the *NaDCLs* suggested that *DCL3* and *DCL4* contribute to this plant's herbivore resistance (Bozorov et al., 2012). Which of the 11 *NaAGOs* play a role in the herbivore-induced smRNA pathway remained elusive, and that was the subject of this study.

RESULTS

Characterization and Domain Organization of AGOs in *N. attenuata*

N. attenuata contains 11 unique AGO homologs (Singh et al., 2015). A neighbor-joining phylogenetic tree (Fig. 1) was reconstructed after multiple sequence alignment (MSA) of all 11 NaAGOs (Supplemental Fig. S1). NaAGO2 and NaAGO7 clustered together; similarly, NaAGO4a, NaAGO4b, NaAGO8, and NaAGO9 formed a cluster; while NaAGO1a, NaAGO1b, NaAGO1c, NaAGO5, and NaAGO10 formed independent branches on the tree (Fig. 1). Overall, the topology of the NaAGO phylogenetic tree was similar to that of the AtAGOs (Supplemental Fig. S1).

In order to further characterize these 11 homologs, we performed a comparative analysis of the sequences of the NaAGOs, the *Homo sapiens* AGO2 (HsAGO2; Protein Data Bank [PDB] code 4F3T; Elkayam et al., 2012), and the *Kluyveromyces polysporus* AGO (KpAGO; PDB code 4F1N [model for yeast AGO]; Nakanishi et al., 2012). HsAGO2 and KpAGO are the two best biochemically characterized eukaryotic AGOs, as their structures have been determined. We identified the characteristic N, PAZ, MID, and PIWI domains in the NaAGOs (Fig. 1). Furthermore, we identified an additional domain of unidentified function between the L1 (linker 1) and PAZ domains (Fig. 1). The PAZ, MID, and PIWI domains contain R/K/V-F-Y, Y-N-K-K, and D-E-D-D/H signature residues, respectively (Hutvagner and Simard, 2008; Nakanishi et al., 2012; Singh et al., 2015). These signature residues were readily identified in the respective domains of the NaAGOs (Fig. 1; Supplemental Fig. S1). Variation in the R-F-Y signature of the PAZ domains was evident; R (position 600; Fig. 1) had been substituted with K in NaAGO4a, NaAGO8, and NaAGO9 and with V in NaAGO2. NaAGO2 displayed the D-D-D variant in the PIWI signature. Additionally, we discovered five, eight, and 11 functionally important sites in the PAZ, MID, and PIWI domains (Elkayam et al., 2012), respectively, that were variable among NaAGOs. Such variations at important positions in PAZ, MID, and PIWI domains (Fig. 1; Supplemental Fig. S1) may have functional consequences related to the mechanism by which AGOs interact with RNA substrates (Singh and Pandey, 2015).

Changes in Transcript Abundance of *NaAGOs* in Response to Herbivory

We quantified transcript abundances of the *NaAGO*s that are elicited in leaves or roots during the attack of

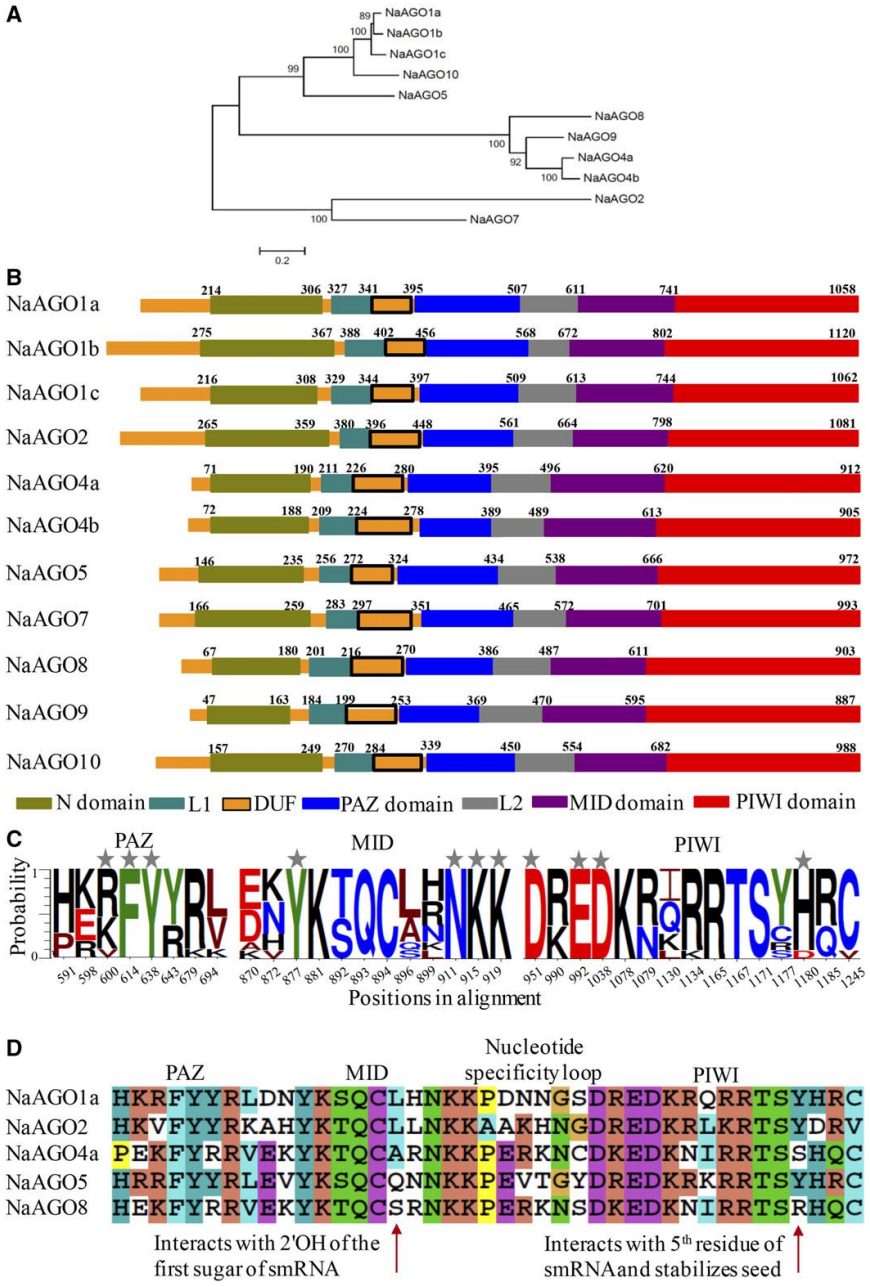

Figure 1. Characterization of AGOs of *N. attenuata*. A, Neighbor-joining phylogenetic tree of *N. attenuata* AGOs. The MSA of the full-length peptide sequences of NaAGOs was performed using ClustalX 2.1, and phylogeny was created using MEGA 5.2. Clade robustness was assessed with 1,000 bootstrap replicates, and the values are shown on the branches. B, Schematic representation of domain architectures in 11 NaAGOs. Different regions were annotated with the help of the conserved domain search tool and compared with the domains of KpAGO and HsAGO2. The MID and the PIWI domains are fused in all the NaAGOs. C, Diversity in signature residues of the PAZ, the MID, and the PIWI domains in NaAGOs. The height of a residue denotes the probability of occurrence of a residue at the given position in MSA (Supplemental Fig. S1). The positions marked with stars are the previously

Manduca sexta larvae (Fig. 2; Supplemental Fig. S2). Immediate application of distilled water-diluted *M. sexta* oral secretions (W+OS) to puncture wounds in leaves recapitulates the responses elicited during attack from this insect (Halitschke et al., 2001). Although no significant differences in transcript profiles in roots were noticed (Supplemental Fig. S2), in leaves 18 h after W+OS treatment (Fig. 2), the accumulation of *NaAGO8* transcripts increased 3-fold over the wounding controls (similarly wounded plants in which the puncture wounds were treated with distilled water). Such an increase in transcript levels suggested that *AGO8* contributes to the smRNA-mediated regulation of defenses. Additionally, we noticed an increase of nearly 2-fold in *NaAGO5* transcripts 1 h after oral secretions (OS) elicitation. A second 6-fold peak in the accumulation of *NaAGO5* transcripts over untreated and wounding controls also was observed 18 h after OS elicitation (Fig. 2). No significant effects were observed in the abundance of transcripts of the other *AGOs* in response to the W+OS treatment (Fig. 2). This analysis was duplicated, and similar results were obtained. W+OS-induced differences in *AGO5* and *AGO8* transcripts at the 18-h time point were validated in independent experiments with at least three (independent) biological replicates. Compared with control plants, a significant increase of 3.5-fold or greater in *AGO8* transcripts (Student's *t* test, $t = 5.937$, $P < 0.05$) and a 5-fold or greater increase in *AGO5* transcripts (Student's *t* test, $t = 8.261$, $P < 0.01$) were recorded. This indicates that AGO5 and AGO8 may be involved in modulating the induced defense responses of *N. attenuata* against herbivore attack. It is plausible that AGO5 may modulate certain defense-signaling events independent of AGO8 or that AGO5 and AGO8 also may have overlapping targets.

Characterization of Transgenic *NaAGO* Lines

The inverted-repeat stable transformants (ir*AGO*) of *NaAGO1* (*a*, *b*, and *c*), *NaAGO2*, *NaAGO4* (*a* and *b*), *NaAGO5*, *NaAGO7*, *NaAGO8*, and *NaAGO10* with complete T-DNA insertions were screened for homozygosity in the T2 generation, as detailed earlier (possibilities of incomplete T-DNA insertions were ruled out as described by Gase et al. [2011]). After testing the transformant's seedling survival rate on hygromycin plates and conducting diagnostic PCRs, we identified two independently transformed lines of *NaAGO2*, *NaAGO4*, *NaAGO5*, *NaAGO7*, *NaAGO8*, and *NaAGO10* and one for *NaAGO1*. These were subjected to DNA gel-blot analysis, which revealed single insertions in both the independent lines of *NaAGO2*, *NaAGO4*, *NaAGO7*, *NaAGO8*, and *NaAGO10* (Fig. 3; Supplemental Fig. S3). For *NaAGO1* (866-1-5) and *NaAGO5* (909-6-2), the analysis revealed that the lines were heterozygous, harboring double insertions (Fig. 3). Upon evaluating the silencing efficiency of the targeted genes in all the ir*AGO* lines, a minimum decrease of 50% transcript levels as compared with the wild type was observed for ir*AGO4a*. Stronger reductions were recorded for all the other genotypes, including a nearly complete silencing of *AGO2*, *AGO5*, and *AGO10* (Fig. 3). The ir*AGOs* with two independent homozygous single insertion lines with significantly reduced transcript levels as compared with the wild type (for *NaAGO2*, *NaAGO4*, *NaAGO7*, *NaAGO8*, and *NaAGO10*) were selected for further experiments.

Silencing *NaAGO8* Improves the Performance of the Specialist Herbivore *M. sexta*

To identify if any of the AGOs are involved in modulating the defense response of *N. attenuata* plants against *M. sexta*, caterpillar performance assays were conducted with all ir*AGO* lines and the wild type. We observed no significant differences in the larval biomass from larvae feeding on lines silenced in *NaAGO1* (*a*, *b*, and *c*), *NaAGO2*, *NaAGO4* (*a* and *b*), *NaAGO7*, and *NaAGO10* expression compared with those feeding on wild-type plants (Fig. 4). Due to the absence of two independent transformants with single T-DNA insertions for ir*AGO5*, ir*AGO5* plants were not included in the caterpillar assays. In contrast, when fed on the two independent homozygous lines of ir*AGO8* (A-12-871-8-8 and A-12-873-5-2, which did not show any developmental or growth abnormalities compared with wild-type plants [Supplemental Fig. S4]; silencing *AGO8* had no effect on the transcript accumulations of any other AGOs [Supplemental Fig. S5]), caterpillars were significantly larger at the 6-, 9-, and 11-d measures. Caterpillar mass was 63% larger on ir*AGO8* lines in comparison with those on wild-type plants after 11 d of feeding (Fig. 4; repeated-measures ANOVA, $P \leq 0.001$). These results were verified in an independent caterpillar bioassay (Supplemental Fig. S6). In order to further evaluate off-target effects other than on the other *NaAGOs* in the *N. attenuata* genome, we used the *AGO8* inverted-repeat sequence present in the pRESC8*AGO8* construct, both with the SGN VIGS tool (Fernandez-Pozo et al., 2015) and a BLAST search against the complete transcriptome of *N. attenuata*. We did not find any off-target effects related to herbivore resistance (Supplemental Fig. S5; detailed further in "Materials and Methods"). From these results, we conclude that silencing *NaAGO8* expression specifically increases

Figure 1. (*Continued.*)
recognized signature residues. The values on the *x* axis show the positions of the residues in the MSA of NaAGOs (Supplemental Fig. S1). D, Signature residues in NaAGO8 at the respective positions of C (Supplemental Fig. S1). Specific signature residues marked with red arrows may contribute to the interaction of AGO8 with the substrate.

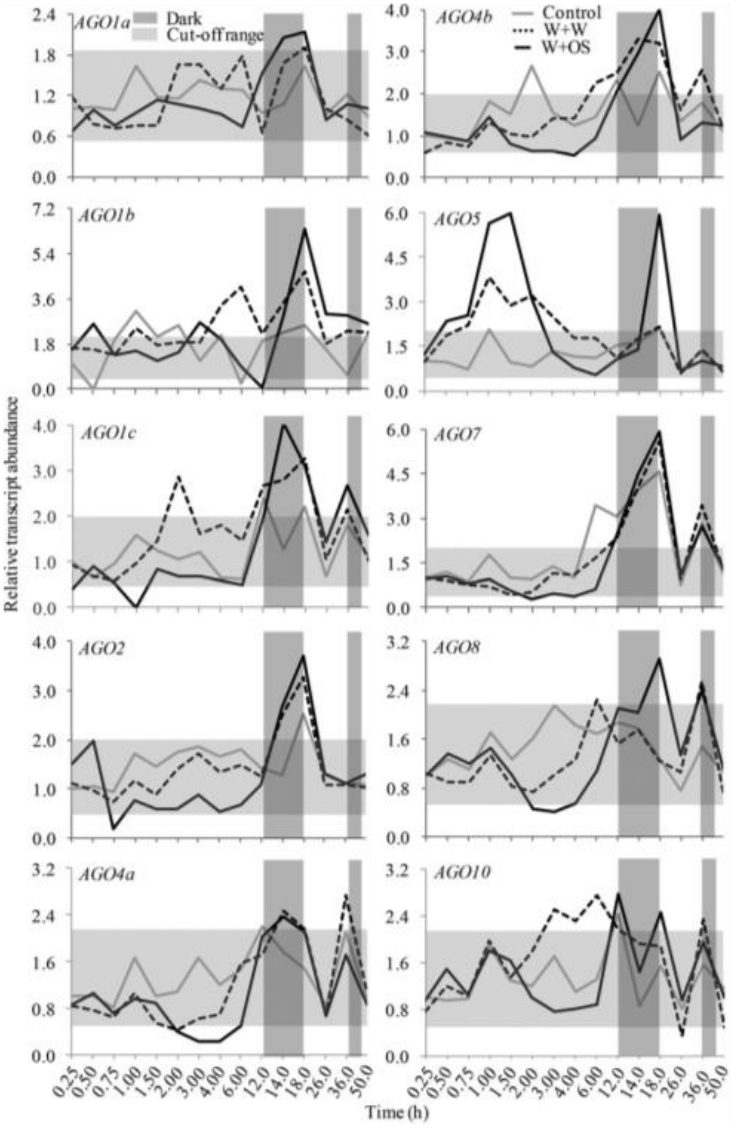

Figure 2. Abundance of *NaAGO* transcripts in the leaves during time-course experiments. Rosette leaves of 3- to 4-week-old wild-type *N. attenuata* plants were wounded with pattern wheels, and 20 μL of water (W+W) or *M. sexta* OS (W+OS; diluted 5-fold in water) were immediately applied to these wounds. Leaf samples from control and treated plants were collected at the time intervals depicted on the *x* axis. SYBR Green assays were performed, and the ΔΔCT method was used to determine relative transcript accumulations. Dark, When lights were off; Cut-off range, relative abundance of transcript, above or below which was considered up- or down-regulated, respectively.

caterpillar performance, suggesting that this AGO plays a key regulatory role in resistance to insect attack.

Silencing *AGO8* Reprograms the *N. attenuata* smRNA Population

We determined how *AGO8* silencing influenced the smRNA profiles of *N. attenuata* before and after simulated herbivory (OS elicitation). We deep sequenced the smRNome (in the range of 15–30 nucleotides) of wild-type and ir*AGO8* plants before (0 h) as well as 0.75 and 18 h after OS elicitation. An average of 18.1 ± 1.6 million reads were generated in each of the samples; after quality-control measures and removing the structural RNAs and mRNAs (Pandey et al., 2008b), we obtained, on average, 4.8 ± 0.9 million unique smRNA reads in each sample in the range of 15 to 30 nucleotides (Fig. 5A). We determined the composition of miRNAs influenced by *AGO8* silencing in this pool using the miRDeep pipeline (Friedländer et al., 2012). We focused our analysis on miRNAs that are conserved across plant species, as these miRNAs may have profound roles for a plant's physiology. A total of 135 miRNA reads corresponding to 125 unique miRNAs (Fig. 5A; Supplemental Table S1), conserved in 32 plant

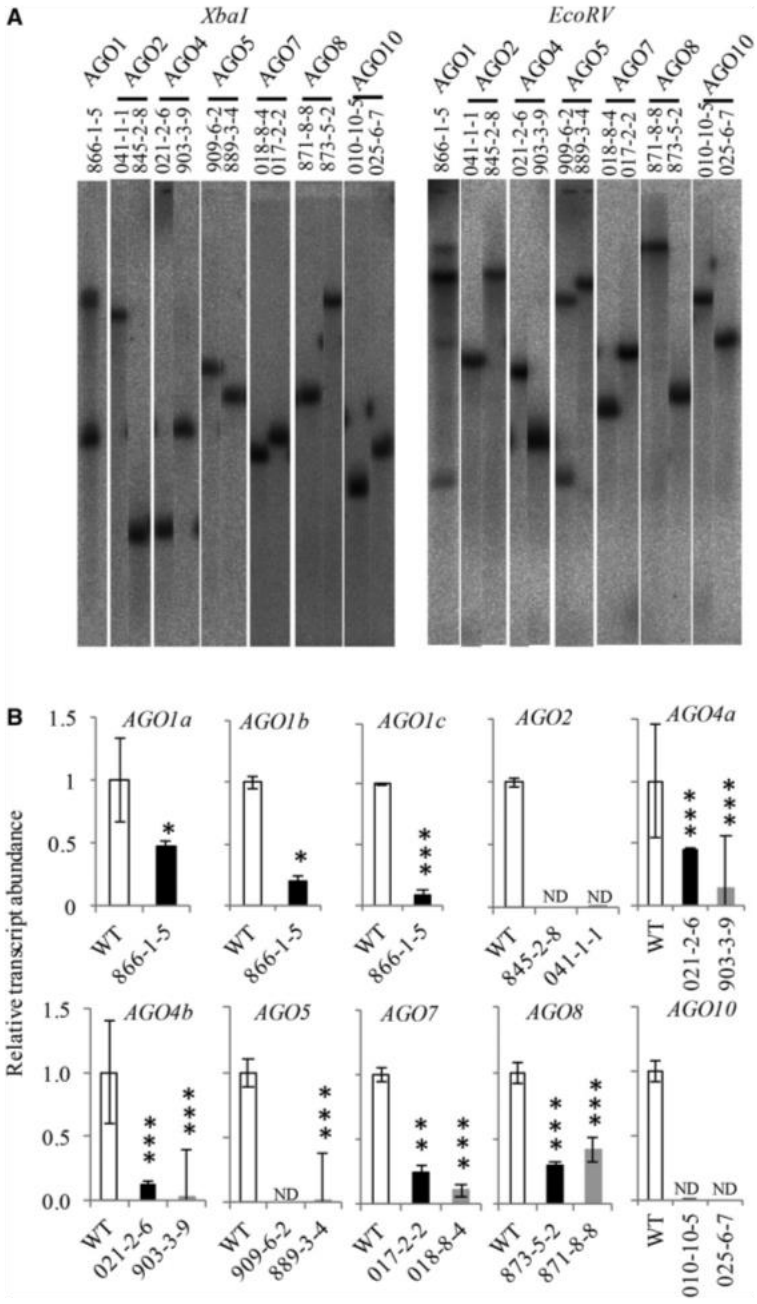

Figure 3. Characterization of ir*AGO* lines. A, Southern-blot analysis of transgenic genotypes to determine lines harboring a single insertion; genomic DNA was digested with *Xba*I (left) and *Eco*RV (right). B, Evaluation of the silencing efficiency of ir*AGO* lines. Wild type (WT) and ir*AGO* genotypes were W+OS elicited, and samples were collected after 18 h. Transcript levels, quantified by qPCR, of *AGO*s were normalized to wild-type levels, which were set to 1. ND, Transcripts not detected. Significant differences from the wild type are indicated with asterisks (ANOVA [Fisher's LSD]: *, $P \leq 0.05$; **, $P \leq 0.01$; and ***, $P \leq 0.001$).

species, were annotated using the miRDeep pipeline (Fig. 5G; Supplemental Table S2). Secondary hairpin structures of 166 putative novel miRNA candidates were produced and evaluated by miRDeep. Overall, the length distributions of small RNA reads indicate that the libraries are highly enriched in miRNAs in the 21- to 24-nucleotide lengths (Supplemental Table S1).

Results of mapping the clean reads to different publicly available databases produced 301 mature and 551 precursor miRNA reads (Fig. 5A): mapping results showed 135 known reads (corresponding to125 miRNAs) and 166 novel miRNA reads (Supplemental Table S1). Complete lists and the main characteristics of miRNAs and their precursors, length, coordinates, and annotation in the

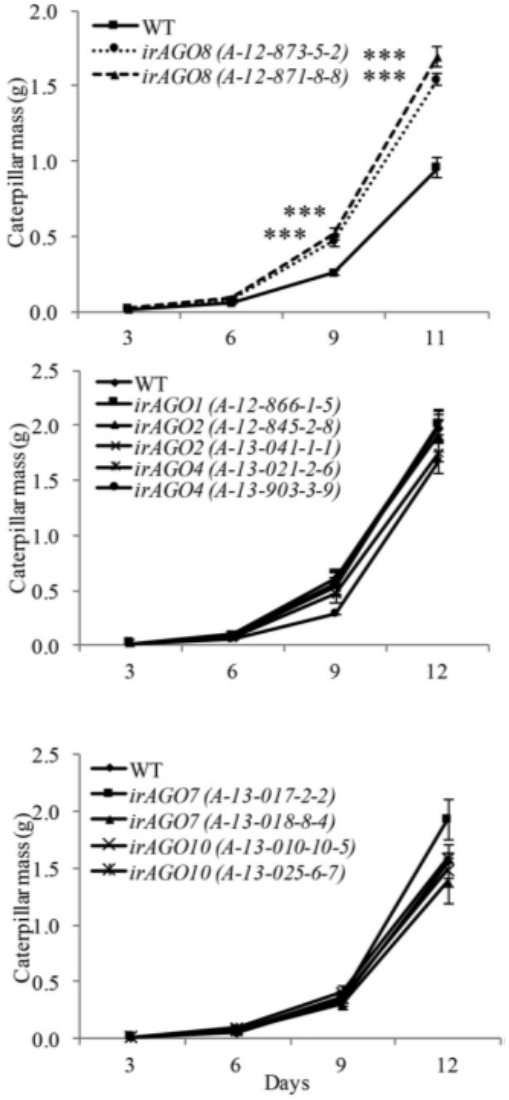

Figure 4. Silencing of *AGO8* makes *N. attenuata* susceptible to *M. sexta* larval attack. Caterpillars (one neonate per plant) were allowed to feed continuously; their mass was recorded at 3, 6, 9, and 12 d of feeding. Significant differences from the wild type (WT) are given (repeated-measures ANOVA: for ir*AGO8* line 873-5-2, $F = 16.71$, $P \leq 0.001$; and for line 871-8-8, $F = 23.57$, $P \leq 0.001$). ***, Significant difference at $P \leq 0.001$.

genome, are provided in Supplemental Table S1. Also, details for miRNAs found in intergenic and intragenic regions are given in Supplemental Table S1. As expected for miRNA genes (conserved in Fig. 5, B and C, and novel miRNA reads in Fig. 5, D and E), most were found in intergenic or intronic regions (conserved, 119 reads [88%]; novel, 134 reads [81%]). However, two conserved and two novel reads mapped to untranslated regions, whereas two conserved and five novel reads mapped to the predicted coding sequence. Furthermore, 12 conserved and 25 novel reads mapped to exonic regions. Precursor miRNA length varied from 45 to 111 nucleotides, with an average of 71 nucleotides; and 50% of conserved and 46% of novel precursor miRNA reads comprised between 71 and 90 nucleotides (Fig. 5F).

Expression Profiles of Conserved and Novel miRNAs

Mature miRNAs from a total of 32 conserved families were detected (Fig. 5G; their expression counts are tabulated in Supplemental Tables S1 and S2). Silencing *AGO8* profoundly influenced the composition of the miRNAs of *N. attenuata* in a complex manner. Of the 125 conserved miRNAs, 71, 74, and 63 miRNAs were detected in ir*AGO8*, whereas 68, 72, and 77 miRNAs were captured in the wild type (presence of *AGO8*), at 0, 0.75, and 18 h after OS elicitation. Similarly, 82, 90, and 64 novel miRNAs were expressed in ir*AGO8*, whereas 75, 67, and 77 novel miRNAs were captured in the wild type, at 0, 0.75, and 18 h after OS elicitation. Wild-type and ir*AGO8* plants shared nearly 57% of conserved and 44% of novel miRNAs, of which a large number were differentially accumulated in ir*AGO8* compared with the wild type (Fig. 6; Supplemental Table S3). The expression level of conserved miRNA families can be classified into three categories, namely as high (reads per million [RPM] > 10,000; e.g. miR167-5p, miR165a-3p, miR156b-5p, miR168a-5p, miR6149a, and miR6021), moderate (RPM = 100–10,000; e.g. miR156a, miR172a-3p, miR1846e, miR403a-3p, miR5386, miR5789, miR6020b, miR7122a, miR8015-3p, and miR8764), and low (RPM < 100; e.g. miR1066, miR1169-3p, miR160-5p, miR394, miR477a-3p, miR6218-5p, miR7504e, and miR9496).

Identification of ir*AGO8*-Specific Conserved and Novel miRNAs

miRNA profiles of wild-type and ir*AGO8* plants, in triplicate, at 0-, 0.75-, and 18-h time points were compared. Thirty-one conserved miRNAs are expressed only after silencing of *AGO8* (Fig. 6A, black line graphs). Of these, miR8703a, miR6484, miR6226-3p, miR5497, miR4358, miR319-3p, miR1066, and miR169j-3p were expressed only at 0 h (before OS elicitation); miR7808, miR7756-3p, miR6295, miR6147, miR5069, miR482c-5p, miR395, miR170-3p, and miR3701 were expressed only at 0.75 h after OS elicitation; and miR9496, miR8769, miR7486h, miR5049-3p, miR5780c, and miR6206 were expressed only at 18 h; whereas miR2596, miR394, miR8129-3p, miR6020b, miR6158a, miR1536, and miR5027 were expressed at both 0 and 0.75 h, and miR6218-5p was expressed at all the three time points only in the ir*AGO8* samples.

Twenty-five conserved miRNAs are expressed only when *AGO8* is present (and, thus, may be regarded as specific to AGO8; Fig. 6A, green line graphs). miRNAs such as miR5781, miR1846e, and miR7725b-3p.1 (and others) are

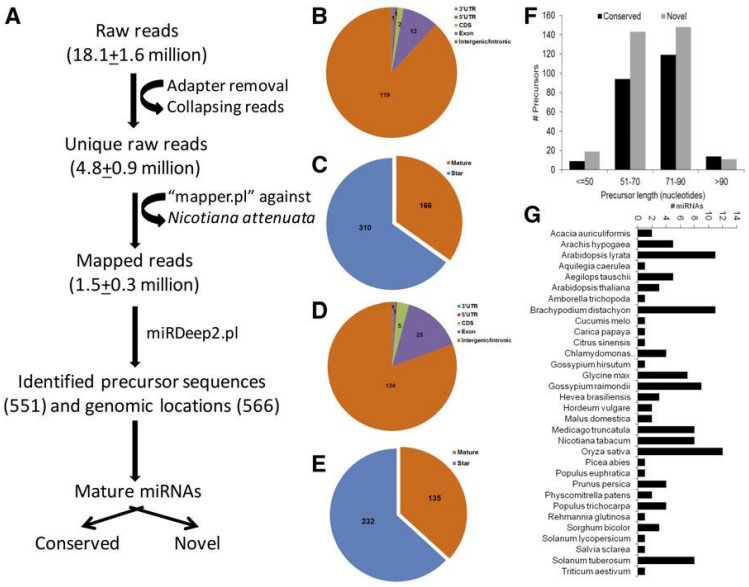

Figure 5. Herbivore-induced ir*AGO8*-dependent smRNA profiling of *N. attenuata*. A, Pipeline used for *N. attenuata* miRNA identification. Counts for reads, unique sequences, genomic locations, and precursor miRNA detected are given at each step. Details on filtering steps are provided in "Materials and Methods." B to E, Pie charts represent the distribution of precursor miRNA genomic loci on the *N. attenuata* genome for the conserved (B) and predicted (D) miRNAs; C and E show the number of mature and star sequences identified for conserved and predicted miRNAs, respectively. CDS, Coding sequence; UTR, untranslated region. F, Histogram shows the size distribution of the precursor miRNAs for the conserved (black bars) and novel (gray bars) miRNAs. The number of miRNAs present in each size class is shown. G, Distribution of mature miRNAs in different species. Mature sequences were found widespread in 32 plant species (analysis performed on miRNAs from 72 plant species obtained from miRBase). Bars represent the number of miRNAs mapping to each species.

expressed only at 0 h; miRNAs such as miR7980a, miR5163a-3p, and miR159b are expressed only at 0.75 h; whereas miRNAs like miR6483, miR5820, and miR6444 are expressed at 18 h specifically.

Fifty-seven novel miRNAs are expressed only in ir*AGO8*: Nat-AGO8-PN119, Nat-AGO8-PN112, and Nat-AGO8-PN26 are expressed only at 0 h; Nat-AGO8-PN72, Nat-AGO8-PN58, and Nat-AGO8-PN39 are expressed at 0.75 h; and miRNAs such as Nat-AGO8-PN96, Nat-AGO8-PN78, and Nat-AGO8-PN20 are expressed at 18 h (Fig. 6B, black line graphs). Thirty-three novel miRNAs are not captured in the absence of *AGO8* (and, thus, are considered dependent on *AGO8*). For example, *AGO8*-dependent novel miRNAs such as Nat-AGO8-PN154, Nat-AGO8-PN115, and Nat-AGO8-PN32 are expressed only at 0 h; Nat-AGO8-PN117, Nat-AGO8-PN68, and Nat-AGO8-PN50 are expressed only at 0.75 h; and Nat-AGO8-PN101, Nat-AGO8-PN76, and Nat-AGO8-PN17 are expressed only at 18 h (Fig. 6B, green line graphs).

Differential Expression of miRNAs

Complex patterns of differential accumulation of miRNAs (commonly expressed in the wild type and ir*AGO8*) were observed across the three time points, 0, 0.75, and 18 h, due to silencing of AGO8. Information on these patterns of differentially expressed miRNAs (DEMs) in both genotypes at the three time points is summarized in Table I and Supplemental Table S4. Most of the miRNAs have higher expression values in the presence of AGO8 at 0 h. Twenty-one miRNAs accumulated more in the wild type compared with irAGO8 (Table I). Only 29 miRNAs were differentially expressed within ir*AGO8* before and after OS elicitation, whereas a large number of miRNAs (66 DEMs) were reprogrammed in the wild type after OS elicitation as compared with the 0-h control (Supplemental Fig. S7). Fifty-one and 32 miRNAs were significantly down-regulated at 0.75 h (compared with 0 and 18 h, respectively) in the wild type, whereas in ir*AGO8*, only 11 and 16 miRNAs were repressed (Table I). For example, miRNAs 162, 1163.2, 4414b, 7504c, and 5789 were down-regulated by more than 1.5-fold in the wild type, whereas only miR4414b was down-regulated in ir*AGO8* at 0.75 h (as compared with 0 h; Supplemental Table S4). We found that miR408-5p and miR8688 were significantly down- and up-regulated, respectively, in the absence of AGO8 (Supplemental Table S4). miRNAs 72a-3p, 4379, 8015-3p, 8165, and 6218-5p were up-regulated in irAGO8 at 0.75 and 18 h when compared with the wild type. miR1846e was significantly highly expressed at the baseline (0 h) in the presence of AGO8, whereas very few reads were obtained in ir*AGO8* samples, indicating that its expression might be dependent on AGO8. These results suggest that (1) AGO8 is needed for the modulation of miRNA levels, as shown by the larger number of DEMs in the wild type compared with ir*AGO8*, and (2) 0.75 h showed the maximum change in AGO8-dependent miRNA expression (Table I).

NaAGO8 Modulates the Accumulation of Key Defense Metabolites

After determining the impact of *AGO8* silencing on miRNA accumulation during herbivory, we determined which physiological processes were impacted by such profound changes. Moreover, specific susceptibility of

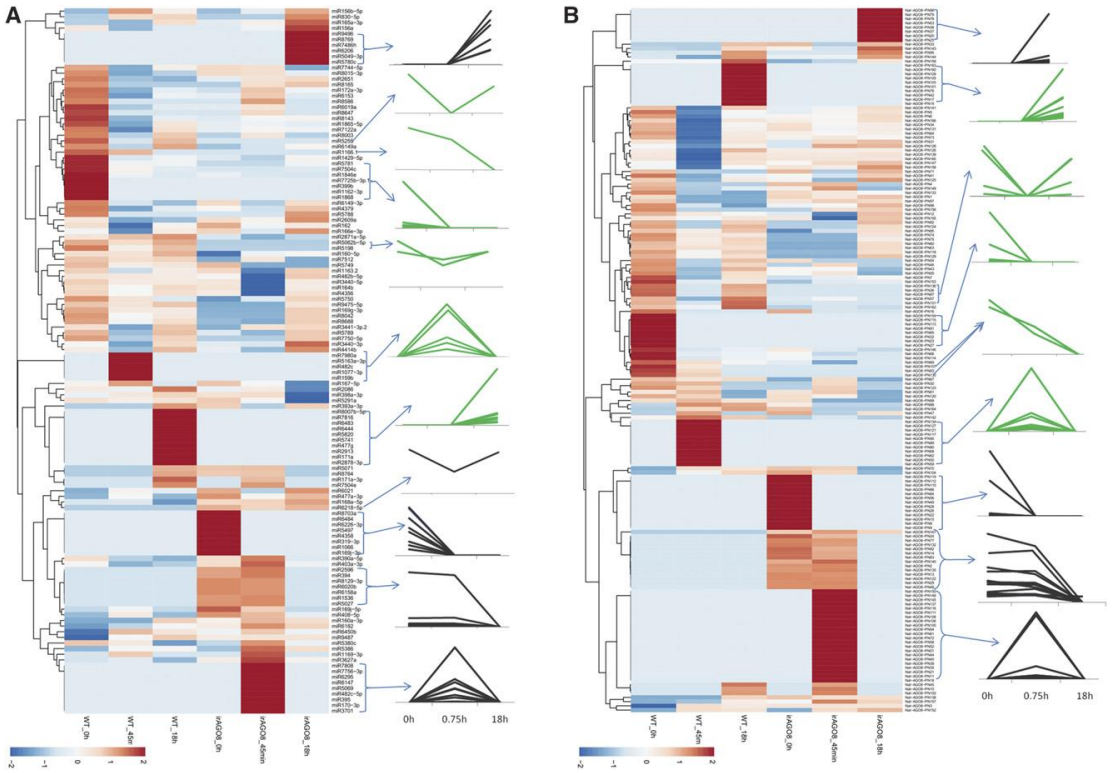

Figure 6. Transcript abundance patterns for conserved and novel miRNAs. Hierarchical clustering of heat maps was performed on the miRNA abundance values using the Pearson correlation method. Higher abundance is represented by dark color, whereas dark blue shows very low abundance. Line graphs are used to highlight changes in abundance for a few miRNAs (explained in the text). Black and green line graphs show patterns for miRNAs present in ir*AGO8* and the wild type (WT), respectively. A, Heat map representing the abundance pattern for 125 conserved miRNAs. Fifty-five miRNAs are differentially abundant in both genotypes across all three time points (0, 0.75, and 18 h). On the other hand, 56 miRNAs (31 in the wild type and 25 in ir*AGO8*) were captured only at one or two time points in one of the two genotypes. For example, miRNAs 5062b-5p and 5198 were captured only in the wild type and were repressed at 0.75 h compared with 0 and 18 h. miR159b was accumulated only at 0.75 h in the wild type, whereas nine miRNAs were captured only in ir*AGO8* at 0.75 h. B, Heat map for 166 predicted novel miRNAs. Ninety novel miRNAs (33 in the wild type and 57 in ir*AGO8*) were accumulated at one or two time points in either the wild type or ir*AGO8*. At 0.75 h, 10 miRNAs accumulated only in the wild type and 22 only in ir*AGO8*.

ir*AGO8* plants to herbivore attack indicated that the complex reprogramming in miRNA accumulation during the course of OS elicitation may lead to compromised inducible defenses. We used an unbiased metabolomics approach to help us identify the changes in metabolites in caterpillar-fed ir*AGO8* plants as compared with the wild type that might be responsible for the changes in resistance (Wu and Baldwin, 2010; Gaquerel et al., 2014). The leaf extracts from 12-d caterpillar-fed wild-type and ir*AGO8* plants were analyzed using liquid chromatography-electrospray ionization-time of flight-mass spectrometry (n = 15 for the wild type and n = 10 for ir*AGO8*). When comparing the peak matrices of the two genotypes, we found mass spectra with reduced peak areas in ir*AGO8* plants that corresponded to several defense-related metabolites, such as nicotine, phenolamides, and HGL-DTG (Fig. 7). The important molecular features identified from loading plots were annotated with elemental formulas and summarized (Fig. 7; Supplemental Table S5). Projection (VIP) scores based on partial least squares-discriminate analysis confirmed the reduced levels of these defense metabolites in ir*AGO8* compared with their levels in the wild type (Fig. 7; $P < 0.05$). No primary metabolites were detected among the key molecular features of the VIP plot, and no significant differences in acyl sugars were observed (Supplemental Table S5). Highly significant silencing of *AGO8* transcripts was observed under both basal (n = 4, ANOVA, F = 28.02, $P < 0.05$) as well as induced (n = 3, ANOVA, $P < 0.001$; Fig. 3) states. Yet, the growth and morphology of the ir*AGO8* plants were fully comparable to those of wild-type plants (Supplemental Fig. S4); no differences in rosette diameter

Table I. *Differentially expressed miRNAs at $P < 0.05$ in six comparisons*
P values were computed using χ^2. C, Conserved; N, novel.

Comparison	Total miRNA Expressed in ir*AGO8* and the Wild Type	DEMs	Up	Down
ir*AGO8* and the wild type at 0 h	95	28 (C = 20; N = 8)	7 (C = 6; N = 1)	21 (C = 14; N = 7)
ir*AGO8* and the wild type at 0.75 h	89	37 (C = 21; N = 16)	29 (C = 15; N = 14)	8 (C = 6; N = 2)
ir*AGO8* and the wild type at 18 h	104	18 (C = 12; N = 6)	11 (C = 8; N = 3)	7 (C = 4; N = 3)
ir*AGO8* at 0.75 and 0 h	115	20 (C = 14; N = 6)	9 (C = 8; N = 1)	11 (C = 6; N = 5)
ir*AGO8* at 18 and 0 h	93	18 (C = 14; N = 4)	16 (C = 12; N = 4)	2 (C = 2; N = 0)
ir*AGO8* at 18 and 0.75 h	87	22 (C = 18; N = 4)	16 (C = 12; N = 4)	6 (C = 6; N = 0)
The wild type at 0.75 and 0 h	105	57 (C = 32; N = 25)	6 (C = 6; N = 0)	51 (C = 26; N = 25)
The wild type at 18 and 0 h	114	35 (C = 20; N = 15)	10 (C = 6; N = 4)	25 (C = 14; N = 11)
The wild type at 18 and 0.75 h	105	38 (C = 20; N = 18)	32 (C = 14; N = 18)	6 (C = 6; N = 0)

($n = 5$, ANOVA, Fisher's LSD, $F = 2.12$, $P > 0.05$), number of rosette leaves ($n = 5$, ANOVA, Fisher's LSD, $F = 0.22$, $P > 0.05$), plant height ($n = 5$, ANOVA, Fisher's LSD, $F = 2.58$, $P > 0.05$), number of flowers ($n = 5$, ANOVA, Fisher's LSD, $F = 0.222$, $P > 0.05$), or chlorophyll content ($n = 5$, ANOVA, Fisher's LSD, $F = 0.3686$, $P > 0.05$) of ir*AGO8* and wild-type plants were observed under unstressed conditions (Supplemental Fig. S4). From these results, we infer that silencing *AGO8* did not affect the primary metabolism of *N. attenuata* plants.

We performed targeted metabolite analysis of caterpillar-fed wild-type and ir*AGO8* leaf samples to reexamine the accumulation patterns of nicotine, rutin, and HGL-DTGs (Fig. 7; Supplemental Fig. S8). The nicotine levels were significantly lower in both ir*AGO8* lines (Fig. 7; ANOVA, $P \leq 0.01$). Similarly, HGL-DTG levels were reduced significantly in both the ir*AGO8* lines (Fig. 7; ANOVA, $P \leq 0.05$ [871-8] and $P \leq 0.001$ [873-5]). As previous work found that insect feeding increases rutin levels in *N. attenuata* (Yang et al., 2013), we examined the concentrations of these metabolites with a targeted analysis, even though rutin had not been found in the unbiased analysis. Rutin levels also were significantly lower in the leaves of ir*AGO8* plants that had been attacked by caterpillars as compared with wild-type fed leaves (ANOVA, $P \leq 0.05$; Fig. 7).

NaAGO8 Modulates *MYB8*-Mediated Defense Responses

Metabolomic analyses revealed that silencing *AGO8* reduced the concentrations of key defense metabolites such as nicotine, phenolamides, and DTGs. *MYB8* is a transcription factor in *N. attenuata* known to regulate the induction of nicotine, phenylpropanoid, and phenolamide pathways (Kaur et al., 2010). We conducted time-course experiments with OS-elicited wild-type and ir*AGO8* plants in the fully expanded rosette stage of growth. The transcript levels of *MYB8* were strongly reduced in ir*AGO8* (Fig. 8). As *NaMYB8* regulates the expression of genes for phenolamide metabolism, we investigated how the transcription of this *MYB8* network of genes was affected: transcripts of *AT1*, *DH29*, and *CV86*, which are elicited 6 h after the wild-type plants are OS elicited (Onkokesung et al., 2012), were reduced in ir*AGO8* (Fig. 8). As phenylpropanoid metabolism is regulated by *MYB8* during herbivory (Onkokesung et al., 2012), we also examined the accumulation of transcripts of key genes in the pathway: *PAL1*, *PAL2*, and *C4H*; lower levels of transcripts of these genes were recorded in the ir*AGO8* lines (Fig. 8). This implies that *AGO8* has a role in regulating the expression of *MYB8* and its associated genes in phenolamide and phenylpropanoid metabolism after herbivore attack.

In congruence with the metabolomic profiles, the transcripts of the key genes involved in the biosynthesis of HGL-DTGs (*NaGGPPS*) and nicotine (*NaODC* and *NaPMT*) were clearly less abundant in the ir*AGO8* lines after simulated herbivory (Fig. 8). These results are consistent with the hypothesis that *AGO8* has a regulatory role in the biosynthesis of defense-responsive metabolites during herbivory.

Silencing *AGO8* Partially Affects Phytohormone Signaling

JA signaling plays a central role in activating robust defenses (that are described above) in *N. attenuata* against herbivore attack (Halitschke and Baldwin, 2003). Therefore, we analyzed JA and JA-Ile levels in the leaves of 12-d caterpillar-fed wild-type and ir*AGO8* plants (Supplemental Fig. S8), which indicated that herbivory-induced JA levels might be lower in ir*AGO8* lines. OS elicitation provides a means of rigorously quantifying JA dynamics in a manner that is not obfuscated by variations in caterpillar feeding behavior; therefore, we examined JA levels in W+OS-treated wild-type and ir*AGO8* plants. JA levels were partly, yet significantly, lower in ir*AGO8* in comparison with the wild type 30 min after OS elicitation (38.83%; ANOVA, $P \leq 0.05$; Supplemental Fig. S8; no differences in JA-Ile levels were observed). JA-Ile levels are typically one-tenth of the JA levels, and the amounts of JA present in ir*AGO8* plants may be sufficient to supply the JA-Ile burst, as the genes responsible for such conversion may not be under AGO8 control. *WRKY3* and *WRKY6* are the major transcription factors in *N. attenuata* that regulate JA signaling (Skibbe et al., 2008). Consistent with a significant reduction in JA levels, at early time points (45 and 60 min), the transcript levels of the *WRKY3* and

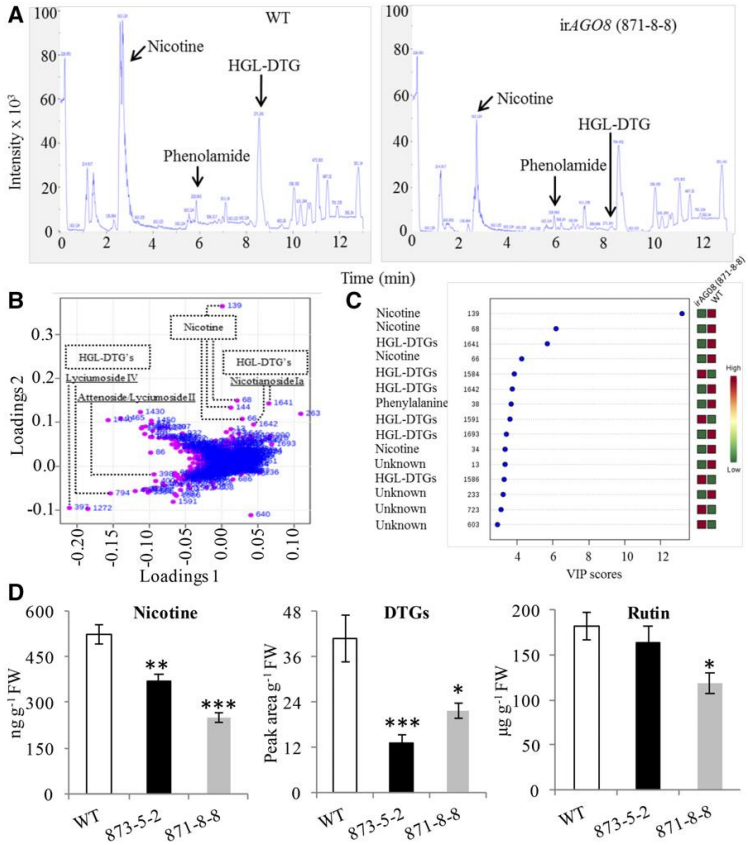

Figure 7. Profiling of metabolomes of *M. sexta* caterpillar-attacked wild-type (WT) and ir*AGO8* leaves. A, Untargeted metabolite profile (from A–C) showing representative tandem mass spectrometry ion chromatograms of wild-type and ir*AGO8* (871-8-8) genotypes exhibiting alterations in major defense metabolites (nicotine, phenolamides, and HGL-DTGs) in response to herbivory. B, Loading plot for the selected principal components of wild-type and ir*AGO8* genotypes, discriminating the major herbivore-responsive defense metabolites, nicotine and HGL-DTGs. C, Key molecular features identified by partial least squares-discriminant analysis among the genotypes. The colored boxes on the right indicate the relative concentrations of the corresponding metabolite in each genotype. D, Targeted metabolite analysis. Silencing of the expression of *NaAGO8* significantly reduces the accumulation of nicotine, DTGs, and rutin in response to herbivore attack. Compromised levels of nicotine, HGL-DTGs, and rutin were validated in herbivore-fed leaves of ir*AGO8* plants, as compared with levels in the wild type. Values presented are means ± SE. All pairwise multiple comparison procedure values are as follows: nicotine (ANOVA, $F = 24.72$, $P \leq 0.001$), DTGs (ANOVA, $F = 8.921$, $P \leq 0.001$), and rutin (ANOVA, $F = 4.074$, $P \leq 0.05$). Asterisks indicate significant differences as follows: *, $P \leq 0.05$; **, $P \leq 0.01$; and ***, $P \leq 0.001$. FW, Fresh weight.

WRKY6 transcription factors and many JA biosynthetic pathway genes (of those tested, *MYC2*, *LOX3*, *AOS*, *AOC*, and *OPR3*) were reduced in OS-elicited ir*AGO8* lines (Supplemental Fig. S10). The modulatory action of the smRNA pathway on defense signaling is complex and not fully understood. Loss of such modulation in cells may result in the misregulation of gene expression networks, which could result in incoherent patterns of accumulation of mRNAs of genes of the JA signaling pathway.

In addition, abscisic acid (ABA) levels, which also are increased strongly by OS elicitation and herbivore attack in the wild type (Dinh et al., 2013), were reduced in ir*AGO8* lines, while SA and JA-Ile levels remained unchanged (Supplemental Fig. S9). Genes involved in ethylene production were either unchanged (*ACS3*) or reduced (*ACO3*) in ir*AGO8* lines as compared with the wild type after OS elicitation (Supplemental Fig. S10).

Taken together, these results are consistent with the hypothesis that *AGO8* has a regulatory role in inducing the biosynthesis of defense-responsive metabolites during herbivory. In a complex manner, *AGO8* appears to modulate several regulatory nodes in the pathway eliciting direct inducible defenses in *N. attenuata*, for example, by moderately regulating WRKY-mediated responses upstream of JA, by partially regulating phytohormone signaling, and by modulating the elicitation of MYB8-dependent gene networks downstream for secondary metabolism (Supplemental Fig. S11).

Structural Insights into Plausible Interactions of NaAGO8 with smRNA Substrates

Variability in residues at important sites (Fig. 1) may affect the structural conformations of NaAGOs during their interaction with a variety of smRNA substrates, which, in turn, may have implications for their functional specificities. To gain mechanistic insights into the functional diversity of the AGOs, we used a comparative structural analysis approach. By modeling the interactions of each NaAGO with two bona fide smRNA substrates (see "Materials and Methods"), we found significant differences (greater than 3 Å) among the three-dimensional structures of the substrate-bound NaAGOs (Fig. 9A, i). The structural conformation of NaAGO8 was significantly different (greater than 3 Å) than those of NaAGO4a, NaAGO7, and NaAGO10. We also found significant differences (3.97 Å) in the overall structure of NaAGO8 and AtAGO8. NaAGOs also showed diversity in surface area

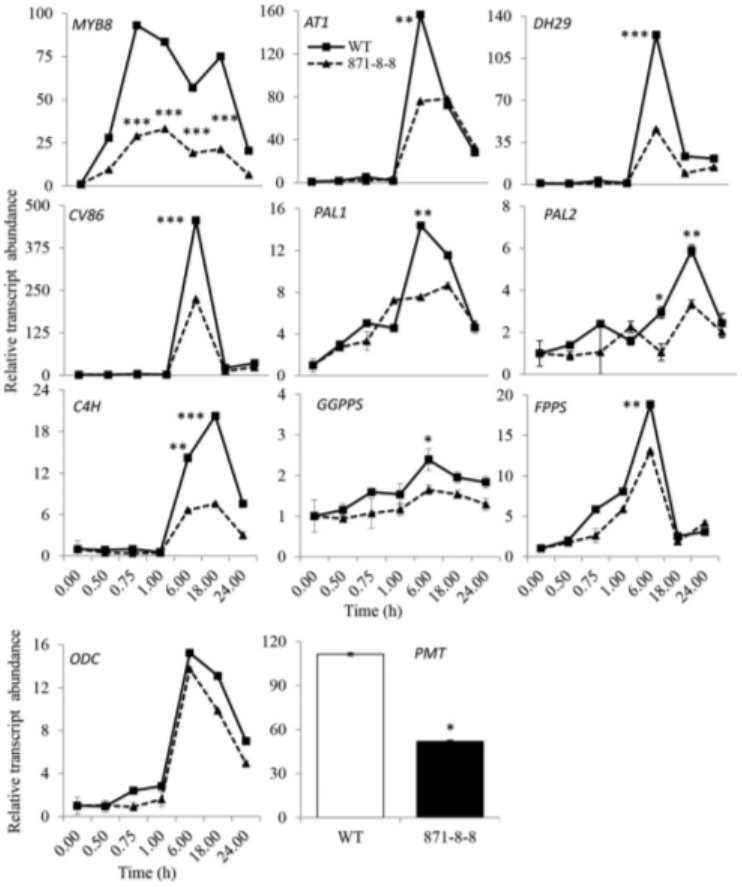

Figure 8. Silencing *AGO8* in *N. attenuata* perturbs the regulation of genes of the *MYB8*-dependent defense network and nicotine pathway in response to herbivore attack. Rosette leaves of the *N. attenuata* wild type (WT) and ir*AGO8* (871-8-8) were subjected to OS elicitation. Samples were collected at time intervals of 0, 0.5, 0.75, 1, 6, 18, and 24 h. Transcript abundance was determined for *MYB8* and key genes of phenolamide metabolism (*AT1*, *DH29*, and *CV86*), the phenylpropanoid pathway (*PAL1*, *PAL2*, and *C4H*), HGL-DTG biosynthesis (*GGPPS*), *FPPS*, and the nicotine biosynthesis pathway (*ODC* and *PMT*). *PMT* levels were evaluated in wild-type and ir*AGO8* genotypes 24 h after OS elicitation. Values are means ± pooled variances. Transcript levels in ir*AGO8* (873-5-2) were significantly different from those in the wild type in the time-course experiment (two-way repeated-measures ANOVA, Fisher's LSD: *, $P \leq 0.05$; **, $P \leq 0.01$; and ***, $P \leq 0.001$). Significant differences in *PMT* transcripts were evaluated with ANOVA: $F = 61.51$, $P \leq 0.05$ (*).

and volume of the largest binding pocket as well as in the properties of the largest positive electrostatic patches on the surface of the protein (Fig. 9A, ii). NaAGO8 possesses the largest area and volume of the binding pocket, whereas it contains the fewest residues in the predicted largest positive electrostatic patch (Fig. 9A, ii). Also, the distance between the nucleotides at the 5′ end of the RNA substrate and the interacting residues in the MID-PIWI lobe varied across the AGOs (Fig. 9B). For instance, the distance between the residue in the PIWI domain corresponding to MSA position 1,185 (Fig. 1C) and the first nucleotide at the 5′ end of the smRNA with which it interacts is 19.4 Å in NaAGO8, while it is 13.1 and 14.9 Å in NaAGO7 and NaAGO10, respectively (Fig. 9B). The physicochemical properties of the residue corresponding to MSA position 1,130 (Fig. 1C), which may interact directly with the second nucleotide at the 5′ end of the smRNA substrate, are different between NaAGO7 (Leu-894), NaAGO8 (Ile-803), and NaAGO10 (Gln-885; Fig. 9B). These findings suggest that the structural conformations of the smRNA-binding and catalytic domains of NaAGO8 differ from those of other NaAGOs and that these differences likely affect substrate and functional specificity. Differences in structural conformations of the smRNA-binding and catalytic domains of the AGOs may have arisen from varying evolutionary constraints on the important residues as well as due to their genetic correlations with residues in other positions (Singh et al., 2015). Revisiting our earlier study (Singh et al., 2015), we found that residue Glu-563 in the nucleotide specificity loop of the MID domain in NaAGO8 (corresponding to MSA position 870; Fig. 1C), which may interact directly with a nucleotide at the 5′ end of the smRNA (Fig. 9B, ii), is evolutionarily correlated with four other residues (Arg-564 and Ile-627 of the MID domain and Arg-850 and His-853 of the PIWI domain; Fig. 9C). We did not observe any such evolutionary correlations at corresponding positions in other NaAGOs.

Mapping of AGO8-Dependent miRNA-mRNA Interactions

Reprogramming of miRNAs as well as defense-related pathways indicated intensive interaction of AGO8-dependent miRNAs and the mRNAs of the disregualted

A(i)

	NaAGO1a	NaAGO2	NaAGO4a	NaAGO7	NaAGO8	NaAGO10
				4F3T:R		
NaAGO1a		2.65	**3.37**	**3.02**	2.68	**3.54**
NaAGO2	2.76		**3.59**	2.87	2.55	**3.08**
NaAGO4a	**3.41**	**3.62**		**3.79**	**3.60**	**4.16**
NaAGO7	**3.17**	2.81	**3.94**		**3.28**	2.58
NaAGO8	2.62	2.56	**3.58**	**3.25**		**3.55**
NaAGO10	**3.16**	**3.19**	**4.20**	2.63	**3.60**	
			4W5O:B			

(ii)

	Largest binding pocket on NaAGO-smRNA complex		Largest positive electrostatic patches on the NaAGO-smRNA complex	
	Area (Å^2)	Volume (Å^3)	Total number of residues	Total number of residues from MID-PIWI lobe
NaAGO1a	2904	6664	664	263
NaAGO2	4982	11827	475	163
NaAGO4a	4927	10851	402	128
NaAGO7	5566	13482	499	202
NaAGO8	8733	20619	396	121
NaAGO10	6491	16214	431	150

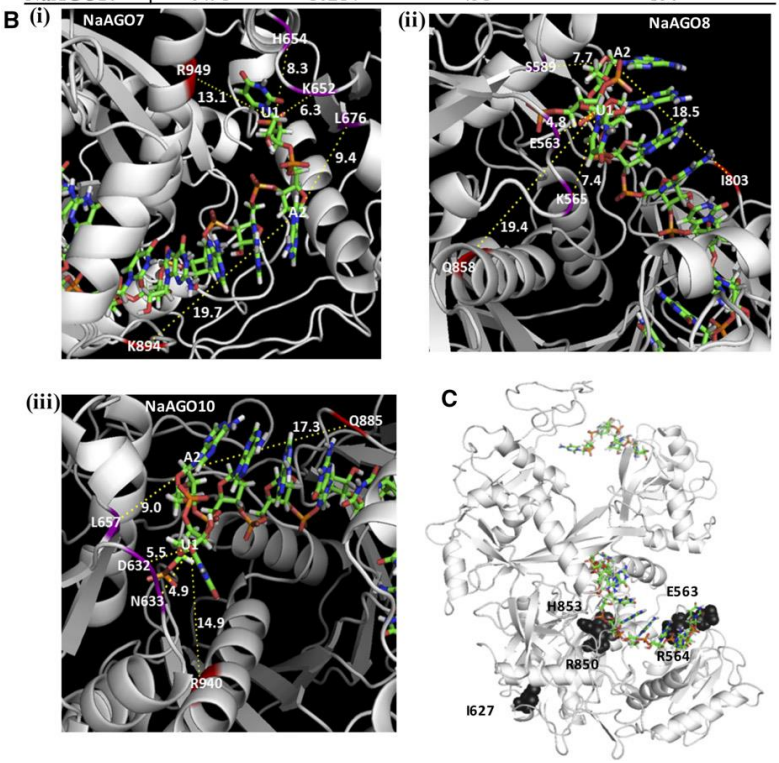

Figure 9. Structural analysis of the interaction of NaAGOs and the smRNAs provides mechanistic insights. A, Root mean square deviations (Å) between NaAGOs bound to smRNAs, 4F3T:R (top diagonal) and 4W5O:B (bottom diagonal), are shown in (i). Details of the largest binding pocket and the positive electrostatic patch on the surface among NaAGOs bound to smRNA, 4F3T:R, are shown in (ii). B, The modeled structures of NaAGO7 (i), NaAGO8 (ii), and NaAGO10 (iii) docked with smRNA (4F3T:R) show variation in the identities of interacting residues as well as the distance between 5′ nucleotide U1 and the interacting residues corresponding to MSA positions 872 and 877 of the MID domain and MSA position 1,185 of the PIWI domain (Fig. 1C). In NaAGO7, distances are 6.3, 8.3, and 13.1 Å; in NaAGO8, distances are 4.8, 7.4, and 19.4 Å; and in NaAGO10, distances are 5.5, 4.9, and 14.9 Å. Residues interacting with the second nucleotide (A2) of the smRNA substrate that differs in NaAGO7, NaAGO8, and NaAGO10 also are shown. C, The modeled structure of NaAGO8 shows residues coevolving only in NaAGO8.

genes. We generated miRNA-mRNA interaction networks by mapping of AGO8-dependent miRNA-binding sites into the mRNAs of the 18 differentially regulated genes of the defense-signaling pathway studied here. Twenty-six differentially changed miRNAs (between two genotypes at 0.75 and 18 h) showed binding to 18 genes (Supplemental Table S6). Of these 26 differentially expressed miRNAs, 16 may target differentially expressed genes at 0.75 h inversely. In other words, these miRNAs were up-regulated in ir*AGO8* at 0.75 h compared with the wild type, and their target genes were down-regulated in the same comparison, as shown in Figure 10A. miR1429-5p

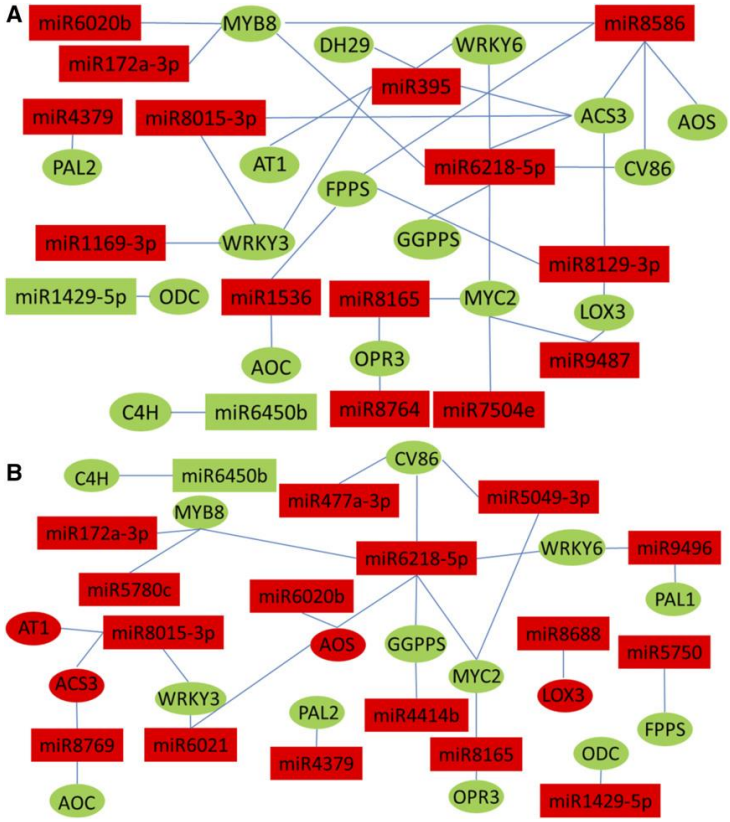

Figure 10. AGO8-dependent inversely related miRNA and their target genes are presented as networks. Differentially accumulated miRNAs in ir*AGO8* compared with the wild type at 0.75 and 18 h showed binding sites in genes involved in the defense-signaling pathway. A, Network representing inversely related differentially accumulated miRNAs in ir*AGO8* compared with the wild type and their target genes at 0.75 h. Fourteen miRNAs showed binding sites in more than one gene. B, Many-to-many miRNA-mRNA interactions are evident in the network. These miRNAs were differentially more accumulated in ir*AGO8* compared with the wild type at 18 h, whereas their target genes were down-regulated in the same comparison.

and miR6450b and their target genes, *ODC* and *C4H*, both were down-regulated in ir*AGO8* at 0.75 h. Similarly, we found that 16 differentially expressed miRNAs (not the same set) were up-regulated at 18 h in ir*AGO8* compared with the wild type and their target genes were down-regulated in the same comparison (Fig. 10B). miR6450b and its target gene, *C4H*, were down-regulated in ir*AGO8* at 18 h when compared with the wild type. For the majority of miRNAs, more than one gene has binding sites and was identified as a possible target. The miRNA-target interaction data set presented here (Fig. 10) gives a unique possibility to find the miRNA-mediated modulation of important biological processes, such as the *MYB8*-dependent defense network.

For example, differentially more accumulated miRNAs, in ir*AGO8* as compared with the wild type, such as miRNAs 395 (at 0.75 h), 6218-5p (at 0.75 and 18 h), 5049-3p (at 18 h), 477a-3p (at 18 h), and 8015-3p (at both 0.75 and 18 h), were predicted to target key genes of phenolamide metabolism that gets perturbed during herbivory attack (Fig. 10). Similarly, differentially more accumulated miRNAs in ir*AGO8* as compared with the wild type, miRNAs 8769 (at 18 h), 8015-3p (at both 0.75 and 18 h), 395 (at 0.75 h), 8586 (at 0.75 h), 8129-3p (at 0.75 h), 6218-5p (at both 0.75 and 18 h), 7504e (at 0.75 h), 8165 (at both 0.75 and 18 h), and 8764 (at 0.7 5h), targeted key genes in the JA signaling pathway and defense pathways such as nicotine biosynthesis, HGL-DTG biosynthesis, and phenylpropanoid and phenolamide metabolism, indicating that these also might be regulated by miRNAs.

DISCUSSION

Regulatory smRNAs modulate the complex responses of plants that are elicited during attack by insect herbivores (Pandey et al., 2008b). Yet, the central component of the RISC machinery, the AGOs, of the herbivore-induced smRNA pathway had remained unknown, and this was addressed in this investigation. Previously, we had shown that *RdR1* and *DCL3/4* mediate herbivore defense in *N. attenuata* (Pandey and Baldwin, 2007; Pandey et al., 2008b; Bozorov et al., 2012). Here, we advance this understanding and propose that, when plants are attacked, they recruit a specific pathway to elicit herbivory-induced smRNAs. The herbivore-induced precursor miRNAs and the RdR1-dependent precursors of other smRNAs are diced by DCL3/4 and loaded onto the RISC that may be largely composed of AGO8.

The silencing signal may further be amplified with the help of RdR1. These herbivory-induced smRNAs modulate defense responses by regulating the expression of genes related to signaling and defense directly or by regulating the expression of major transcription factors. This analysis suggests that the smRNA machinery has specialized components devoted to regulating complex herbivore responses. Further mechanistic insights related to this hypothesis may be tested by the AGO HITS-CLIP technique (Chi et al., 2009), which has been demonstrated to work with virus-cell culture interactions, but not yet with intact plants, and hence is beyond the scope of this article.

Comparative sequence and structure analyses of domains indicated conformational diversity, specifically in the smRNA-binding pocket. NaAGO8 has specific residues that may recognize smRNAs with different preferences. Indeed, the analysis of various domains of NaAGOs (Fig. 1, C and D) showed variability in the physicochemical properties of residues at functionally important sites. NaAGO8 has significantly different area and volume of the smRNA-binding pocket and the distribution of electrostatic patches that may help in recognizing/differentiating the incoming, herbivory-induced RNA substrate (as evident in Fig. 9). Specific biochemical studies with site-directed mutagenesis, and dedicated crystallization efforts using the herbivore-induced smRNAs as substrates, may further improve the mechanistic understanding of the specificity of AGO8.

In *N. attenuata*, an array of metabolites, including nicotine, phenolics, diterpenoids, and volatiles, are produced to counter herbivore attack at many different levels (Wu and Baldwin, 2010; Gaquerel et al., 2014). These induced defenses are largely downstream of JA (Halitschke and Baldwin, 2003). Interestingly, both in the OS-elicited and the caterpillar-fed leaf samples of *NaAGO8*-silenced lines, JA concentrations were partially reduced, which phenocopies the JA accumulations in attacked ir*RdR1* and ir*DCL4* (Pandey et al., 2008b; Bozorov et al., 2012). One of the most important defenses of *N. attenuata* is nicotine (Steppuhn et al., 2004), and in ir*AGO8* plants, nicotine levels are reduced significantly, a result likely explained by reduced transcript accumulations of *NaODC* and *NaPMT*, important genes in nicotine biosynthesis (Steppuhn et al., 2004). Again, lower nicotine levels of ir*AGO8* plants after herbivory phenocopy those of attacked ir*RdR1* and ir*DCL3*/ir*DCL4* plants (Pandey and Baldwin, 2007; Bozorov et al., 2012). Furthermore, ir*AGO8* plants accumulated very low levels of HGL-DTGs and phenylamine defense compounds. Abundant herbivore-induced HGL-DTGs, such as lyciumoside IV, attenoside/lyciumoside II, and malonylated nicotianoside Ia, accumulated little in ir*AGO8*, as evident from their VIP scores. Silencing *NaGGPPS*, which supplies geranylgeranyl diphosphates for the production of HGL-DTGs, significantly lowers the accumulation levels of HGL-DTGs (Jassbi et al., 2008; Heiling et al., 2010). Transcripts of two prenyltransferase genes, *NaGGPPS* and *NaFPPS*, were reduced significantly in response to *NaAGO8* silencing. These results are consistent with the hypothesis that the NaAGO8-dependent smRNA pathway modulates the biosynthesis of secondary metabolites required for herbivore defenses.

In *N. attenuata*, NaMYB8 is a key transcription factor that regulates the accumulation of major phenolamides, caffeoylputrescine and dicaffeoylspermidine, upon herbivore attack (Kaur et al., 2010; Onkokesung et al., 2012). The key biosynthetic genes of shikimate and polyamine metabolism are regulated in a MYB8-dependent manner (Kaur et al., 2010): *AT1* mediates caffeoylputrescine biosynthesis, while *DH29* and *CV86* mediate the dicaffeoylspermidine biosynthesis (Supplemental Fig. S10; Onkokesung et al., 2012). Silencing *NaAGO8* reduces the accumulation of transcripts of these key downstream genes, which is consistent with the observed reduced levels of *MYB8* and the increased susceptibility of ir*AGO8* plants to herbivores.

It is often observed that herbivore-induced defense signaling results in a positive feedback on the expression of genes of the signaling pathway. A classical example of such a feedback is commonly seen in the JA signaling pathway itself, where W+OS treatment results in a rapid increase of JA and JA-Ile within 15 to 30 min, whereas the maximum transcript levels are observed after 45 min to 1 h (Halitschke and Baldwin, 2003; Paschold et al., 2008; Gulati et al., 2013; Hettenhausen et al., 2013). As AGO8 is downstream in the smRNA pathway, it is plausible that basal levels of AGO8 may be sufficient to bind to herbivory-induced smRNAs that may help in overcoming the suppression of defense signaling under basal conditions. We also noticed that several miRNAs were repressed after OS elicitation in wild-type plants. We postulate that such down-regulation of miRNAs may help in eliciting defense signaling in the wild type (such reprograming is altered in ir*AGO8* plants). Once the defense signaling is induced (resulting in active biosynthesis of, for example, MYB8-dependent defenses as well as nicotine), signals may exert a positive feedback for further modulation and fine-tuning of expression levels. Additionally, an initial suppression of *AGO8* transcript may result in additive induction of positive regulators of the defense-signaling network. It is evident that the smRNA-mediated regulation of defense signaling is highly complex and may exert roles that are modulatory in nature to optimize the induction of costly defense responses.

Because of the negative regulatory nature of the AGO-mediated RISC, and the complex nature of defense signaling, we also postulate the presence of negative regulators or suppressors of defense-signaling responses. It is plausible that, under constitutive conditions (absence of herbivore attack), such a suppressor(s) of defense signaling is expressed in the cells to prevent the synthesis of costly defense responses. During herbivore attack, plants reprogram their smRNome profiles (Figs. 5 and 6), and AGO8-dependent RISC may target such repressors of defense signaling, leading to the induction of defense responses, which are largely regulated by the MYB8 transcription factor.

In conclusion, we propose that AGO8, DCL3/4, and RdR1 participate in the herbivore-induced smRNA

pathway to modulate the reprogramming of plant defenses in *N. attenuata*. Plants have diverse populations of smRNAs that are recruited differentially in response to various biotic and abiotic stress conditions and have specific regulatory roles to combat these stresses (Pandey and Baldwin, 2008; Pandey et al., 2008a, 2008b; Khraiwesh et al., 2012; Kruszka et al., 2012). Herbivore attack results in changes in expression of smRNAs that are produced in an RdR1- and DCL3/4-dependent manner. These smRNAs may be channeled to modulate targets specific to herbivore resistance in an AGO8-dependent manner. In the 11 *AGOs* of *N. attenuata* (Singh et al., 2015), the functionally important nucleotide specificity loop between the MID and PIWI domains shows diversity (Fig. 1; Supplemental Fig. S1), as do the largest binding pocket and the positive electrostatic patch involved in interaction with substrate RNAs (Fig. 9). Importantly, positions in the MID and PIWI domains (Figs. 1 and 9), which are thought to be involved in the interaction and stabilization of smRNA, have residues that differ in their physicochemical properties in NaAGO8 and may help AGO8 in sorting and recruiting smRNAs that are specific to herbivore resistance processes.

MATERIALS AND METHODS

Plant Growth

Seeds of the 31st inbred generation of *Nicotiana attenuata*, originally collected from the native population in Utah, were used. Seeds from wild-type and transformed plants were germinated, and plant populations were grown under a day/night cycle of 16 h (26°C–28°C)/8 h (22°C–24°C) as described earlier (Krügel et al., 2002; Halitschke and Baldwin, 2003; Onkokesung et al., 2012).

Sequence Characterization of *N. attenuata* AGOs

The recently reported 11 *N. attenuata* AGOs (Singh et al., 2015) were aligned, and distance values were calculated with 1,000 bootstrap replicates. Various domains in NaAGOs were annotated by performing a comparative sequence analysis of NaAGOs against the two well-studied eukaryotic AGOs whose structures have been solved: HsAGO2 (PDB code 4F3T; Elkayam et al., 2012) and KpAGO (PDB code 4F1N [model for yeast AGO]; Nakanishi et al., 2012). The NaAGO sequences were then subjected to the conserved domain search tool (http://www.ncbi.nlm.nih.gov/Structure/cdd/wrpsb.cgi; Marchler-Bauer et al., 2011). MSA and neighbor-joining phylogeny of NaAGOs was performed with the help of ClustalX 2.1 (Larkin et al., 2007) and MEGA 5.2 (Tamura et al., 2011), respectively. WebLogo 3 (Crooks et al., 2004) was used to display the position-specific residues at the functionally important sites.

Transcript Accumulation by Quantitative Real-Time PCR

To determine the changes in transcript accumulation of *AGOs* in leaves and roots after herbivore attack, the leaves of three to four replicates of sand-grown rosette-stage *N. attenuata* plants were wounded with a fabric pattern wheel, and the punctured wounds were immediately treated with 20 μL of W+OS. Leaves and roots were harvested at 0.25, 0.5, 0.75, 1, 1.5, 2, 3, 4, 6, 12, 14, 18, 26, 36, and 50 h after elicitation (Bozorov et al., 2012). Total RNA was isolated using the TRIZOL method, and DNA traces were removed with DNase I (DNA-free kit; Ambion).

To analyze the transcript accumulation of genes of phytohormone signaling and defense pathways, time-course experiments were conducted. Fully expanded rosette leaf samples were harvested at 0, 0.5, 0.75, 1, 6, 18, and 24 h after W+OS elicitation of wild-type and *AGO8*-silenced (ir*AGO8*) lines. All samples were obtained from four independent biological replicates for each time point, genotype, and treatment.

cDNA synthesis (SuperScript II Reverse Transcriptase; Invitrogen) and qPCR (qPCR Core Kit for SYBR Green I; Eurogentec) were done following each manufacturer's protocol. qPCR assays were performed using gene-specific primers (designed with the help of Primer Express software version 3.0.1; http://www.appliedbiosystems.com) on cDNA corresponding to 100 ng of total RNA before transcription (Supplemental Table S7). The *N. attenuata* sulfite reductase (*ECI*), a housekeeping gene, was used as an endogenous reference (Bubner et al., 2004). The $2^{-\Delta\Delta CT}$ method was used for data analysis. For data interpretation, the expression level in control plants (time 0) was fixed to 1, and relative expression levels for other time points were calculated with respect to this reference value (Bubner et al., 2004; Pandey and Baldwin, 2007; Bozorov et al., 2012).

Generation and Characterization of Stable Transgenic Lines Silenced for *AGO* Expression

Partial cDNA fragments of *NaAGO1* (common to *AGO1a*, *AGO1b*, and *AGO1c*), *NaAGO2*, *NaAGO4* (common to *AGO4a* and *AGO4b*), *NaAGO5*, *NaAGO7*, *NaAGO8*, and *NaAGO10* were inserted into a derivative of pRESC800 (GenBank accession no. JQ354897) binary transformation vector backbone as inverted repeats as described earlier (Steppuhn et al., 2004). Primers for cloning are indicated in Supplemental Table S7. Wild-type *N. attenuata* plants from the 31st inbred generation were used for *Agrobacterium tumefaciens*-mediated plant transformation (Krügel et al., 2002; Gase et al., 2011). In the subsequent T1 generation, plants were tested for homozygocity by segregation analysis. Characterization of stable transformants and screening of individual transgenic lines were conducted as described earlier (Gase et al., 2011). Transgenic lines with complete T-DNA insertions were tested for homozygosity through the T2 generation. Transgenic seeds were germinated on agar plates containing 35 mg L^{-1} hygromycin B. Ten healthy seeds of each transgenic (T1) line were inbred through the T2 generation to obtain homozygous lines. Complete T-DNA insertion was determined by diagnostic PCR (Gase et al., 2011). Total genomic DNA was isolated by a modified cetyl-trimethyl-ammonium bromide method (Bubner et al., 2004). Positive lines with complete insertion of T-DNA were assayed further to determine single insertion by using Southern hybridization (Bubner et al., 2004), which was performed as described earlier using a ^{32}P-labeled fragment of the *hptII* gene as a probe (Jassbi et al., 2008). Seven micrograms of genomic DNA, digested with *Xba*I and *Eco*RV (New England Biolabs), was blotted onto a nylon membrane (Gene-ScreenPlus; PerkinElmer) according to the manufacturer's protocol. Homozygous T2 plants with single T-DNA insertions were used for further experiments. To determine the silencing efficiency of the transgenic lines, plants were grown in a controlled environment in a glasshouse as described above. At fully expanded rosette stage, leaves were W+OS elicited, and leaf samples were collected after 18 h. Transcript abundance was measured to determine the silencing efficiency using qPCR assays as described above. The silencing efficiency of *AGO8* in ir*AGO8* lines was determined by qPCR assays, both before elicitation (basal levels; Supplemental Fig. S4C) as well as after simulated herbivory (Fig. 3). Possibilities of off-target effects in the *N. attenuata* genome were evaluated by exposing the *AGO8* silencing sequence (inverted repeat sequence present in the pRESC8*AGO8* construct) to both the SGN VIGS tool (Fernandez-Pozo et al., 2015) and a BLAST search against the complete transcriptome of *N. attenuata*. The only identical stretch longer than 19 bp in the entire transcriptome was a 22-nucleotide fragment from the xylem Cys proteinase1-like transcript (*XCP1*). This single short stretch is less likely to cause significant silencing in off-target effects; furthermore, the xylem *XCP1* is not involved in the herbivore defense response (Thomas et al., 2001; Gulati et al., 2013; Zhirnov et al., 2015). Still, to completely rule out any off-target effects, we evaluated the transcript levels of *XCP1*: no differences in levels were recorded between the wild-type and ir*AGO8* genotypes (Supplemental Fig. S5). Thus, it is safe to conclude that silencing of *AGO8* did not generate any off-target effects in ir*AGO8* plants.

Herbivore Performance Assay

Manduca sexta performance assays were conducted on stably transformed lines as described earlier (Pandey and Baldwin, 2007; Oh et al., 2013). Fifteen to 25 replicates from each ir*AGO* genotype and wild type were used. Plants were grown in a glasshouse as described above in a completely randomized design. Neonates were placed on the lower surface of the +2 leaf of rosette stage plants, and larvae were allowed to feed for 11 to 13 d. Caterpillar biomass was recorded every 2 to 3 d. Caterpillar performance on ir*AGO8* lines was verified in an independent biological experiment with a similar setup.

Evaluation of the *AGO8*-Dependent smRNome

In order to evaluate the expression and composition of *AGO8*-dependent smRNAs, deep sequencing was performed in triplicates on +2 leaf samples of

rosette stage wild-type and ir*AGO8* plants before (0 h) as well as 0.75 and 18 h after OS elicitation. Clean reads were populated after filtering out low-quality reads such as reads with N (unidentified nucleotides) as well as reads with single nucleotide stretches of more than five nucleotides, trimming the adaptors, and discarding reads with short stretches of six nucleotides; clean reads in the range of 15 to 30 nucleotides were finally retained (Pandey et al., 2008b). Next, the structural RNAs, such as tRNA, rRNA, snoRNA, and snRNA, were annotated (and removed) by aligning the clean reads to the Rfam 11.0 database (ftp://ftp.sanger.ac.uk/pub/databases/Rfam). Reads mapped to the *N. attenuata* transcriptome were discarded using bowtie with the -norc parameter (no reverse complement; Langmead et al., 2009). For the remaining reads, replicates were merged for each condition/time point, and reads present in at least two of the three replicates were retained for further analysis. These are referred to as miRNA-mappable reads. These were aligned to the *N. attenuata* genome sequence using bowtie with a maximum of two mismatches. Conserved miRNAs were identified using the mirDeep2 software version 2.0.0 (Friedländer et al., 2012) with default parameters and Viridiplantae miRNAs deposited in miRBase 21.0 (www.mirbase.org). Sequences with perfect matches to known miRNAs were regarded as bona fide conserved miRNAs. Furthermore, counts were normalized using RPM. Median values were calculated, and differential accumulation of miRNAs and other smRNAs was evaluated using the χ^2 test with a stringent $P \leq 0.05$ after Benjamini-Hochberg multiple correction (Benjamini and Hochberg, 1995). Reads with counts greater than 2 in at least one comparison were considered for this analysis.

Differential Expression of miRNAs

The raw counts for each miRNA, both conserved and novel, were normalized using the RPM method (Jia et al., 2014). To evaluate the expression of conserved and novel miRNAs between the two genotypes and at the three time points, pairwise comparison was performed on the RPM value for each miRNA. Furthermore, to identify significantly differentially expressed miRNAs, χ^2 (Li et al., 2016) was performed and $P < 0.05$ was set as the cutoff.

Untargeted Metabolomic Analysis

A total of 100 mg of leaf tissue was homogenized to fine powder with a GenoGrinder (SPEX SamplePrep), and 1 mL of extraction buffer (40% methanol/water and 50 mM acetate buffer, pH 4.8) was added and mixed well. The samples were centrifuged at 16,100*g* for 20 min at 4°C, and the supernatant were transferred to a new 1.5-mL microcentrifuge tube (Eppendorf); samples were recentrifuged, and the supernatant was transferred carefully into glass vials. The samples were injected into a C18 Acclaim column (2.2-μm particle size, 150 × 2.1 mm i.d.; Dionex) and separated using an RSLC system (Dionex). As mobile phase, solvent A (0.1% [v/v] acetonitrile and 0.05% [v/v] formic acid in deionized water) and solvent B (acetonitrile and 0.05% [v/v] formic acid) were used with the following gradient conditions: 0 to 0.5 min, 10% B; 0.5 to 6.5 min, linear gradient to 80% B; 6.5 to 10 min, 80% B; and reequilibration at 10% B for 3 min with a flow rate of 300 μL min^{-1}. A MicroToF mass spectrometer (Bruker Daltonics) coupled with an electrospray ionization source in positive ion mode was used to detect the eluted compounds with the following settings: capillary voltage, 4,500 V; capillary exit, 130 V; dry gas temperature, 200°C; dry gas flow, 8 L min^{-1}. Mass calibration was done with the help of sodium formate clusters (10 mM solution of NaOH in 50%:50% [v/v] isopropanol:water containing 0.2% formic acid). The Data Analysis version 4.0 software (Bruker Daltonics) was used to convert raw data files to netCDF format and processed using the XCMS package and the R package CAMERA (http://www.bioconductor.org/biocLite.R). The Metaboanalyst software (Xia et al., 2009; Xia and Wishart, 2011) was used to perform multivariate analysis. The data were filtered using coefficient of variation, and Pareto scaling was used for normalization (Xia et al., 2009; Gaquerel et al., 2010). Insilico viewer was used to view the peaks.

Targeted Secondary Metabolite Analysis

Approximately 100 mg of frozen leaf tissue was ground to a fine powder and homogenized with extraction buffer (40% methanol with acetate buffer [4:6], 10 μL mg^{-1} tissue) in a GenoGrinder for 1 min at 1,200 strokes min^{-1}. The samples were centrifuged at 16,100*g* for 20 min at 4°C, and the supernatants were carefully transferred into new 1.5-mL tubes, recentrifuged to remove any particles, transferred into 1.5-mL glass vials, and analyzed by ultra-HPLC as described previously (Keinänen et al., 2001; Jassbi et al., 2008). One microliter of the sample was injected into a Chromolith Fast Gradient (RP18e, 50 × 2 mm; Merck) column connected to a precolumn (Gemini NX RP18, 3 μm, 2 × 4.6 mm). As mobile phase, solvent A (0.1% formic acid and 0.1% ammonium hydroxide solution in water) and solvent B (methanol) were used in a gradient mode with the following conditions: 0% B for 0.5 min; to 80% B in 6.5 min; and isocratic for 3 min with a flow rate of 0.8 mL min^{-1}. External standard calibration was done with a dilution series of nicotine, chlorogenic acid, and rutin in 40% methanol, and samples were normalized by gram fresh weight. Secondary metabolites were detected on diode array detector channels (260, 254, 210, 320, and 360 nm; ELS1A) and data were analyzed using Chrom software. Representative runs of standards are presented in Supplemental Figure S8.

Phytohormone Extraction

For the analysis of phytohormones (JA, JA-Ile, ABA, and SA), ~100 mg of frozen, fine-powdered leaf tissue was homogenized with 1 mL of extraction buffer (ethyl acetate containing 2 μL of the internal standard mix [D_2-dihydro-JA and D_5-JA, 50 ng μL^{-1}; D_6-ABA, D_4-SA, and $^{13}C_6$-JA-Ile, 10 ng μL^{-1}]) in a GenoGrinder for 1 min at 1,200 strokes min^{-1}. Samples were centrifuged at 16,100*g* for 20 min at 4°C, and the supernatant was transferred into fresh 2-mL microcentrifuge tubes. To the residue, 0.5 mL of ethyl acetate (without internal standards) was added and ground using a GenoGrinder for 1 min at 1,200 strokes min^{-1} (setting: 1× at 200). After centrifugation of samples at 16,100*g* for 20 min at 4°C, the supernatants were pooled. The samples were placed in a vacuum concentrator (Speed-Vac) at a temperature of 30°C, and the dried residues were dissolved in 0.5 mL of 70% (v/v) methanol for analysis on a liquid chromatography-electrospray ionization-tandem mass spectrometry instrument (1200 Triple-Quadrupole-LC-MS system; Varian) as described previously (Oh et al., 2012). The samples were injected in a ProntoSIL column (C18-ace-EPS, 50 × 2 mm, 5 μm, 120 Å; Bischoff) connected to a precolumn (C18, 4 × 2 mm; Phenomenex). Gradient mode was used with mobile phases 0.05% formic acid and 0.1% acetonitrile in water (solvent A) and methanol (solvent B) with the following conditions (time/%B/flow [mL min^{-1}]): 0/15/0.4, 1/15/0.4, 1.5/15/0.2, 2.5/15/0.2, and 4.5/98/0.2. Compounds were detected in the electrospray ionization negative mode with the help of the multiple reaction monitoring method (Bonaventure et al., 2011).

Structural Analysis

HMM profile-based homology modeling of structure was used to predict the secondary structure of NaAGOs using the HHpred server (http://toolkit.tuebingen.mpg.de/hhpred/; Söding et al., 2005). NaAGO peptide sequences were used as input in the HHpred server to search similarities in secondary structure with default parameters. HHpred produces pairwise query-template alignment to generate HMM profiles that search through various databases, such as PDB, SCOP, Pfam, SMART, COGs, and CDD. The final three-dimensional structural models were calculated by MODELER. The ClusPro server (https://cluspro.bu.edu/login.php; Comeau et al., 2004) was used for the docking of smRNAs (PDB codes 4F3T:R and 4W5O:B) with each of the modeled NaAGOs, and their potential energies were calculated. These two smRNAs are bona fide substrates for AGOs and have been used widely in crystallographic studies (Elkayam et al., 2012; Schirle et al., 2014). Root mean square deviations (Å) between NaAGOs were calculated using the TMalign server (http://zhanglab.ccmb.med.umich.edu/TM-align/; Zhang and Skolnick, 2005). The area and volume of the largest binding pocket on the each docked NaAGO were calculated using the CASTp server (http://sts.bioe.uic.edu/castp/calculation.php; Dundas et al., 2006). CASTp uses the weighted Delaunay triangulation and the alpha complex to measure the area and volume of solvent-accessible structural pockets and cavities (Dundas et al., 2006). The distribution of positive electrostatic patches on the surface of docked NaAGOs was computed using the Patch Finder plus server (http://pfp.technion.ac.il/index.html; Shazman et al., 2007). Using the Poisson Boltzmann equation, it first calculates the electrostatic potential (using APBS software) of the protein on a three-dimensional grid and then extracts all the three-dimensional patches of adjacent grid points that meet the defined cutoff of 2kT/e. PyMOL (DeLano, 2002) was used for the visualization and figure preparation of the modeled structures.

Target Prediction and Mapping of miRNAs on mRNAs

With the aim to better understand the biological role of conserved and AGO8-specific miRNAs, we searched for putative binding sites and identified miRNAs

in the sequences of previously reported genes that are involved in defense mechanisms against herbivory attack. We adopted approaches used previously (Pandey et al., 2008b) for binding site identification.

Statistical Analysis

Data were analyzed using StatView software. Caterpillar assay, phytohormone, secondary metabolite, and gene expression data were analyzed by ANOVA (repeated measures wherever applicable) at a significance level of $P \leq 0.05$.

Accession Numbers

The smRNA sequencing data have been deposited in the National Center for Biotechnology Information under accession number PRJNA335958.

Supplemental Data

The following supplemental materials are available.

Supplemental Figure S1. MSA of NaAGOs corresponding to Figure 1A, and phylogenetic tree of Arabidopsis AGOs.

Supplemental Figure S2. Transcript abundance of *NaAGOs* in roots in a time-course experiment.

Supplemental Figure S3. Complete southern blots of all the transgenic genotypes.

Supplemental Figure S4. Silencing of *AGO8* expression does not affect the development and growth of *N. attenuata*.

Supplemental Figure S5. Evaluation of the silencing efficiency of nine *NaAGOs* and *XCP1* in ir*AGO8* samples.

Supplemental Figure S6. Validation of the susceptibility of ir*AGO8* plants to herbivore attack.

Supplemental Figure S7. DEMs in the wild type and ir*AGO8*.

Supplemental Figure S8. Chromatograms of the standards used for targeted analysis of nicotine, DTGs, and rutin.

Supplemental Figure S9. Evaluation of phytohormones in the wild type and ir*AGO8* upon herbivory attack.

Supplemental Figure S10. Dynamics of transcript accumulation in phytohormone signaling genes in response to herbivory.

Supplemental Figure S11. Simplified scheme for the synthesis of major components of defense-related metabolites in *N. attenuata*.

Supplemental Table S1. Conserved and predicted novel miRNAs identified in the wild type and ir*AGO8* across the three time points: 0, 0.75, and 18 h.

Supplemental Table S2. Mature miRNAs conserved to other species when mapped against 72 plant species in miRBase.

Supplemental Table S3. Accumulation of miRNAs at each time point (0, 0.75, and 18 h) for ir*AGO8* and the wild type.

Supplemental Table S4. DEMs for ir*AGO8* and the wild type.

Supplemental Table S5. Differentially accumulated metabolites on silencing *NaAGO8*.

Supplemental Table S6. DEMs showed binding sites in defense-signaling pathway genes.

Supplemental Table S7. List of primers used in this study.

ACKNOWLEDGMENTS

We thank Mario Kallenbach, Sven Heiling, Depeng Li, Wibke Kröber, Antje Wissgott, and Tamara Krügel along with the greenhouse team, Department of Molecular Ecology, Max Planck Institute for Chemical Ecology, for technical help and support in growing plants in the glasshouse.

Received May 31, 2017; accepted August 11, 2017; published August 15, 2017.

LITERATURE CITED

Axtell MJ (2013) Classification and comparison of small RNAs from plants. Annu Rev Plant Biol **64:** 137–159

Baumberger N, Baulcombe DC (2005) *Arabidopsis* ARGONAUTE1 is an RNA Slicer that selectively recruits microRNAs and short interfering RNAs. Proc Natl Acad Sci USA **102:** 11928–11933

Benjamini Y, Hochberg Y (1995) Controlling the false discovery rate: a practical and powerful approach to multiple testing. J R Stat Soc Ser B Methodological **57:** 289–300

Bonaventure G, Schuck S, Baldwin IT (2011) Revealing complexity and specificity in the activation of lipase-mediated oxylipin biosynthesis: a specific role of the *Nicotiana attenuata* GLA1 lipase in the activation of jasmonic acid biosynthesis in leaves and roots. Plant Cell Environ **34:** 1507–1520

Borges F, Martienssen RA (2015) The expanding world of small RNAs in plants. Nat Rev Mol Cell Biol **16:** 727–741

Borsani O, Zhu J, Verslues PE, Sunkar R, Zhu JK (2005) Endogenous siRNAs derived from a pair of natural cis-antisense transcripts regulate salt tolerance in Arabidopsis. Cell **123:** 1279–1291

Bouché N, Lauressergues D, Gasciolli V, Vaucheret H (2006) An antagonistic function for Arabidopsis DCL2 in development and a new function for DCL4 in generating viral siRNAs. EMBO J **25:** 3347–3356

Bozorov TA, Pandey SP, Dinh ST, Kim SG, Heinrich M, Gase K, Baldwin IT (2012) DICER-like proteins and their role in plant-herbivore interactions in *Nicotiana attenuata*. J Integr Plant Biol **54:** 189–206

Brodersen P, Sakvarelidze-Achard L, Bruun-Rasmussen M, Dunoyer P, Yamamoto YY, Sieburth L, Voinnet O (2008) Widespread translational inhibition by plant miRNAs and siRNAs. Science **320:** 1185–1190

Brodersen P, Voinnet O (2006) The diversity of RNA silencing pathways in plants. Trends Genet **22:** 268–280

Bubner B, Gase K, Baldwin IT (2004) Two-fold differences are the detection limit for determining transgene copy numbers in plants by real-time PCR. BMC Biotechnol **4:** 14

Chi SW, Zang JB, Mele A, Darnell RB (2009) Argonaute HITS-CLIP decodes microRNA-mRNA interaction maps. Nature **460:** 479–486

Comeau SR, Gatchell DW, Vajda S, Camacho CJ (2004) ClusPro: an automated docking and discrimination method for the prediction of protein complexes. Bioinformatics **20:** 45–50

Crooks GE, Hon G, Chandonia JM, Brenner SE (2004) WebLogo: a sequence logo generator. Genome Res **14:** 1188–1190

DeLano WL (2002) The PyMOL Molecular Graphics System. DeLano Scientific, San Carlos, CA

Dinh ST, Baldwin IT, Galis I (2013) The HERBIVORE ELICITOR-REGULATED1 gene enhances abscisic acid levels and defenses against herbivores in *Nicotiana attenuata* plants. Plant Physiol **162:** 2106–2124

Dundas J, Ouyang Z, Tseng J, Binkowski A, Turpaz Y, Liang J (2006) CASTp: computed atlas of surface topography of proteins with structural and topographical mapping of functionally annotated residues. Nucleic Acids Res **34:** W116–W118

Elkayam E, Kuhn CD, Tocilj A, Haase AD, Greene EM, Hannon GJ, Joshua-Tor L (2012) The structure of human argonaute-2 in complex with miR-20a. Cell **150:** 100–110

Fernandez-Pozo N, Rosli HG, Martin GB, Mueller LA (2015) The SGN VIGS tool: user-friendly software to design virus-induced gene silencing (VIGS) constructs for functional genomics. Mol Plant **8:** 486–488

Friedländer MR, Mackowiak SD, Li N, Chen W, Rajewsky N (2012) miRDeep2 accurately identifies known and hundreds of novel microRNA genes in seven animal clades. Nucleic Acids Res **40:** 37–52

Gaquerel E, Gulati J, Baldwin IT (2014) Revealing insect herbivory-induced phenolamide metabolism: from single genes to metabolic network plasticity analysis. Plant J **79:** 679–692

Gaquerel E, Heiling S, Schoettner M, Zurek G, Baldwin IT (2010) Development and validation of a liquid chromatography-electrospray ionization-time-of-flight mass spectrometry method for induced changes in *Nicotiana attenuata* leaves during simulated herbivory. J Agric Food Chem **58:** 9418–9427

Gase K, Weinhold A, Bozorov T, Schuck S, Baldwin IT (2011) Efficient screening of transgenic plant lines for ecological research. Mol Ecol Resour **11:** 890–902

Gulati J, Kim SG, Baldwin IT, Gaquerel E (2013) Deciphering herbivory-induced gene-to-metabolite dynamics in Nicotiana attenuata tissues using a multifactorial approach. Plant Physiol **162:** 1042–1059

Halitschke R, Baldwin IT (2003) Antisense LOX expression increases herbivore performance by decreasing defense responses and inhibiting growth-related transcriptional reorganization in *Nicotiana attenuata*. Plant J **36:** 794–807

Halitschke R, Schittko U, Pohnert G, Boland W, Baldwin IT (2001) Molecular interactions between the specialist herbivore *Manduca sexta* (Lepidoptera, Sphingidae) and its natural host *Nicotiana attenuata*. III. Fatty acid-amino acid conjugates in herbivore oral secretions are necessary and sufficient for herbivore-specific plant responses. Plant Physiol **125:** 711–717

Havecker ER, Wallbridge LM, Hardcastle TJ, Bush MS, Kelly KA, Dunn RM, Schwach F, Doonan JH, Baulcombe DC (2010) The *Arabidopsis* RNA-directed DNA methylation argonautes functionally diverge based on their expression and interaction with target loci. Plant Cell **22:** 321–334

Heiling S, Schuman MC, Schoettner M, Mukerjee P, Berger B, Schneider B, Jassbi AR, Baldwin IT (2010) Jasmonate and ppHsystemin regulate key malonylation steps in the biosynthesis of 17-hydroxygeranyllinalool diterpene glycosides, an abundant and effective direct defense against herbivores in *Nicotiana attenuata*. Plant Cell **22:** 273–292

Hettenhausen C, Baldwin IT, Wu J (2013) *Nicotiana attenuata* MPK4 suppresses a novel jasmonic acid (JA) signaling-independent defense pathway against the specialist insect Manduca sexta, but is not required for the resistance to the generalist *Spodoptera littoralis*. New Phytol **199:** 787–799

Höck J, Meister G (2008) The Argonaute protein family. Genome Biol **9:** 210

Howe GA, Jander G (2008) Plant immunity to insect herbivores. Annu Rev Plant Biol **59:** 41–66

Hutvagner G, Simard MJ (2008) Argonaute proteins: key players in RNA silencing. Nat Rev Mol Cell Biol **9:** 22–32

Jassbi AR, Gase K, Hettenhausen C, Schmidt A, Baldwin IT (2008) Silencing geranylgeranyl diphosphate synthase in *Nicotiana attenuata* dramatically impairs resistance to tobacco hornworm. Plant Physiol **146:** 974–986

Jia L, Zhang D, Qi X, Ma B, Xiang Z, He N (2014) Identification of the conserved and novel miRNAs in mulberry by high-throughput sequencing. PLoS ONE **9:** e104409

Jones-Rhoades MW, Bartel DP, Bartel B (2006) MicroRNAS and their regulatory roles in plants. Annu Rev Plant Biol **57:** 19–53

Kaur H, Heinzel N, Schöttner M, Baldwin IT, Gális I (2010) R2R3-*NaMYB8* regulates the accumulation of phenylpropanoid-polyamine conjugates, which are essential for local and systemic defense against insect herbivores in *Nicotiana attenuata*. Plant Physiol **152:** 1731–1747

Keinänen M, Oldham NJ, Baldwin IT (2001) Rapid HPLC screening of jasmonate-induced increases in tobacco alkaloids, phenolics, and diterpene glycosides in *Nicotiana attenuata*. J Agric Food Chem **49:** 3553–3558

Khraiwesh B, Zhu JK, Zhu J (2012) Role of miRNAs and siRNAs in biotic and abiotic stress responses of plants. Biochim Biophys Acta **1819:** 137–148

Krügel T, Lim M, Gase K, Halitschke R, Baldwin IT (2002) *Agrobacterium*-mediated transformation of *Nicotiana attenuata*, a model ecological expression system. Chemoecology **12:** 177–183

Kruszka K, Pieczynski M, Windels D, Bielewicz D, Jarmolowski A, Szweykowska-Kulinska Z, Vazquez F (2012) Role of microRNAs and other sRNAs of plants in their changing environments. J Plant Physiol **169:** 1664–1672

Langmead B, Trapnell C, Pop M, Salzberg SL (2009) Ultrafast and memory-efficient alignment of short DNA sequences to the human genome. Genome Biol **10:** R25

Larkin MA, Blackshields G, Brown NP, Chenna R, McGettigan PA, McWilliam H, Valentin F, Wallace IM, Wilm A, Lopez R, et al (2007) Clustal W and Clustal X version 2.0. Bioinformatics **23:** 2947–2948

Li X, Shahid MQ, Wu J, Wang L, Liu X, Lu Y (2016) Comparative small RNA analysis of pollen development in autotetraploid and diploid rice. Int J Mol Sci **17:** 499

Liu X, Williams CE, Nemacheck JA, Wang H, Subramanyam S, Zheng C, Chen MS (2010) Reactive oxygen species are involved in plant defense against a gall midge. Plant Physiol **152:** 985–999

Ma X, Kim EJ, Kook I, Ma F, Voshall A, Moriyama E, Cerutti H (2013) Small interfering RNA-mediated translation repression alters ribosome sensitivity to inhibition by cycloheximide in *Chlamydomonas reinhardtii*. Plant Cell **25:** 985–998

Maffei ME, Mithöfer A, Boland W (2007) Before gene expression: early events in plant-insect interaction. Trends Plant Sci **12:** 310–316

Mallory A, Vaucheret H (2010) Form, function, and regulation of ARGONAUTE proteins. Plant Cell **22:** 3879–3889

Mallory AC, Hinze A, Tucker MR, Bouché N, Gasciolli V, Elmayan T, Lauressergues D, Jauvion V, Vaucheret H, Laux T (2009) Redundant and specific roles of the ARGONAUTE proteins AGO1 and ZLL in development and small RNA-directed gene silencing. PLoS Genet **5:** e1000646

Marchler-Bauer A, Lu S, Anderson JB, Chitsaz F, Derbyshire MK, DeWeese-Scott C, Fong JH, Geer LY, Geer RC, Gonzales NR, et al (2011) CDD: a Conserved Domain Database for the functional annotation of proteins. Nucleic Acids Res **39:** D225–D229

Mi S, Cai T, Hu Y, Chen Y, Hodges E, Ni F, Wu L, Li S, Zhou H, Long C, et al (2008) Sorting of small RNAs into *Arabidopsis* argonaute complexes is directed by the 5′ terminal nucleotide. Cell **133:** 116–127

Montgomery TA, Howell MD, Cuperus JT, Li D, Hansen JE, Alexander AL, Chapman EJ, Fahlgren N, Allen E, Carrington JC (2008) Specificity of ARGONAUTE7-miR390 interaction and dual functionality in TAS3 trans-acting siRNA formation. Cell **133:** 128–141

Nakanishi K, Weinberg DE, Bartel DP, Patel DJ (2012) Structure of yeast Argonaute with guide RNA. Nature **486:** 368–374

Oh Y, Baldwin IT, Gális I (2012) *NaJAZh* regulates a subset of defense responses against herbivores and spontaneous leaf necrosis in *Nicotiana attenuata* plants. Plant Physiol **159:** 769–788

Oh Y, Baldwin IT, Galis I (2013) A jasmonate ZIM-domain protein *NaJAZd* regulates floral jasmonic acid levels and counteracts flower abscission in *Nicotiana attenuata* plants. PLoS ONE **8:** e57868

Onkokesung N, Gaquerel E, Kotkar H, Kaur H, Baldwin IT, Galis I (2012) MYB8 controls inducible phenolamide levels by activating three novel hydroxycinnamoyl-coenzyme A:polyamine transferases in *Nicotiana attenuata*. Plant Physiol **158:** 389–407

Pandey SP, Baldwin IT (2007) RNA-directed RNA polymerase 1 (RdR1) mediates the resistance of Nicotiana attenuata to herbivore attack in nature. Plant J **50:** 40–53

Pandey SP, Baldwin IT (2008) Silencing RNA-directed RNA polymerase 2 increases the susceptibility of *Nicotiana attenuata* to UV in the field and in the glasshouse. Plant J **54:** 845–862

Pandey SP, Gaquerel E, Gase K, Baldwin IT (2008a) RNA-directed RNA polymerase3 from *Nicotiana attenuata* is required for competitive growth in natural environments. Plant Physiol **147:** 1212–1224

Pandey SP, Shahi P, Gase K, Baldwin IT (2008b) Herbivory-induced changes in the small-RNA transcriptome and phytohormone signaling in *Nicotiana attenuata*. Proc Natl Acad Sci USA **105:** 4559–4564

Paschold A, Bonaventure G, Kant MR, Baldwin IT (2008) Jasmonate perception regulates jasmonate biosynthesis and JA-Ile metabolism: the case of COI1 in *Nicotiana attenuata*. Plant Cell Physiol **49:** 1165–1175

Qi Y, Denli AM, Hannon GJ (2005) Biochemical specialization within *Arabidopsis* RNA silencing pathways. Mol Cell **19:** 421–428

Rasmann S, De Vos M, Casteel CL, Tian D, Halitschke R, Sun JY, Agrawal AA, Felton GW, Jander G (2012) Herbivory in the previous generation primes plants for enhanced insect resistance. Plant Physiol **158:** 854–863

Rayapuram C, Baldwin IT (2007) Increased SA in NPR1-silenced plants antagonizes JA and JA-dependent direct and indirect defenses in herbivore-attacked *Nicotiana attenuata* in nature. Plant J **52:** 700–715

Rogers K, Chen X (2013) Biogenesis, turnover, and mode of action of plant microRNAs. Plant Cell **25:** 2383–2399

Schirle NT, Sheu-Gruttadauria J, MacRae IJ (2014) Structural basis for microRNA targeting. Science **346:** 608–613

Shazman S, Celniker G, Haber O, Glaser F, Mandel-Gutfreund Y (2007) Patch Finder Plus (PFplus): a web server for extracting and displaying positive electrostatic patches on protein surfaces. Nucleic Acids Res **35:** W526–W530

Singh RK, Gase K, Baldwin IT, Pandey SP (2015) Molecular evolution and diversification of the Argonaute family of proteins in plants. BMC Plant Biol **15:** 23

Singh RK, Pandey SP (2015) Evolution of structural and functional diversification among plant Argonautes. Plant Signal Behav **10:** e1069455

Skibbe M, Qu N, Galis I, Baldwin IT (2008) Induced plant defenses in the natural environment: *Nicotiana attenuata WRKY3* and *WRKY6* coordinate responses to herbivory. Plant Cell **20:** 1984–2000

Söding J, Biegert A, Lupas AN (2005) The HHpred interactive server for protein homology detection and structure prediction. Nucleic Acids Res **33:** W244–W248

Steppuhn A, Gase K, Krock B, Halitschke R, Baldwin IT (2004) Nicotine's defensive function in nature. PLoS Biol **2:** E217

Takeda A, Iwasaki S, Watanabe T, Utsumi M, Watanabe Y (2008) The mechanism selecting the guide strand from small RNA duplexes is different among argonaute proteins. Plant Cell Physiol **49:** 493–500

Tamura K, Peterson D, Peterson N, Stecher G, Nei M, Kumar S (2011) MEGA5: molecular evolutionary genetics analysis using maximum likelihood, evolutionary distance, and maximum parsimony methods. Mol Biol Evol **28:** 2731–2739

Thomas CL, Jones L, Baulcombe DC, Maule AJ (2001) Size constraints for targeting post-transcriptional gene silencing and for RNA-directed methylation in *Nicotiana benthamiana* using a potato virus X vector. Plant J **25:** 417–425

von Dahl CC, Winz RA, Halitschke R, Kühnemann F, Gase K, Baldwin IT (2007) Tuning the herbivore-induced ethylene burst: the role of transcript accumulation and ethylene perception in *Nicotiana attenuata*. Plant J **51:** 293–307

Vrbsky J, Akimcheva S, Watson JM, Turner TL, Daxinger L, Vyskot B, Aufsatz W, Riha K (2010) siRNA-mediated methylation of *Arabidopsis* telomeres. PLoS Genet **6:** e1000986

War AR, Paulraj MG, Ahmad T, Buhroo AA, Hussain B, Ignacimuthu S, Sharma HC (2012) Mechanisms of plant defense against insect herbivores. Plant Signal Behav **7:** 1306–1320

Wu J, Baldwin IT (2010) New insights into plant responses to the attack from insect herbivores. Annu Rev Genet **44:** 1–24

Xia J, Psychogios N, Young N, Wishart DS (2009) MetaboAnalyst: a web server for metabolomic data analysis and interpretation. Nucleic Acids Res **37:** W652–W660

Xia J, Wishart DS (2011) Web-based inference of biological patterns, functions and pathways from metabolomic data using MetaboAnalyst. Nat Protoc **6:** 743–760

Xie Z, Johansen LK, Gustafson AM, Kasschau KD, Lellis AD, Zilberman D, Jacobsen SE, Carrington JC (2004) Genetic and functional diversification of small RNA pathways in plants. PLoS Biol **2:** E104

Yang DH, Baldwin IT, Wu J (2013) Silencing brassinosteroid receptor BRI1 impairs herbivory-elicited accumulation of jasmonic acid-isoleucine and diterpene glycosides, but not jasmonic acid and trypsin proteinase inhibitors in *Nicotiana attenuata*. J Integr Plant Biol **55:** 514–526

Zhang Y, Skolnick J (2005) TM-align: a protein structure alignment algorithm based on the TM-score. Nucleic Acids Res **33:** 2302–2309

Zhirnov IV, Trifonova EA, Kochetov AV, Shumny VK (2015) Virus-induced silencing as a method for studying gene functions in higher plants. Genetika **51:** 558–567

Manuscript II

Argonaute 4 modulates resistance against hemibiotrophic fungal infection by regulating jasmonic acid signaling in *Nicotiana attenuata* plants

Maitree Pradhan, Priyanka Pandey, Ian T. Baldwin*, and Shree P. Pandey*

(Plant Physiology (2019) under revision)

ABSTRACT

Argonautes (AGOs) associate with non-coding RNAs to regulate gene expression during development and stress adaptation. Their role in plant immunity against hemibiotrophic fungal infection remains poorly understood. Here, we explore the function of AGOs in *Nicotiana attenuata's* interaction with a naturally-occurring hemibiotrphic pathogen, *Fusarium brachygibbosum*. Amongst six AGOs, only AGO4 responded to fungal infection. The disease progressed more rapidly in AGO4-silenced (irAGO4) plants than in WT, and small RNA (smRNA) profiling revealed that irAGO4 plants were severely abrogated in 24-nucleotide smRNA accumulations. Unique microRNAs (miRNAs: 130 conserved and 208 novel, including 11 isomiRs) were identified in infected plants; silencing AGO4 strongly changed the dynamics of their accumulations. Time-course studies revealed that infection increased accumulations of ABA, jasmonates and salicylic acid in WT; irAGO4 plants accumulated only lower jasmonate levels and lower transcripts of JA biosynthetic genes. Treatment of irAGO4 plants with JA, methyl jasmonate and cis-(+)-12-oxo-phytodienoic acid restored WT levels of susceptibility. Additionally, silencing the expression of *RdR1, RdR2* (not *RdR3*) and *DCL3* (not *DCL2/4*) increased susceptibility to this fungal pathogen. The real-world relevance of the *AGO4*, *RdR1*, *RdR2* and *DCL3* sector of the smRNA machinery was revealed when plants individually silenced in *AGO4*, *RdR1*, *RdR2* and *DCL3* expression (and their binary combinations) were planted into a diseased field plot in the Great Basin Desert, and found to be more susceptible and accumulated lower JA levels than WT's. We infer that AGO4-dependent smRNAs play a central role in modulating JA biogenesis and signaling during hemibiotrophic fungal infections.

Keywords: Argonaute, AGO4, *Nicotiana attenuata*, hemibiotrophy, *Fusarium brachygibbosum*, plant-pathogen interaction, disease resistance

INTRODUCTION

The genus *Fusarium,* which originated 91.3 million years ago following the diversification of flowering plants, harbors some of the most devastating phytopathogenic ascomycete fungi (Ma et al., 2013). They infect plants by colonizing roots (e.g. *F. oxysporum*) as

well as the above-ground parts such as leaves and floral tissues (e.g. *F. graminearum*). For many of these interactions, the infection process starts asymptomatically, in which biotrophic phase transitions into a necrotrophic phase, during which plant cells are killed and consumed. Thus, many *Fusaria* species broadly follow a hemibiotrophic life-style characteristic of a variety of diseases (including blights, cankers, rots and wilts) in hundreds of plant species in both agricultural and natural habitats.

Nicotiana attenuata (a wild tobacco species) is a post-fire native of south-western USA. Due to three decades of intensive research, the molecular basis of its interactions with native herbivores and pollinators are well understood. After fires, seeds of *N. attenuata* germinate from long-lived seed banks in a highly synchronized manner. This results in populations which resemble agricultural monocultures. The infection of *N. attenuata* with *Fusarium* species was recently discovered, when field plantations of this species in the Great Basin Desert of Utah (USA) started suffering from a sudden wilt-like disease that was first observed in 2005 and steadily progressed over the subsequent 13 years (Santhanam et al., 2015). This sudden wilt-like disease shared many similarities with a dynamic fungal infection characterized in 2011 of a native population of plants growing adjacent to the field plots (Schuck et al., 2014). *F. brachygibbosum* was identified as an important component of symptomatic plants in both the native population and the plantation (Schuck et al., 2014; Santhanam et al., 2015). Due to its recent identification, knowledge of the infection as well as the molecular components regulating host signaling and responses against *F. brachygibbosum* remains in its infancy (Luu et al., 2015; Luu et al., 2017).

Jasmonic acid (JA) signaling forms the backbone of a multi-layered molecular defense response that plants, including *N. attenuata,* mount against the attack of specialized herbivores (Howe and Jander, 2008; Meredith and Baldwin, 2016). JA signaling also plays a central role in *N. attenuata's* resistance to the sudden wilt-like disease (Luu et al., 2015), but the molecular details of *F. brachygibbosum*-triggered responses in *N. attenuata* remain poorly characterized. During herbivore attack, various facets of JA-mediated defense responses of *N. attenuata* are modulated by regulatory non-coding small RNAs (smRNAs (Pandey and Baldwin, 2007; Pandey et al., 2008a; Pradhan et al., 2017)) and we were interested to see if smRNAs were also modulated by infection of the sudden-wilt-like pathosystem.

smRNA pathways are important modulators of phenotypic plasticity as they are known to be involved in plant development, abiotic and biotic stress adaptation, genome stability and reproduction. Ranging in size between 18-30 nucleotides (nt), several diverse classes of smRNAs are found in plants (Axtell, 2013; Borges and Martienssen, 2015). Endogenous plant smRNAs may be broadly classified into microRNAs (miRNAs) and small interfering RNAs (siRNAs), which are further subdivided as heterochromatic siRNAs, secondary siRNAs, natural-*cis* and -*trans* siRNAs, secondary phased siRNAs and *trans*-acting siRNAs. Hairpin miRNA precursors (double stranded stem-loops, formed from single stranded RNA) are transcribed from the miRNA genes by RNA-polymerase II. Conversely, single stranded RNA are converted into double-stranded RNA (dsRNA) precursors of siRNAs by the RNA directed RNA polymerases (RdRs). Dicer-like (DCL) endonucleases act on these dsRNA intermediates to produce mature smRNA duplexes, which can be loaded onto the Argonaute (AGO) proteins to regulate gene expression by sequence complementarity. Depending on the types of the smRNAs and the associated AGOs, these complexes can directly catalyze target mRNA cleavage, repress translation, or, along with recruitment of other cofactors, orchestrate chromatin modifications (Axtell, 2013; Böhmdorfer et al., 2014; Borges and Martienssen, 2015).

AGOs are regarded as the 'effectors' of RNA-interference processes (Fang and Qi, 2016). The AGO gene family has expanded during the evolution of higher plants after their divergence from green algae as a consequence of several genome duplication events and other smaller scale duplication processes (Singh et al., 2015; Singh and Pandey, 2017). In Arabidopsis, 10 AGOs are reported, whereas in *N. attenuata*, 11 genes have been identified (Singh et al., 2015; Singh and Pandey, 2015; Pradhan et al., 2017). AGOs are classified into 4 phylogenetic clades of AGO1/10, AGO5, AGO2/3/7 and AGO4/6/8/9 (Singh et al., 2015; Rodriguez-Leal et al., 2016). Recently, in *N. attenuata*, we discovered the function of AGO8 in mediating the induction of direct defenses in response to herbivore attack (Pradhan et al., 2017); the biological functions of other members of the NaAGO family remain largely uncharacterized. In Arabidopsis, AGO2 and AGO4 have been associated with plant immunity against bacteria and viruses (Zhang et al., 2011; Fang and Qi, 2016; Ludman et al., 2017).

In Arabidopsis, AGO4 (AtAGO4) mediates resistance against the gram-negative bacteria, *Pseudomonas syringae* (Agorio and Vera, 2007). In *N. benthamiana*, AGO4 is involved in virus

resistance induced by NB-LRR proteins (Bhattacharjee et al., 2009) as well as in systemic silencing (Jones et al., 2006). In Arabidopsis, AGO4 is specifically required for the accumulation of a subset of secondary heterochromatic siRNAs (Wang and Axtell, 2017). AtAGO4 forms a component of RNA-directed DNA methylation (RdDM) pathway (Borges and Martienssen, 2015). In Arabidopsis, dynamic DNA methylation changes are reported during infection of bacteria and in regulating the salicylic acid (SA) response (Dowen et al., 2012). Although the Arabidopsis response to *P. syringae* attack is negatively regulated by methylation (Dowen et al., 2012), AtAGO4 appears to be a positive regulator as it is required for Arabidopsis immunity against *P. syringae* (Agorio and Vera, 2007). The RdDM pathway can induce gene expression in petunia (Shibuya et al., 2009). AtAGO4 is thought to operate independently of the canonical RdDM pathway (Agorio and Vera, 2007; López et al., 2011; Dowen et al., 2012) and hence there's much to learn about the functions of AGO4, which are clearly complex. It should be noted that all of research on AGO4 function comes from laboratory investigations; hence the 'real-world' relevance of the function of AGO4 (or AGO2) in regulating plant immunity against pathogens remains unknown. Here, we examine the role of the *N. attenuata* AGO4 in modulating immune responses against its natural hemibiotrophic phytopathogen, *F. brachygibbosum* in both laboratory and field-based assays.

Which AGOs are involved in host-pathogen interaction in *N. attenuata* remains unexplored. Here we (1) explore which of the *N. attenuata* AGOs might modulate immunity against infection from a natural, hemibiotrophic fungal pathogen, *F. brachygibbosum*. Our results demonstrate a crucial role played by AGO4. (2) We characterize the progress of infection of WT and plants silenced in *AGO4* expression to determine temporal dynamics of disease progression and host susceptibility. (3) We investigate how host smRNAs are reprogrammed during infection and their dependence on AGO4. We (4) elucidate the signaling and molecular components of *N. attenuata* that are modulated by AGO4 during infection, and (5) explore other components of the core-smRNA machinery that may cooperate with AGO4 in modulating plant immunity. We infer a miRNA-target network that modulates JA signaling during pathogenesis. (6) Lastly, we evaluate the real world-relevance of the inferred RNA-interference pathway by characterizing the susceptibility of plants silenced in *AGO, DCL* and *RdR* expressions in *N. attenuata*'s native habitat.

RESULTS

Nicotiana attenuata AGO4 specifically responds to *Fusarium brachygibbosum* infection

Nicotiana attenuata contains 11 genes that correspond to 8 unique AGOs (*NaAGOs 1, 2, 4, 5, 7, 8, 9* and *10*). While *AGO1* has been implicated in development-related plant processes and *NaAGO8* has been implicated in herbivore-resistance (Pradhan et al., 2017), the biological functions of the other *NaAGO*s are unknown. In order to determine which *NaAGO*s may be involved in regulating plant immunity against the naturally occurring hemibiotrophic pathogen of *N. attenuata*, *Fusarium brachygibbosum*, we characterized the expression dynamics of *NaAGO2, 4, 5, 7, 9* and *10* in time-course infection studies. We quantified the changes in transcript abundances of genes 12-48 h post inoculation (hpi) of the wild type (WT) *N. attenuata* leaves with *F. brachygibbosum*, relative to the uninoculated controls (0 hpi). No differences in the expression profiles of *NaAGOs 2, 5, 7, 9* and *10* were observed before or after pathogen infection (Fig. 1A). On the other hand, transcript abundance of *NaAGO4* was rapidly increased by nearly 3-fold within 12 hpi (Fig. 1A). Transcripts levels of *NaAGO4* remained significantly elevated at 24 (2.5-fold) and 48 hpi (≤2-fold), as compared to the 0 hpi controls (Fig. 1A).

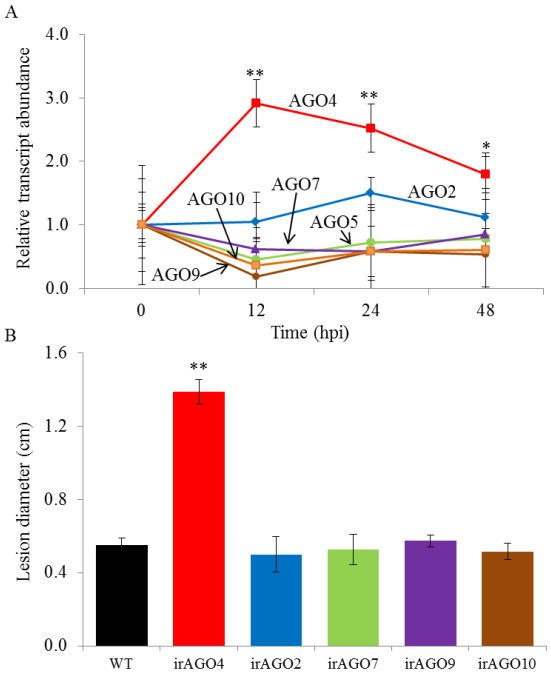

Figure 1.

Figure 1. Response of *Nicotiana attenuata* to *Fusarium brachygibbosum* infection shows specificity to AGO4. A, Elicitation dynamics of *AGO* transcripts in *N. attenuata* leaves during *F. brachygibbosum* infection. A time-course experiment with WT plants whose leaves were inoculated at t_0 was conducted. Only *AGO4* transcripts responded to pathogen infection, with significant increases within 12 h post infection (hpi). Levels of *ECI* gene was used as internal control for normalization. Transcript level at t_0 was set to 1 and used for calculating relative abundances after infection. Values presented are means ± SD. ANOVA, F=7.88, n=3, * and ** represent significant differences from 0h at $P \leq 0.05$, and $P \leq 0.01$. B, Silencing of AGO4 specifically makes *N. attenuata* susceptible to *F. brachygibbosum* infection. Plants silenced in AGO2, 4, 5, 7, 9 and 10 expression (irAGO) were infected with 10 µL of spore suspension (10^6 spores/mL) and disease severity was measured by recording lesion diameter after 5 days of inoculation (** significantly different from wild type (WT), ANOVA, F = 14.93, n=30, $P \leq 0.01$).

These results indicated that *NaAGO4* might be functionally relevant for plant immunity against the hemibiotrophic fungal pathogens. To evaluate this hypothesis, we performed a loss-of-function characterization of plants silenced in the expression of *NaAGOs 2, 4, 7, 9,* and *10* (irAGOs (Pradhan et al., 2017)) in response to *F. brachygibbosum* infection. The expression of each of the individual AGOs was silenced in stably transformed homozygous lines harboring a single insertion of an RNAi construct specifically targeting the individual AGOs. These lines are characterized in (Pradhan et al., 2017) and were all created in the same genetic background as the WT plants. Indeed, only irAGO4 plants were hyper-susceptible (Fig. 1B), which was consistent with the hypothesis that *AGO4* in *N. attenuata* specifically modulates plant immunity.

Silencing *NaAGO4* enhances infection and susceptibility of *N. attenuata* against *F. brachygibbosum*

irAGO4 did not display developmental abnormalities, and the isogenic WT and irAGO4 plants were indistinguishable in their growth and fitness traits, such as rosette diameter, leaf number, chlorophyll content, plant height, and flower numbers (Supplemental Fig. S1). We studied the process of infection of *N. attenuata* plants over a period of 12 days. The leaves of *N. attenuata* plants were inoculated with *F. brachygibbosum* spore suspension (10^6/mL), and microscopic observations were made after chlorophyll de-staining for 48 hpi. Aggressive colonization of the host surface, specifically on irAGO4 plants was particularly noticeable (Fig. 2A, Supplemental Fig. S2). The spores germinated within 12h on WT as well as on irAGO4 plants (Fig. 2A) and hyphae started to spread on the surface of leaves. The hyphae germinating

from the spores around the stomata approached the stomatal opening by 24 hpi. Also, hyphae germinating from spores often aligned towards the stomatal opening and parallel to the junctions between epidermal cells, suggesting directional growth towards stomata. Short infection hyphae were noticed, which indicated direct penetration and entry into the host from the plant's stomata and junctions of the epidermal cells. On irAGO4 plants, septate runner hyphae were found to give rise to foot structures, appressoria-like structures, and hyphae that appeared to penetrate into cells (infection hyphae). Infection cushions were noticed at 24-48 hpi. Similar structures have been reported during the fungal infection of other hosts, such as on wheat by *F. graminearum* (Boenisch and Schäfer, 2011). A few infection cushions were noticed on WT plants at 24 hpi. Initiation of browning of cells near stomata was also evident at 24-48 hpi, indicating the initiation of necrosis in WT plants around 48 hpi (Fig. 2A). WT stomata were occupied by mycelia at 48 hpi and increased frequencies of infection cushions were also visible on WT plants at 48 hpi (Fig. 2A). On the other hand, stomata were already colonized by 24 hpi and large numbers of infection cushions were observed on irAGO4 plants at 24 hpi, which increased by 48 hpi, indicating the more rapid colonization of irAGO4 plants as compared to WT (Fig. 2A). Numerous lobate appressoria and foot structures were also visible on irAGO4 plants at 48 hpi (Supplemental Fig. S2), as compared to their more limited numbers on WT plants. These results indicated that irAGO4 plants were more rapidly and vigorously colonized by the pathogen than were WT plants.

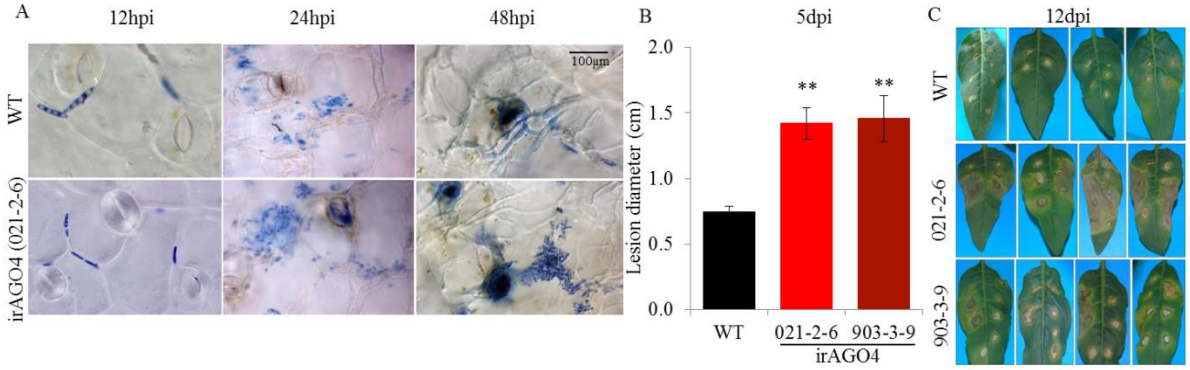

Figure 2.

Figure 2. Silencing *AGO4* expression in *N. attenuata* increases disease progression and susceptibility to infection by *F. brachygibbosum.* A, Interaction of wild type (WT) *N. attenuata* with *F. brachygibossum*

reveals germination of spores on the host leaf surface within 12 h post infection (hpi). The newly formed mycelia approaches stomata and few infection cushions are formed by 24-48 hpi, which results in colonization of tissues surrounding stomata. Initiation of necrosis was recorded between 24-48 hpi (light brown pigmentation around stomata) in WT tissue and infection cushions. In irAGO4 plants (B), colonization by large number of mycelia and spores around stomatal openings led to destruction of stomata and the formation of large number of infection cushions by 48 hpi. In infected irAGO4 leaves, large numbers of sites of penetration through stomatal openings and through junctions of epidermal cells were observed; the multiplication of mycelia occurs within 24h, and by 48h large numbers of conidia are developed that may initiate a new cycle of infection. Structures similar to lobate appresoria were visible at 48 hpi. Large numbers of 'foot' structures from runner hyphae were visible in irAGO4 plants. The irAGO4 plants were highly susceptible to *F. brachygibossum* infection by 5 days post inoculation (dpi; B); susceptibility of irAGO4 was verified in two independent transformants (021-2-6 and 903-3-9). Disease severity was measured by lesion diameter (ANOVA, n=8, $P \leq 0.01$, **significantly different from WT). By 12 dpi (C), irAGO4 leaves were completely colonized and necrotic.

On WT plants, it appears that the pathogen might survive as a biotroph, without initiating visible symptoms for 24-48 hpi as only a few infection cushions were observed, and browning was limited to those cells near the mycelia. As necrosis was observed 48 hpi, this may portend the time when the pathogen may switch from biotrophic to necrotrophic phases. This switching may happen more quickly on irAGO4 plants, as indicated by increased browning of the cells and extensive infection cushions observed on irAGO4 plants already by 24-48 hpi (Fig. 2A, Supplemental Fig. S2).

Symptoms of chlorosis and necrotic lesions were visible by 3 days post inoculation (dpi). The lesions size on the irAGO4 plants increased rapidly compared to WT. After 5 dpi, irAGO4 plants sustained lesions that were already two-fold larger than those on WT plants (Fig. 2B). These lesions on the irAGO4 leaves coalesced, and leaves were fully necrotic by 12 dpi (Fig. 2C). By 12 days, plants started to wilt, indicating the spread of pathogen to other tissues. On the other hand, the necrotic lesions on WT plants remained restricted at 12 dpi, with symptoms of enhanced chlorosis in tissues surrounding the inoculation sites (Fig. 2C). The greater susceptibility of irAGO4 plants was verified on an independently transformed line (Fig. 2B, C). Clearly, the fungus grew faster on irAGO4 plants than the WT, including at 24-48 hpi, when

symptoms were not visible, and rapidly colonized large parts of leaf tissues, plausibly by drawing upon nutrients from the dying cells of irAGO4 plants.

From this analysis, we conclude that silencing *AGO4* expression in *N. attenuata* enhanced disease progression, compromised immunity and resulted in increased susceptibility to the hemibiotrophic *F. brachygibbosum*.

Large-scale reprogramming of smRNA accumulations during various stages of *F. brachygibbosum* infection

Next, we determined how the accumulation of regulatory non-coding smRNAs in *N. attenuata* are reprogrammed during the course of infection and how these changes are regulated by *AGO4* expression. We deep-sequenced smRNomes of WT and irAGO4 leaves at various stages, after 0 (no infection), 12 (spore germination), 24 (initiation of infection) and 48 h (establishment) of *F. brachygibbosum* infection. A total of 24 smRNome libraries (2 genotypes, 4 time points and 3 replicates each) were sequenced. An average of (98.58$\pm$0.53) % unique smRNA reads per sample, in the range of 15-30 nucleotide (nt) length, were obtained after the quality control measures were implemented and the reads that aligned to structural and messenger RNAs were removed.

As AGO4 has been implicated in generating 24 nt siRNAs in Arabidopsis (Zilberman et al. 2003, Wang and Axtell 2016), we determined how this size class (24 nt) of smRNAs was reprogrammed during infection in both WT and AGO4-silenced lines of *N. attenuata* (Fig. 3, Supplemental Fig. S3). Nearly 100 X 10^3 unique 24 nt smRNAs were expressed in healthy (uninfected) WT leaves. Infection of *F. brachygibbosum* fungus extensively reprogrammed the patterns of 24 nt smRNAs accumulation, which were maximally reduced at 24 hpi (Fig. 3A). Silencing of *NaAGO4*, strongly reduced the constitutive accumulation of 24 nt smRNAs as well as pathogen-induced levels. Strongest reductions in 24 nt smRNA accumulation were recorded in irAGO4 plants at 12 hpi (Fig. 3A).

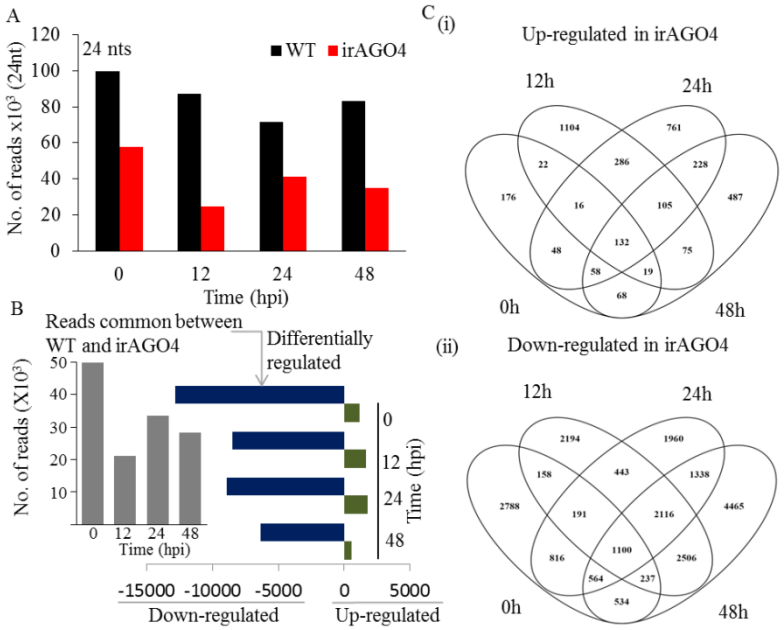

Figure 3.

Figure 3. Silencing *AGO4* results in strong down-regulation of 24 nt non-coding smRNAs during *F. brachygibossum* infection. A, Overall, irAGO4 plants show reduced accumulation of 24 nt smRNAs (0-48 hpi). B, 24 nt-reads that are commonly expressed (grey bar graph insert) between WT and irAGO4 further show strong down-regulation in irAGO4 (blue bars). C, A total of 132 smRNAs were uniformly up-regulated (i) in irAGO4 during the process of infection, whereas 1100 smRNAs were uniformly down-regulated (ii) at all the time points during pathogenesis in irAGO4 compared to WT.

Approximately 50,000 24 nt smRNAs were commonly expressed between WT and irAGO4 plants in healthy plants; infection of *F. brachygibbosum* further induced changes in their accumulation patterns (Fig. 3B). The commonly occurring smRNAs were differentially accumulated between the WT and irAGO4 plants in a time-dependent manner, with a majority being down-regulated (Fig. 3B and C). Strongest down-regulation of 2194 unique 24 nt smRNAs was recorded at 12 hpi (Fig. 3C). Only a total of 132 unique 24 nt smRNA reads were commonly up-regulated, whereas 1100 were down-regulated at all the 4 time points (Fig. 3C). Principle component analysis of these smRNAs reinforced that the patterns of expression of these smRNAs were genotype- and time-dependent (Supplemental Fig. S3).

These results show that the expression of 24 nt smRNAs is highly dynamic during the process of infection in an AGO4-dependent manner, and that silencing AGO4 might also up-regulate a very small fraction of 24 nt smRNAs during the infection process.

Pathogen induced reprogramming of the miRNome of *N. attenuata*

Overview of N. attenuata miRNome and its dependency on AGO4. We studied how *F. brachygibbosum* infection alters the expression of conserved and novel miRNAs of *N. attenuata* and how this pathogen-induced reprograming of miRNome is regulated by AGO4 expression using a miRDeep-based pipeline. A total of 842 miRNAs were captured in 24 samples (Supplemental Table S1). Of these, 237 miRNAs were captured in at least one of the 12 WT samples (but not in irAGO4). Similarly, 313 miRNAs were captured in one of the 12 irAGO4 samples (but not in WT). 292 miRNAs were captured in both, WT and irAGO4, of which 44 miRNAs were present in all the 24 samples.

We observed that several of the 842 miRNAs were expressed in only one of the three replicates. Median-centering the data (miRNAs that were captured in at least 2 of the 3 replicates of each treatment-condition; Pradhan et al., 2017; Pandey et al., 2018) resulted in 338 miRNAs across 8 'treatment-conditions' *viz.* 4 time points and 2 genotypes (Supplemental Table S2). We used this data set for further analysis. A detailed description of the important characteristics of the miRNAs is provided in SI Tables 1 and 2.

As the conserved miRNAs are expected to have profound regulatory roles in a plant's physiology, we determined the conserved fraction of the miRNome of *N. attenuata*. Of 338, 131 miRNA reads, corresponding to 119 unique miRNAs, were conserved, whereas 207 miRNA reads were novel, being found only in *N. attenuata*. The conserved miRNAs mapped to 24 plant species (Supplemental Table S3). Of 131 conserved miRNA reads, 59 were commonly expressed in WT and irAGO4 genotypes, whereas 39 miRNAs were expressed only in WT (whose expression was completely abrogated after silencing of AGO4), whereas 33 were identified only in irAGO4 samples (i.e. their accumulation was associated with the loss of AGO4 expression). Similarly, of the 207 novel miRNA reads, 82 were commonly identified in both the genotypes, whereas 69 were specific to WT and 56 were specific to irAGO4. Thus, transcription of these 72

conserved and 125 novel miRNAs completely depended on AGO4, and thus could be considered as AGO4-specific miRNAs.

Expression profiles and differential accumulation of miRNAs during pathogenesis. Infection by *F. brachygibbosum* resulted in complex changes in accumulation patterns of miRNA (Fig. 4, Supplemental Table S4, Supplemental Fig. S4). In WT plants, at 12 hpi (compared to 0 hpi controls), 42 miRNAs (18 conserved, 24 novel) were up-regulated, whereas 39 (17 conserved, 22 novel) were down-regulated (Supplemental Table S4). At 24 hpi, 16 miRNAs (6 conserved, 10 novel) were up- and 71 (34 conserved, 37 novel) were down-regulated. Further, at 48 hpi, 32 (17 conserved, 15 novel) were up- and 50 (20 conserved, 30 novel) were down-regulated (Supplemental Table S4).

Silencing *AGO4* further changed the miRNA expression landscape during infection (Fig. 4, Supplemental Table S4, Supplemental Fig. S4). At 0 hpi, 36 miRNAs (20 conserved, 16 novel) were up-regulated in irAGO4, whereas 33 (11 conserved, 22 novel) were down-regulated. At 12 hpi, 15 miRNAs (9 conserved, 9 novel) were up-, whereas 51 (21 conserved, 30 novel) were down-regulated. At 24 and 48 hpi, 49 (24 conserved, 25 novel) and 52 miRNAs (27 conversed, 25 novel) were up-regulated, respectively, whereas 24 (8 conserved, 16 novel) and 28 (6 conserved, 22 novel) miRNAs were down-regulated, respectively (Fig. 4, Supplemental Table S4). The novel miRNt0326, and miR7785-5p were the most down-regulated miRNAs at 0 hpi, whereas miRNt0172 and miRNt0014 were amongst the highly up-regulated miRNAs at 0 hpi in irAGO4 compared to WT plants. miRNt0167, 0072, and 0157 were amongst the most strongly down-regulated miRNAs in irAGO4 at 12, 24 and 48 hpi compared to WT respectively, whereas, miRNt0153, 0017 and miR1222d were the most up-regulated miRNAs. miRNt0015 is an example of a miRNA that is consistently up-regulated during infection (12-48 hpi) in irAGO4 over WT, while novel miRNAs such as miRNt0163, 0172, 0015, 0156 are examples of miRNAs that are consistently up-regulated at late stages of infection at 24 and 48 hpi in irAGO4 compared to WT.

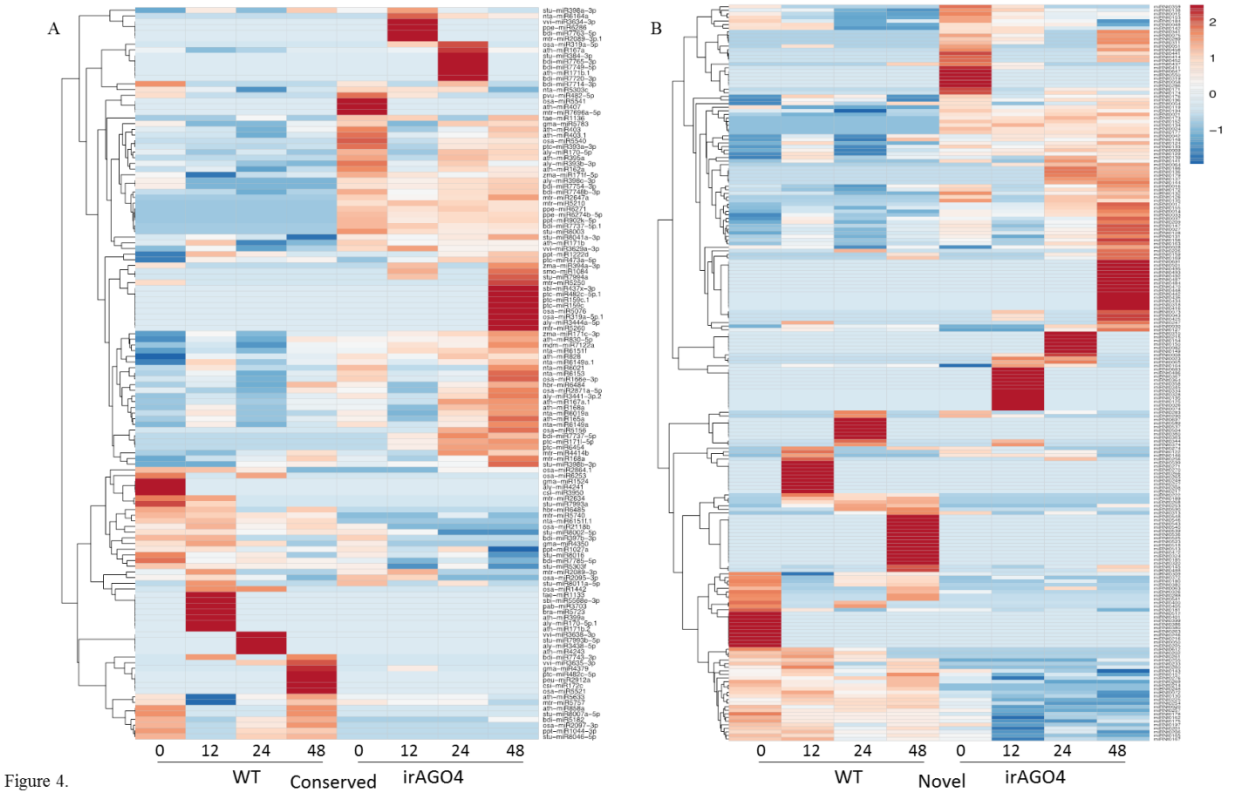

Figure 4.

Figure 4. Silencing AGO4 reprograms the microRNA expression during *F. brachygibossum* infection. Heat maps reveal the patterns of change in accumulation of (A) conserved and (B) novel miRNAs in WT and irAGO plants after infection. A total of 338 unique miRNAs (sequences) were identified, of which 130 were conserved and 208 were novel miRNAs.

Time- and genotype-specific clusters of conserved miRNA expression were also evident during infection (Fig. 4). For instance, the cluster of aly-miR170-5p.1, ath-miR171b.2, ath-miR399a, bra-miR5723, osa-miR1442, pab-miR3703, sbi-miR5568e-3p, tae-miR1133 was specifically expressed at 12 hpi in WT (Fig. 4). aly-miR3438-5p, ath-miR4243, stu-miR7993b-5p, vvi-miR3638-3p formed the cluster of miRNAs that were expressed only 24 hpi in WT, whereas the 48 hpi-WT-specific miRNA cluster included csi-miR172c, gma-miR4379, osa-miR5521, peu-miR2912a, ptc-miR482c-5p (Fig. 4). On the other hand, nta-miR6164a, vvi-miR3634-3p, ppe-miR6286, bdi-miR7763-5p, mtr-miR2089-3p formed a cluster of miRNAs specifically up-regulated only in irAGO4 at 12 hpi (Fig. 4). The 24 hpi irAGO4 specific cluster included, for example, stu-miR384-3p, bdi-miR7765-3p, bdi-miR7749-5p, ath-miR171b, bdi-

miR7720-3p, whereas mtr-miR5250, sbi-miR437x-3p, ptc-miR482c-5p, ptc-miR159c, ptc-miR159c, osa-miR5076, osa-miR319a-5p, aly-miR3444a-5p, mtr-miR5260 were amongst the 48 hpi specific cluster of irAGO4-specific miRNAs (Fig. 4). Similar time- and genotype-specific clusters of novel miRNAs were clearly apparent (Fig. 4).

Further, some miRNA may express their sequence variants in condition- or cell-specific manners (isomiRs; (Pandey et al., 2018)). Amongst the group of the 131 conserved miRNAs, 11 expressed isomiRs (23 miRNA sequences, Fig. 5). miR171b expressed 3 isomiRs, whereas the other 10 miRNAs expressed 2 each, respectively. These isomiRs demonstrated a genotype- and time-specific pattern of expression. For instance, miR170-5p, miR171b, expressed isomiRs specifically at 12 hpi in WT plants only, whereas, miR2089-3p expressed an isomiR at 12 hpi only in irAGO4 plants. An isomiR of miR6151f was specifically expressed at all the 4 time points only in WT plants (whereas the other isomiR was expressed in WT as well as irAGO4, Fig. 5). Furthermore, miR7737-5p isomiRs were specifically expressed only in irAGO4 plants (Fig. 5).

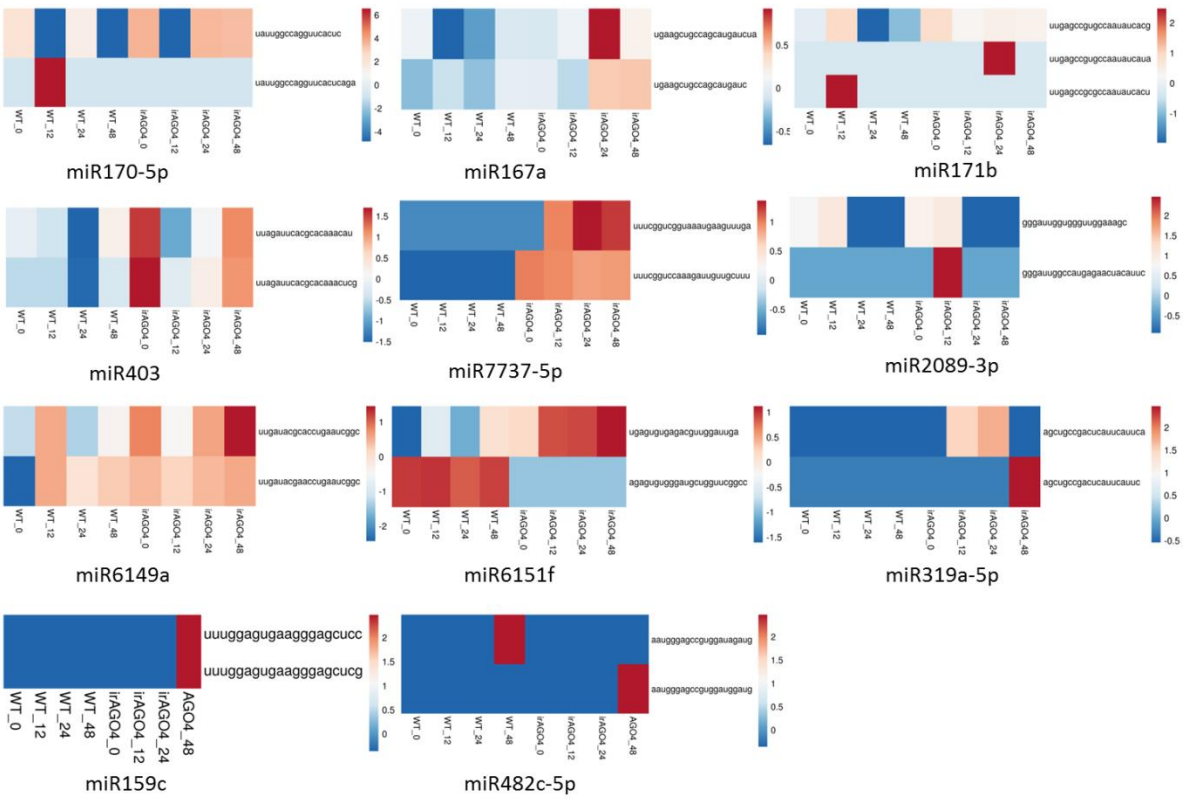

Figure 5.

Figure 5. Characterization of isomiRs during *F. brachygibossum* infection in WT and irAGO4 plants. 11 isomers (aly-miR170-5p, ath-miR167a, ath-miR171b, ath-miR403, bdi-miR7737-5p, mtr-miR2089-3p, nta-miR6149a, nta-miR6151f, osa-miR319a-5p, ptc-miR159c, ptc-miR482c-5p) were identified. Their expression patterns are represented as heat maps in WT and irAGO4 genotypes during pathogen infection.

These results demonstrate that the process of infection of *F. brachygibbosum* has profound effects on the patterns of accumulation of miRNAs, many of which express only at specific stages of infection, and this reprogramming is partly under the control of AGO4 expression.

Phytohormone signaling during the *N. attenuata-F. brachygibbosum* interaction

Disease progression on the susceptible irAGO4 plants was more rapid than on WT plants; this suggests that irAGO4 plants might be perturbed in signal transduction pathways mediating resistance mechanisms, such as those mediated by phytohormones. Jasmonic acid (JA, along with its isoleucine conjugate, JA-Ile) and salicylic acid (SA) have long been implicated as the important phytohormones regulating plant-pathogen interactions (Pieterse et al., 2009): they often act in an antagonistic manner, whereas their action is also predicted to be synergistic/co-operative in regulating immunity of plants against hemibiotrophic fungal pathogens (Sahu et al., 2016). Additionally, a role for abscisic acid (ABA) in modulating plant-pathogen interactions is becoming increasingly evident (Overmyer et al., 2018). To obtain a detailed analysis of how these hormones accumulate during the *Nicotiana-Fusarium* interaction, we conducted time-series experiments (0-72 hpi) to determine the elicitation dynamics of these phytohormones during the course of infection in both WT and irAGO4 plants (Fig. 6). At t_0 (0 hpi), the levels of JA and JA-Ile were extremely low (<1.5 ng per gram fresh mass (FM) of leaf). JA and JA-Ile levels were rapidly increased in response to infection with maximum levels being recorded at 48 hpi in WT plants (Fig. 6). On the other hand, irAGO4 plants accumulated 3-times lower levels of pathogen induced JA, and >2 times lower levels of JA-Ile at 48 hpi (Fig. 6). *F. brachygibbosum* infection elicited similar patterns of the accumulation of ABA and SA in WT and irAGO4 plants (Fig. 6). Thus, silencing *AGO4* specifically compromised pathogen-induced jasmonate accumulations during infection of *N. attenuata*.

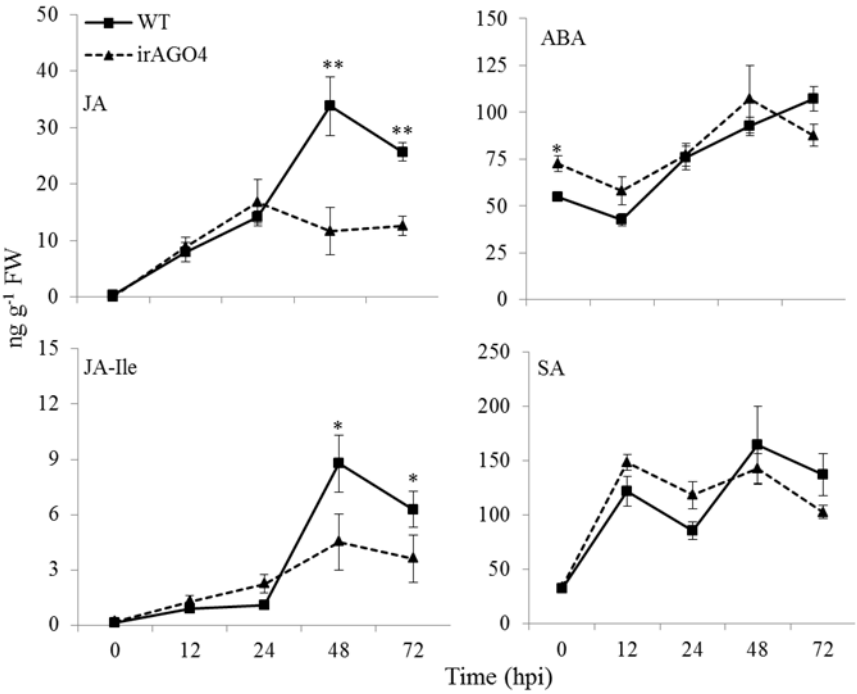

Figure 6.

Figure 6. Silencing AGO4 abrogates *Fusarium*-induced jasmonate accumulation in *N. attenuata*. Jasmonic acid (JA), JA-isolucine (JA-Ile), abscisic acid (ABA) and salicylic acid (SA) were assayed during the time-course of infection (0-72 hpi). irAGO4 plants specifically accumulated significantly lower amounts of JA and JA-Ile after 48-72 hpi, whereas ABA and SA levels did not differ from those of WT plants after infection. Values are means ± SD, and significance was tested with the help of two-way repeated measures ANOVA (Fisher's LSD; $P \leq 0.05$ (*) and $P \leq 0.01$(**)).

Silencing *AGO4* attenuates pathogen-induced transcriptional reprogramming of the JA pathway

In order to understand the molecular basis of compromised jasmonate accumulation in irAGO4 plants during *F. brachygibbosum* infection, we determined the transcriptional response of biosynthetic genes of the JA and JA-Ile pathway (summarized in Fig. 7A) in time-course experiments. *LOX3* is specifically implicated in JA biogenesis in leaves of *N. attenuata* (Halitschke and Baldwin, 2003): irAGO4 plants consistently accumulated lower *NaLOX3* levels during the course of infection (Fig. 7B). Next, *NaOPR3* expression, in WT, was already up-regulated by >2-fold at 12 hpi, and reached a maximum of 4-fold at 24 hpi compared to the 0 hpi controls (Fig. 7B). On the other hand, irAGO4 plants failed to elicit any changes in *NaOPR3*

transcripts over the full time course of 0-48 hpi (Fig. 7B). Similar patterns of significant compromises in pathogen-induced accumulation of *NaAOC* and *NaAOS* in irAGO4 plants (as compared to their respective time-matched WT's) were evident (Fig. 7B). Additionally, we noticed that *NaGLA1* accumulated similar transcript levels in WT and irAGO4 plants (Supplemental Fig. S5). Also, *N. attenuata* encodes another member of the lipoxygenase gene family (*NaLOX2*), which is involved mainly in green leaf volatile production (Allmann et al., 2010). Expression of *NaLOX2* was unaffected by pathogen infection (Supplemental Fig. S5). Thus, highly significantly reduced expression of *LOX3, OPR3, AOC* and *AOS* in time course studies suggested that irAGO4 plants failed to optimally induce the JA biosynthesis pathway, which is consistent with the reduced JA-levels observed after infection (Fig. 6).

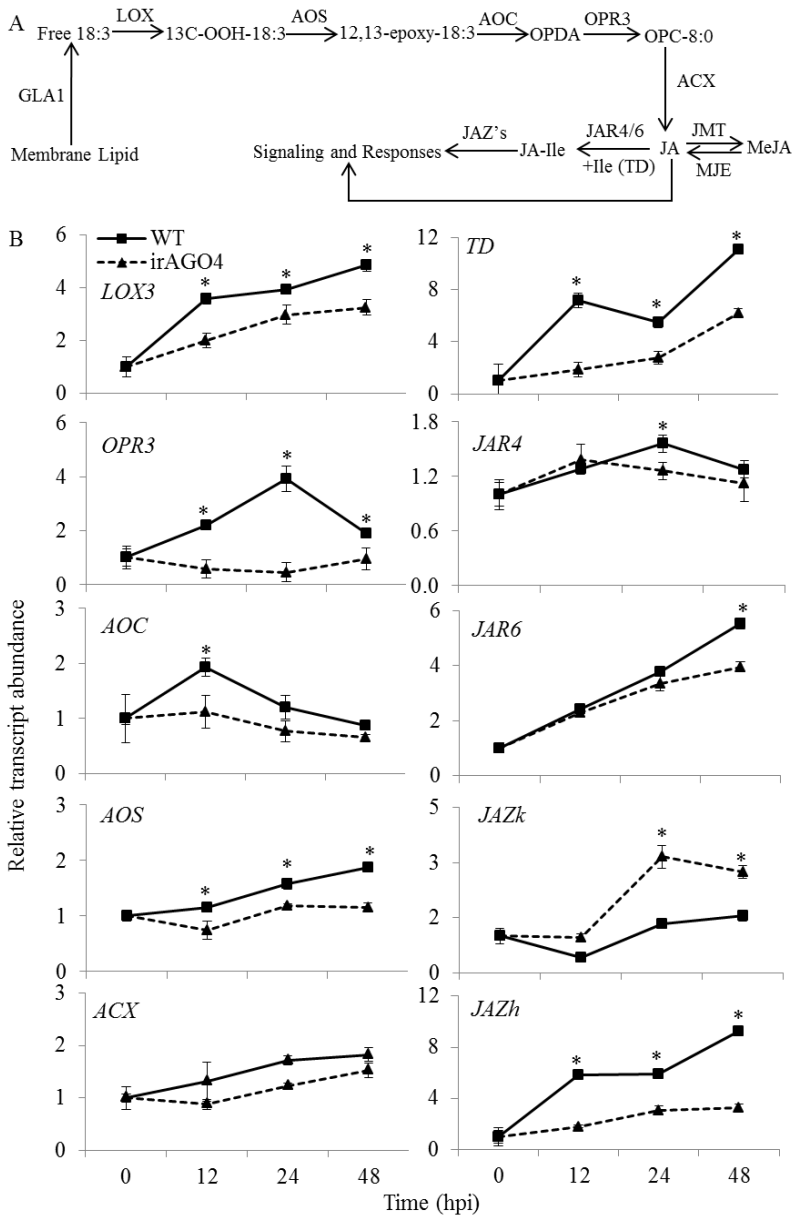

Figure 7.

Figure 7. Elicitation dynamics of JA biosynthesis and signaling genes. A, A simplified scheme of JA-biogenesis and signaling pathway showing the functions of genes investigated below. B, *Fusarium*-induced transcript levels of all the JA-biosynthetic genes (except *ACX*) were significantly different between ir*AGO4* and WT plants in a time course experiment. Transcripts of *ECI* gene was used as internal control for normalization. Transcript level at t_0 was set to 1 and relative abundances were calculated accordingly (two-way repeated measures ANOVA, Fisher's LSD; $P \leq 0.05$; *, significantly different from the respective WT).

Typically, 10-20% of JA is conjugated into JA-Ile, which acts as the canonical signaling molecule in JA signaling (Wang et al., 2007; Stitz et al., 2011). Threonine deaminase (TD) delivers Ile required for this conjugation (Kang et al 2006), and the JA-adenylation reaction during JA-Ile conversion is catalyzed by two members of the JAR gene family (*NaJAR4* and *6*; (Wang et al., 2008). More than 7-11-fold increases in *NaTD* transcripts was recorded in WT plants at 12-48 hpi, whereas irAGO4 plants accumulated significantly lower transcript levels during this time of infection (Fig. 7). Compared to WT, irAGO4 plants had significant reduced levels of *NaJAR4* transcripts at 24 hpi, whereas *NaJAR6* transcript levels were significantly lower at 48 hpi (Fig. 7). These results are consistent with the observed reduced JA-Ile levels after infection (Fig. 6).

Biosynthesis of JA-Ile is connected to the activation of responsive genes through signaling modules that are believed to be centered around the Jasmonate-ZIM domain (*JAZ*) family of proteins (Howe et al., 2018). A large number of JAZ genes are found in *N. attenuata*'s genome and these are thought to provide functional diversity (Li et al., 2016; Howe et al., 2018). In *N. attenuata*, at least 13 JAZ genes are already known (Oh et al., 2012; Lee et al., 2017), but which of these respond to *F. brachygibbosum* infection was unknown. Furthermore, whether JAZ genes are regulated by smRNAs in an AGO4-dependent manner was also unknown. We profiled the elicitation dynamics of these genes during 0-48 hpi time course study, which revealed complex patterns. In WT plants, expressions of 7 JAZs were induced, whereas 4 were repressed during infection (Fig. 7, Supplemental Fig. S5). Transcripts of *NaJAZg* and *NaJAZl* were not detected in the leaves of *N. attenuata* plants. When we compared the profiles of WT and irAGO4 plants during infection, transcript levels of 7 genes were lower in irAGO4 plants, whereas those of *NaJAZk* and *NaJAZc* were higher in irAGO4 plants. *NaJAZb* and *NaJAZm* transcript levels were similar between the two genotypes (Fig. 7, Supplemental Fig. S5). These results show that *JAZ* transcription is complex, a large number of JAZs are reprogrammed in response to infection, and that several of these are under the control of AGO4-modulated pathway.

Three transcription factors, *MYC2*, *WRKY3* and *WRKY6* have been associated to the JA-signaling pathway (Skibbe et al., 2008; Woldemariam et al., 2013), but their roles in the

Nicotiana-Fusarium interaction is less known: patterns of transcriptional response of these genes were largely similar between WT and irAGO4 plants during infection (Supplemental Fig. S6).

Thus, transcriptional profiling revealed that irAGO4 plants were compromised in the elicitation of genes of JA and JA-Ile biogenesis and signaling. These results are consistent with the observed reduced accumulations of JA and JA-Ile in irAGO4 plants during infection.

Exogenous application of JA, methyl jasmonate (MeJA) and OPDA restores irAGO4 resistance to *F. brachygibbosum* infection

To further evaluate if the compromised immunity of irAGO4 plants to *F. brachygibbosum* infection was due to attenuated JA levels, we performed complementation assays. irAGO4 plants were exogenously complemented with 1 mM JA (by 1 mL per plant, spray, until run-off) or methyl-jasmonate (MeJA; 0.15-0.30 µg per plant, applied in lanolin) prior to conducting a pathogen assay. The data was recorded at 5 and 12 dpi. The disease severity of JA and MeJA-supplemented irAGO4 plants were highly significantly reduced to WT levels (Fig. 8, Supplemental Fig. S7). In independent experiments, we also complemented the irAGO4 plants with 50µM OPDA (an important intermediate substrate in JA biogenesis, Fig. 7) and performed pathogenesis assays. Treating plants with OPDA also restored the resistance of irAGO4 plants to WT levels (Fig. 8). We used plants silenced in *AOC* (irAOC) and *OPR3* (irOPR3) expressions (Kallenbach et al., 2012) as positive controls in the OPDA complementation assays, as they are attenuated in the substrates for JA biogenesis: both, irAOC and irOPR3 were highly susceptible to *F. brachygibbosum* infection (Fig. 8). Their enhanced susceptibility, as in case of irAGO4, was restored to WT levels when they were supplemented with OPDA (Fig. 8, Supplemental Fig. S8). Thus, the results of complementation assays confirmed that the enhanced susceptibility of irAGO4 plants was associated with compromised amounts of JA produced during infection.

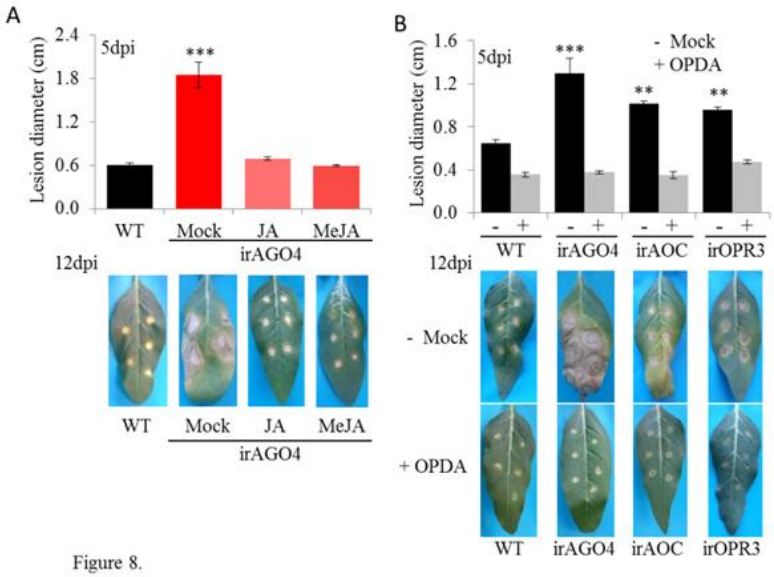

Figure 8.

Figure 8. Exogenous complementation of (A) jasmonic acid (JA, 1mM), methyl jasmonate (MeJA, 7.5µg/mL) and OPDA (50µM; B) rescues pathogenesis phenotype for irAGO4. Data on lesion diameter were recorded at 5dpi, whereas the pictures were taken at 12dpi. Only representative pictures are included. Pictures of several biological replicates are presented in SI Figures S7 and S8. Stars indicate significant differences from WT (ANOVA, $P \leq 0.01$ (**), $P \leq 0.001$ (***)).

Identification of other core components of smRNA machinery during *F. brachygibbosum infection* of *N. attenuata*

Next, we asked which other core components of smRNA machinery might be involved in regulating plant immunity against infection of hemibiotrophic pathogens. Dicer-like (DCLs) and RNA-directed RNA polymerases (RdRs) are two important components of the core smRNA machinery. *N. attenuata* contains 4 DCLs and 3 functional RdR genes (Pandey and Baldwin, 2007; Bozorov et al., 2012). We performed pathogenesis assays with previously characterized lines silenced in expression of *NaDCL2*, *3* and *4* (irDCL2-4; (Bozorov et al., 2012)), and *NaRdR1*, *2* and *3* (Pandey and Baldwin, 2007, 2008; Pandey et al., 2008b). irDCL3 plants were more susceptible to *F. brachygibbosum* infection, whereas silencing *NaDCL2* and *4* did not significantly increase pathogen performance as compared to WT (Fig. 9, Supplemental Fig. S9). Amongst the three RdRs, silencing *NaRdR1* and *NaRdR2* increased the susceptibility of plants, but irRdR3 were comparable in their resistance to WT plants (Fig. 9, Supplemental Fig. S9).

These results suggest that along with *AGO4*, *DCL3*, *RdR1* and *RdR2* act in a pathway that regulates plant immunity. We further asked whether *DCL3*, *RdR1* and *RdR2* regulate similar molecular targets as *AGO4* and profiled the pathogen-induced levels of JA, JA-Ile, SA and ABA after 48 hpi. irDCL3, irRdR1 and irRdR2 plants accumulated only one-fourth of the WT levels of JA and JA-Ile (Fig. 9), whereas, SA levels in these genotypes were similar to those of WT (Supplemental Fig. S10; irRdR2 plants had marginally higher SA as compared to WT plants). Constitutive or pathogen-induced ABA levels were also not compromised amongst WT, irDCL3, irRdR1 and irRdR2 (Supplemental Fig. S10). These results indicate that *AGO4*, *DCL3*, *RdR1* and *RdR2* regulate plant immunity by commonly modulating JA signaling.

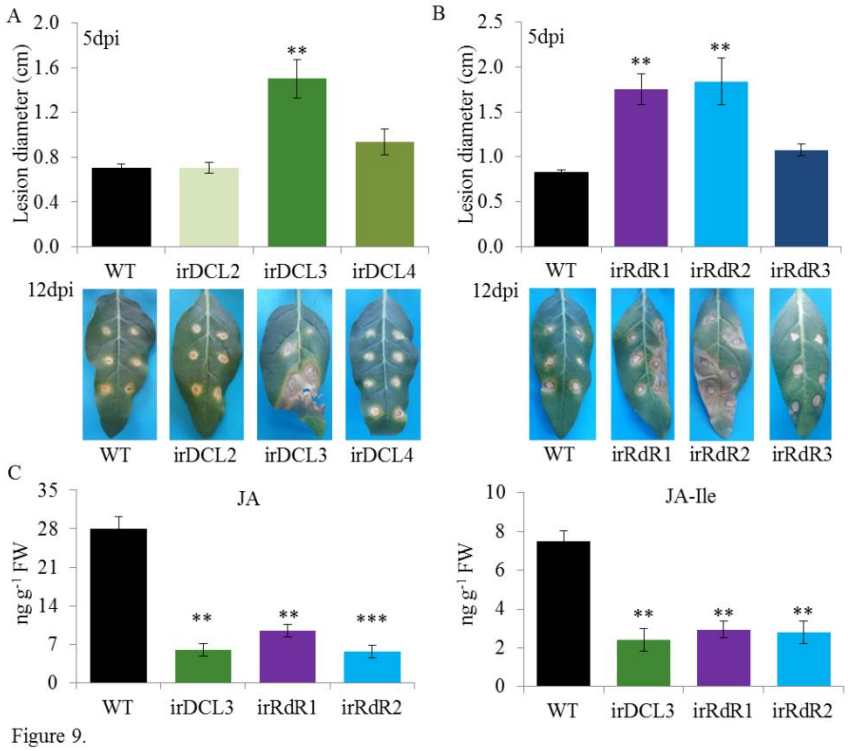

Figure 9.

Figure 9. Plants individually silenced in *RdR1, RdR2* and *DCL3* expression are highly susceptible to *F. brachgibbosum* infection. Evaluation of the lines silenced in the expression of the *Dicer-like* (*DCL*s; A) and three independent *RNA directed RNA polymerases* (*RdR*s; B) reveal that *DCL3, RdR1*, and *RdR2* form the component of the smRNA machinery involved in immune response during infection. Lesion diameters were measured at 5 dpi and pictures were taken at 12 dpi (representative pictures, middle panel). A pictorial record of several biological replicates of plants at 12 dpi is presented in Supplemental

Real-world verification of the function of AGO4-centered smRNA machinery

In order to determine the ecological and functional relevance of AGO4-centered smRNA machinery, we conducted field experiments in the native habitat of *N. attenuata* in the Great Basin Desert (Utah, USA). irAGO4, irDCL3, irRdR1 and irRdR2 plants were planted into an *Alternaria/Fusarium* infected field plot (Fig. 10). Further, irAGO4 plants were crossed with irDCL3 (irAGO4 X irDCL3), irRdR1 (irAGO4 X irRdR1), and irRdR2 (irDCL3 X irRdR2) to generate plants co-silenced in the biogenesis and effector components of smRNA machinery (Supplemental Fig. S11A). These crosses were also planted into the same field plot along with their parents (Fig. 10). The plants grown in the field displayed symptoms of chlorosis, necrosis and wilting (Fig. 10), which ultimately resulted in sudden plant death, as described in (Schuck et al., 2014; Santhanam et al., 2015). Microscopic observations of diseased plants showed fungal colonization, infection cushions and other cytological features (of *Fusarium* pathogens), similar to those displayed by plants inoculated by *Fusarium* in the glasshouse (Fig. 10). First disease symptoms appeared 4 days after planting (DAP) in the field, and the disease progression was recorded at an interval of 3 days, till 25 DAP. Disease symptoms were noticed on ≥10% of the WT plants on 13 DAP; at this time, ≥45% of irAGO4 plants already displayed symptoms (Fig. 10). By 16 DAP, ≥60% of irAGO4, irAGO4 X irDCL3 and irAGO4 X irRdR2 plants were already diseased, while ≤20% WT plants showed disease symptoms. Similarly, at the end of experiments, ≥85% of irAGO4 plants had died while a cumulative death of 32.7% WT plants was recorded at 25 DAP (Fig. 10). All the other genotypes (irDCL3, irRdR1, irRdR2 and the three crosses) suffered ≥50% death (Fig. 10). Thus, plants compromised in the AGO4 effector and biogenesis (DCL3, RdR1 and RdR2) components were more susceptible to native pathogens present in the field (Fig. 10); irAGO4 plants were most susceptible.

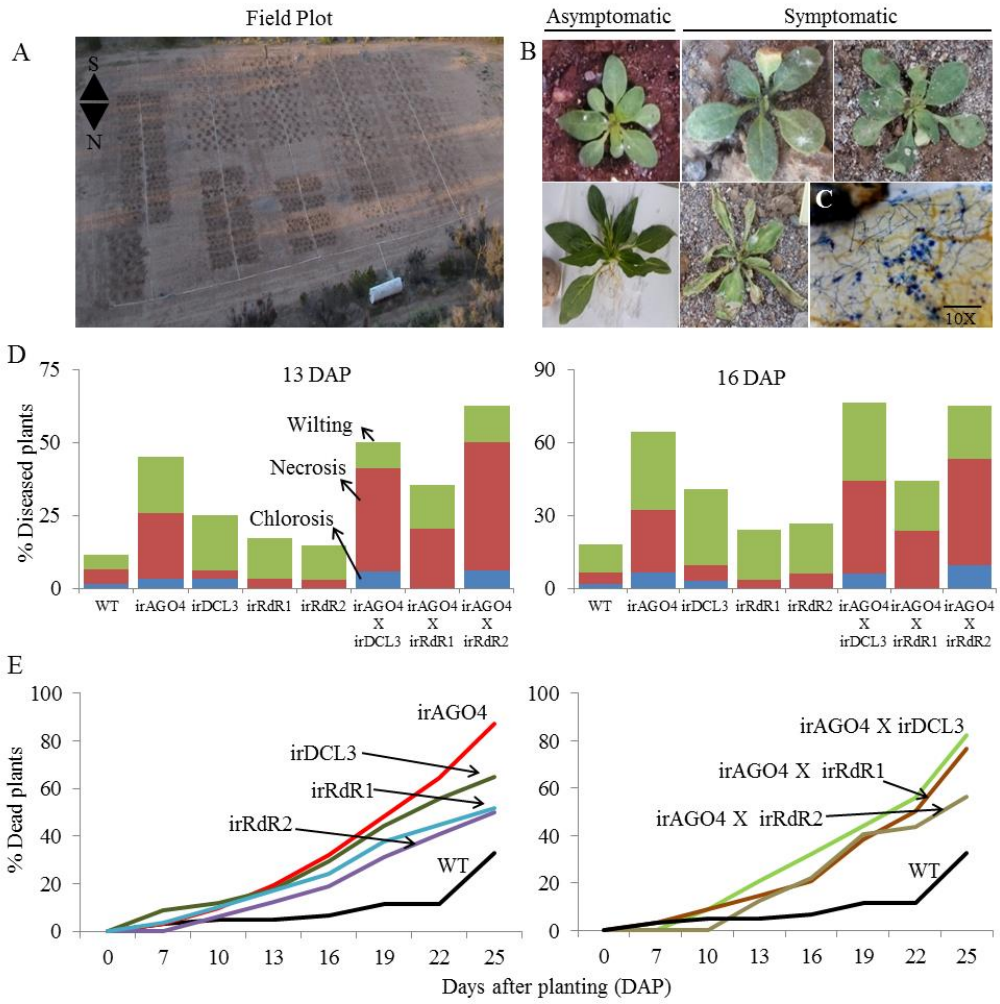

Figure 10.

Figure 10. Real-world test of the inferred smRNA machinery involved in immune response during pathogen infection in *N. attenuata*. A shows the field plot in *N. attenuata*'s native habitats in the Utah deserts, USA (N 37.1412, W 114.0275). B, Representative pictures of the asymptomatic and symptomatic plants in the field. C, Microscopic observations of field-grown symptomatic plants show fungal mycelium colonizing the leaves of *N. attenuata* plants and forming infection cushions similar to those grown in glass house (Fig. 2), indicating presence of *Fusarium* species. D, Disease progression was recorded by evaluating various disease symptoms such as chlorosis, necrosis and wilting in WT, irAGO4, irDCL3, irRdR1, and irRdR2 plants 13 and 16 days after planting (DAP). E, Cumulative plant death was recorded for WT, irAGO4, irDCL3, irRdR1, irRdR2 and the crosses of irAGO4 X irDCL3, irAGO4 X irRdR1, irAGO4 X irRdR2 over the study period of 25 DAP compared to the total number of plants transplanted into the field plot (day 0). irAGO4 plants were the most susceptible to the natural fungal disease complex.

In order to evaluate whether this susceptibility of the irAGO4 and other genotypes planted into the field was also associated with compromised jasmonate signaling, we profiled the accumulation of phytohormones from asymptomatic and symptomatic plants, grown under field conditions for 16 and 25 days, respectively. Symptomatic irAGO4 plants accumulated 5-fold lower levels of JA and JA-Ile than the symptomatic WT (Fig. 11). Diseased irDCL3, irRdR2 and irRdR1 plants were also highly significantly attenuated in JA and JA-Ile levels as compared to the diseased WT (Fig. 11). SA and ABA accumulations were not compromised in genotypes silenced in various components of smRNA machinery (Supplemental Fig. S11B). These results are consistent with the hypothesis that the AGO4-centered smRNA machinery is essential for plant resistance against invading pathogens in natural habitats by modulating jasmonate pathway.

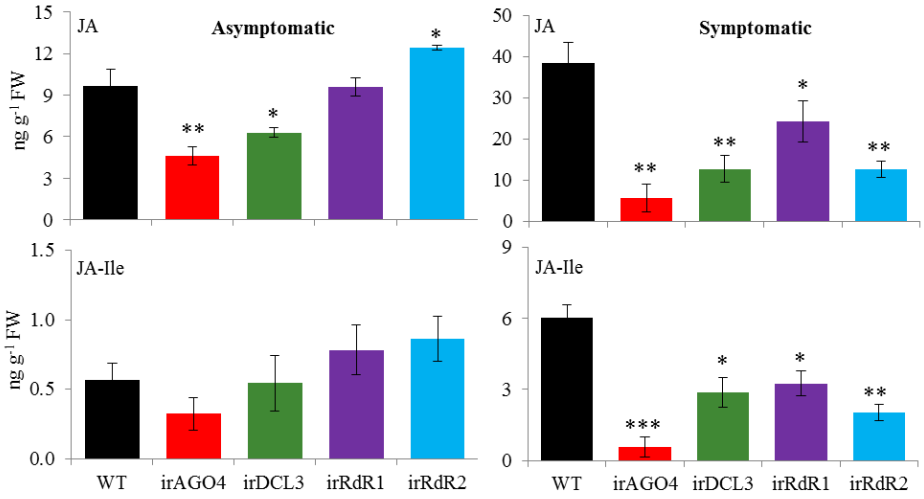

Figure 11.

Figure 11. Phytohormone profiles of field grown plants. Evaluation of jasmonic acid (JA) and jasmonic acid isoleucine (JA-Ile) contents of both, asymptomatic and symptomatic field grown plants. Error bars represent SEM; significant differences between the WT and the RNAi lines were evaluated with the help of ANOVA; $P \leq 0.05$ (*) and $P \leq 0.01$ (**).

Mapping interaction between jasmonate pathway and AGO4-dependent miRNAs

Metabolite profiling, gene expression, complementation studies and field investigations consistently showed that modulation of jasmonate pathway was critical for *N. attenuata* to deploy reliable resistance against hemibiotrophic phytopathogens such as *F. brachygibbosum*, and this was modulated in an AGO4-dependent manner. Reprogramming of miRNA expression

after infection in an AGO4-dependent manner further indicated a plausible miRNA-jasmonate interaction module. An intensive network of interaction of AGO4-dependent miRNAs and mRNAs of genes of the disregulated jasmonate pathway was uncovered. We mapped the AGO4-dependent miRNA-binding sites on to the mRNAs of 18 genes of the jasmonate pathway. Seventy-one miRNAs showed binding sites, of which 67 were differentially accumulated between the WT and irAGO4 plants (Fig. 12). At least 45 predicted miRNA-mRNA interactions showed inverse expression patterns between the mRNAs and miRNAs. In other words, when a miRNA was up-regulated, its target was down-regulated in irAGO4 plants compared to WT after pathogen infection, indicating those might indeed be regulated by miRNAs (Fig. 12).

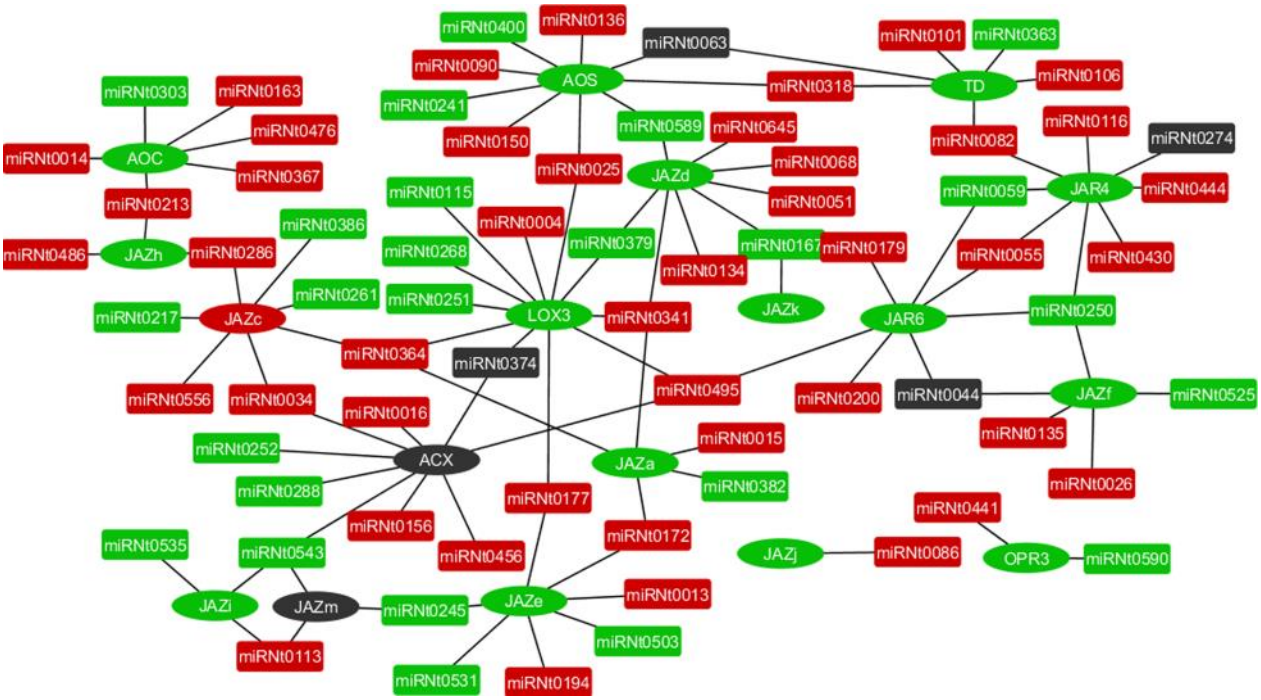

Figure 12. AGO4-dependent smRNA-mediated regulation of jasmonate signaling during interaction of *N. attenuata* and the hemibiotrophic *F. brachygibbosum* pathogen. AGO4-dependent miRNA-target network of JA-pathway genes was constructed. Red, blue and black represent up-, down- and no-regulation, respectively, in irAGO4 compared to WT. Gene sequences were obtained from NCBI (accession numbers are provided in Supplemental Table S5), whereas miRNA sequences were from this study (Fig. 4, Supplemental Table S2). miRNA target predictions were made as described earlier (Srivastava et al., 2014; Pandey et al., 2018). Network was constructed with the help of Cytoscape 3.6.1 tool.

DISCUSSION

Fusarium infection results in the reprogramming of the expression of thousands of host genes (Lanubile et al., 2014; Huang et al., 2016). *Fusarium* is also an important challenge in natural habitats as it rapidly wipes out substantial portions of plant populations (Schuck et al., 2014; Santhanam et al., 2015). Here, we demonstrate the ecological function of *N. attenuata's* AGO4 in regulating jasmonate signaling and resistance against the naturally occurring hemibiotrophic fungal pathogen, *F. brachygibbosum*. Only the loss of AGO4 (and not any other AGOs) increased the susceptibility of *N. attenuata* to *F. brachygibbosum* infection. The specificity of NaAGO4 function in regulating *Fusarium* resistance is consistent with: (i) The outcomes of the kinetic studies where only *AGO4* was transcriptionally reprogrammed after pathogen infection; (ii) the observation that irAGO4 plants did not display any growth or developmental abnormalities (Supplemental Fig. S1), (iii) were indistinguishable from the WT plants in defending themselves against the insect herbivores, and (iv) *AGO4* did not responded transcriptionally to other biotic elicitors, such as of herbivory (Pradhan et al., 2017). Furthermore, irAGO4 plants were specifically compromised in pathogen-induced jasmonate biogenesis and signaling (but not in SA or ABA). Infection of *F. brachygibbosum* extensively altered the host smRNome, including the miRNAs, in a manner that depended on the infection stage and *NaAGO4* expression. We further demonstrate the real-world relevance of our findings by showing that plants compromised in AGO4-centered machinery were abrogated in jasmonates, were more susceptible and rapidly died when planted into a field plot teaming with fungal pathogens (Schuck et al., 2014; Santhanam et al., 2015). The underlying biochemical mechanisms warrant further investigation.

We also show that *DCL3*, *RdR1*, and *RdR2* are the other members of the smRNA core machinery that were essential for an unabrogated JA signaling and resistance against *F. brachygibbosum*. In *N. attenuata*, *AGO4, DCL3, RdR1* and *RdR2* may act cooperatively to deploy resistance against the hemibiotrophic pathogens in nature. Whereas, in *Arabidopsis*, *AGO4* is essential for resistance against the *Pseudomonas syringae* bacteria, in a manner independent of *DCL3*, *RdR2* or other components of RNA-dependent DNA methylation (RdDM) pathway (Agorio and Vera, 2007). As AGO4 can mediate methylation, another biological function of AGO4 is to defend plants against DNA viruses (Raja et al., 2008). In *N.*

benthamiana, AGO4 is required for systemic silencing and control of viral transcripts (Jones et al., 2006). AGO4 also controls megaspore formation in Arabidopsis (Hernández-Lagana et al., 2016). In rice, knock-down of AGO4 homologues resulted in dwarfism due to changes in methylation mediated by 24 nt siRNAs (Wei et al., 2014). In *N. attenuata*, although we observed changes in 24 nt smRNA populations upon silencing *AGO4*, it did not affect plant height (or the other growth or development-related traits), nor did the release of irAGO4 plants in nature reveal any viral symptoms. These observations further highlight the biological and ecological relevance of AGO4 machinery that is specialized in modulating resistance against complex fungal diseases in nature by regulating JA signaling.

In Arabidopsis, in response to *P. syringae* bacteria and SA treatments, Dowen et al. explored the genome-wide dynamics of DNA methylation and searched for its correlations with gene expression (Dowen et al., 2012): they found that differentially methylated regions were accompanied with up-regulations of 21 nt siRNAs within repetitive sequences or transposons, which could regulate neighboring genes. Some components of the RdDM pathway have indeed been implicated to have a role in plant immunity in *Arabidopsis*, but whether their effect on disease related gene expression is direct or indirect is unclear (López et al., 2011). López et al report that Pol V defective mutants (but not Pol IV mutants) had enhanced disease resistance to *P. syringae* due to enhanced SA-mediated defenses that are effective against this bacterium. The conclusions on the involvement of RdDM in SA-mediated plant defenses were largely based on the studies using marker genes such as *PR1* (López et al., 2011). We show that infection of *F. brachygibbosum* elicits changes in SA accumulation, but that these patterns are unaffected by silencing of *AGO4, DCL3* or *RdRs*. These results were verified in the field studies: the field grown WT, irAGO4, irDCl3, irRdR1 and irRdR2 plants accumulated largely similar SA (and ABA) levels, but were severely attenuated in jasmonate accumulations. Thus, our study further highlights the importance of verifying the biological functions of genes under real-world scenarios. Our study also provides hints on how phytohormone signaling may shape the interaction of *N. attenuata* with its natural pathogens such as *Fusarium* species, by cooperatively eliciting JA and SA pathways. Indeed, such cooperative elicitations have been recorded in other hemibiotrophic fungal interactions in agro-ecological habitats (Sahu et al., 2016).

Phytohormone signaling networks, comprising mainly of SA, JA, ABA and auxin, have emerged as key regulators of host interaction with *Fusaria*. During infection of *F. oxysporum,* SA acts as a positive regulator of resistance, may promote resistance, and could reduce susceptibility (Berrocal-Lobo and Molina, 2008; Xue et al., 2014; Di et al., 2016). It is hypothesized that SA signaling might be activated at late stages of infection of Arabidopsis with *Fusarium*. Instead, in the *N. attenuata-F. brachygibbosum* interaction, we noticed a rapid elicitation of SA within 12-48 hpi, which is not regulated by the NaAGO4-dependent machinery.

On the other hand, in other *Fusarium*-host interactions, JA signaling might promote resistance as well as susceptibility in complex manners, and that JA signaling might be 'hijacked' by *F. oxysporum* to manipulate its host (Di et al., 2016). In Arabidopsis, JA biogenesis is not regarded as being crucial for defense against *Fusarium* (Thatcher et al., 2009; Di et al., 2016), however, *COI1* was found to influence its interactions with *F. oxysporum* (Thatcher et al., 2009; Cole et al., 2014). The caveat of such (lab-based) studies have been that the phenotype of *coi1*-mutant depended on the method used for inoculating the pathogen: studies employing uprooted plants allow for additional entry points during pathogen inoculation and promote strong vascular colonization by the pathogen (Thatcher et al., 2009; Cole et al., 2014; Di et al., 2016). In *N. attenuata's* infection with *F. brachygibbosum*, we observe a central role of JA biogenesis and that JA positively regulates resistance: the JA biogenesis pathway was upregulated in WT plants during infection, and plants compromised in various steps of JA biogenesis, such as the loss of AOC- or OPR3-functions, showed increased susceptible, which was comparable to that of irAGO4 plants. The increased susceptibility of irAGO4 (as well as irDCL3 and irRdR1 and 2) plants were consistently associated with compromised pathogen-induced JA and JA-Ile levels, and irAGO4 plants failed to optimally induce expression of most of the JA biogenetic genes upon *Fusarium* infection. Further, the increased susceptibility of these JA-compromised plants could be rescued by exogenous complementation with a substrate for JA biosynthesis (OPDA), as well as by JA and methyl-jasmonate. Such multiple complementation assays lessen the possibility that the complemented resistance phenotypes might be due to the high doses of JA used or direct fungal toxicity of treatments.

In Arabidopsis, it is still unclear how JA signaling is reprogrammed to promote disease, and the dependency on JA for infection may be governed by the strain of *Fusarium* used in the

studies (Cole et al., 2014; Di et al., 2016). In contrast, we show that the host-*Fusarium* interaction in nature is indeed governed by JA and that compromised JA levels is associated with increased susceptibility, which is mostly *COI1*-independent in *N. attenuata* (Luu et al., 2015). Our data suggests that during pathogen infections, the JA pathway is partly regulated by the AGO4-dependent smRNA machinery, which includes a network of miRNAs that could plausibly regulate components of JA biogenesis and signaling.

This investigation advances our understanding on the biological functions of AGOs, in particular during host-environment interactions, specifically of AGO4 by expanding its arena to the resistance of hemibiotrophic fungal pathogens. We propose that when plants are stressed, they recruit specific smRNA pathways by eliciting AGOs in a stimulus-dependent manner (Alazem et al., 2017; Pradhan et al., 2017). We infer that infection of *Nicotiana* by hemibiotrohic *Fusarium* pathogens specifically elicits AGO4 activity, which could rapidly help in pathogen-triggered reprogramming of smRNAs, including the miRNAs and their isomiRs. Furthermore, pathogen-infection elicits *RdR1, RdR2* and *DCL3*, to plausibly help in generation/amplification of pathogen induced smRNAs. We hypothesize that the pathogen-induced smRNAs in *N. attenuata* could regulate the expression of JA-biogenesis and -signaling genes, plausibly by (a) post-transcriptionally modulating the levels of mRNAs via miRNAs, and (b) transcriptionally, for example, by changing the methylation status of relevant portions of DNA (Dowen et al., 2012). At the genomic scale, during various stages of infection, a combination of both the processes could provide the much-needed, stimulus-dependent, effective and temporally dynamic modulation of gene expression (Supplemental Fig. S12). It is plausible that AGO4 could act as a facilitator of such crosstalk of transcriptional and post-transcriptional regulation of gene expression. Such a model requires further investigation by generating genome-wide methylomes in time-course experiments during pathogenesis, and overlaying them with stage-specific transcriptomes, along with the time-matched degradome analysis, at each of the infection stages. Further investigations are also needed to explore the crosstalk between JA and SA signaling during *F. brachygibbosum*'s infection of *N. attenuata*.

MATERIALS AND METHODS

Plant material and growth conditions

Seeds of the 30th and 31st generations of an inbred *N. attenuata* wild-type plants (WT) originally collected from the native south western Utah, USA were used for all experiments. Transgenic irAGO lines have been described previously (Pradhan et al., 2017). Lines silenced in *OPR3* and *AOC* are described in (Kallenbach et al., 2012), whereas, lines silenced in expression of *DCL*s and *RdRs* 1-3 were from following studies (Pandey and Baldwin, 2007, 2008; Pandey et al., 2008b; Bozorov et al., 2012). As all of these RNAi lines are homozygous and harbor single insertions of the T-DNAs, which provide powerful silencing of the targeted genes even when expressed in hemizygous plants, *irAGO4 X irDCL3, irAGO4 X irRdR1, irDCL3 X irRdR2* were crossed to generate plants co-silenced in expression of both genes. Seeds from WT and all the transgenic plants were germinated in Gamborg B5 medium (Krügel et al., 2002). Seeds were germinated and plant populations were grown and maintained under a day/night cycle of 16 h (26 to 28°C)/8 h (22 to 24°C) (Krügel et al., 2002; Halitschke and Baldwin, 2003; Onkokesung et al., 2012) for 30 days.

Fusarium brachygibbosum culture, creation of disease conditions and bioassays for determining susceptibility

F. brachygibbosum Padwick Utah 4 strain, used in this study, was isolated from diseased *N. attenuata* plants growing in the native habitats of Utah, USA, and is an important component of the disease causing fungal complex in nature (Schuck et al., 2014; Luu et al., 2015). The fungal cultures were maintained on potato dextrose agar (PDA, Fluka Analytical, Steinheim, Germany) at 25 ^{0}C in the dark with repeated re-isolation from infected plants (Luu et al., 2015).

Mechanical damage created due to uprooting of plants during the inoculation of *Fusaria* pathogens may significantly enhance disease development and phenotypes of the genotypes that are inoculated (Thatcher et al., 2009; Cole et al., 2014; Di et al., 2016). Therefore, in order to avoid the confounding effects of wounding and pathogen infection, we inoculated the *N. attenuata* plants without creating any mechanical damage. Spores of *F. brachygibbosum* were harvested from 12-15 day old pure cultures grown on PDA. Droplets (10 µL) of this spore suspension (10^6 spore mL^{-1}) were inoculated on the '+2-leaves' of rosette-stage *N. attenuata*

plants (defined in: (Van Dam et al., 2001)) under high humidity (≥80%) in a growth chamber under controlled conditions (day/night cycle of 16 h (26°C)/8 h (22°C) with 80 ± 5% humidity). First disease symptoms appeared within 3-4 dpi.

During the bioassays for determining the susceptibility of plants to *F. brachygibbosum* infection, high humidity was maintained throughout the experiment. Disease symptoms were assessed at 5 dpi and 12 dpi by determining lesion size in 10-12 independent biological replicates per genotype per treatment condition.

Initial steps in the infection of *F. brachygibbosum* on the WT and irAGO4 plants were microscopically studied in a time-course experiments: +2 leaves were inoculated with the *F. brachygibbosum* spore suspension at t_0 and microscopic observations were made at 12, 24, and 48 hpi, after removing the chlorophyll by soaking it into the de-staining solution (1:1 absolute ethanol and glacial acetic acid (v/v)) for 30h. Subsequently, the leaves were washed in distilled water for 1h, followed by fixation in a solution containing equal proportion of lactic acid, glycerol and water, for 2h. Next, the leaves were stained using 0.1% trypan blue for 2h. Excess stain was removed by rinsing with water briefly followed by mounting on the slides using lactoglycerol. Zeiss Imager.Z1 with Axiocam HRC (Carl Zeiss) was used for the microscopic analysis.

Plant treatments and sampling of plant material

In order to understand molecular changes elicited by *F. brachygibbosum* infection in WT and irAGO4 plants, time course experiments were conducted. Fully expanded rosette-stage plants of all genotypes were droplet-inoculated with *F. brachygibbosum* spore suspension (10 µL, 10^6 spore mL^{-1}). Four independent biological replicates at 5 time points (0, 12, 24, 48, and 72 hpi) were harvested in liquid nitrogen and stored at -80°C until further use for phytohormone profiling, gene expression and smRNome profiling studies.

For the JA complementation experiments, 1 mM aqueous solutions of JA (Sigma Aldrich) were used (Rayapuram and Baldwin, 2007; Pandey et al., 2008a). JA was first dissolved in a small amount of ethanol and made up to a concentration of 1 mM with distilled water. JA was sprayed on the entire plant until run-off. No phytotoxic affects were observed between the

JA-sprayed and the control plants, which were mock-sprayed. 10 biological replicates from both genotypes were used in each of the treatment groups.

For complementation experiments with MeJA treatments, 7.5 µg of MeJA (Sigma Aldrich) was dissolved in 1 mL of melted lanolin (Acros Organics), and 20 µL of this lanolin paste, containing an equivalent of 0.15-0.30 µg of MeJA, was applied per leaf (Baldwin et al., 1996; Halitschke et al., 2000). An aliquot of 20 µL of pure lanolin was used in control treatments (Baldwin et al., 1996; Halitschke et al., 2000). Ten biological replicates from each of the genotypes were used.

OPDA complementation experiments were conducted by using 50 µM aqueous solutions of OPDA (Larodan Fine Chemicals) (Scalschi et al., 2015). OPDA was first dissolved in a small amount of ethanol and made to a concentration of 50 µM with distilled water. OPDA was sprayed on the entire plant until run-off (Scalschi et al., 2015). Control plants were sprayed with distilled water. 10 biological replicates from both genotypes were used in both treated and untreated groups.

Evaluation of plant-pathogen interactions under field conditions

WT, irAGO4, irDCL3, irRDR1, irRDR2, and the three crosses (irAGO4 X irDCL3, irAGO4 X irRdR1, irDCL3 X irRdR2) were planted in a paired design (each transgenic line paired to WT) into the experimental field plot in the natural habitat of *N. attenuata* in the southwestern United States, at the Lytle Preserve research station (Santa Clara, Utah, USA: N 37.1412, W 114.02). Seeds were directly germinated on 'jiffy' pots (Jiffy 703, jiffygroup.com) in the natural habitat of the Great Basin Desert for 25 days. These 25 day old seedlings were transplanted to the irrigated field plot that naturally harbors a complex pathogen load, dominated by *Fusarium* (Schuck et al., 2014; Santhanam et al., 2015). Plants were regularly monitored at an interval of 3 days for disease symptoms for 7-25 days after transplanting into the field. Data on the number of plants showing chlorosis, necrosis or wilting symptoms as well as cumulative deaths over time was recorded (Santhanam et al., 2015).

Asymptomatic and symptomatic plants, grown under the field conditions, were harvested at 16 and 25 days after transplanting, respectively, and stored on dry ice until further analysis.

Phytohormone measurements were made on leaves of 6 independent biological replicates from each of the genotypes.

Transcript accumulation by quantitative real-time PCR

To determine the changes in transcript accumulation of *AGO*s in leaves after pathogen infection, 3 to 4 biological replicates of +2 leaves of *N. attenuata* plants were harvested at 0, 12, 24, and 48 h after infection. Total RNA was isolated using the TRIZOL method following the manufacturer's instructions (Ambion, Life Technologies, Carlsbad, CA, USA), and DNA traces were removed with DNase I (DNA free kit, Ambion). cDNA synthesis (Super Script II Reverse Transcriptase, Invitrogen), and qPCR (qPCR core kit for Taykon^{TM} SYBR master mix, Eurogentec) were done following the manufacturer's protocol. qPCR assays were performed using gene-specific primers (designed with the help of Primer Express software v 3.0.1 (http://www.appliedbiosystems.com, Supplemental Table S5) on cDNA templates corresponding to 50 ng total RNA before reverse-transcription. The *N. attenuata* sulfite reductase (*ECI*), a housekeeping gene, was used as an endogenous reference (Bubner et al., 2004). The $2^{-\Delta\Delta CT}$ method was used for data analysis (Bubner et al., 2004). For determining relative transcript abundances, levels corresponding to time point 0 hpi (controls) were set to 1 (as reference) and relative expressions of genes at various time points were determined (Bubner et al., 2004; Pandey and Baldwin, 2007; Bozorov et al., 2012).

Evaluation of *AGO4*-dependent smRNome

To determine the composition and changes of pathogen-induced, *AGO4*-dependent smRNome of *N. attenuata*, deep sequencing was performed on +2 leaves of rosettes of WT and irAGO4 plants in time-course experiments at 0, 12, 24 and 48 hpi of *F. brachygibbosum* in triplicates. Data was analyzed following the already optimized pipeline for *N. attenuata* smRNome (Pandey et al., 2018). Briefly, clean reads, in the range of length of 15-30 nt were populated and retained after quality control measures were implemented, such as filtering out low quality reads, and discarding reads with short stretch of 6 nucleotide (Pandey et al., 2008a). Next, the clean reads were aligned to Rfam database (ftp://ftp.sanger.ac.uk/pub/databases/Rfam) to annotate and remove the structural RNAs such as tRNA, rRNA, snoRNA and snRNA. Using

Bowtie with *-norc* parameter (no reverse complement (Langmead et al., 2009)), the reads were mapped to *N. attenuata* transcriptome and discarded. Reads existing in at least two of the three replicate for each condition/time point were retained for further analysis (Pradhan et al., 2017; Pandey et al., 2018). These 'miRNA-mappable reads' were aligned to the *N. attenuata* genome sequence (Xu et al., 2017) using Bowtie with a maximum of two mismatches. The pipeline of mirDeep2 v2.0.0, with default parameters (Friedländer et al., 2012), was used to identify novel and conserved miRNAs amongst the *Viridiplantae* miRNAs deposited in miRBase 21.0 (www.mirbase.org). For analysis of 24 nt smRNAs, these were size selected and analyzed for differential accumulations (described below).

Differential expression of smRNAs

Differential accumulation of smRNAs during pathogen infection was analyzed following the method recently described (Pandey et al., 2018). The raw counts of the smRNAs were normalized using RPM (reads per million) method (Jia et al., 2014). Medians were calculated, and differential accumulation was evaluated at the three time-points, and between genotypes by performing pairwise comparisons on the RPM values (Pradhan et al. 2017, Pandey et al. 2018). Significant differences were tested with the help of Chi-square test at P-value ≤ 0.05 after Benjamini-Hochberg (Benjamini and Hochberg, 1995) multiple correction (Li et al. 2016). Reads with the count >2 in at least one comparison were considered for this analysis (Pradhan et al., 2017; Pandey et al., 2018). Analysis of differential accumulation of the isomiRs was done as recently described (Pandey et al., 2018).

Phytohormone extraction from glasshouse and field-grown plants

For analysis of phytohormones (JA, JA-Ile, ABA, and SA) at 5 time points (0, 12, 24, 48 and 72 hpi) from glasshouse experiments as well as from field-grown plants, around 100 mg of frozen, fine-powdered leaf tissue was homogenized with 1mL of extraction buffer [ethyl acetate containing 1µL of the internal standard mix (D_2-dihydro-JA, D_5-JA, 50ng/µL; D_6-ABA, D_4-SA, $^{13}C_6$-JA-Ile, 20ng/µL)] in a GenoGrinder for 1min at 1200 strokes/min (Bonaventure et al., 2011; Oh et al., 2012). Samples were centrifuged at 16,100g for 20 min at 4°C and the supernatant was transferred into a fresh 2 mL microcentrifuge tube. To the residue, 0.5 mL of ethyl acetate

(without internal standards) was added and processed in a GenoGrinder for 1 min at 1200 strokes/min (setting: 1x at 200). After centrifugation of samples at 16,100g for 20min at 4°C, the supernatants were pooled. The samples were placed in a vacuum concentrator (Speed-Vac) at 30 °C and the dried residues were dissolved in 0.5 mL of 70% methanol (v/v) for analysis on an LC-ESI-MS/MS (Varian 1200 Triple-Quadrupole-LC-MS system; Varian) as previously described (Bonaventure et al., 2011, Oh et al*.,* 2012). The samples were injected in a ProntoSIL column (C18-ace-EPS, 50 × 2 mm, 5 µm, 120 Å; Bischoff) connected to a pre-column (C18, 4 × 2 mm; Phenomenex). Gradient mode was used with mobile phases 0.05% formic acid; 0.1% acetonitrile in water (solvent A) and methanol (solvent B) with the following conditions: time/%B/flow (mL/min); 0/15/0.4; 1/15/0.4; 1.5/15/0.2; 2.5/15/0.2; 4.5/98/0.2. Compounds were detected in the ESI negative mode with the help of multiple-reaction monitoring (MRM) method (Bonaventure et al., 2011, Oh et al*.,* 2012).

Target prediction and mapping of miRNAs on mRNAs

In order to get better insight into the biological roles of miRNAs in regulating jasmonate signaling during *Nicotiana-Fusarium* interaction, we determined the putative targets of the miRNAs in genes of JA biogenesis and signaling pathway (Pandey et al., 2019). We adapted approaches used previously (Pandey et al., 2008a; Pradhan et al., 2017; Pandey et al. 2019) for binding site identification, employing psRNATarget (Dai and Zhao, 2011; Srivastava et al., 2014). Network of interaction between the miRNAs and the mRNAs of JA biogenesis and signaling genes was visualized with the help of Cytoscape (Shannon et al., 2003; Pandey et al., 2019).

Statistical analysis

Data were analyzed using StatView software. Caterpillar assay, phytohormone, secondary metabolite and gene expression data were analyzed by ANOVA (repeated measures wherever applicable) at a significance level of $p \leq 0.05$.

Accession numbers

The smRNA sequencing data is deposited at NCBI under the BioProject database with BioProject ID PRJNA510758. Complete sequence of the pRESC8AGO4 cloning vector is submitted at NCBI with the GenBank accession number MK317973.

Supplemental Data

Following supplemental data is included.

Supplemental Figure S1. No abnormalities in development and growth were evident in plants silenced in *AGO4* expression. Rosette diameter, number of rosette leaves, plant height, total chlorophyll content and number of flowers of the WT plants were similar to the plants of the two independently transformed irAGO4 lines (021-2-6 and 903-3-9, respectively) under pathogen-free conditions.

Supplemental Figure S2. Microscopic observations of *F. brachygibbosum* reveal infection structures on plant surface. Light microscopy was performed after de-staining chlorophyll and staining with trypan blue. A, Germinating spores align themselves towards stomata and in parallel to the junctions of epidermal cells, indicating initial polarity in spore germination/hyphae movement. B, Hyphae penetrate the stomata, which are heavily colonized by pathogen. The runner hyphae (RH) formed is septate (S). The surface is colonized by numerous short hyphae that spread and appear to penetrate inside the hosts (infection hyphae, IH). Foot structures (FS, also shown as insert) are also visible. C, Numerous infection cushions, of various sizes are easily visible throughout the surface, near which the necrosis in plant cells was also observed.

Supplemental Figure S3. Study of 24 nt smRNAs in AGO4 and WT plants at various stages of infection. A, Distribution of 24 nt smRNAs in AGO4 vs WT samples at 0, 12, 24 and 48 hpi, as visualized with the help of scatter plots. B, Principal component analysis (PCA) of siRNAs common to irAGO4 and WT show that silencing of AGO4 had profound effects on siRNA accumulation.

Supplemental Figure S4. Principal component analysis (PCA) of the accumulation of conserved (A) and novel (B) miRNAs during infection of irAGO4 and WT.

Supplemental Figure S5. Dynamics of transcript accumulation in genes of Jasmonic acid (JA) pathway during pathogen infection. Biogenesis (*GLA1*, and *LOX2*) and signaling genes such as of *JAZ* (*JASMONATE-ZIM-DOMAIN PROTEIN*) genes, encoding for the key regulators in the JA-pathway are shown (*, **, and *** show significant difference from the respective WT at $P < 0.05$, 0.01 and 0.005, respectively, ANOVA, n=4).

Supplemental Figure S6. Three transcription factors, known to regulate JA signaling, show similar patterns of transcript accumulation in irAGO4 and WT plants during infection suggesting that their expression was not compromised during pathogenesis in irAGO4 plants.

Supplemental Figure S7. Phenotypes of 12 dpi (days post inoculation) symptoms on wild type (WT) and *AGO4*-silenced plants (irAGO4) and when irAGO4 were complemented with jasmonic acid (JA) and methyl jasmonate (MeJA). 4 random replicates (other than one presented in Figure 8A) are shown.

Supplemental Figure S8. Phenotypic representation of disease at 12 dpi (days post inoculation) on the WT, irAGO4, irAOC and irOPR3 plants that were not complemented (buffer treated mock, left panel) or complemented with OPDA. 4 random replicates (other than one presented in Figure 8B) are shown.

Supplemental Figure S9. Characterization of plants silenced in expression of the three *Dicer like* genes (*DCL*'s; A) and *RNA-directed RNA polymerase* genes (*RdR*'s; B) against 12 days infection of *F. brachygibbosum*. Four randomly chosen replicates (other than the one's in Fig. 9) are presented.

Supplemental Figure S10. Evaluation of salicylic acid (SA) and abscisic acid (ABA) levels after 48 hpi of *F. brachygibbosum* in irDCL3, irRdR1, and irRdR2 as compared to WT. Infection induced the accumulation of both the hormones in all the four genotypes. Levels across the genotypes were largely comparable; both before and after infection. irRdR2 recorded maximum levels of SA after infection (ANOVA, significant differences at $P \leq 0.05$, represented by a, b and c).

Supplemental Figure S11. Characterization of lines silenced in expression of *AGO4, DCL3, RdR1* and *RdR2* under field condition. (A) Evaluation of silencing efficiency of the respective genes in the crosses of irAGO4 X irDCL3, irAGO4 X irRdR1 and irAGO4 X irRdR2, relative to the levels in WT, which were set to 1. Values represented are mean ± SEM (ANOVA, significantly different at $P \leq 0.05$ (*), $P \leq 0.01$ (**), $P \leq 0.001$(***)). (B) Evaluation of salicylic acid (SA) and abscisic acid (ABA), in asymptomatic and symptomatic plants, show similar patterns of accumulation in WT or plants silenced in expression of *AGO4, DCL3, RdR1* and *RdR2* under field condition.

Supplemental Figure S12. A simplified model of the action of AGO4, DCL3 and RdR1/2 sector of the smRNA machinery during modulation of immune response of *N. attenuata* against *F. brachygibbosum* infection.

Supplemental Table S1. miRNA reads sequenced in 24 samples.

Supplemental Table S2. Conserved and predicted novel miRNAs identified in this study.

Supplemental Table S3. Mature miRNAs conserved to other species when mapped against 72 plant species in miRBase.

Supplemental Table S4. Differentially accumulated miRNAs for irAGO4 and WT. p-value <0.05. RPM=Reads Per Million.

Supplemental Table S5. List of primers used in the study.

ACKNOWLEDGEMENTS

We thank Klaus Gase, and Wibke Seibt, for technical assistance, Eva Rothe for help with crossing, greenhouse team for help with plant propagation, Rayko Halitschke for analytical help and useful discussions, the field team for help with field work, Karin Groten and Lucas C. Llorca and other members of Department of Molecular Ecology for all the support and helpful discussion, Brigham Young University for the use of their field station, Lytle Ranch Preserve,

and APHIS for constructive regulatory oversight and the Max Planck Society for financial support.

Literature Cited

Agorio A, Vera P (2007) ARGONAUTE4 is required for resistance to *Pseudomonas syringae* in Arabidopsis. Plant Cell **19:** 3778-3790

Alazem M, He MH, Moffett P, Lin NS (2017) Abscisic Acid Induces Resistance against Bamboo Mosaic Virus through Argonaute2 and 3. Plant Physiol **174:** 339-355

Allmann S, Halitschke R, Schuurink RC, Baldwin IT (2010) Oxylipin channelling in *Nicotiana attenuata*: lipoxygenase 2 supplies substrates for green leaf volatile production. Plant Cell Environ **33:** 2028-2040

Axtell MJ (2013) Classification and comparison of small RNAs from plants. Annu Rev Plant Biol **64:** 137-159

Baldwin IT, Schmelz EA, Zhang ZP (1996) Effects of octadecanoid metabolites and inhibitors on induced nicotine accumulation in *Nicotiana sylvestris*. J Chem Ecol **22:** 61-74

Benjamini Y, Hochberg Y (1995) Controlling the false discovery rate: a practical and powerful approach to multiple testing. J R Stat S. Series B (Methodological) **57:** 289-300

Berrocal-Lobo M, Molina A (2008) Arabidopsis defense response against *Fusarium oxysporum*. Trends Plant Sci **13:** 145-150

Bhattacharjee S, Zamora A, Azhar MT, Sacco MA, Lambert LH, Moffett P (2009) Virus resistance induced by NB–LRR proteins involves Argonaute4-dependent translational control. Plant J **58:** 940-951

Boenisch MJ, Schäfer W (2011) *Fusarium graminearum* forms mycotoxin producing infection structures on wheat. BMC Plant Biol **11:** 110-110

Böhmdorfer G, Rowley MJ, Kuciński J, Zhu Y, Amies I, Wierzbicki AT (2014) RNA-directed DNA methylation requires stepwise binding of silencing factors to long non-coding RNA. Plant J **79:** 181-191

Bonaventure G, Schuck S, Baldwin IT (2011) Revealing complexity and specificity in the activation of lipase-mediated oxylipin biosynthesis: a specific role of the *Nicotiana attenuata* GLA1 lipase in the activation of jasmonic acid biosynthesis in leaves and roots. Plant Cell Environ **34:** 1507-1520

Borges F, Martienssen RA (2015) The expanding world of small RNAs in plants. Nat Rev Mol Cell Biol **16:** 727-741

Bozorov TA, Pandey SP, Dinh ST, Kim SG, Heinrich M, Gase K, Baldwin IT (2012) DICER-like proteins and their role in plant-herbivore interactions in *Nicotiana attenuata*. J Integr Plant Biol **54:** 189-206

Bubner B, Gase K, Baldwin IT (2004) Two-fold differences are the detection limit for determining transgene copy numbers in plants by real-time PCR. BMC Biotechnol **4:** 1-14

Cole SJ, Yoon AJ, Faull KF, Diener AC (2014) Host perception of jasmonates promotes infection by *Fusarium oxysporum* formae speciales that produce isoleucine- and leucine-conjugated jasmonates. Mol Plant Pathol **15:** 589-600

Dai X, Zhao PX (2011) psRNATarget: a plant small RNA target analysis server. Nucleic Acids Res **39:** W155-159

Di X, Takken FLW, Tintor N (2016) How phytohormones shape interactions between plants and the soil-borne fungus *Fusarium oxysporum*. Front Plant Sci **7:** 170-170

Dowen RH, Pelizzola M, Schmitz RJ, Lister R, Dowen JM, Nery JR, Dixon JE, Ecker JR (2012) Widespread dynamic DNA methylation in response to biotic stress. Proc Natl Acad Sci USA **109:** E2183-E2191

Fang X, Qi Y (2016) RNAi in Plants: An Argonaute-Centered View. Plant Cell **28:** 272-285

Friedländer MR, Mackowiak SD, Li N, Chen W, Rajewsky N (2012) miRDeep2 accurately identifies known and hundreds of novel microRNA genes in seven animal clades. Nucleic Acids Res **40:** 37-52

Halitschke R, Baldwin IT (2003) Antisense LOX expression increases herbivore performance by decreasing defense responses and inhibiting growth-related transcriptional reorganization in *Nicotiana attenuata*. Plant J **36:** 794-807

Halitschke R, Keßler A, Kahl J, Lorenz A, Baldwin IT (2000) Ecophysiological comparison of direct and indirect defenses in *Nicotiana attenuata*. Oecologia **124:** 408-417

Hernández-Lagana E, Rodríguez-Leal D, Lúa J, Vielle-Calzada JP (2016) A Multigenic Network of ARGONAUTE4 Clade members controls early megaspore formation in Arabidopsis. Genetics **204:** 1045-1056

Howe GA, Jander G (2008) Plant immunity to insect herbivores. Annu Rev Plant Biol **59:** 41-66

Howe GA, Major IT, Koo AJ (2018) Modularity in jasmonate signaling for multistress resilience. Annu Rev Plant Biol **69:** 387-415

Huang Y, Li L, Smith KP, Muehlbauer GJ (2016) Differential transcriptomic responses to *Fusarium graminearum* infection in two barley quantitative trait loci associated with *Fusarium* head blight resistance. BMC Genomics **17:** 387-387

Jia L, Zhang D, Qi X, Ma B, Xiang Z, He N (2014) Identification of the conserved and novel miRNAs in Mulberry by high-throughput sequencing. PLoS ONE **9:** e104409-e104409

Jones L, Keining T, Eamens A, Vaistij FE (2006) Virus-induced gene silencing of argonaute genes in Nicotiana benthamiana demonstrates that extensive systemic silencing requires Argonaute1-like and Argonaute4-like genes. Plant Physiol **141:** 598-606

Kallenbach M, Bonaventure G, Gilardoni PA, Wissgott A, Baldwin IT (2012) Empoasca leafhoppers attack wild tobacco plants in a jasmonate-dependent manner and identify jasmonate mutants in natural populations. Proc Natl Acad Sci USA **109:** E1548-E1557

Krügel T, Lim M, Gase K, Halitschke R, Baldwin IT (2002) *Agrobacterium*-mediated transformation of *Nicotiana attenuata*, a model ecological expression system. Chemoecology **12:** 177-183

Langmead B, Trapnell C, Pop M, Salzberg SL (2009) Ultrafast and memory-efficient alignment of short DNA sequences to the human genome. Genome Biol. **10:** 1

Lanubile A, Ferrarini A, Maschietto V, Delledonne M, Marocco A, Bellin D (2014) Functional genomic analysis of constitutive and inducible defense responses to *Fusarium verticillioides* infection in maize genotypes with contrasting ear rot resistance. BMC Genomics **15:** 710-710

Lee G, Joo Y, Kim SG, Baldwin IT (2017) What happens in the pith stays in the pith: tissue-localized defense responses facilitate chemical niche differentiation between two spatially separated herbivores. Plant J **92:** 414-425

Li D, Baldwin IT, Gaquerel E (2016) Beyond the Canon: Within-plant and population-level heterogeneity in jasmonate signaling engaged by plant-insect interactions. Plants **5:** 14

López A, Ramírez V, García-Andrade J, Flors V, Vera P (2011) The RNA silencing enzyme RNA polymerase V is required for plant immunity. PLoS Genet **7:** e1002434-e1002434

Ludman M, Burgyán J, Fátyol K (2017) Crispr/Cas9 mediated inactivation of Argonaute 2 reveals its differential involvement in antiviral responses. Sci Rep **7:** 1010-1010

Luu VT, Schuck S, Kim SG, Weinhold A, Baldwin IT (2015) Jasmonic acid signalling mediates resistance of the wild tobacco *Nicotiana attenuata* to its native Fusarium, but not Alternaria, fungal pathogens. Plant Cell Environ **38:** 572-584

Luu VT, Weinhold A, Ullah C, Dressel S, Schoettner M, Gase K, Gaquerel E, Xu S, Baldwin IT (2017) O-acyl sugars protect a wild tobacco from both native fungal pathogens and a specialist herbivore. Plant Physiol **174:** 370-386

Ma LJ, Geiser DM, Proctor RH, Rooney AP, O'Donnell K, Trail F, Gardiner DM, Manners JM, Kazan K (2013) Fusarium pathogenomics. Annu Rev Microbiol **67:** 399-416

Meredith CS, Baldwin IT (2016) The layers of plant responses to insect herbivores. Annu Rev Entomol **61:** 373-394

Oh Y, Baldwin IT, Galis I (2012) *NaJAZh* regulates a subset of defense responses against herbivores and spontaneous leaf necrosis in *Nicotiana attenuata* plants. Plant Physiol **159:** 769-788

Onkokesung N, Gaquerel E, Kotkar H, Kaur H, Baldwin IT, Galis I (2012) MYB8 controls inducible phenolamide levels by activating three novel hydroxycinnamoyl-coenzyme A:polyamine transferases in *Nicotiana attenuata*. Plant Physiol **158:** 389-407

Overmyer K, Vuorinen K, Brosché M (2018) Interaction points in plant stress signaling pathways. Physiologia Plantarum **162:** 191-204

Pandey P, Srivastava PK, Pandey SP (2019) Prediction of plant miRNA targets. In: de Folter S.(ed.), Plant microRNAs: methods and protocols, Methods Mol Biol, vol. 1932, Chapter 7

Pandey P, Wang M, Baldwin IT, Pandey SP, Groten K (2018) Complex regulation of microRNAs in roots of competitively-grown isogenic *Nicotiana attenuata* plants with different capacities to interact with arbuscular mycorrhizal fungi. BMC Genomics **19:** 937

Pandey SP, Baldwin IT (2007) RNA-directed RNA polymerase 1 (RdR1) mediates the resistance of *Nicotiana attenuata* to herbivore attack in nature. Plant J **50:** 40-53

Pandey SP, Baldwin IT (2008) Silencing RNA-directed RNA polymerase 2 increases the susceptibility of *Nicotiana attenuata* to UV in the field and in the glasshouse. Plant J **54:** 845-862

Pandey SP, Gaquerel E, Gase K, Baldwin IT (2008b) RNA-directed RNA polymerase3 from *Nicotiana attenuata* is required for competitive growth in natural environments. Plant Physiol **147:** 1212-1224

Pandey SP, Shahi P, Gase K, Baldwin IT (2008a) Herbivory-induced changes in the small-RNA transcriptome and phytohormone signaling in *Nicotiana attenuata*. Proc Natl Acad Sci USA **105:** 4559-4564

Pieterse CMJ, Leon-Reyes A, Van der Ent S, Van Wees SCM (2009) Networking by small-molecule hormones in plant immunity. Nat Chem Biol **5:** 308

Pradhan M, Pandey P, Gase K, Sharaff M, Singh RK, Sethi A, Baldwin IT, Pandey SP (2017) Argonaute 8 (AGO8) mediates the elicitation of direct defenses against herbivory. Plant Physiol **175:** 927-946

Raja P, Sanville BC, Buchmann RC, Bisaro DM (2008) Viral genome methylation as an epigenetic defense against geminiviruses. J Virol **82:** 8997-9007

Rayapuram C, Baldwin IT (2007) Increased SA in NPR1-silenced plants antagonizes JA and JA-dependent direct and indirect defenses in herbivore-attacked *Nicotiana attenuata* in nature. Plant J **52:** 700-715

Rodriguez-Leal D, Castillo-Cobian A, Rodriguez-Arevalo I, Vielle-Calzada JP (2016) A primary sequence analysis of the ARGONAUTE protein family in plants. Front Plant Sci **7:** 1347

Sahu R, Sharaff M, Pradhan M, Sethi A, Bandyopadhyay T, Mishra VK, Chand R, Chowdhury AK, Joshi AK, Pandey SP (2016) Elucidation of defense-related signaling responses to spot blotch infection in bread wheat (*Triticum aestivum* L.). Plant J **86:** 35-49

Santhanam R, Luu VT, Weinhold A, Goldberg J, Oh Y, Baldwin IT (2015) Native root-associated bacteria rescue a plant from a sudden-wilt disease that emerged during continuous cropping. Proc Natl Acad Sci USA **112:** E5013-5020

Scalschi L, Sanmartín M, Camañes G, Troncho P, Sánchez-Serrano JJ, García-Agustín P, Vicedo B (2015) Silencing of OPR3 in tomato reveals the role of OPDA in callose deposition during the activation of defense responses against *Botrytis cinerea*. Plant J **81:** 304-315

Schuck S, Weinhold A, Luu VT, Baldwin IT (2014) Isolating fungal pathogens from a dynamic disease outbreak in a native plant population to establish plant-pathogen bioassays for the ecological model plant *Nicotiana attenuata*. PLoS ONE **9:** e102915

Shannon P, Markiel A, Ozier O, Baliga NS, Wang JT, Ramage D, Amin N, Schwikowski B, Ideker T (2003) Cytoscape: a software environment for integrated models of biomolecular interaction networks. Genome Res **13:** 2498-2504

Shibuya K, Fukushima S, Takatsuji H (2009) RNA-directed DNA methylation induces transcriptional activation in plants. Proc Natl Acad Sci USA **106:** 1660-1665

Singh RK, Gase K, Baldwin IT, Pandey SP (2015) Molecular evolution and diversification of the Argonaute family of proteins in plants. BMC Plant Biol **15:** 23

Singh RK, Pandey SP (2015) Evolution of structural and functional diversification among plant Argonautes. Plant Signal Behav **10:** e1069455

Singh RK, Pandey SP (2017) Phylogenetic and evolutionary analysis of plant Argonautes. In: Carbonell A. (eds) Plant Argonaute Proteins. Methods in Molecular Biology, **1640:** 267-294

Skibbe M, Qu N, Galis I, Baldwin IT (2008) Induced plant defenses in the natural environment: *Nicotiana attenuata WRKY3* and *WRKY6* coordinate responses to herbivory. Plant Cell **20:** 1984-2000

Srivastava PK, Moturu TR, Pandey P, Baldwin IT, Pandey SP (2014) A comparison of performance of plant miRNA target prediction tools and the characterization of features for genome-wide target prediction. BMC Genomics **15:** 348

Stitz M, Gase K, Baldwin IT, Gaquerel E (2011) Ectopic expression of AtJMT in *Nicotiana attenuata*: creating a metabolic sink has tissue-specific consequences for the jasmonate metabolic network and silences downstream gene expression. Plant Physiol **157:** 341-354

Thatcher LF, Manners JM, Kazan K (2009) *Fusarium oxysporum* hijacks COI1-mediated jasmonate signaling to promote disease development in Arabidopsis. Plant J **58:** 927-939

Van Dam NM, Horn M, Mares M, Baldwin IT (2001) Ontogeny constrains systemic protease inhibitor response in *Nicotiana attenuata*. J Chem Ecol **27:** 547-568

Wang F, Axtell MJ (2017) AGO4 is specifically required for heterochromatic siRNA accumulation at Pol V-dependent loci in *Arabidopsis thaliana*. Plant J **90:** 37-47

Wang L, Allmann S, Wu J, Baldwin IT (2008) Comparisons of LIPOXYGENASE3- and JASMONATE-RESISTANT4/6-silenced plants reveal that jasmonic acid and jasmonic acid-amino acid conjugates play different roles in herbivore resistance of *Nicotiana attenuata*. Plant Physiol **146:** 904-915

Wang L, Halitschke R, Kang JH, Berg A, Harnisch F, Baldwin IT (2007) Independently silencing two JAR family members impairs levels of trypsin proteinase inhibitors but not nicotine. Planta **226:** 159-167

Wei L, Gu L, Song X, Cui X, Lu Z, Zhou M, Wang L, Hu F, Zhai J, Meyers BC, Cao X (2014) Dicer-like 3 produces transposable element-associated 24-nt siRNAs that control agricultural traits in rice. Proc Natl Acad Sci USA **111:** 3877-3882

Woldemariam MG, Dinh ST, Oh Y, Gaquerel E, Baldwin IT, Galis I (2013) NaMYC2 transcription factor regulates a subset of plant defense responses in *Nicotiana attenuata*. BMC Plant Biol **13:** 73

Xu S, Brockmöller T, Navarro-Quezada A, Kuhl H, Gase K, Ling Z, Zhou W, Kreitzer C, Stanke M, Tang H, Lyons E, Pandey P, Pandey SP, Timmermann B, Gaquerel E, Baldwin IT (2017) Wild tobacco genomes reveal the evolution of nicotine biosynthesis. Proc Natl Acad Sci USA **114:** 6133-6138

Xue RF, Wu J, Wang LF, Blair MW, Wang XM, Ge WD, Zhu ZD, Wang SM (2014) Salicylic Acid Enhances Resistance to *Fusarium oxysporum* f. sp. phaseoli in common beans (*Phaseolus vulgaris* L.). J Plant Growth Regul **33:** 470-476

Zhang X, Zhao H, Gao S, Wang WC, Katiyar-Agarwal S, Huang HD, Raikhel N, Jin H (2011) Arabidopsis Argonaute 2 regulates innate immunity via miRNA393(*)-mediated silencing of a Golgi-localized SNARE gene, MEMB12. Mol Cell **42:** 356-366

Manuscript III

Argonaute7 (AGO7) moderates plant fitness and arbuscular mycorrhizal fungal associations under competitive and resource limited conditions in *Nicotiana attenuata*

Maitree Pradhan, Klaus Gase[+], Ling Chuang[+], Ian T. Baldwin[*], Karin Groten[*], Shree P. Pandey[*]

(Manuscript under preparation-Plant Physiology)

Summary

Plant AGOs have diversified in their biological functions due to the expansion of the number of genes in this family due to duplication and loss events. The genome of the ecological model plant *Nicotiana attenuata* contains 8 unique AGO genes, whose biological functions have only been described for a few. *N. attenuata* interacts with arbuscular mycorrhizal fungi entailing reprograming of miRNAs and their target genes. We demonstrate that NaAGO7 moderates such reprograming of miRNAs and mRNAs during host-AMF interaction under competitive resource-limited conditions. Silencing of AGO7 (and no other AGO) significantly reduced the competitive fitness of *N. attenuata* under resource limited conditions, while we could not observe any change in leaf development or juvenile to adult phase transition as described in other species. In these competitively growing plants, ir*AGO7* roots were over-colonized with AMF as ir*AGO7* plants had >3-fold higher numbers of arbuscules. AMF-induced miRNA expressions were altered in ir*AGO7* plants, consequently, the expression of the target genes was also inversely regulated. The results indicate that hypercolonization has a negative impact on plant competitiveness, probably due to P starvation and changes in auxin signaling. The biological function of NaAGO7 was validated in nature, confirming that the roles for NaAGO7 have diverged. The next step is to evaluate the function of individual miRNAs that are reprogramed in an AGO7-dependent manner during the progress of AMF-colonization of roots.

Keywords: *Nicotiana attenauta*, AMF, AGO7, miRNA, biological function, competition, field studies

Introduction

The proteins of the Argonaute (AGO) family are a central component of all small-RNA (smRNA) driven regulatory processes. They are regarded as the 'effectors' of the smRNA-machinery in a critical cellular process of RNA-interference (Axtell, 2013; Carbonell, 2017, Fang and Qi, 2016, Meister, 2013). A large variety of smRNAs is produced by plants that are involved in many aspects of phenotypic plasticity (Borges and Martienssen, 2015). smRNAs regulate molecular events in the development of plants, their reproduction, and their adaptation to unpredictable fluctuations in the abiotic and biotic environment (Brant and Budak, 2018, Manavella *et al.* 2019,; Song *et al*., 2019). Despite their diversity, all characterized smRNA processes involve an AGO protein that is the direct binding partner of the smRNAs during formation of the RNA-induced silencing complex (RISC). The complex is formed by loading 20- to 24-nucleotide duplexes with two-nucleotide overhangs onto the AGOs that retain one of the strands to form the RISC. This procedure determines the specificity of target selection based on smRNA-mRNA complementarities. AGOs facilitate endonucleolytic cleavage of the transcripts, translational repression, RNA directed DNA methylation, synthesis of secondary small interfering RNAs (siRNAs), Dicer (DCL)-independent pre-microRNA (miRNA) synthesis and co-transcriptional regulation of miRNA gene expression (Carbonell 2017; Fang and Qi, 2016). Engagement in these processes makes the AGOs an indispensable component of the smRNA pathways.

The family of *AGO*s in flowering plants encompasses a large number of genes, such as 10 in Arabidopsis and 19 in rice, whereas the genomes of Chlamydomonas (algae) and Physcomitrella (moss) contain 3 and 6 *AGO* genes. Evolution of AGOs has been a dynamic process, during which an ancient *AGO* plausibly underwent duplications after the divergence of unicellular algae giving rise to large number of extant AGOs (Singh *et al.,* 2015). Plant AGOs are classified into four major clades (Singh *et al*., 2015) of AGO1/10 (class I), AGO5 (class II), AGO2/3/7 (class III) and AGO4/6/8/9 (class IV). The expansion of the AGO family in plants equally suggests functional diversification during the evolution of specialized smRNA pathways (Carbonell 2017; Pradhan *et al.,* 2017); but the biological roles have not been fully elucidated for all plant AGOs yet. While members of class I and class IV AGOs are rather well-characterized,

biological functions of class III AGOs (AGO2/3/7) have been only known in a limited set of plant species. In Arabidopsis, AGO2 is primarily involved in resistance to a broad spectrum of viruses; AtAGO3 is closely located to AtAGO2 and could bind siRNAs, but the biological function remains unknown. Loss of AGO7 accelerates juvenile to adult phase change and leaf morphogenesis (Carbonell 2017; Fang and Qi, 2016; Hunter *et al.,* 2003; Xu *et al.,* 2006). AGO7 specifically binds to miR390 and is required for biogenesis of ta-siRNAs (Jouannet *et al.,* 2012; Montgomery *et al.,* 2008). The functions of AGO7 in leaf development and ta-siRNA biogenesis are conserved in crop species of maize and rice (Douglas *et al.,* 2010; Nagasaki *et al.,* 2007). On the other hand, in the ecological model species *Nicotiana attenuata*, for which the identity of components of smRNA machinery is now well established (Pandey and Baldwin, 2007; 2008, Pandey *et al.,* 2008; Gase *et al*., 2011; Pradhan *et al*., 2017), the biological function of class III AGOs, in particular NaAGO7, remains largely unknown. Under laboratory conditions, loss-of-AGO7 function neither affected *N. attenuata*'s defense against insect herbivores (Pradhan *et al*., 2017), nor its resistance to phyto-pathogens (Pradhan *et al.,* 2019).

Nicotiana attenuata, or Coyote tobacco, is an annual, wild herb species, native to Southwestern North America that germinates from long-lived seed banks in post-fire environments (Baldwin and Morse 1994). In the post-fire burns, where soils have a high nitrogen content, these plants form a pioneering species as the seeds of *N. attenuata* germinate in a highly synchronized manner, often forming populations of mono-cultures that resemble in primordial agricultural niches. The genome of this ecological model plant encodes for 11 AGOs from 8 unique genes homologous to *AGO1* (NaAGO1a, b, c), *AGO2, AGO4* (Na*AGO4a, b*), *AGO5*, *AGO7*, *AGO8*, *AGO9* and *AGO10* (Singh *et al.,* 2015). Analysis of gene expression and loss-of-function characterization studies have helped to associate the biological functions to candidate genes of class I and IV.

The biological function of AGO1 in development is conserved in *N. attenuata* (Pradhan *et al*., 2017). *N. attenuata* grows in a complex biotic environment. Every year, it faces a community of unpredictable insect herbivores (Baldwin 2001). AGO8 modulates *N. attenuata*'s direct defenses induced against such herbivores (Pradhan *et al*., 2017). The monoculture-like population structure of *N. attenuata* has resulted in the evolution of a complex wilt-like disease (Santhanam *et al.,* 2015; Schuck *et al.,* 2014), resistance to which is modulated by AGO4

(Pradhan *et al*., 2019). In their native habitats, *N. attenuata* also interacts with AMF (Groten *et al.,* 2015), and under competitive conditions plants impaired in their interaction with AMF are outcompeted by a fully functional isogenic line (Wang *et al.,* 2018). Amongst the diverse effects of smRNAs in plants their role in the interaction with arbuscular mycorrhizal fungi (AMF) has not been investigated in full detail. Multiple beneficial effects of AMF on plants could be demonstrated, the most prominent one is improved nutrient supply, in particular with inorganic phosphorus (Smith *et al.,* 2011), but also with other nutrients. Despite of the very limited number of characterized species (Redecker *et al.,* 2013) AMF can colonize about 70% of all land plants effectively (Cosme *et al.,* 2018). This promiscuity results in an underground AMF network connecting the same and different plant species leading to a change in plant competitiveness depending on its capacity to interact with AMF (Kiers *et al.,* 2011; Walder *et al.,* 2012; Wang *et al*, 2017). A number of studies analyzed the changes in the smRNAome of AMF colonized and non-colonized plants and observed significant reprogramming in its expression (Pandey *et al.,* 2018; Silvestri *et al.,* 2019; Song *et al.,* 2018; Wu *et al.,* 2016). The roles of miR171h, miR396 and miR393 (Couzigou and Combier, 2016) as well as miR399 due to its involvement in P-starvation response (Kuo and Chiou, 2011; Wang *et al*, 2017) could be clearly associated with AMF colonization.

Nicotiana-AMF interaction entails a large-scale reprogramming in the root miRNome (Pandey *et al.*, 2018), but which AGO modulates this interaction remains elusive and is the subject of this study. Here, we determine the biological function of *N. attenuata*'s AGO7 and test how it affects plant fitness in nature.

Results

Silencing AGO7 does not affect plant development, juvenile to adult transition, or plant fitness in resource rich condition

Previous studies in Arabidopsis identified AGO7 to function in juvenile to adult phase change, in leaf morphogenesis and ta-siRNA formation (Carbonell 2017; Fang and Qi 2016; Hunter *et al.*, 2003; Xu *et al*., 2006). Such functions were shown to be conserved in maize and rice. In *N. attenuata*, loss-of-*AGO7* function (in ir*AGO7* plants) did not produce any noticeable change in plant development under standard growth conditions when resources were not

limiting. The rosettes of ir*AGO7* plants grew similar to WT plants, produced a similar number of leaves, and transited to elongation stage identically to the WT plants (Figure 1A). The chlorophyll contents of both, rosette stage leaves and stem leaves of elongating plants, were also similar (Figure 1A). Further, no differences in reproductive performance of ir*AGO7* and WT plants were noticed as both genotypes produced similar numbers of seed capsules.

AGO7-silenced plants show reduced fitness under resource-limited competitive conditions in *Nicotiana attenuata*.

Compared to above, when ir*AGO7* and WT plants were allowed to compete in resource limited conditions with AMF inoculum (Wang *et al*., 2018; Pandey *et al*., 2018), ir*AGO7* plants were outcompeted by the WT conspecies neighbors (Figure 1B). The rosettes of WT and ir*AGO7* plants expanded at a similar rate and no significant developmental abnormalities between the WT and ir*AGO7* plants were recorded (Figure 1B). However, under these competitive growth conditions, WT plants out-competed the ir*AGO7* plants. Stalks of WT plants were significantly longer (Figure 1B, repeated measures ANOVA, n=10 pairs, $P<0.01$). The fresh and dry mass of the shoots of the WT plants were significantly higher than the ir*AGO7* plant in the same pot (paired t-test, n=10 pairs, $P<0.01$ for fresh mass and <0.05 for dry mass). Similarly, WTs had significantly more numbers of seed capsule than ir*AGO7* plants (Figure 1B, 42%; paired t-test, n=10 pairs, $P<0.01$).

Further, we tested whether the reduced competitive ability of ir*AGO7* was a trait specific for AGO7, or if plants silenced in other AGOs (the other class II member-AGO2, AGO4 and AGO10) were also impaired in their competitive ability. We also included one line of ir*AGO1* (Pradhan *et al*., 2017). Rosette diameters were recorded at 1, 2 and 3 weeks of AMF inoculation, stalk lengths were measured at 2, 3 4 and 5 weeks after inoculation and seed capsules were counted at the end of the experiment: none of the traits showed any significant differences between the WT and the respective ir*AGO* lines (Figure S1). This confirmed that only ir*AGO7* plants were compromised in their competitiveness when grown in AMF inoculum under resource limited conditions.

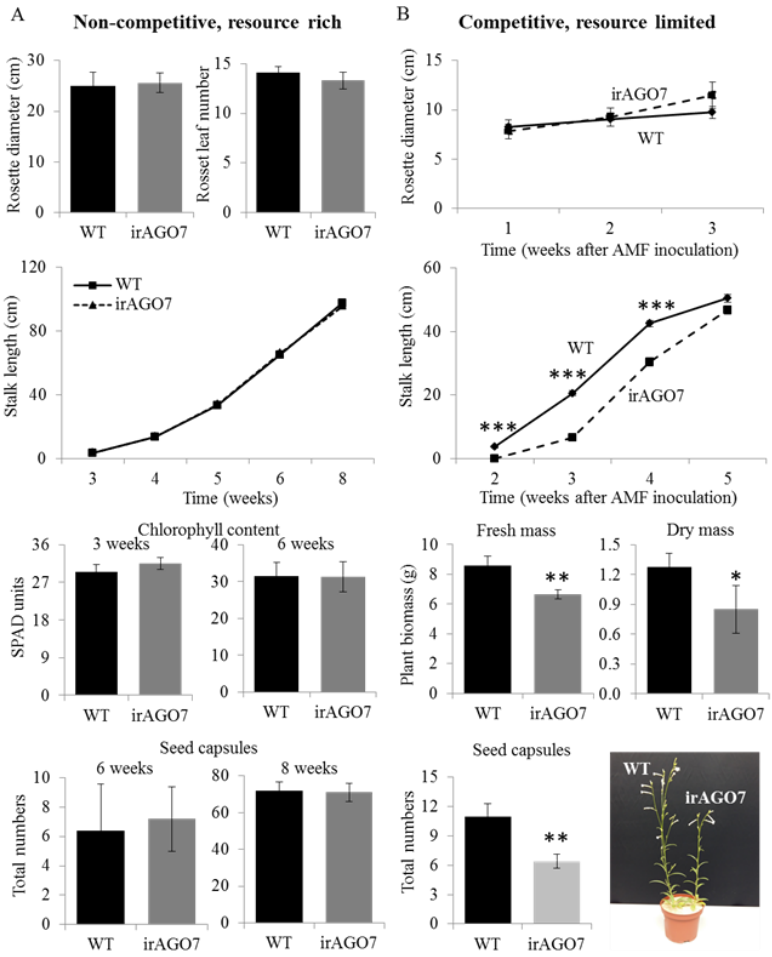

Figure 1. Silencing AGO7 impairs *Nicotiana attenuata*'s competitive fitness under resource limited and AMF conditions. Values presented are means ± SD, solid lines represent WT and broken lines represent irAGO7. (a) Silencing of AGO7 does not affect plant growth and fitness under non-competitive, resource rich conditions. Parameters such as rosette diameter, rosette leaf number, chlorophyll content and total capsule number of irAGO7 and WT plants were similar. (b) Under competitive, resource limited (low-P) conditions with AMF inoculum, irAGO7 plants were out-competed by WT. irAGO7 plants had shorter stalk length (***significantly different from WT, paired t-test, t-value=5.38686E-07 for 3-weeks comparison and t-value=0.00029 for 4 weeks comparison, n=10 WT-irAGO7 pairs, P<0.001), less fresh and dry mass (paired t-test, n=10 pairs, P ≤ 0.01), and significantly lower numbers of seed capsules (paired t-test, t-value=0.018, n=10 WT-irAGO7 pairs; ** significant differences from WT at P ≤ 0.01). A representative picture of WT and irAGO7 plants grown in competitive settings in 2-L pots in sand.

Loss-of-AGO7 expression increases AMF colonization of roots of *N. attenuata*

As plants have a high demand for phosphorous, which is limited in soil, they often resort to form an association with AMF and in return pay with 4-20% of their photosynthesis carbon (Johnson *et al.,* 1997). Therefore, we evaluated how loss-of-*AGO7* function affected the AMF-*N. attenuata* interactions during conspecific resource-limited competitive conditions (Figure 2). To estimate root colonization, we first measured 11-carboxyblumenol-C glucoside content as measure of arbuscule number (Wang *et al.,* 2018) of the two genotypes over the period of 8 weeks after AMF inoculation (Figure 2). ir*AGO7* plants had >2-fold higher levels of 11-carboxyblumenol C glucoside than those of WT plants at 6 weeks after inoculation (Figure 2A; paired t-test, n=10, $P<0.01$). At 8 weeks after AMF inoculation the 11-carboxyblumenol levels were still 50% higher in ir*AGO7* than those in WT plants (Figure 2A; paired t-test, n=10, $P<0.01$). These results clearly show that silencing *AGO7* increased AMF colonization.

To further confirm that ir*AGO7* roots were indeed hyper-colonized by AMF, and to determine, which fungal structures were in abundance, we estimated root colonization by Trypan Blue staining (Figure 2B-C). Total root colonization of ir*AGO7* was >2-fold as compared to WT (Figure 2B; paired t-test, $P<0.01$). The total number of arbuscules in ir*AGO7* roots were >3-fold as compared to WT when identical numbers of fields were counted. No significant differences in vesicles were observed, whereas a slight reduction in the number of hyphae was noticed (Figure 2).

Taken together, the results of Figure 1 and 2 suggest that AGO7 moderates optimal colonization of *N. attenuata* roots, and silencing of AGO7 leads to hyper-colonization. Such hyper-colonization may negatively impact plant productivity and competitive ability as the 'investment costs' from the plant side in terms of photo assimilates in AMF associations are high.

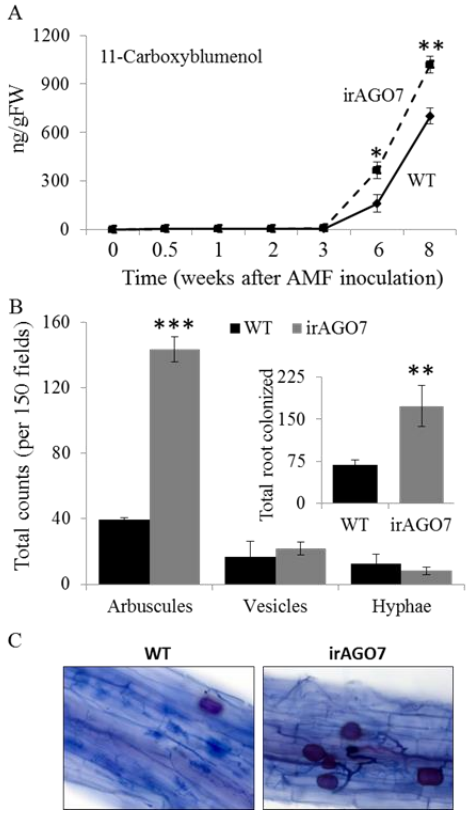

Figure 2. Loss-of-AGO7 function increases AMF colonization of roots of N. attenuata. (a) 6 to 8 weeks after inoculation, the AMF marker metabolite 11-carboxyblumenol C glucosides accumulates significantly more in leaves of ir*AGO7* than in WT. Values presented are means ± SD, solid line represent WT and broken, ir*AGO7*. paired t-test, n=6 per genotype, * and ** represent significant differences from WT at $P \leq 0.05$ and $P \leq 0.01$. (b) Microscopic estimation of AMF colonization structures in WT (black bars) and ir*AGO7* roots after staining with Trypan blue (grey bars). Arbuscules, vesicles, and hyphae were counted. Values presented are means ± SD. Paired t-test, n=5 biological replicates per genotype (50 observations were made on each replicate); t-value = ** and *** represent significant differences from WT at $P \leq 0.01$ and $P \leq 0.001$. The insert in panel b represents the total AMF colonization by integrating the amounts of arbuscules, vesicles and hyphae in each of the genotypes. **significantly different from WT, paired t-test, n=5 biological replicates; 50 observations per replicate, $P<0.01$ (c) A representative microscopic image of WT and ir*AGO7* roots stained with Trypan blue.

AGO7 regulates the reprogramming of miRNA expression during host-AMF interaction

Association of AMF with the *N. attenuata* host roots entails a large-scale reconfiguration of miRNome: expression of 149 unique miRNA – 67 conserved and 82 novel- change during root's AMF colonization (Pandey *et al*., 2018). The abundances and distribution of these

miRNAs is shown to be highly dynamic to the extent that several miRNAs accumulated distinct sequence-specific variants under AMF-colonized and non-colonized states (Pandey *et al*., 2018). Based on these findings we investigated if this AMF-induced reprograming in the miRNome is modulated by *AGO7*. In time-course experiments, we profiled the change in expression of 35 miRNAs, including 6 novel miRNAs in WT and ir*AGO7* genotypes. We determined how their accumulation changed during the course of AMF-colonization, and whether this change was globally affected by AGO7.

Root colonization by AMF starts with a pre symbiotic phase during the first 1-3 days, hyphopodium formation, colonization of the root cortex and eventually arbuscule formation, the main sites of exchange, and eventually spread in the root system. During the mature stage of root colonization corresponding to six weeks after inoculation in our experimental set-up roots are colonized with hyphae and vesicles and with arbuscules of different age. Earlier, we showed that ir*AGO7* plants had high arbuscule-formation by 6 weeks (Figure 2). It implied that the molecular signaling events in preceding stages might be perturbed in ir*AGO7* as compared to WT. Indeed, time/stage- and genotype-dependent changes in miRNA accumulation patters were evident. A complex pattern of change in expression of miRNAs was seen (Figure 3). Of the total of 35 miRNAs, all of them showed a similar expression before transfer to AMF. After transfer, at least 25 were down-regulated in ir*AGO7* roots, mostly during early stages of AMF colonization (by 3 weeks), indicating their strong dependency on *AGO7* for expression/function in early stages of AMF establishment.

Specificity in isomiR-expression was also evident (Figure 3). For example, a total of 6 sequence variants of miR156 were expressed. Most of these miRNAs were maximum expressed at the 6 week time point. Of the 6 sequences, 2 were specifically up-regulated in ir*AGO7* compared to WT only at 6 weeks. miR156b-5p was strongly down-regulated in ir*AGO7* roots in the early stages of AMF infection. Maximum up-regulation in ir*AGO7* at 6 weeks was noticed for miR156a-5p_2 (Figure 3). Such complex reprograming of the miR156 variants during AMF colonization as well as during AGO7-silencing indicates that plants are able to selectively recruit such sequence variants and that AGO7 has a plausible role in their accumulation and/or function.

An example of AMF-repressed miRNAs in WT is the novel miRNA, Nat-R-PN59 (Pandey *et al*., 2018). It was suppressed between 1-3 weeks of AMF inoculation in WT. This miRNA was constantly down-regulated at all time-points in ir*AGO7*.

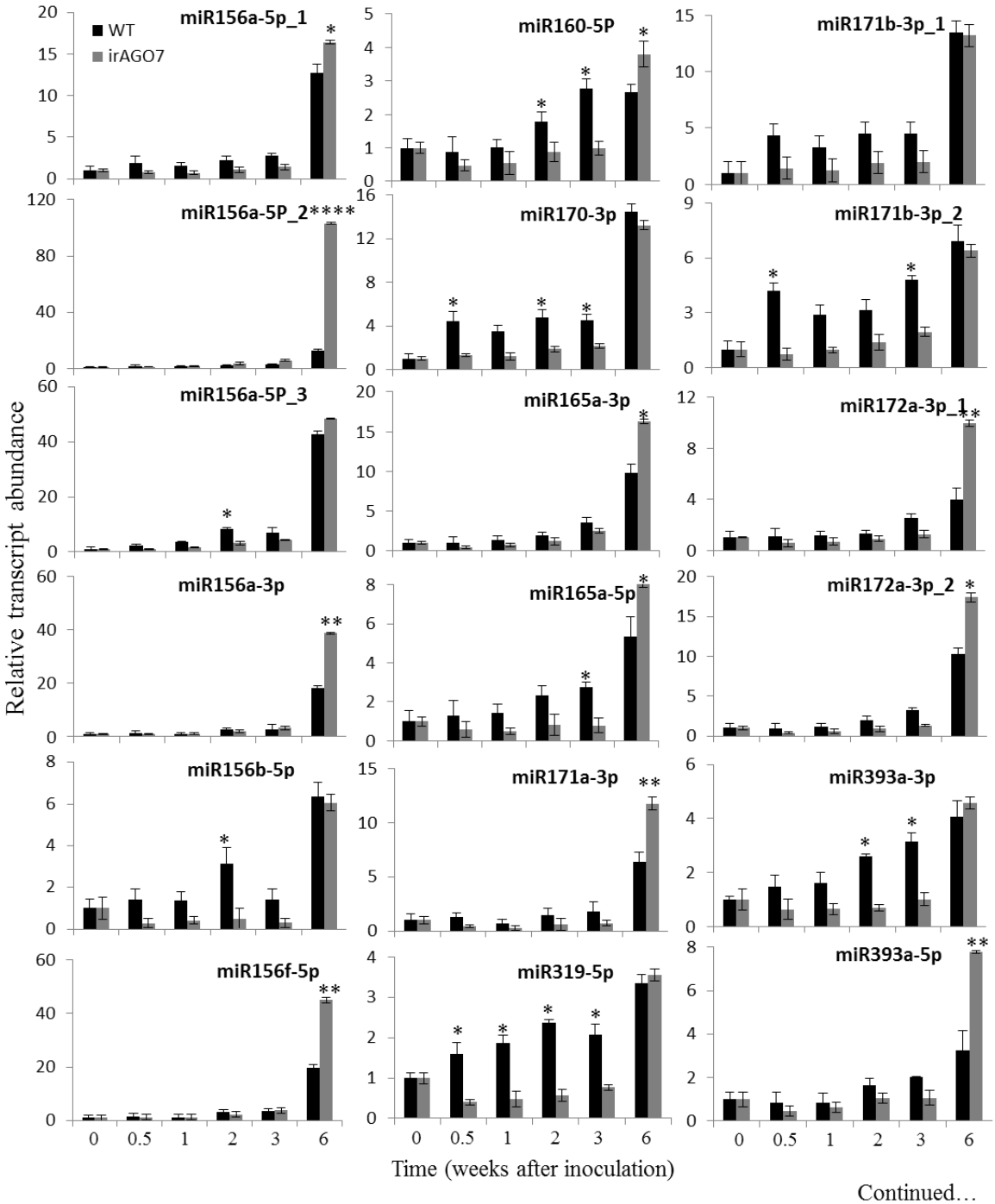

Continued…

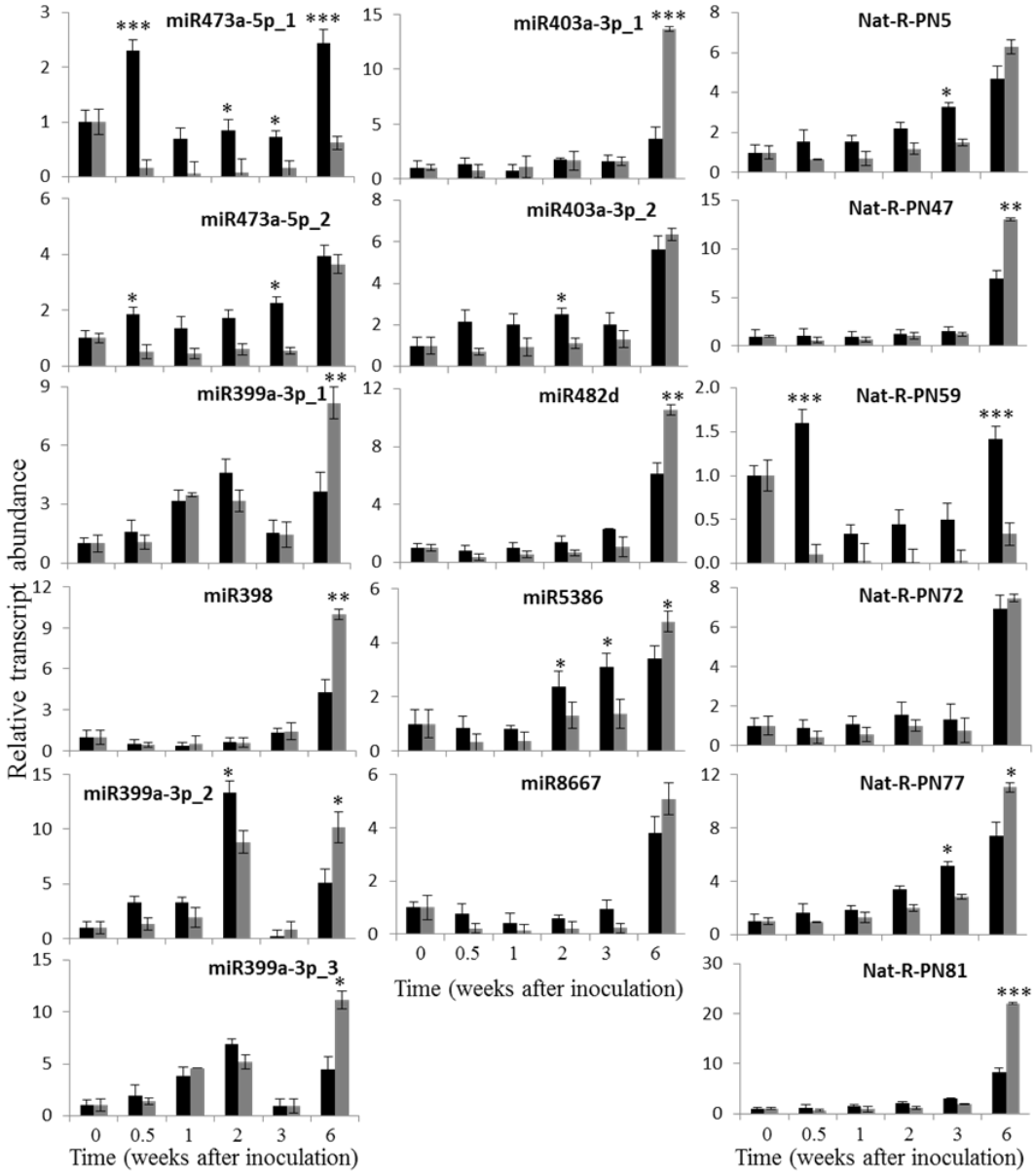

Figure 3. Temporal dynamics of miRNA expression in WT and ir*AGO7* roots during AMF colonization using quantitative real time PCR (qPCR) analysis. Transcripts of 5S rRNA gene were used as internal control for normalization. Transcript levels at t0 were set to 1 and relative abundances were calculated accordingly at other time points in both the genotypes. Significant differences were evaluated with the help of two-way repeated measures ANOVA, Fisher's LSD; * $P \leq 0.05$, ** $P \leq 0.01$, *** $P \leq 0.001$ between ir*AGO7* and WT at a given time point

Temporal changes in putative target gene expressions in WT and irAGO7 during AMF infection and colonization

Above-stated complex changes in miRNA expression after AMF inoculation and their dependency on AGO7 motivated us to examine the expression patterns of their putative targets in both genotypes during the course of 6 weeks of AMF inoculation. Changes in transcript accumulation of a total of 15 genes after AMF inoculation are presented in Figure 4. These genes were selected as they were predicted as targets of several miRNAs in our previous analysis (Pandey *et al*., 2018). They are summarized in supplemental Table S1. Of the 15 genes, transcript accumulation of 2 genes, *SPL9 and RAP2-7*, were not significantly different between WT and ir*AGO7* before or after AMF inoculation (Figure 4). Overall, an inverse pattern of expression between ir*AGO7* and WT roots was observed for most of these genes (Figure 4). *SPL3*, *PEX14* and *PHT1-4* were consistently down-regulated in ir*AGO7* during early (up to 3 weeks) and late (6-week time point) stages of AMF-inoculation. Inversely, *PUB45* was consistently up-regulated in ir*AGO7* compared to WT. *PMT29* was down-regulated in AMF-inoculated WT roots, whereas it was up-regulated in inoculated ir*AGO7* roots. The remaining genes also showed inverse correlation in their expression: if a gene was up-regulated after inoculation at a given time-point in WT, it was down-regulated at that time-point in ir*AGO7* and *vice versa*. These results show that ir*AGO7* plants have inversed molecular events, which could be attributed to the regulation of these genes by miRNAs. As many of the dis-regulated putative miRNA target genes belong to the signaling (mainly auxin) and phosphate transport (Pandey *et al*., 2018), these results also indicate that ir*AGO7* plants are perturbed in pathways related to hormone signaling (such as auxin) and phosphate-transport during AMF colonization.

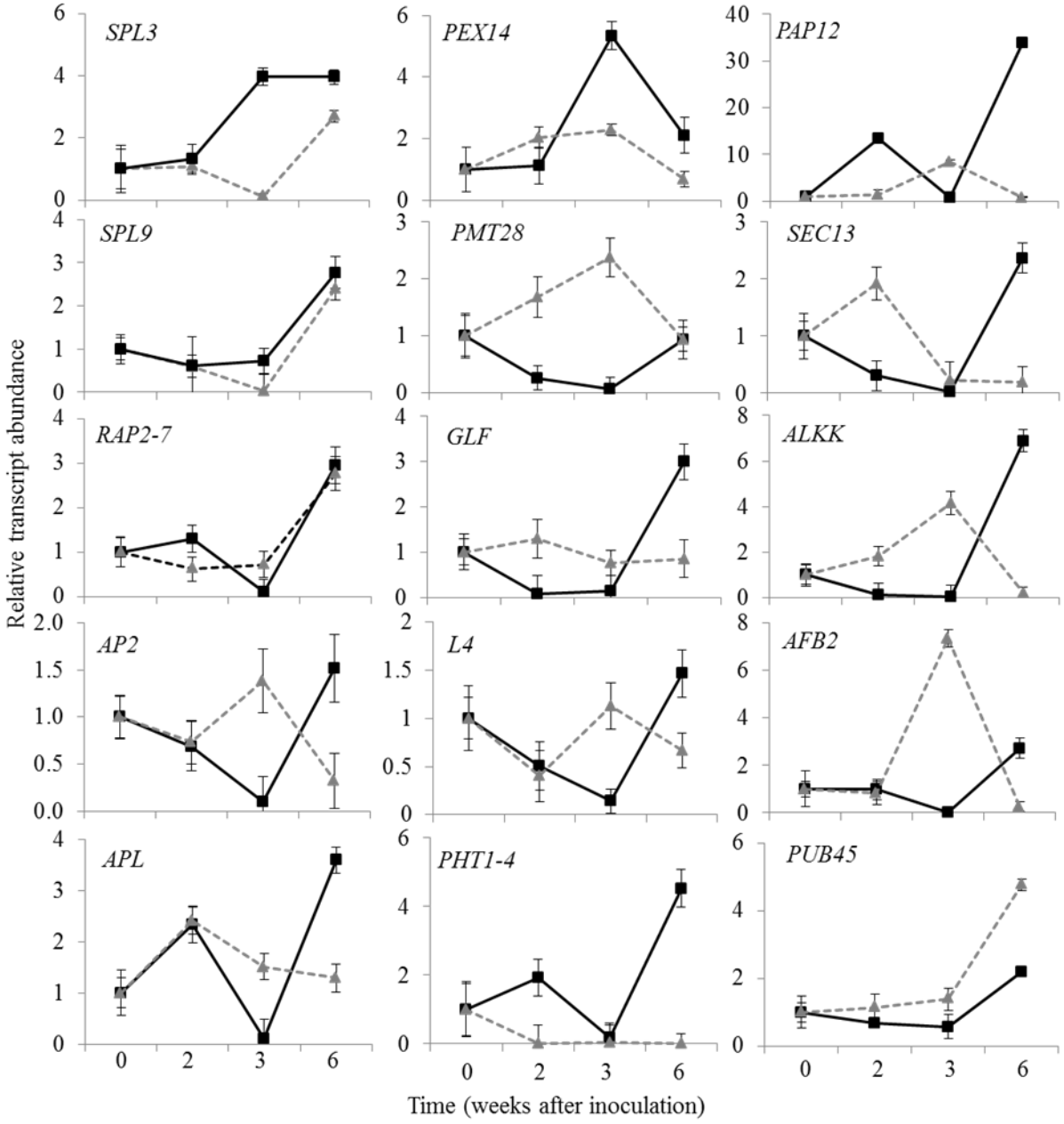

Figure 4. Elicitation dynamics of putative target genes in in AMF inoculated roots of WT and ir*AGO7*.Transcripts of ECI gene were used as internal control for normalization. Transcript level at t0 was set to 1 and relative abundances were calculated accordingly (significantly different from the respective WT, two-way repeated measures ANOVA, Fisher's LSD; $P \leq 0.05$ *, $P \leq 0.01$ **, $P \leq 0.001$ ***).

AGO7-impaired *N. attenuata* plants are strongly impaired in competitive plant fitness but not in herbivory in the field

In our glasshouse studies, we found that *AGO7* gene expression did not affect caterpillar performance or disease progression when ir*AGO7* plants were subjected to *Manduca sexta* attack (Pradhan *et al*., 2017) or *F. brachygibbosum* infections (Pradhan *et al*., 2019), respectively. In order to determine the ecological relevance of AGO7 and to validate its biological functions in nature, we introduced ir*AGO7* plants into the natural habitat of *N. attenuata* on an experimental plot at Lytle Ranch Preserve (Utah USA). We grew plants in conspecies paired designs where each ir*AGO7* plant was paired with a WT plant in close proximity and assessed their performance (Pandey *et al*., 2008b). No artificial fertilizers were applied in the field. ir*AGO7* plants were able to defend themselves against herbivore damages as well as their WT neighbors, as the total canopy areas damaged were similar for WT and ir*AGO7* plants at the end of 4 weeks after transplanting into the field plot (Figure 6). This confirmed that loss of AGO7 does not affect herbivore resistance in nature.

Growth measurements showed that the majority of ir*AGO7* plants were outcompeted by their WT-neighbors (Figure 5). Rosette diameter and plant height were measured from 3-8 weeks after transplanting in the field. WT plants started to elongate around the 4th week after transplanting; stalk length of ir*AGO7* plants was significantly shorter than those of WT plants at the end of 4 weeks (Figure 5). Overall, ir*AGO7* plants continued to lag-behind the WT counterparts even at the end of 8 weeks (Figure 5). Although we could not measure the life time fitness parameters (to prevent any introduction of the transgenic seeds in nature), loss of *AGO7* clearly had negative effects on plant fitness, as inferred from following traits: WT plants started to 'flower' 1 week earlier than the ir*AGO7* competitors, and eventually produced significantly more numbers of flowers (Figure 5). At the end of 8 weeks, WT plants were already producing, on an average, 4-5 seed capsules per plant, but no capsules were noticed on ir*AGO7* plants. At the end of 8 weeks, the plants were uprooted and fresh mass was recorded: ir*AGO7* plants had accumulated significantly lower biomass (Figure 5). These observations confirm that loss of *AGO7* impaired the capacity of *N. attenuata* plants to compete with their WT conspecies in nature when resources were limited.

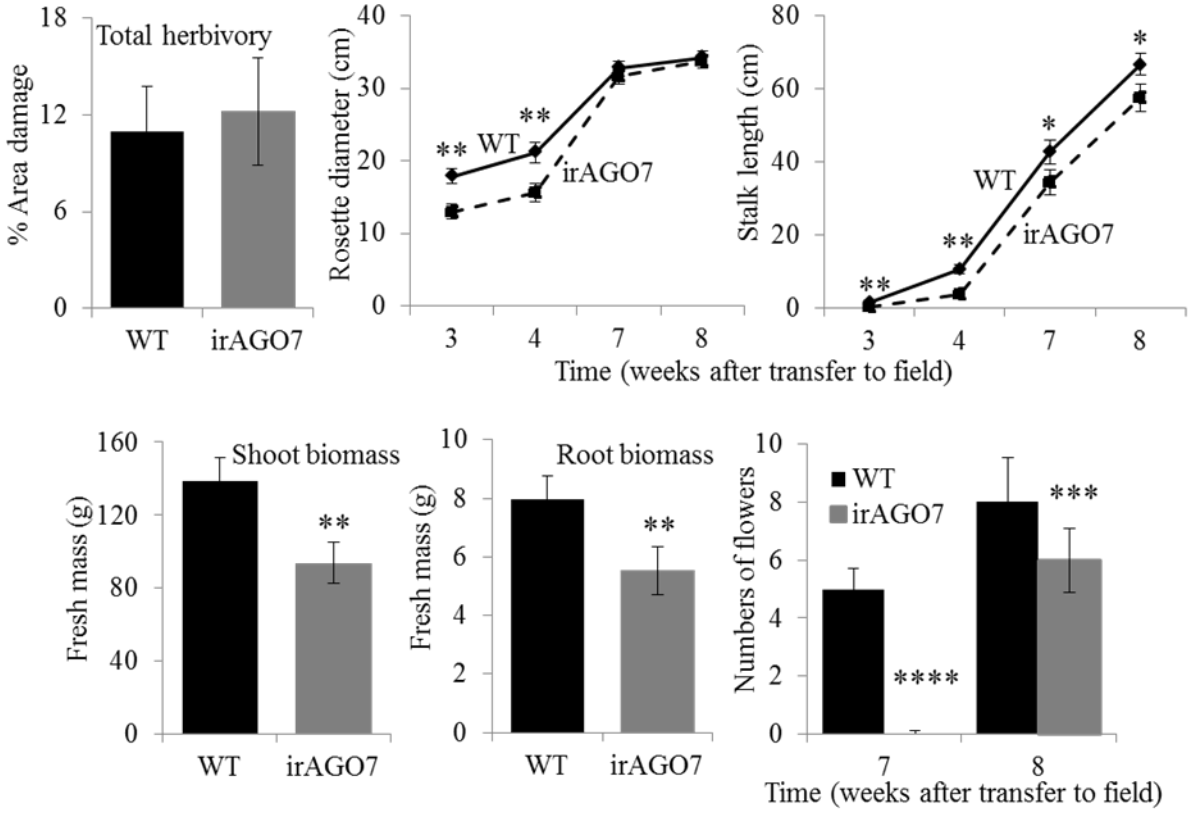

Figure 5. Evaluation of AGO7-function in nature confirms that AGO7-silenced *N. attenuata* plants have impaired competitive plant fitness. ir*AGO7* and WT pairs suffered similar herbivore damage, but ir*AGO7* plants were significantly smaller in rosette diameter (paired t-test, t-value=0.013 and 0.0021 for 3 weeks and 4th weeks data sets, respectively, n=25 per genotype, ** significant differences at $P \leq 0.01$), and in stalk length (paired t-test, t-value = 0.004, 0.01, 0.052 and 0.048 for datasets of 3, 4, 7, and 8 weeks respectively, n=25, * and ** significant differences from WT at $P \leq 0.05$ and $P \leq 0.01$, respectively). Fresh shoot and root biomass of ir*AGO7* was significantly lower than WT (paired t-test, t-value=0.012 for shoot biomass and 0.013 for root biomass, n=23, $P<0.01$). ir*AGO7* also produced significantly fewer flowers than WT (paired t-test, n=27, **** and *** represent significant differences from WT at $P \leq 0.001$ and 0.005, respectively).

Discussion

The central component of the smRNA pathway, the AGOs, has been well characterized for some classes of AGOs, but due to their diversification and their highly variable numbers in different plant species the function of several AGOs remain unknown or only described for a few

model species. In particular, publications on the role of class III AGOs (AGO2, AGO3 and *AGO7*) are limited and focused on Arabidopsis and a few crop species. This lack was addressed in this investigation by using plants silenced in the expression of *AGO7* of the model ecological plant *N. attenuata*. Previously, we had shown that the AGO protein family of *N. attenuata* encompasses 11 AGOs (Singh *et al.*, 2015). We could not find a homologue to AGO3 in the genome (Singh *et al.*, 2015), so that initially we used all viable irAGO-lines available including ir*AGO2* (Pradhan *et al*., 2017), but we decided to focus on *AGO7* only due to its phenotype. Here, we advance our understanding and propose that *AGO7* affects the plant's competitive capacity under resource limited conditions and when plants are colonized by AMF. They recruit this pathway to modulate smRNA expression.

An Arabidopsis loss-of-function mutant in *AGO7* (*ZIPPY*) was the first AGO7 mutant line to be described mainly characterized by the premature change in leaf morphology without accelerating the onset of flowering time (Hunter *et al*., 2003). The mutant line produced elongated leaves that curl downward, have a serrate margin and short petioles, and had abaxial trichomes (Hunter *et al*., 2003). Similarly in the two crop monocots maize and rice mutations in *AGO7* affect leaf development (Douglas *et al*., 2010; Nagasaki *et al.* 2007). However, in *N. attenuata* we could not find such a phenotype. When grown in single pots under full nutrient regimes plants silenced in *AGO7* grew similar to wild type plants; rosette diameter, stalk length and fitness were not altered (Fig. 1A) and we did not observe any changes in leaf morphology nor changes in flowering. Based on these results we conclude that *AGO7* in *N. attenuata* does not directly regulate developmental traits. However, when grown in competition in the presence of AMF either in the glasshouse or in the field, ir*AGO7* plants had severely reduced stalk elongation and delayed production of flowers and capsules (Fig. 1B), while herbivore damage and pathogen infection was similar in both genotypes, confirming previous data from glasshouse studies (Pradhan *et al*., 2017; Pradhan *et al*., 2019). The phenotype closely mimics the reduced competitive ability of irRdR3 plants. RNA-Directed RNA Polymerases (RdRs) are an important element to for the synthesis of dsRNAs during smRNA biogenesis (Wassenegger and Krczal 2006); and we showed earlier that RdR3 in *N. attenuata* is involved in conspecific competition and loss of RdR3 affects siRNA accumulation (Pandey *et al*., 2008). In ir*RdR3* plants the phenotype was associated with altered phytohormone homeostasis, in particular auxin. In

Arabidopsis, AGO7 is known to interact with miR390 directing the production of tasiRNAs, which in turn regulate AUXIN RESPONSIVE FACTOR (ARF) genes, critical for auxin signaling (Montgomery *et al.*, 2008; Xia *et al.* 2017). It is tempting so speculate that *AGO7* helps to regulate hormone balance when plants compete with conspecifics in natural environments.

In this context the expression pattern of miR398 and the three sequence variants of miR399 is interesting. Their expression is similar in both lines or even tends to be higher in WT during the early stages of AMF-colonization, but at 6 weeks after AMF root colonization expression is much higher in ir*AGO7* roots. These miRNAs are very well described to be induced by N- and P-starvation and involved in regulating P starvation responses (Yang and Finnegan 2010). The expression pattern of miR399 partially corresponds with the expression of its putative targets laccase 4 and phosphate transporter 1-4 (PT1-4). A down-regulation of PT1 was also observed in plants overexpressing miR399 in Arabidopsis (Fujii *et al.,* 2005). Hence, we assume that at the early stage of AMF colonization both plants are equally competent to acquire N and P, and due to their size they may not be competing for nutrients yet. However, at 6 weeks of AMF colonization despite of the higher root colonization of ir*AGO7* plants their competitive ability is impaired and they may suffer from P-starvation.

In the natural environment all land plants are exposed to AMF which ubiquitously occur in soil (Davison *et al.,* 2015), and in natural populations as well as field-grown *N. attenuata* plants are colonized by AMF (Groten *et al*., 2015; Wang *et al*., 2017). The growth phenotype we observed in the field for ir*AGO7* plants grown in pairs with WT was also observed in the glasshouse when the same pair of plants was cultivated in 2L pots with AMF under low P fertilization regimes (Fig. 1). The growth effect was specific for AGO7; silencing of other AGOs in *N. attenuata* did not result in a decreased growth pattern under these conditions (Fig. S1). In a previous study we showed that plants impaired in the interaction with AMF (ir*CCaMK*) are smaller, less fit and P-starved when competing for nutrients with a fully functional neighbor (Wang *et al*., 2017). Therefore, we expected to find lower AMF colonization rates in ir*AGO7*. However, we observed the opposite: 11 carboxyblumenol C glucoside levels were significantly higher in *AGO7* leaves compared to WT (Fig. 2). We confirmed the results by microscopy, and in particular the relative number of arbuscules was significantly higher in ir*AGO7* roots grown compared to WT plants grown in the same pot (Fig. 2). The symbiotic relationship with AMF is

costly for the plant; the plants have to provide photoassimilates to the fungus while receiving P and other micronutrients in exchange (Smith and Smith 2011). Hyper-colonization may negatively impact plant productivity and competitive ability as the 'investment costs' in AMF associations are as high as 20% of photosynthesis. It is plausible that hyper-colonization increases the investment cost for plants such that the 'returns' due to increased P-mobilization do not benefit the plants. For the symbiosis of legumes and rhizobia it is known that plants can autoregulate nodulation to avoid hypernodulation (Penmetsa *et al.,* 2003; Schnabel *et al.,* 2005), and, similar to our findings for AMF, mutations in *AGO7* in *Medicago truncatula* enhance nodulation and rhizobial infection (Hobecker *et al.,* 2017). We hypothesize that *AGO7* may have a similar role in the AMF-plant symbiosis – it controls the number of arbuscules to avoid non-beneficial symbiotic costs.

The expression of miRNAs during AMF colonization provides first evidence to support this hypothesis. During AMF colonization, plants reprogram their smRNome profiles (Pandey *et al*., 2018), and AGO7-dependent RISC may target such repressors of AMF signalling. Based on a previous study we selected further miRNAs shown to be differentially enriched in AMF inoculated and non-inoculated roots of WT plants and plants impaired in the interaction with AMF (Pandey *et al*., 2018) and followed their expression pattern over time. In particular during early time-points of root colonization (3 days to 3 weeks after AMF inoculation) when AMF starts to enter the plants, form hyphopodia and hyphae and the first arbuscules are build (Pimprikar and Gutjahr, 2018) the selected miRNAs were mostly up-regulated in AMF colonized WT roots compared to ir*AGO7*, while the expression was mostly equal or even reversed during the mature stage of the interaction. This expression pattern is particularly well represented by miR393a. Interestingly, one of on the miR393a sequence variants (miR393a-5p) was strongly up-regulated in ir*AGO7* plants during the mature stage of the interaction with AMF, while the other one was much more strongly expressed in AMF colonized WT during the early stages of root colonization (miR393a-3p). miR393 regulates TIR and several AFB genes enconding auxin receptors (Navarro *et al.,* 2006; Vidal *et al.,* 2010), and it was shown to act synergistically with miR390 and its targets auxin response factor2 (ARF2), ARF3, and ARF4 to regulate lateral root development (Lu *et al.,* 2018). miR393 is considered as a negative regulator of arbuscule formation, because its overexpression in three different plant species strongly impaired arbuscule

formation (Etemadi *et al.,* 2014). At first glimpse this contradicts our findings; however, the comparison of AMF-inoculated *N. attenuata* plants compared to non-inoculated plants clearly showed a down-regulation of miR393a-3p in a previous study (Pandey *et al*., 2018); hence, the relative high levels compared of WT to ir*AGO7* may have a strong down-stream effect; and as shown by our kinetic analysis sequence variants most probably interact with different targets leading to different down-stream effects. Here, we see a negative correlation of miR393a-5 expression with the expression pattern of its putative target AFB2. The two sequence variants of miR172a showed a similar expression pattern as miR393a with higher values for WT compared to ir*AGO7* during the early stages of root colonization and depending on the sequence variant higher enrichment in ir*AGO7* or WT. miR172a plays a role in the rhizobium-Lotus interaction and strongly accumulates in dependency of both nodulation (Nod) factor and compatible rhizobia (Holt *et al.,* 2015).

The expression pattern of miR156a sequence variants was even more complex and varied strongly among the variants. In *Lotus japonicus* ectopic expression of miR156a led to enhanced branching, delayed flowering, underdeveloped roots, reduced nodulation and repression of several nodulation genes (Wang and Chua, 2014). Its function in AMF has not been described yet, though (Couzigou *et al.,* 2017) speculated that it might act similarly to miR171b, having a positive effect on symbiosis (Couzigou *et al*., 2017). However, our expression analysis shows a higher expression of miR171b during early stages of root colonization in AMF-colonized WT roots than in ir*AGO7* roots; and during the mature stage of AMF colonization miR171a - which acts as a repressor of AMF colonization in *L. japonicus* (Couzigou *et al*., 2017) is enriched in ir*AGO7* compared to WT. Further studies are needed to resolve this controversy.

In conclusion, we propose that AGO7 participates in the AMF-induced smRNA pathway to control root colonization, most probably via controlling auxin responses. AMF root colonization results in changes in expression of miRNAs. These miRNAs may be channelled to modulate targets specific to AMF colonization in an AGO7-dependent manner. In future studies we will use selected miRNAs (such as miR156, miR172a, miR393a, miR473, miR398, miR399a, and the novel, miR Nat-R-PN59) and overexpress them in WT and background after inoculation with AMF to further investigate the relationship between AGO7 and these miRNAs for AMF colonization. The mechanistic basis of recruitment of miRNAs by AGO7 during host-AMF

interaction needs further elucidation as AGO7 might be involved in differential accumulation and recruitment of AMF-associated miRNAs; multiple checkpoints and sequence dependent recruitment mechanisms cannot be ruled out. An additional unresolved aspect to be further investigated is why AMF colonized irAGO7 plants express markers of P-starvation despite of higher arbuscule numbers.

Material and Methods

Plant material and growth conditions in the glasshouse

Seeds of 31st generations of an inbred *N. attenuata* wild-type plant (WT), originally collected from Southwestern Utah, USA were used for all experiments. Two independent transgenic irAGO7 lines (A-13-018-8-4 and A-13-017-2-2) have been described previously and did not show any significant differences among each other (Pradhan *et al*., 2017). Therefore, we randomly selected line A-13-018-8-4 for the experiments presented here. Seeds from WT and all the transgenic plants were germinated on Gamborg B5 medium (Krügel *et al.,* 2002). Seeds were germinated and plant populations were grown and maintained under a day/night cycle of 16 h (26 to 28°C)/8 h (22 to 24°C) and 45 to 55% humidity (Halitschke *et al.* 2004; Krügel *et al*., 2002, Onkokesung *et al.* 2012).

For the glasshouse experiments with AMF, plants were first transferred to sand in Teku pots, and 10-12 days later into inactive (autoclaved twice at 121 °C for 30 min; non-inoculated controls) and living inoculum (*R. irregularis*, Biomyc Vital, www.biomyc.de, inoculated plants), diluted 1:10 with expanded clay (size: 2-4 mm). Plants were watered with distilled water for the first day of pot transfer and then fertilized every second day with a hydroponic solution with a low P hydroponics fertilizer (Groten *et al*., 2015) with 1/10 of the regular inorganic Pi concentration during rosette stage, and starting with the elongation stage with 1/4 Pi concentration (Wang *et al*., 2018). For experiments presented in Figure 1A, all plants were grown in standard soil conditions, in 1L pots without competition (Krügel *et al*., 2002). Plant performance in terms of rosette diameter, chlorophyll content, stalk length, total capsule number, and shoot and root fresh mass, were recorded at respective time points. For experiments presented in Figure 1B and later plants were subjected to resource-limited conditions by growing

them in pairs in 2L pots, in expanded clay with AMF inoculum and low-P as described above. A WT plant was always paired with an irAGO7 stage-matched plant in the same pot to allow the two genotypes to compete for resources as previously described (Pandey *et al*., 2008). During sample harvests, roots were carefully washed, briefly dried with a paper towel, cut into approximately 1 cm pieces and mixed. An aliquot was stored in root storage solution (99% ethanol and 60% acetic acid, 3:1, v : v) and stored at 4 °C for microscopic analysis, while the remaining root material was immediately frozen in liquid nitrogen and stored at −80 °C for future use.

Blumenol analysis and microscopic observations for estimating host-AMF interaction

11-Carboxyblumenol-C-glucoside is a reliable quantitative marker for root colonization of AMF (Wang *et al*., 2018). For estimation of 11-Carboxyblumenol-C-glucoside, leaf samples were aliquoted into reaction tubes, containing two steel balls after their mass was recorded for later normalization. For 100 mg plant tissues, approximately 1 mL 80% MeOH was added to the samples, and shaken in a GenoGrinder 2000 (SPEX SamplePrep) for 60 s at 1150 strokes min^{-1}. After centrifugation, the supernatant was collected and analyzed with a Ultra-high performance liquid chromatography (UHPLC), using a Dionex UltiMate 3000 rapid separation LC system (Thermo Fisher) as described in detail previously (Wang *et al*., 2018).

To determine the fungal colonization rates and mycorrhizal structures, root samples were stained and analyzed by microscopy. Roots were first washed with distilled water and then boiled in a 2% (w/v) KOH solution for 5 min. After rinsing with water, the roots were boiled in 2% HCl solution for 5 min, rinsed with water and subsequently Trypan blue staining was performed as described (Brundrett *et al.,* 1984; McGonigle *et al.,* 1990) to visualize mycorrhizal structures. For determining mycorrhizal colonization, 10 root fragments, each about 1 cm long, were stained with either trypan blue and placed on the slide by mounting. Around 150 view fields per slide were surveyed with Axioskop/Zeiss Imager.Z1 at 200x magnification and visible structures were classified into three groups: arbuscules, vesicles and hyphae.

RNA extraction and quantitative real time PCR

To analyze miRNA accumulation and gene expression, approximately 200 mg of powdered root sample was used for RNA extraction. Total RNA was extracted from the root

samples using the lithium chloride method as previously described by (Kistner and Matamoros 2005) and adapted to *N. attenuata* (Pradhan *et al*., 2017). Reverse transcription (RT) was performed using oligo (dT) and Superscript II reverse transcriptase according to the manufacturer's instruction (www.invitrogen.com). Real-time q-PCR was performed on a Mx3005P qPCR system (Stratagene, Santa Clara, CA, USA; http://www.stratagene.com) with qPCR (qPCR core kit for Taykon^{TM} SYBR master mix, Eurogentec) were done following the manufacturer's protocol. qPCR assays were performed using gene-specific primers (designed with the help of Primer Express software v 3.0.1). (http://www.appliedbiosystems.com) on cDNA templates corresponding to 50 ng total RNA before reverse-transcription. The *N. attenuata* sulfite reductase (*ECI*), a housekeeping gene, was used as an endogenous reference (Bubner and Baldwin 2004). The $2^{-\Delta\Delta CT}$ method was used for data analysis (Bubner and Baldwin 2004). For determining relative transcript abundances, levels corresponding to time point 0 hpi (controls) were set to 1 (as reference) and relative expressions of genes at various time points were determined (Bozorov *et al.* 2012; Bubner and Baldwin 2004; Pandey and Baldwin 2007).

To check the miRNA transcript abundance, a total of 1 ug of total RNA was converted to cDNA according to the manufacturer's instruction (www.qiagen.com). Real-time q-PCR was performed on a Mx3005P qPCR system (Stratagene, Santa Clara, CA, USA; http://www.stratagene.com). qPCR was performed with the help of miScript SYBR Green PCR kit, by following the manufacturer's protocol. QPCR assay were performed using the specific miRNA sequences from Pandey et al., (2018). A total of 10 ng of cDNA was used for detection of miRNA in each sample. 5S rRNA gene was used for normalization of microRNA expression by real-time reverse transcription PCR. The $2^{-\Delta\Delta CT}$ method was used for data analysis (Bubner and Baldwin 2004).

A list of sequences of all the primers (genes and miRNAs) used in the study is provided in Supplemental Table 2.

Field experiments

All the field experiments were conducted at the Lytle Ranch Preserve, located in the Great Basin Desert of Southwestern Utah, USA (latitude 37.146, longitude 114.020). Seeds were germinated directly on borax-soaked Jiffy 703 pots (AlwaysGrows), which were transplanted

into the field plot 3 to 4 weeks later. 10-15 pairs of sized adapted seedlings of WT and ir*AGO7* genotypes were transplanted. 10-15 pairs of sized adapted seedlings of WT and ir*AGO7* genotypes were transplanted. Pairs of WT and ir*AGO7* (A-13-018-8-4) were planted around 15-20 cm apart in a quadrant design and randomized over the field plot to avoid any spatial variation in the diversity of root-associated microbial communities. Rosette diameter of the plants was measured until they started to elongate, followed by measurements of the stalk length, flower number and start of setting of the capsules. Experiments were terminated after 8 weeks (when the plants started to produce seed capsules) by uprooting the plants. Before the capsules were matured, they were removed as per the requirements of APHIS regulation. To get the fitness data plants were harvested carefully separated into shoots and roots which were washed with water, briefly dried and weighed. Herbivory was estimated as percentage of total plant canopy area of WT and ir*AGO7* plants damaged at 4 weeks and 8 weeks.

Statistical analysis

Data were analyzed using OriginLab 2016 software. All the fitness related parameters (rosette diameter, stalk length fresh and dry biomass, and seed capsule data) from the competition experiments were analyzed using paired T-test at a significance level of $p \leq 0.05$, $p \leq 0.01$ and $p \leq 0.001$; gene expression and miRNA expression data were analyzed by ANOVA (repeated measures wherever applicable) at a significance level of $p \leq 0.05$, $p \leq 0.01$ and $p \leq 0.001$.

Acknowledgments

We thank the glasshouse team of the Max Planck Institute for Chemical Ecology for plant cultivation and the Brigham Young University for use of their field station. This work was supported by the Max Planck Society.

References

Axtell, M.J. (2013) Classification and comparison of small RNAs from plants. *Annual Review of Plant Biology*, **64**, 137-159.

Baldwin, I.T. (2001) An ecologically motivated analysis of plant-herbivore interactions in native tobacco. *Plant Physiology*, **127**, 1449-1458.

Baldwin, I.T. and Morse, L. (1994) Up in smoke 2. germination of *Nicotiana attenuata* in response to smoke-derived cues and nutrients in burned and unburned soils. *Journal of Chemical Ecology*, **20**, 2373-2391.

Gase, K., Weinhold, A., Bozorov, T.A., Schuck, S. and Baldwin, I.T. (2011) Efficient screening of transgenic plant lines for ecological research. *Molecular Ecology Resources*, **11**, 890 - 902.

Borges, F. and Martienssen, R.A. (2015) The expanding world of small RNAs in plants. *Nature Reviews. Molecular Cell Biology*, **16**, 727-741.

Bozorov, T.A., Baldwin, I.T. and Kim, S.-G. (2012) Identification and profiling of miRNAs during herbivory reveals jasmonate-dependent and -independent patterns of accumulation in *Nicotiana attenuata*. *BMC Plant Biology*, **12**.

Brant, E.J. and Budak, H. (2018) Plant small non-coding RNAs and their roles in biotic stresses. *Frontiers in Plant Science*, **9**, 1038-1038.

Brundrett, M.C., Piché, Y. and Peterson, R.L. (1984) A new method for observing the morphology of vesicular–arbuscular mycorrhizae. *Canadian Journal of Botany*, **62**, 2128-2134.

Bubner, B. and Baldwin, I.T. (2004) Use of real-time PCR for determining copy number and zygosity in transgenic plants. *Plant Cell Reports*, **23**, 263-271.

Carbonell, A. (2017) Immunoprecipitation and high-throughput sequencing of ARGONAUTE-bound target RNAs from plants. In *Plant Argonaute Proteins: Methods and Protocols* (Carbonell, A. ed. New York, NY: Springer New York, pp. 93-112.

Cosme, M., Fernández, I., Van der Heijden, M.G.A. and Pieterse, C.M.J. (2018) Non-mycorrhizal plants: The exceptions that prove the rule. *Trends in Plant Science*, **23**, 577-587.

Couzigou, J.-M., Lauressergues, D., André, O., Gutjahr, C., Guillotin, B., Bécard, G. and Combier, J.-P. (2017) Positive gene regulation by a natural protective miRNA enables arbuscular mycorrhizal symbiosis. *Cell Host & Microbe*, **21**, 106-112.

Couzigou, J.M. and Combier, J.P. (2016) Plant microRNAs: key regulators of root architecture and biotic interactions. *New Phytol*, **212**, 22-35.

Davison, J., Moora, M., Öpik, M., Adholeya, A., Ainsaar, L., Bâ, A., Burla, S., Diedhiou, A.G., Hiiesalu, I., Jairus, T., Johnson, N.C., Kane, A., Koorem, K., Kochar, M., Ndiaye, C., Pärtel, M., Reier, Ü., Saks, Ü., Singh, R., Vasar, M. and Zobel, M. (2015) Global assessment of arbuscular mycorrhizal fungus diversity reveals very low endemism. *Science*, **349**, 970-973.

Douglas, R.N., Wiley, D., Sarkar, A., Springer, N., Timmermans, M.C.P. and Scanlon, M.J. (2010) ragged seedling2 Encodes an ARGONAUTE7-like protein required for mediolateral expansion, but not dorsiventrality, of maize leaves. *The Plant Cell*, **22**, 1441-1451.

Etemadi, M., Gutjahr, C., Couzigou, J.-M., Zouine, M., Lauressergues, D., Timmers, A., Audran, C., Bouzayen, M., Becard, G. and Combier, J.-P. (2014) Auxin perception is required for arbuscule development in arbuscular mycorrhizal symbiosis. *Plant Physiology*, **166**, 281-292.

Fang, X. and Qi, Y. (2016) RNAi in plants: An Argonaute-centered view. *The Plant Cell*, **28**, 272-285.

Fujii, H., Chiou, T.-J., Lin, S.-I., Aung, K. and Zhu, J.-K. (2005) A miRNA involved in phosphate-starvation response in Arabidopsis. *Current Biology*, **15**, 2038-2043.

Groten, K., Nawaz, A., Nguyen, N.H.T., Santhanam, R. and Baldwin, I.T. (2015) Silencing a key gene of the common symbiosis pathway in *Nicotiana attenuata* specifically impairs arbuscular mycorrhizal infection without influencing the root-associated microbiome or plant growth. *Plant, Cell & Environment*, **38**, 2398-2416.

Halitschke, R., Ziegler, J., Keinanen, M. and Baldwin, I.T. (2004) Silencing of hydroperoxide lyase and allene oxide synthase reveals substrate and defense signaling crosstalk in *Nicotiana attenuata*. *Plant Journal*, **40**, 35-46.

Hobecker, K.V., Reynoso, M.A., Bustos-Sanmamed, P., Wen, J., Mysore, K.S., Crespi, M., Blanco, F.A. and Zanetti, M.E. (2017) The microRNA390/TAS3 pathway mediates symbiotic nodulation and lateral root growth. *Plant Physiology*, **174**, 2469-2486.

Holt, D.B., Gupta, V., Meyer, D., Abel, N.B., Andersen, S.U., Stougaard, J. and Markmann, K. (2015) micro RNA 172 (miR172) signals epidermal infection and is expressed in cells primed for bacterial invasion in *Lotus japonicus* roots and nodules. *New Phytol*, **208**, 241-256.

Hunter, C., Sun, H. and Poethig, R.S. (2003) The *Arabidopsis* heterochronic gene *ZIPPY* is an *ARGONAUTE* family member. *Current Biology*, **13**, 1734-1739.

Johnson, N.C., Graham, J.H. and Smith, F.A. (1997) Functioning of mycorrhizal associations along the mutualism-parasitism continuum. *New Phytol*, **135**, 575-586.

Jouannet, V., Moreno, A.B., Elmayan, T., Vaucheret, H., Crespi, M.D. and Maizel, A. (2012) Cytoplasmic Arabidopsis AGO7 accumulates in membrane-associated siRNA bodies and is required for ta-siRNA biogenesis. *The EMBO Journal*, **31**, 1704-1713.

Kiers, E.T., Duhamel, M., Beesetty, Y., Mensah, J.A., Franken, O., Verbruggen, E., Fellbaum, C.R., Kowalchuk, G.A., Hart, M.M., Bago, A., Palmer, T.M., West, S.A., Vandenkoornhuyse, P., Jansa, J. and Buecking, H. (2011) Reciprocal rewards stabilize cooperation in the mycorrhizal symbiosis. *Science*, **333**, 880-882.

Kistner, C. and Matamoros, M. (2005) RNA isolation using phase extraction and LiCl precipitation. In *Lotus Japonicus Handbook* (Márquez, A.J., Stougaard, J., Udvardi, M., Parniske, M., Spaink, H., Saalbach, G., Webb, J., Chiurazzi, M., Márquez, A.J. ed. Netherlands: Springer, pp. 123-124.

Krügel, T., Lim, M., Gase, K., Halitschke, R. and Baldwin, I.T. (2002) Agrobacterium-mediated transformation of *Nicotiana attenuata*, a model ecological expression system. *Chemoecology*, **12**.

Kuo, H.-F. and Chiou, T.-J. (2011) The role of microRNAs in phosphorus deficiency signaling. *Plant Physiology*, **156**, 1016-1024.

Lu, Y., Feng, Z., Liu, X., Bian, L., Xie, H., Zhang, C., Mysore, K.S. and Liang, J. (2018) MiR393 and miR390 synergistically regulate lateral root growth in rice under different conditions. *BMC Plant Biology*, **18**, 261-261.

Manavella, P.A., Yang, S.W. and Palatnik, J.(2019) Keep calm and carry on: miRNA biogenesis under stress. *The Plant Journal*, doi: 10.1111/tpj.14369.

McGonigle, T.P., Miller, M.H., Evans, D.G., Fairchild, G.L. and Swan, J.A. (1990) A new method which gives an objective measure of colonization by vesicular arbuscular mycorrhizal fungi. *New Phytol*, **115**, 495-501.

Meister, G. (2013) Argonaute proteins: functional insights and emerging roles. *Nature Reviews Genetics*, **14**, 447.

Montgomery, T.A., Howell, M.D., Cuperus, J.T., Li, D., Hansen, J.E., Alexander, A.L., Chapman, E.J., Fahlgren, N., Allen, E. and Carrington, J.C. (2008) Specificity of ARGONAUTE7-miR390 interaction and dual functionality in *TAS3 Trans*-acting siRNA formation. *Cell*, **133**, 128-141.

Nagasaki, H., Itoh, J.-i., Hayashi, K., Hibara, K.-i., Satoh-Nagasawa, N., Nosaka, M., Mukouhata, M., Ashikari, M., Kitano, H., Matsuoka, M., Nagato, Y. and Sato, Y. (2007) The small interfering RNA production pathway is required for shoot meristem initiation in rice. *Proceedings of the National Academy of Sciences*, **104**, 14867-14871.

Navarro, L., Dunoyer, P., Jay, F., Arnold, B., Dharmasiri, N., Estelle, M., Voinnet, O. and Jones, J.D.G. (2006) A plant miRNA contributes to antibacterial resistance by repressing auxin signaling. *Science*, **312**, 436-439.

Onkokesung, N., Gaqkimuerel, E., Kotkar, H., Kaur, H., Baldwin, I.T. and Galis, I. (2012) MYB8 controls inducible phenolamide levels by activating three novel hydroxycinnamoyl-coenzyme A: polyamine transferases in *Nicotiana attenuata*. *Plant Physiology*, **158**.

Pandey, P., Wang, M., Baldwin, I.T., Pandey, S.P. and Groten, K. (2018) Complex regulation of microRNAs in roots of competitively-grown isogenic *Nicotiana attenuata* plants with different capacities to interact with arbuscular mycorrhizal fungi. *BMC Genomics*, **19**, 937.

Pandey, S.P. and Baldwin, I.T. (2007) RNA-directed RNA polymerase 1 (RdR1) mediates the resistance of *Nicotiana attenuata* to herbivore attack in nature. *The Plant Journal*, **50**, 40 - 53.

Pandey, S.P., Gaquerel, E., Gase, K. and Baldwin, I.T. (2008) RNA-directed RNA polymerase 3 from *Nicotiana attenuata* is required for competitive growth in natural environments. *Plant Physiology*, **147**, 1212 - 1224.

Penmetsa, R.V., Frugoli, J.A., Smith, L.S., Long, S.R. and Cook, D.R. (2003) Dual genetic pathways controlling nodule number in *Medicago truncatula*. *Plant Physiology*, **131**, 998-1008.

Pimprikar, P. and Gutjahr, C. (2018) Transcriptional regulation of arbuscular mycorrhiza development. *Plant and Cell Physiology*, pcy024-pcy024.

Pradhan, M., Pandey, P., Baldwin, I.T. and Pandey, S.P. (2019) Argonaute 4 modulates resistance against hemibiotrophic fungal infection by regulating jasmonic acid signaling in Nicotiana attenuata plants *Plant Physiology*, **under revision**.

Pradhan, M., Pandey, P., Gase, K., Shraff, M., Singh, R.K., Sethi, A., Baldwin, I.T. and Pandey, S.P. (2017) Argonaute 8 (AGO8) mediates the elicitation of primary defense against herbivory. *Plant Physiology*.

Redecker, D., Schuessler, A., Stockinger, H., Stuermer, S.L., Morton, J.B. and Walker, C. (2013) An evidence-based consensus for the classification of arbuscular mycorrhizal fungi (Glomeromycota). *Mycorrhiza*, **23**, 515-531.

Santhanam, R., Luu, V.T., Weinhold, A., Goldberg, J., Oh, Y. and Baldwin, I.T. (2015) Native root-associated bacteria rescue a plant from a sudden-wilt disease that emerged during continuous cropping. *Proceedings of the National Academy of Sciences of the United States of America*, **112**, E5013-E5020.

Schnabel, E., Journet, E.-P., de Carvalho-Niebel, F., Duc, G. and Frugoli, J. (2005) The *Medicago truncatula* SUNN gene encodes a CLV1-like leucine-rich repeat receptor kinase that regulates nodule number and root length. *Plant Molecular Biology*, **58**, 809-822.

Schuck, S., Weinhold, A., Luu, V.T. and Baldwin, I.T. (2014) Isolating fungal pathogens from a dynamic disease outbreak in a native plant population to establish plant-pathogen bioassays for the ecological model plant *Nicotiana attenuata*. *Plos One*, **9**.

Silvestri, A., Fiorilli, V., Miozzi, L., Accotto, G.P., Turina, M. and Lanfranco, L. (2019) In silico analysis of fungal small RNA accumulation reveals putative plant mRNA targets in the symbiosis between an arbuscular mycorrhizal fungus and its host plant. *BMC Genomics*, **20**, 169.

Singh, R.K., Gase, K., Baldwin, I.T. and Pandey, S.P. (2015) Molecular evolution and diversification of the Argonaute family of proteins in plants. *BMC Plant Biology*, **15**, 23-23.

Smith, S.E., Jakobsen, I., Gronlund, M. and Smith, F.A. (2011) Roles of arbuscular mycorrhizas in plant phosphorus nutrition: Interactions between pathways of phosphorus uptake in arbuscular mycorrhizal roots have important implications for understanding and manipulating plant phosphorus acquisition. *Plant Physiology*, **156**, 1050-1057.

Smith, S.E. and Smith, F.A. (2011) Roles of arbuscular mycorrhizas in plant nutrition and growth: new paradigms from cellular to ecosystem scales. In *Annual Review of Plant Biology* (Merchant, S.S., Briggs, W.R. and Ort, D. eds), pp. 227-250.

Song, F., He, C., Yan, X., Bai, F., Pan, Z., Deng, X. and Xiao, S. (2018) Small RNA profiling reveals involvement of microRNA-mediated gene regulation in response to mycorrhizal symbiosis in *Poncirus trifoliata* L. Raf. *Tree Genetics & Genomes*, **14**, 42.

Song, X., Li, Y., Cao, X. and Qi, Y. (2019) MicroRNAs and their regulatory roles in plant–environment interactions. *Annual Review of Plant Biology*, **70**, 489-525.

Vidal, E.A., Araus, V., Lu, C., Parry, G., Green, P.J., Coruzzi, G.M. and Gutiérrez, R.A. (2010) Nitrate-responsive miR393/AFB3 regulatory module controls root system architecture in *Arabidopsis thaliana*. *Proceedings of the National Academy of Sciences*, **107**, 4477-4482.

Walder, F., Niemann, H., Natarajan, M., Lehmann, M., Boller, T. and Wiemken, A. (2012) Mycorrhizal networks: common goods of plants shared under unequal terms of trade. *Plant Physiology*, **159**, 789.

Wang, H. and Chua, N.H. (2014) Big effects of small RNAs on legume root biotic interactions. *Genome Biology*, **15**.

Wang, M., Schäfer, M., Li, D., Halitschke, R., Dong, C., McGale, E., Paetz, C., Song, Y., Li, S., Dong, J., Heiling, S., Groten, K., Franken, P., Bitterlich, M., Harrison, M.J.,

Paszkowski, U. and Baldwin, I.T. (2018) Blumenols as shoot markers of root symbiosis with arbuscular mycorrhizal fungi. *eLife*, **7**, e37093.

Wang, M., Wilde, J., Baldwin, I.T. and Groten, K. (2018) *Nicotiana attenuata*'s capacity to interact with arbuscular mycorrhiza alters its competitive ability and elicits major changes in the leaf transcriptome. *Journal of Integrative Plant Biology*, **60**, 242-261.

Wassenegger, M. and Krczal, G. (2006) Nomenclature and functions of RNA-directed RNA polymerases. *Trends in Plant Science*, **11**, 142-151.

Wu, P., Wu, Y., Liu, C.-C., Liu, L.-W., Ma, F.-F., Wu, X.-Y., Wu, M., Hang, Y.-Y., Chen, J.-Q., Shao, Z.-Q. and Wang, B. (2016) Identification of arbuscular mycorrhiza (AM)-responsive microRNAs in tomato. *Frontiers in Plant Science*, **7**.

Xia, R., Xu, J. and Meyers, B.C. (2017) The emergence, evolution, and diversification of the miR390-*TAS3*-*ARF* pathway in land plants. *The Plant Cell*, **29**, 1232-1247.

Xu, L., Yang, L., Pi, L., Liu, Q., Ling, Q., Wang, H., Poethig, R.S. and Huang, H. (2006) Genetic interaction between the AS1–AS2 and RDR6–SGS3–AGO7 pathways for leaf morphogenesis. *Plant and Cell Physiology*, **47**, 853-863.

Yang, X.J. and Finnegan, P.M. (2010) Regulation of phosphate starvation responses in higher plants. *Annals of Botany*, **105**, 513-526.

Supplemental material

Figure S1. Silencing AGOs 1, 2, 4, and 10 does not affect competitive fitness of *N. attenauta* plants under resource limited conditions. Rosette diameter (c), stalk length (b) as well as total number of seed capsules produced by ir*AGO*s and WT plants were similar.

Table S1. miRNA and their putative target genes tested in *Nicotiana*-AMF interaction

Table S2. List of primers (a, of genes, and b, of miRNAs) used in this study.

3. DISCUSSION

3.1 Overview

The overarching objective of this study was to uncover the biological functions of the genes of the Argonaute (AGO) family of *Nicotiana attenuata* during plant's adaptive responses to biotic challenges posed by the ecological habitats. *N. attenuata* genome codes for 11 AGOs that correspond to 8 unique genes. We performed loss-of-function characterization of these AGOs and determined functional specificities towards modulating defense and signalling responses during interaction with herbivores, hemibiotrophic phytopathogens and AMF colonization (presented in three manuscripts here). As AGO's are the central components of the smRNA-function, our findings strongly suggest specialization of biological functions of AGOs during stress adaptation and modulation of defense signaling, while the overall biochemical functions (of such as association with nucleic acids and the slicer activity) might remain intact. Evolutionary studies suggest that an ancestral AGO duplicated after the divergence of unicellular green algae, and consequently four major classes of plant AGOs have evolved (Figure 1; (Singh et al., 2015)). Context-dependent changes in sequence of AGOs may have had consequences for gene function (Singh et al., 2015). AGO proteins have diverged resulting in evolution of their differential affinities to various types of smRNA-duplexes (Figure 1).

Discussion

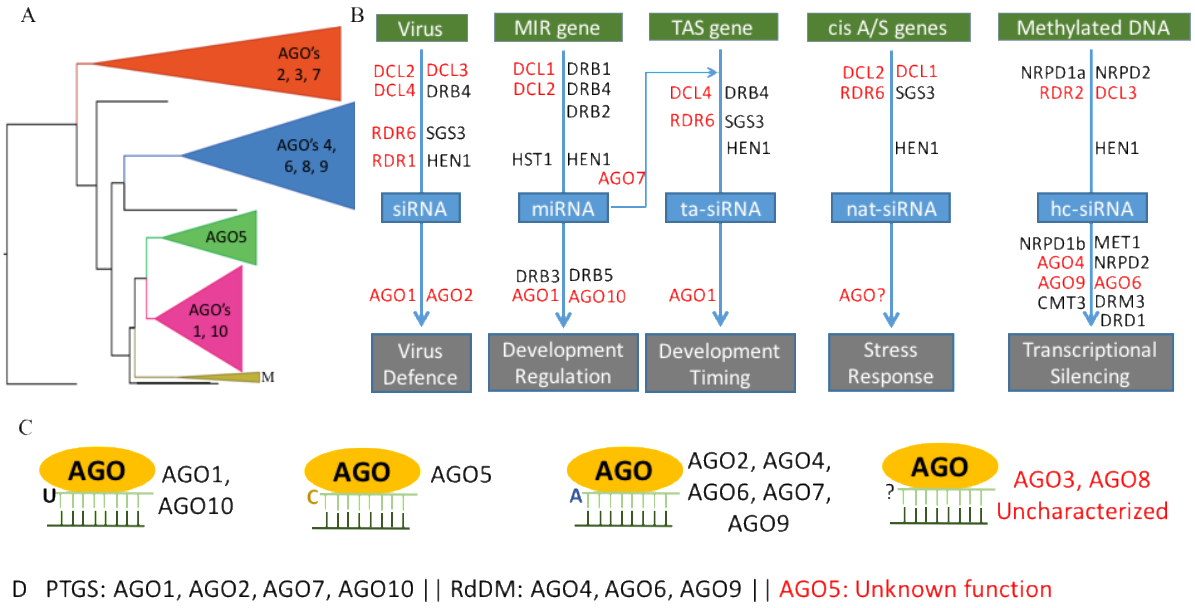

Figure 1. Classification and functions of plant AGO's. (A) Phylogenetic tree showing 4 clusters of AGOs (B) Association of AGOs with various types of smRNAs. (C) 5'-nucleotide preference of AGOs. (D) Molecular functions of AGOs. PTGS-post transcriptional gene silencing, RdDM-RNA directed DNA methylation (Nakasugi et al., 2013; Borges and Martienssen, 2015; Singh et al., 2015).

Changes in structure-function relationship due to evolutionary diversifications plausibly had implications on interaction with the smRNAs (Singh and Pandey, 2015). These evolutionary events have given rise to a variety of distinct non-coding smRNA pathways for gene silencing (Figure 1). The identity of 5'-terminal residue of the smRNA influences its loading on to the specific AGO's as well as their activity. Most plant lineages have multiple paralogs for the AGO genes due to gene-family expansion during evolution, which is believed to have resulted in functional diversification. Specialization of AGOs in various smRNA processes have been described to their intrinsic biochemical properties and the patterns on their interaction with the substrate smRNAs (Figure 1). Most of the identified biological functions of AGOs have been attributed to aspects of plant development such as reproduction, growth, and differentiation ((Fang and Qi, 2016; Carbonell, 2017) and Table 1). Their role in biotic stress response has been largely investigated in the context of antiviral defense, and to some extent in the context of bacterial immunity (Table 1). Little, if anything, is known on their role(s) in herbivore defense, resistance against hemibiotrophic fungal pathogens or root colonizing AMF. Neither have the

ecological relevance of AGOs been tested in a real-world setting before.

Table 1. Known biological functions of plant Argonautes in other plant species (adapted from (Fang and Qi, 2016; Carbonell, 2017)

Function	AGO involved[a]
Antibacterial immunity	AtAGO2 AtAGO4
Antiviral defense	AtAGO1 AtAGO2 AtAGO4 AtAGO5 AtAGO7 AtAGO10 NbAGO1 NbAGO2 OsAGO1a/b OsAGO18
Cell specification	AtAGO9 ZmAGO9
Gamete, Somatic Chromosome segregation	ZmAGO9
Development	AtAGO1 OsAGO1a/b/c SiAGO1b
DNA methylation	AtAGO3 AtAGO4 AtAGO6 OsAGO4a OsAGO4b
DNA repair	AtAGO2 AtAGO9
Germ cell development	ZmAGO18b
Leaf development	AtAGO1 AtAGO7 OsAGO10 ZmAGO7
Meiosis	AtAGO4 OsAGO5c
Megagametogenesis	AtAGO5
Phase transition	AtAGO7
SAM development	AtAGO10 OsAGO7
SAM maintenance	OsAGO10
Small RNA biogenesis	AtAGO1 AtAGO4 AtAGO1 AtAGO7 OsAGO7 ZmAGO7
Stress response	AtAGO1 SiAGO1b
Tapetum development	ZmAGO18b

[a]At, *Arabidopsis thaliana*; Nb, *Nicotiana benthamiana*; Os, *Oryza sativa*; Si, *Setaria italica*; Zm, *Zea mays*

3.2 Stimulus-dependent specialization in biological functions of AGOs in *N. attenuata*

N. attenuata genome encodes three genes homologous to AGO1 (NaAGO1a, b, c; 78-87% identity with AtAGO1), 2 genes homologous to AGO4 (NaAGO4a,b; 74-87% identity to AtAGO4), and 1 each to AGO2, AGO5, AGO7, AGO8, AGO9 and AGO10. Herbivore attack induces the expression of only NaAGO5 and NaAGO8 in the leaves of *N. attenuata* (Pradhan et al., 2017), indicating their roles in herbivore resistance, which was validated in loss-of-function studies. Whereas, infection of the hemibiotrophic pathogen, *Fusarium brachygibbosum* reprogrammed only NaAGO4 expression and its role in fungal resistance was further validated (Pradhan et al. 2019). NaAGO7 was identified to function in modulating colonization of roots by the AMF (Pradhan et al. in preparation). It can be inferred that the recruitment/expression of

AGO's happen in a stimulus-dependent (and plausibly for some AGO's, also in a tissue specific) manner(s), which might dictate functional specialization in biogenesis, and recruitment/loading of smRNAs during response to various stresses.

3.3 Framework of action of specialized smRNA-pathways in modulating eco-physiological responses of *N. attenuata*

According to an estimate, there could be more than a million smRNAs transcribed in a plant cell (Lu et al., 2005). This population of smRNAs is highly dynamic in nature and modulate gene expression in a sequence dependent manner by base-pairing with the target nucleic acids. The essentiality of base-pairing rule is variable, depending on the type of organisms. For instance, a small seed of just 6-7 nucleotide is sufficient to undertake pairing of miRNAs and mRNAs in several organisms including humans (Lewis et al., 2005), whereas longer complementarities are required in plants (Srivastava et al., 2014; Pandey et al., 2019). In order to explore the functional relevance of smRNAs in controlling defense-signaling networks during stress adaptation, we have adapted a genetics-guided loss-of-function approach at organism level. Such studies of smRNA-controlled pathways are crucial for an integrative understanding of how RNA-interference functions in broader contexts of plant's adaptation to unforeseen ecological challenges in annuals in their native habitats. *N. attenuata* offers a perfect model system as the ecological challenges of this plant are well characterized in past 25 years of research.

In order to study the eco-biological functions of AGOs, we adapted an unbiased approach by silencing the expression of the AGOs individually and testing their roles. A detailed investigation on the role of AGOs in herbivore resistance (Manuscript I, (Pradhan et al., 2017)) not only described the biological relevance and specificity of AGO8 (and AGO5), it also uncovered the time-resolved changes in accumulation patterns of miRNAs and siRNAs that correlated to the elicitation dynamics of targets in defense signaling network. We uncovered the smRNA-transcription factor network (e.g. the MYB8-miRNA network; Figure 2) that could fine-tune expression of downstream genes (Figure 2).

Previous studies have characterized the biological function on RdRs and DCLs in herbivore resistance: of the three RdRs of *N. attenuata*, only RdR1 modulates herbivore resistance by regulating direct defense traits such as nicotine (Pandey and Baldwin, 2007; Pandey et al., 2008a). Similarly, DCL3 and 4 were implicated in herbivore resistance (Bozorov et al., 2012). Here we have filled the missing link of the core machinery of herbivore-induced smRNA pathway by discovering herbivore-responding AGOs (Figure 2). As stated above, we have also uncovered the dynamic nature of accumulation of miRNAs and their dependence on AGO8 to regulate defense signalling by (i) modulating the expression of crucial transcription factors such as MYB8, as well as by targeting other genes (Figure 2; (Pradhan et al., 2017)). As the core components of the herbivore-induced smRNA pathway (RdRs, DCL and AGOs) have now been elucidated, the next step is to determine the genetic framework of interaction and function of these genes amongst themselves and refine the canonical components of such a pathway.

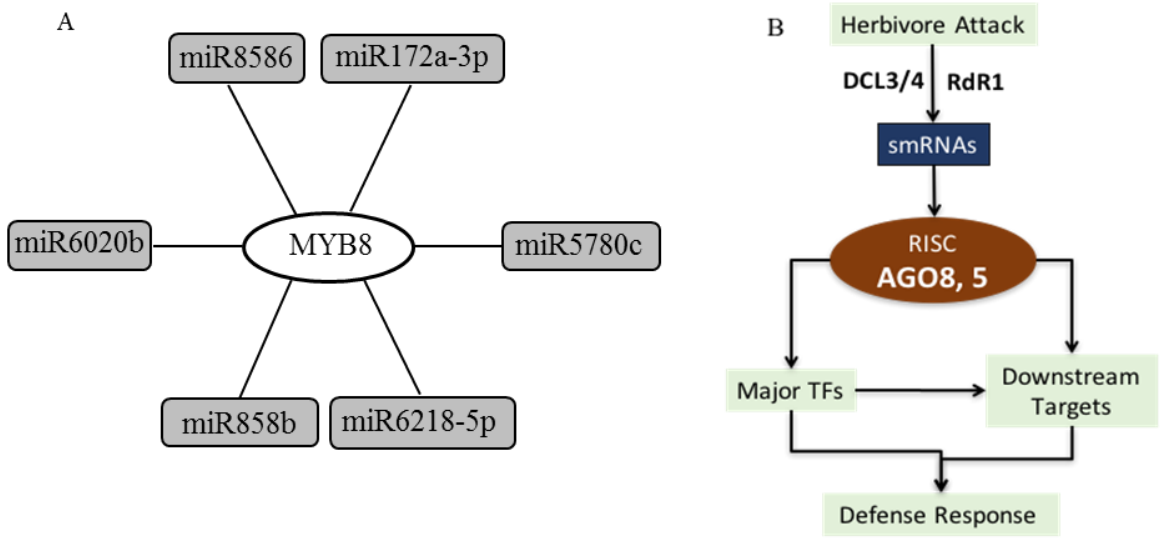

Figure 2. Herbivore-induced smRNA pathway in *N. attenuata*. (A) AGO8-dependent MYB8-miRNA network. (B) A schematic model of herbivore-induced smRNA pathway in *N. attenuata*.

In the second manuscript (Pradhan et al. 2019), we show the specificity of AGO4 in modulating resistance against hemibiotorpic fungal pathogens by regulating jasmonic acid (JA)

signalling (Figure 2). We not only performed gene expression studies of several AGO's to determine candidates involved in pathogen resistance, we also performed unbiased genome-wide loss-of-function screens to confirm that AGOs other than AGO4 were not involved in pathogen resistance. Silencing NaAGO4 resulted in *N. attenuata* plants susceptible to *F. brachygibbosum* infection, whereas silencing other AGO's did not affect susceptibility against pathogens. The susceptibility of AGO4-silenced plants could be easily attributed to perturbation of resistance signalling. Infection of hemibiotrophic fungal infection elicits the recruitment of both, JA and Salicylic acid (SA) signalling pathways (Sahu et al., 2016). JA pathway had been already characterised to act as a positive regulator for *F. brachygibbosum* resistance (Luu et al., 2015). Profiling of elicitation dynamics of JA and SA in time course experiments in the second manuscript supported the idea that both the pathways may be activated during *Fusarium* infection in *N. attenuata*; but that only the JA-signalling cascade is modulated by AGO4-dependent smRNAs. Silencing AGO4 compromised both, JA- biogenesis as well as -signal transduction pathways. Exogenous complementation of JA, methyl jasmonate conjugate as well as the substrate of JA biogenesis (OPDA) could restore the resistance of AGO4-silenced plants to the WT levels. The durability of modulation of JA-dependent resistance against *F. brachygibbosum* by AGO4-centric smRNA pathway was verified in real-world setting. Further, the identity and reprograming of *Fusarium* dependent miRNAs and 24 nt siRNAs was also deciphered and their AGO4-dependency was illustrated. Loss-of-function and genetics studies further demonstrated a framework for action of AGO4-dependent smRNAs, including miRNAs and 24 nt siRNAs (Figure 3).

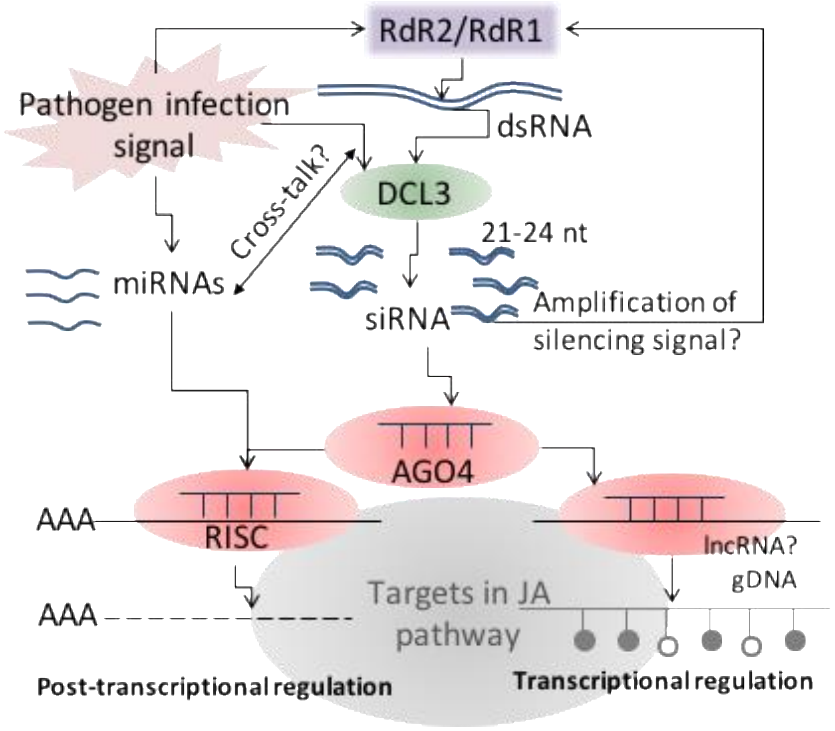

Figure 3. Resistance to hemibiotrophic fungal infection is modulated specifically by AGO4.

As RdRs and DCLs are the other core components of the biogenesis of smRNAs, it was demonstrated that RdR2, along with RdR1 but not RdR3, is involved in *Fusarium* resistance, whereas only DCL3 (and not DCL2 or DCL4) is involved. And, that RdR2/RdR1 and DCL3, like AGO4, target JA signalling pathway. Such a genetic framework was verified under field conditions when plants silenced only in biogenesis and effector components as well as those silenced in pair-wise combinations of biogenesis and effector components (AGO4XRdR2, AGO4XRdR1 and AGO4XDCL3) were highly susceptible to natural pathogens and lacked the efficacy of eliciting JA-signalling pathway.

RdR2 and DCL3 also form the component of RNA-directed DNA methylation pathway, involving 24 nt AGO4-related siRNAs. Involvement of RdR2 and DCL3, cooperatively together with AGO4, and reprograming of 24 nt siRNAs during *Fusarium* response hints towards a plausible transcriptional regulation deploying processes such as DNA methylation to modulate resistance in *N. attenuata*. Large-scale and rapid reprograming of miRNAs that might target genes of JA biogenesis and signalling indicates involvement of PTGS mode of action during

Nicotiana-Fusarium interaction. Given the complex nature of JA biogenesis and signalling, involving a large number of genes in the pathway, we infer a model deploying both the modes (PTGS and TGS) of regulation (Figure 3). The biochemical mode of action of this model needs further investigation.

3.4 Plausible biological functions of other NaAGO's

NaAGO1 is essential for the survival of plants. Further, NaAGO1 expression does not change when plants are attacked by herbivores or pathogens. AGO1 associates with several essential developmental events and this modulation of plant growth and development appears to be a conserved function of AGO1 across plant species including *N. attenuata* (Fang and Qi, 2016; Pradhan et al., 2017).

AGO7 has been associated with phase transition, development related events and antiviral resistance in Arabidopsis (and to limited extent in rice; Table 1 and Figure 2). Now, a novel function of NaAGO7 is discovered as it specifically modulates the interactions of *N. attenuata* roots with the AMF. Knock-down of AGO7 expression does not significantly affect *N. attenuata* development, growth and fitness parameters under controlled and unstressed conditions. Further, AGO7-silenced plants are not compromised in their defense against herbivores or resistance against pathogens. Rather, AGO7-silenced plants (and not other AGO's such as AGO4, which modulates resistance against pathogenic fungi) are compromised in their ability to facilitate AMF colonization, are impaired in their competitive ability when they are grown in resource limited conditions and thus suffer significant fitness consequences (Pradhan et al. 2019, manuscript under preparation). NaAGO7-silenced plants phenocopy NaRdR3-silenced plants hinting that they might act in a genetic framework. Indeed, AtAGO7 and AtRdR6 (homolog of NaRdR3) act together in the biochemical pathway for biogenesis of trans-acting siRNAs (ta-siRNAs; Figure 2).

NaAGO9's expression is mostly confined to flowers, specifically in the nectaries and ovaries, indicating its role in modulating traits critical for flower ecology. Silencing of AGO9 does not significantly impact plant fitness under unstressed conditions. Nor, AGO9-silenced

plants are impaired in their defences against herbivores, pathogens or interaction with AMF. It is plausible that NaAGO9 might influence process of process of fertilization by helping in screening and providing access to pollens tubes growing out of a variety of pollens that might land on the stigma during pollination events. This warrants further investigation.

3.5 CONCLUSIONS

In the current investigation, we studied the small-RNA (smRNA) mediated regulation of the induced responses on plants when they face biotic challenges in the ecological model species, *N. attenuata*. Because the AGOs are central components of smRNA action and are coded by several genes in the genome, we characterized their biological functions against various critical ecological stresses under controlled environments as well as natural habitats.

smRNA pathways involve the broad steps of biogenesis, maturation and action of regulatory non-coding RNAs in modulating gene expression. While biogenesis and maturation steps involve the RdRs and DCLs, the action steps essentially require the AGO effector proteins. Three RdRs and 4 DCL genes have been previously identified in *N. attenuata* genome, but the role of NaAGO gene family had been unknown. This study fills the essentially missing piece in the identity and function of the core machinery of the smRNA pathways. We have reverse-engineered specificity in smRNA pathways that may be recruited in specific contexts of tissues and stresses encountered.

N. attenuata genome has 11 genes that correspond to eight unique AGOs. Of these 8 unique AGO's, this investigation could associate functions to 6 genes supporting the hypothesis of specialization of function in smRNA pathways. NaAGO1 was found as essential for plants suggesting conserved roles in development and differentiation. NaAGO4 was associated to hemibiotrophic fungal resistance, whereas NaAGO7 specifically modulates colonization of plant roots with the beneficial AMF. Further, AGO8 and AGO5 are recruited during induction of direct defences against the insect herbivores attack plants. The function of NaAGO9 is postulated to be associated with flower ecology and plant fitness where their expression in nectaries and ovaries may assist the female magetophyte to distinguish pollen sources for fertilization after the stigmas are pollinated, and requires further investigation. Maximum specialization in function is attained by expanding and diversifying genes of AGO family that act as effectors of smRNA pathway.

This investigation also uncovers the *N. attenuata* miRNome and its temporal reprograming during herbivory and pathogenesis as well as their dependence on AGO's. Deep-sequencing assisted miRNome profiling clearly establish that the miRNome composition is

highly temporally dynamic and is dictated in manner specific to the stimulus due to the stress encountered by plants. These large-scale context-dependent reprograming of smRNome inflicts modulation of defense-signalling network during adaptive responses of plants.

By putting functional studies together (reported here such as (Pradhan et al., 2017), 2019) with evolutionary studies (Singh et al., 2015; Singh and Pandey, 2015), it may be inferred that expansion after gene duplications in AGO family offer sufficient genomic plasticity to modulate specialized biological processes driving phenotypic plasticity while adapting to ecological challenges. The evolution and expansion of smRNA machinery is hypothesized to have played crucial roles during the evolution of plants. It is proposed that plants produce diverse classes of regulatory non-coding RNAs by evolving several smRNA pathways so that plants could successfully carry out development and differentiation events by enhancing their adaptive plasticity and fitness (Singh et al., 2015; Singh and Pandey, 2017). Expansion amongst the biogenesis and maturation factors (such as RdRs and DCLs) could have resulted in the creating diversity in the classes of smRNAs whereas, gene family expansion and divergence amongst the effectors (AGO's) plausibly gave rise to a diversity in the biological functions that could be modulated by these smRNAs. Genetic studies integrating genome-wide manipulation of expression of biosynthetic and effector components coupled to molecular, analytical and genomics driven characterization have proven helpful in understanding the biological functions of large pools of smRNAs.

3.6 REFERENCES

Axtell MJ (2013) Classification and comparison of small RNAs from plants. Annu Rev Plant Biol **64:** 137-159

Baldwin IT, Staszak-Kozinski L, Davidson R (1994) Up in smoke: I. Smoke-derived germination cues for postfire annual,Nicotiana attenuata torr. Ex. Watson. Journal of Chemical Ecology **20:** 2345-2371

Borges F, Martienssen RA (2015) The expanding world of small RNAs in plants. Nat Rev Mol Cell Biol **16:** 727-741

Bozorov TA, Pandey SP, Dinh ST, Kim SG, Heinrich M, Gase K, Baldwin IT (2012) DICER-like proteins and their role in plant-herbivore interactions in *Nicotiana attenuata*. J Integr Plant Biol **54:** 189-206

Carbonell A (2017) Plant ARGONAUTEs: Features, Functions, and Unknowns. *In* A Carbonell, ed, Plant Argonaute Proteins: Methods and Protocols. Springer New York, New York, NY, pp 1-21

Dresselhaus T, Hückelhoven R (2018) Biotic and Abiotic Stress Responses in Crop Plants. Agronomy **8:** 267

Fang X, Qi Y (2016) RNAi in Plants: An Argonaute-Centered View. Plant Cell **28:** 272-285

Groten K, Nawaz A, Nguyen NHT, Santhanam R, Baldwin IT (2015) Silencing a key gene of the common symbiosis pathway in Nicotiana attenuata specifically impairs arbuscular mycorrhizal infection without influencing the root-associated microbiome or plant growth. Plant Cell Environ **38:** 2398-2416

Hibbett DS, Binder M, Bischoff JF, Blackwell M, Cannon PF, Eriksson OE, Huhndorf S, James T, Kirk PM, Lücking R, Thorsten Lumbsch H, Lutzoni F, Matheny PB, McLaughlin DJ, Powell MJ, Redhead S, Schoch CL, Spatafora JW, Stalpers JA, Vilgalys R, Aime MC, Aptroot A, Bauer R, Begerow D, Benny GL, Castlebury LA, Crous PW, Dai Y-C, Gams W, Geiser DM, Griffith GW, Gueidan C, Hawksworth DL, Hestmark G, Hosaka K, Humber RA, Hyde KD, Ironside JE, Kõljalg U, Kurtzman CP, Larsson K-H, Lichtwardt R, Longcore J, Miądlikowska J, Miller A, Moncalvo J-M, Mozley-Standridge S, Oberwinkler F, Parmasto E, Reeb V, Rogers JD, Roux C, Ryvarden L, Sampaio JP, Schüßler A, Sugiyama J, Thorn RG, Tibell L, Untereiner WA, Walker C, Wang Z, Weir A, Weiss M, White MM, Winka K, Yao Y-J, Zhang N (2007) A higher-level phylogenetic classification of the Fungi. Mycological Research **111:** 509-547

Huang Y, Li L, Smith KP, Muehlbauer GJ (2016) Differential transcriptomic responses to Fusarium graminearum infection in two barley quantitative trait loci associated with Fusarium head blight resistance. BMC Genomics **17:** 387-387

Lanubile A, Ferrarini A, Maschietto V, Delledonne M, Marocco A, Bellin D (2014) Functional genomic analysis of constitutive and inducible defense responses to Fusarium verticillioides infection in maize genotypes with contrasting ear rot resistance. BMC Genomics **15:** 710-710

Lewis BP, Burge CB, Bartel DP (2005) Conserved Seed Pairing, Often Flanked by Adenosines, Indicates that Thousands of Human Genes are MicroRNA Targets. Cell **120:** 15-20

Lu C, Tej SS, Luo S, Haudenschild CD, Meyers BC, Green PJ (2005) Elucidation of the Small RNA Component of the Transcriptome. Science **309:** 1567-1569

Luu VT, Schuck S, Kim SG, Weinhold A, Baldwin IT (2015) Jasmonic acid signalling mediates resistance of the wild tobacco Nicotiana attenuata to its native Fusarium, but not Alternaria, fungal pathogens. Plant Cell Environ **38:** 572-584

Luu VT, Weinhold A, Ullah C, Dressel S, Schoettner M, Gase K, Gaquerel E, Xu S, Baldwin IT (2017) O-Acyl Sugars Protect a Wild Tobacco from Both Native Fungal Pathogens and a Specialist Herbivore. Plant Physiol **174:** 370-386

Nakasugi K, Crowhurst RN, Bally J, Wood CC, Hellens RP, Waterhouse PM (2013) De Novo Transcriptome Sequence Assembly and Analysis of RNA Silencing Genes of Nicotiana benthamiana. PLOS ONE **8:** e59534

Pandey P, Srivastava PK, Pandey SP (2019) Prediction of Plant miRNA Targets. *In* de Folter S.(ed.), Plant microRNAs: methods and protocols, Methods Mol Biol, vol. 1932, Chapter 7

Pandey SP, Baldwin IT (2007) RNA-directed RNA polymerase 1 (RdR1) mediates the resistance of Nicotiana attenuata to herbivore attack in nature. Plant J **50:** 40-53

Pandey SP, Shahi P, Gase K, Baldwin IT (2008a) Herbivory-induced changes in the small-RNA transcriptome and phytohormone signaling in *Nicotiana attenuata*. Proc Natl Acad Sci USA **105:** 4559-4564

Pradhan M, Pandey P, Gase K, Sharaff M, Singh RK, Sethi A, Baldwin IT, Pandey SP (2017) Argonaute 8 (AGO8) Mediates the Elicitation of Direct Defenses against Herbivory. Plant Physiol **175:** 927-946

Ralph S, Oddy C, Cooper D, Yueh H, Jancsik S, Kolosova N, Philippe RN, Aeschliman D, White R, Huber D, Ritland CE, Benoit F, Rigby T, Nantel A, Butterfield YSN, Kirkpatrick R, Chun E, Liu J, Palmquist D, Wynhoven B, Stott J, Yang G, Barber S, Holt RA, Siddiqui A, Jones SJM, Marra MA, Ellis BE, Douglas CJ, Ritland K, Bohlmann J (2006) Genomics of hybrid poplar (Populus trichocarpa× deltoides) interacting with forest tent caterpillars (Malacosoma disstria): normalized and full-length cDNA libraries, expressed sequence tags, and a cDNA microarray for the study of insect-induced defences in poplar. Molecular Ecology **15:** 1275-1297

Sahu R, Sharaff M, Pradhan M, Sethi A, Bandyopadhyay T, Mishra VK, Chand R, Chowdhury AK, Joshi AK, Pandey SP (2016) Elucidation of defense-related signaling responses to spot blotch infection in bread wheat (Triticum aestivum L.). Plant J **86:** 35-49

Santhanam R, Luu VT, Weinhold A, Goldberg J, Oh Y, Baldwin IT (2015) Native root-associated bacteria rescue a plant from a sudden-wilt disease that emerged during continuous cropping. Proc Natl Acad Sci USA **112:** E5013-5020

Schmidt DD, Voelckel C, Hartl M, Schmidt S, Baldwin IT (2005) Specificity in Ecological Interactions. Attack from the Same Lepidopteran Herbivore Results in Species-Specific Transcriptional Responses in Two Solanaceous Host Plants. Plant Physiol **138:** 1763-1773

References

Schuck S, Weinhold A, Luu VT, Baldwin IT (2014) Isolating fungal pathogens from a dynamic disease outbreak in a native plant population to establish plant-pathogen bioassays for the ecological model plant Nicotiana attenuata. PLoS ONE **9:** e102915

Schüßler A, Schwarzott D, Walker C (2001) A new fungal phylum, the Glomeromycota: phylogeny and evolution**Dedicated to Manfred Kluge (Technische Universität Darmstadt) on the occasion of his retirement. Mycological Research **105:** 1413-1421

Singh RK, Gase K, Baldwin IT, Pandey SP (2015) Molecular evolution and diversification of the Argonaute family of proteins in plants. BMC Plant Biol **15:** 23

Singh RK, Pandey SP (2015) Evolution of structural and functional diversification among plant Argonautes. Plant Signal Behav **10:** e1069455

Singh RK, Pandey SP (2017) Phylogenetic and Evolutionary Analysis of Plant ARGONAUTES. Methods Mol Biol **1640:** 267-294

Srivastava PK, Moturu TR, Pandey P, Baldwin IT, Pandey SP (2014) A comparison of performance of plant miRNA target prediction tools and the characterization of features for genome-wide target prediction. BMC Genomics **15:** 348

Voelckel C, Baldwin IT (2004) Generalist and specialist lepidopteran larvae elicit different transcriptional responses in Nicotiana attenuata, which correlate with larval FAC profiles. Ecology Letters **7:** 770-775

Wang M, Wilde J, Baldwin IT, Groten K (2018) Nicotiana attenuata's capacity to interact with arbuscular mycorrhiza alters its competitive ability and elicits major changes in the leaf transcriptome. J Integr Plant Biol **60:** 242-261

Xu S, Brockmöller T, Navarro-Quezada A, Kuhl H, Gase K, Ling Z, Zhou W, Kreitzer C, Stanke M, Tang H, Lyons E, Pandey P, Pandey SP, Timmermann B, Gaquerel E, Baldwin IT (2017) Wild tobacco genomes reveal the evolution of nicotine biosynthesis. Proc Natl Acad Sci USA **114:** 6133-6138

4. SUMMARY

Plants display extensive transcriptional and phenotypic plasticity to adapt to unforeseen challenges and maximize their fitness. Such massive reprogramming requires an efficient reprogramming of gene expression in tissue and time-specific manner. At the same time, plants contain numerous non-coding small RNAs (smRNAs) such as microRNAs and small-interfering RNAs (siRNAs) that might generate an efficient and dynamic regulatory network during stress adaptation. An effective way to study ecological functions of smRNAs is to manipulate the expression of the genes responsible for their biosynthesis and action. The Argonaute (AGO) family of genes are amongst the core functional components of the machinery of the smRNA pathways as they form the RNA-induced silencing complex. As AGOs are the effectors of smRNA pathways and directly interact with smRNAs as well as their targets to modulate gene expression, they are one of the most important candidates for studying smRNA-mediated gene regulation. Here, we investigated the biological functions of the AGO's in *Nicotiana attenuata* during its response to ecological challenges such as attack by insect herbivores and fungi.

The *N. attenuata* genome encodes for 11 AGOs from 8 unique genes homologous to AGO1 (NaAGO1a, b, c), AGO2, AGO4 (NaAGO4a, b), AGO5, AGO7, AGO8, AGO9 and AGO10. In this investigation we determined which AGO(s) moderate the interaction of *N. attenuata* with its biotic challengers, namely insect herbivores, fungal pathogens and arbuscular mycorrhizal fungi (AMF). We performed loss-of-function characterization of the AGOs by stably silencing their expression. We discovered a high degree of specificity in response of AGOs to these diverse ecological interactions. AGO1 is an established regulator of plant development in Arabidopsis, it was also found to be essential in *N. attenuata* and stably silenced lines (homozygous with single insertions) could not be recovered. Our results show that AGO8 (along with AGO5) regulates plant direct defenses against herbivore attack, whereas only AGO4 is the regulator of signaling and resistance during infection with hemibiotrophic pathogenic fungi. Further, AGO7 is involved in installing optimum colonization of *N. attenuata* roots with mycorrhizal fungi and competitive fitness in resource limited environments. These conclusions are described in three manuscripts included in this thesis. Furthermore, our investigation hints at

novel functions for AGO9 in impacting traits important to flower ecology and warrants further investigation.

We have also described a large part of the non-coding smRNA fraction of *N. attenuata*'s transcriptome (smRNome), specially the miRNAs in the genome (miRNome). Using the high-throughput, next-generation sequencing (NGS, also often referred to as deep sequencing) approach of the Illumina-platform, we investigated the composition and temporal dynamics of expression of *N. attenuata* miRNome when the plants are subjected to herbivorous larvae of *Manduca sexta* and to the hemibiotrophic fungal pathogen, *Fusarium brachygibbosum*. On mapping the conservation across 34 families of plants, it was evident that nearly half of the miRNAs of *N. attenuata* miRNome are conserved. The patterns of accumulation of miRNAs were highly dependent on the type of stress (insect attack or fungal infection), and they were highly temporally dynamic in nature. A large fraction of these miRNAs was influenced by silencing specific AGOs such as AGO8 and AGO4 during response to insect and pathogen attack, respectively. Direct defenses on *N. attenuata* are under the control of the jasmonic acid (JA) signaling pathway, and a MYB-family transcription factor (MYB8) is a master regulator of biosynthesis of several key inducible defense metabolites. Therefore, we constructed networks of miRNA-modulated signaling and defense processes, such as the miRNA-MYB8 network for regulation of biosynthesis of direct defense metabolites during herbivore attack and the miRNA-mRNA network of JA-biogenesis and -signaling pathway during pathogen infection.

Moreover, we validated the ecological functions of the AGOs by testing them in nature. The AGO4-silenced lines, the lines silenced in expression of other component of the smRNA biogenesis machinery, namely RNA-directed RNA polymerases 1 and 2 (RdR1, RdR2) and the Dicer-like protein (DCL3) as well as the binary combinations of AGO4 with RdR1/2 and DCL3 were released and evaluated under field conditions in the natural habitats of *N. attenuata*. We show the functional specificity of the smRNA machinery during hemibiotrophic pathogen interaction of the host. The pathway comprising the three core components of DCL3, RdR2/1 and AGO4 modulates disease resistance by regulating pathogen-induced JA-biogenesis and signaling.

In conclusion, (i) the biological functions of the AGO family of genes was investigated during the plant response to three types of biotic interactions; a high level of specificity in AGO

function was discovered. (ii) The miRNome and its stimulus-dependent reprograming to modulate defense signaling was uncovered. (iii) From our results, we infer that plants rely heavily on smRNAs to regulate signaling and defense responses in nature to circumvent stress and that a stress-dependent specialized smRNA-machinery is recruited for their action. The next step in this direction is to determine the function of other AGOs as well as to determine the biochemical mechanism underlying such eco-biological functions.

5. ZUSAMMENFASSUNG

Pflanzen weisen eine große Plastizität der Transkription und des Phänotyps auf, um sich an unvorhergesehene Herausforderungen anzupassen und ihre Fitness zu maximieren. Eine derart umfassende Neuprogrammierung erfordert eine wirksame Modulation der Genexpression, die für jedes Gewebe und die Zeit nach dem Befall spezifisch ist. Gleichzeitig enthalten Pflanzen zahlreiche nichtkodierende kleine RNAs (smRNAs), wie Mikro-RNAs und kleine interferierende RNAs (siRNAs), die während der Anpassung an Stress ein wirksames und dynamisch-regulatorisches Netzwerk erzeugen können. Eine effiziente Möglichkeit, die ökologischen Funktionen von smRNAs zu untersuchen, besteht darin, die Expression der Gene zu verändern, die für Biosynthese und Wirkung von smRNAs verantwortlich sind. Die Genfamilie der Argonauten (AGO) gehört zu den funktionellen Kernkomponenten der smRNA-Maschinerie, da sie den RNA-induzierten Silencing-Komplex bilden. Da AGOs die Effektoren von smRNA-Biosynthesewegen sind und direkt mit smRNAs sowie deren Zielen interagieren, um die Genexpression zu modulieren, gehören sie zu den wichtigsten Kandidaten für die Untersuchung der smRNA-vermittelten Genregulation. Hier haben wir die biologischen Funktionen der AGOs in *N. attenuata* als Reaktion auf ökologische Herausforderungen wie den Befall durch pflanzenfressende Insekten und Pilze untersucht.

Das Genom von *N. attenuata* kodiert für 11 AGOs aus 8 Genen, die zu AGO1 (NaAGO1a, b, c), AGO2, AGO4 (NaAGO4a, b), AGO5, AGO7, AGO8, AGO9 und AGO10 homolog sind. In dieser Untersuchung haben wir herausgefunden, welche AGO(s) die Wechselwirkung von *N. attenuata* mit seinen biotischen Herausforderern, nämlich Herbivoren, pathogenen Pilzen und arbuskulären Mykorrhizapilzen (AMF), vermitteln. Wir haben die AGOs durch den Verlust ihrer Funktion charakterisiert, indem wir ihre Expression stabil stumm schalteten. Wir haben ein hohes Maß an Spezifität bei der Reaktion von AGOs auf diese vielfältigen ökologischen Wechselwirkungen entdeckt. AGO1 reguliert bekanntermaßen die Pflanzenentwicklung in Arabidopsis. Auch in *N. attenuata* stellte sich AGO1 als essentiell heraus, und stabil stummgeschaltete Linien (homozygot mit einem Insert) konnten nicht regeneriert werden. Unsere Ergebnisse zeigen, dass AGO8 (zusammen mit AGO5) die pflanzliche Abwehr gegen Angriffe von Pflanzenfressern moduliert, während nur AGO4 die

Signal- und Resistenzregulierung bei der Infektion mit hemibiotrophen pathogenen Pilzen übernimmt. Weiterhin, ist AGO7 an den Wechselwirkungen von *N. attenuata* mit arbuskulären Mykorrhizapilzen (AMF) durch AGO7 beteiligt. Diese Schlussfolgerungen werden in drei Manuskripten beschrieben, die in dieser Arbeit enthalten sind. Darüber hinaus geben unsere Untersuchungen Hinweise auf neuartige Funktionen von AGO9 zur Modulation von Merkmalen, die für die Blütenökologie wichtig sind, und erfordern weitere Untersuchungen.

Wir haben auch einen großen Teil der nicht-kodierenden smRNA-Fraktion des *N. attenuata*-Transkriptoms (smRNome) beschrieben, insbesondere die miRNAs im Genom (miRNome). Unter Verwendung der Hochdurchsatz-Next-Generation-Sequenzierung (NGS, auch Deep Sequencing genannt) der Illumina-Plattform haben wir die Zusammensetzung und die zeitliche Dynamik der Expression des *N. attenuata* miRNome untersucht, wenn die Pflanzen Larven des Pflanzenfressers *Manduca sexta* und dem hemibiotrophen pathogenen Pilz *Fusarium brachygibbosum* ausgesetzt sind. Bei der Kartierung der konservierten miRNAs aus 34 Pflanzenfamilien wurde deutlich, dass fast die Hälfte der miRNAs des *N. attenuata* miRNomes konserviert sind. Die Muster der Anreicherung von miRNAs waren stark von der Art des Stresses (Insektenbefall oder Pilzinfektion) abhängig, und diese Muster waren in der Natur zeitlich hoch dynamisch. Ein großer Teil dieser miRNAs wurde durch die Stummschaltung spezifischer AGOs, wie AGO8 und AGO4, während der Reaktion auf Insekten- bzw. Pathogenbefall beeinflusst. Direkte Abwehrmechanismen sind unter der Kontrolle des Jasmonsäuresignalwegs, und ein Transkriptionsfaktor der MYB-Familie (MYB8) ist der Hauptregulator der Biosynthese von einigen entscheidenden, induzierbaren Abwehrmetaboliten Daher haben wir Netzwerke von miRNA-modulierten Signal- und Abwehrprozessen aufgebaut, wie das miRNA-MYB8-Netzwerk zur Regulation der Biosynthese direkter Abwehrmetaboliten während des Befalls mit Pflanzenfressern und das miRNA-mRNA-Netzwerk der JA-Biogenese und des JA-Signalwegs während der Pilzinfektion.

Darüber hinaus haben wir die ökologischen Funktionen der AGOs validiert, indem wir sie in der Natur getestet haben. Wir haben AGO4 als Modell verwendet und seine Funktion bei der Wechselwirkung zwischen Pflanzen und Krankheitserregern in der Natur untersucht. Dazu haben wir die in der Expression von anderen Komponenten der Maschinerie für die Biosynthese von smRNAs, nämlich die RNA-geleiteten RNA Polymerasen 1 und 2 (RdR1, RdR2) und das

Dicer-ähnliche Protein 3 (DCL3), stummgeschalteten Linien sowie die binären Kombinationen von AGO4 mit RdR1 / 2 und DCL3 freigesetzt und unter Freilandbedingungen in den natürlichen Lebensräumen von *N. attenuata* evaluiert. Wir haben die funktionelle Spezifität der smRNA-Maschinerie während der hemibiotrophen Pathogen-Interaktion des Wirts gezeigt. Der Signalweg aus den drei Kernkomponenten DCL3, RdR2 / 1 und AGO4 moduliert die Krankheitsresistenz, indem die pathogen-induzierte JA-Biogenese und JA-Signalübertragung aktiviert wird.

Zusammenfassend wurde i) die biologische Funktion der AGO-Genfamilie während der Reaktion der Pflanzen auf drei Arten von biotischen Wechselwirkungen untersucht und ein hohes Maß an Spezifität in der AGO-Funktion entdeckt. ii) Das miRNome und seine stimulusabhängige Umprogrammierung zur Modulation des Abwehrsignalwegs wurden ebenfalls aufgedeckt. iii) Aus unseren Ergebnissen schließen wir, dass Pflanzen in hohem Maße auf smRNAs angewiesen sind, um Signal- und Abwehrreaktionen in der Natur zu regulieren, um Stress zu umgehen, und dass Stress-abhängige, spezialisierte smRNA-Maschinerien für ihre Wirkung rekrutiert werden. Der nächste Schritt in diese Richtung ist die Bestimmung der Funktion anderer AGOs sowie die Bestimmung des biochemischen Mechanismus, der solchen öko-biologischen Funktionen zugrunde liegt.

6. REFERENCES

Axtell MJ (2013) Classification and comparison of small RNAs from plants. Annu Rev Plant Biol **64:** 137-159

Baldwin IT, Staszak-Kozinski L, Davidson R (1994) Up in smoke: I. Smoke-derived germination cues for postfire annual,Nicotiana attenuata torr. Ex. Watson. Journal of Chemical Ecology **20:** 2345-2371

Borges F, Martienssen RA (2015) The expanding world of small RNAs in plants. Nat Rev Mol Cell Biol **16:** 727-741

Bozorov TA, Pandey SP, Dinh ST, Kim SG, Heinrich M, Gase K, Baldwin IT (2012) DICER-like proteins and their role in plant-herbivore interactions in *Nicotiana attenuata*. J Integr Plant Biol **54:** 189-206

Carbonell A (2017) Plant ARGONAUTEs: Features, Functions, and Unknowns. *In* A Carbonell, ed, Plant Argonaute Proteins: Methods and Protocols. Springer New York, New York, NY, pp 1-21

Dresselhaus T, Hückelhoven R (2018) Biotic and Abiotic Stress Responses in Crop Plants. Agronomy **8:** 267

Fang X, Qi Y (2016) RNAi in Plants: An Argonaute-Centered View. Plant Cell **28:** 272-285

Groten K, Nawaz A, Nguyen NHT, Santhanam R, Baldwin IT (2015) Silencing a key gene of the common symbiosis pathway in Nicotiana attenuata specifically impairs arbuscular mycorrhizal infection without influencing the root-associated microbiome or plant growth. Plant Cell Environ **38:** 2398-2416

Hibbett DS, Binder M, Bischoff JF, Blackwell M, Cannon PF, Eriksson OE, Huhndorf S, James T, Kirk PM, Lücking R, Thorsten Lumbsch H, Lutzoni F, Matheny PB, McLaughlin DJ, Powell MJ, Redhead S, Schoch CL, Spatafora JW, Stalpers JA, Vilgalys R, Aime MC, Aptroot A, Bauer R, Begerow D, Benny GL, Castlebury LA, Crous PW, Dai Y-C, Gams W, Geiser DM, Griffith GW, Gueidan C, Hawksworth DL, Hestmark G, Hosaka K, Humber RA, Hyde KD, Ironside JE, Kõljalg U, Kurtzman CP, Larsson K-H, Lichtwardt R, Longcore J, Miądlikowska J, Miller A, Moncalvo J-M, Mozley-Standridge S, Oberwinkler F, Parmasto E, Reeb V, Rogers JD, Roux C, Ryvarden L, Sampaio JP, Schüßler A, Sugiyama J, Thorn RG, Tibell L, Untereiner WA, Walker C, Wang Z, Weir A, Weiss M, White MM, Winka K, Yao Y-J, Zhang N (2007) A higher-level phylogenetic classification of the Fungi. Mycological Research **111:** 509-547

Huang Y, Li L, Smith KP, Muehlbauer GJ (2016) Differential transcriptomic responses to Fusarium graminearum infection in two barley quantitative trait loci associated with Fusarium head blight resistance. BMC Genomics **17:** 387-387

Lanubile A, Ferrarini A, Maschietto V, Delledonne M, Marocco A, Bellin D (2014) Functional genomic analysis of constitutive and inducible defense responses to Fusarium verticillioides infection in maize genotypes with contrasting ear rot resistance. BMC Genomics **15:** 710-710

REFERENCES

Lewis BP, Burge CB, Bartel DP (2005) Conserved Seed Pairing, Often Flanked by Adenosines, Indicates that Thousands of Human Genes are MicroRNA Targets. Cell **120:** 15-20

Lu C, Tej SS, Luo S, Haudenschild CD, Meyers BC, Green PJ (2005) Elucidation of the Small RNA Component of the Transcriptome. Science **309:** 1567-1569

Luu VT, Schuck S, Kim SG, Weinhold A, Baldwin IT (2015) Jasmonic acid signalling mediates resistance of the wild tobacco Nicotiana attenuata to its native Fusarium, but not Alternaria, fungal pathogens. Plant Cell Environ **38:** 572-584

Luu VT, Weinhold A, Ullah C, Dressel S, Schoettner M, Gase K, Gaquerel E, Xu S, Baldwin IT (2017) O-Acyl Sugars Protect a Wild Tobacco from Both Native Fungal Pathogens and a Specialist Herbivore. Plant Physiol **174:** 370-386

Nakasugi K, Crowhurst RN, Bally J, Wood CC, Hellens RP, Waterhouse PM (2013) De Novo Transcriptome Sequence Assembly and Analysis of RNA Silencing Genes of Nicotiana benthamiana. PLOS ONE **8:** e59534

Pandey P, Srivastava PK, Pandey SP (2019) Prediction of Plant miRNA Targets. *In* de Folter S.(ed.), Plant microRNAs: methods and protocols, Methods Mol Biol, vol. 1932, Chapter 7

Pandey SP, Baldwin IT (2007) RNA-directed RNA polymerase 1 (RdR1) mediates the resistance of Nicotiana attenuata to herbivore attack in nature. Plant J **50:** 40-53

Pandey SP, Shahi P, Gase K, Baldwin IT (2008a) Herbivory-induced changes in the small-RNA transcriptome and phytohormone signaling in *Nicotiana attenuata*. Proc Natl Acad Sci USA **105:** 4559-4564

Pradhan M, Pandey P, Gase K, Sharaff M, Singh RK, Sethi A, Baldwin IT, Pandey SP (2017) Argonaute 8 (AGO8) Mediates the Elicitation of Direct Defenses against Herbivory. Plant Physiol **175:** 927-946

Ralph S, Oddy C, Cooper D, Yueh H, Jancsik S, Kolosova N, Philippe RN, Aeschliman D, White R, Huber D, Ritland CE, Benoit F, Rigby T, Nantel A, Butterfield YSN, Kirkpatrick R, Chun E, Liu J, Palmquist D, Wynhoven B, Stott J, Yang G, Barber S, Holt RA, Siddiqui A, Jones SJM, Marra MA, Ellis BE, Douglas CJ, Ritland K, Bohlmann J (2006) Genomics of hybrid poplar (Populus trichocarpa× deltoides) interacting with forest tent caterpillars (Malacosoma disstria): normalized and full-length cDNA libraries, expressed sequence tags, and a cDNA microarray for the study of insect-induced defences in poplar. Molecular Ecology **15:** 1275-1297

Sahu R, Sharaff M, Pradhan M, Sethi A, Bandyopadhyay T, Mishra VK, Chand R, Chowdhury AK, Joshi AK, Pandey SP (2016) Elucidation of defense-related signaling responses to spot blotch infection in bread wheat (Triticum aestivum L.). Plant J **86:** 35-49

Santhanam R, Luu VT, Weinhold A, Goldberg J, Oh Y, Baldwin IT (2015) Native root-associated bacteria rescue a plant from a sudden-wilt disease that emerged during continuous cropping. Proc Natl Acad Sci USA **112:** E5013-5020

Schmidt DD, Voelckel C, Hartl M, Schmidt S, Baldwin IT (2005) Specificity in Ecological Interactions. Attack from the Same Lepidopteran Herbivore Results in Species-Specific Transcriptional Responses in Two Solanaceous Host Plants. Plant Physiol **138:** 1763-1773

Schuck S, Weinhold A, Luu VT, Baldwin IT (2014) Isolating fungal pathogens from a dynamic disease outbreak in a native plant population to establish plant-pathogen bioassays for the ecological model plant Nicotiana attenuata. PLoS ONE **9:** e102915

Schüßler A, Schwarzott D, Walker C (2001) A new fungal phylum, the Glomeromycota: phylogeny and evolution**Dedicated to Manfred Kluge (Technische Universität Darmstadt) on the occasion of his retirement. Mycological Research **105:** 1413-1421

Singh RK, Gase K, Baldwin IT, Pandey SP (2015) Molecular evolution and diversification of the Argonaute family of proteins in plants. BMC Plant Biol **15:** 23

Singh RK, Pandey SP (2015) Evolution of structural and functional diversification among plant Argonautes. Plant Signal Behav **10:** e1069455

Singh RK, Pandey SP (2017) Phylogenetic and Evolutionary Analysis of Plant ARGONAUTES. Methods Mol Biol **1640:** 267-294

Srivastava PK, Moturu TR, Pandey P, Baldwin IT, Pandey SP (2014) A comparison of performance of plant miRNA target prediction tools and the characterization of features for genome-wide target prediction. BMC Genomics **15:** 348

Voelckel C, Baldwin IT (2004) Generalist and specialist lepidopteran larvae elicit different transcriptional responses in Nicotiana attenuata, which correlate with larval FAC profiles. Ecology Letters **7:** 770-775

Wang M, Wilde J, Baldwin IT, Groten K (2018) Nicotiana attenuata's capacity to interact with arbuscular mycorrhiza alters its competitive ability and elicits major changes in the leaf transcriptome. J Integr Plant Biol **60:** 242-261

Xu S, Brockmöller T, Navarro-Quezada A, Kuhl H, Gase K, Ling Z, Zhou W, Kreitzer C, Stanke M, Tang H, Lyons E, Pandey P, Pandey SP, Timmermann B, Gaquerel E, Baldwin IT (2017) Wild tobacco genomes reveal the evolution of nicotine biosynthesis. Proc Natl Acad Sci USA **114:** 6133-6138

7. ACKNOWLEDGEMENT

I would like to express my deepest gratitude to all whose support has been immensely helpful for getting me to this stage of thesis submission. I want to thank especially the following people whose kind advice has made my thesis possible.

I would like to thank Professor Ian T. Baldwin for his supervision, scientific discussion and support.

Dr. Shree P. Pandey my supervisor, I would like to express my deepest gratitude to you for your continuous encouragement and guidance towards my scientific thinking that has been shaping me into a scientist. Also, I am grateful for all your personal support during my ups and downs in life. It is always encouraging working with you for the last 5 years.

Dr. Karin Groten, I thank you for all your support during the experiments, scientific discussions and help with shaping my manuscript on AGO7, for correcting my thesis and an all-time help and encouragement.

I want to express my special thanks to my parents and my brother for all of their support and backing.

My super nice office co-inhabitants, Klaus and Lucas, I thank you for helping me with everything. Lucas has been a great friend and supporter throughout: thank you and your family for all the fun time and support.

I would like to express my heartfelt gratitude to my colleagues at the Max Planck Institute for Chemical Ecology for helping me in all possible way, specially the department office manager, Evelyn Claussen for taking care of all my administrative needs, continuous help from Matthias Schöttner, Thomas Hahn, Eva, Wibke, are thankfully appreciated and the support of all the members of the group is acknowledged. A special thanks to the field-team 2018, especially Gundega for all the care in the Utah field station.

My thesis could not have completed without the extra-ordinary support of the greenhouse team. Thank you.

I also thank all the people at Friedrich-Schiller-University, who are directly or indirectly involved in the dissertation procedure.

Last but not the least, I thank Max Planck Society for funding support.

8. EIGENSTÄNDIGKEITSERKLÄRUNG AND EHRENWÖRTLICHE ERKLÄRUNG

Entsprechend der geltenden, mir bekannten Promotionsordnung der Biologisch-Pharmazeutischen Fakultät der Friedrich-Schiller-Universität Jena erkläre ich, daß ich die vorliegende Dissertation eigenständig angefertigt und alle von mir benutzten Hilfsmittel und Quellen angegeben habe. Personen, die mich bei der Auswahl und Auswertung des Materials sowie bei der Fertigstellung der Manuskripte unterstützt haben, sind am Beginn eines jeden Kapitels genannt. Es wurde weder die Hilfe eines Promotionsberaters in Anspruch genommen, noch haben Dritte für Arbeiten, welche im Zusammenhang mit dem Inhalt der vorliegenden Dissertation stehen, geldwerte Leistungen erhalten. Die vorgelegte Dissertation wurde außerdem weder als Prüfungsarbeit für eine staatliche oder andere wissenschaftliche Prüfung noch als Dissertation an einer anderen Hochschule eingereicht.

_____

Maitree Pradhan

9. CURRICULUM VITAE

Personal Information

Name: Maitree Pradhan

Date of Birth: 15.07.1988

Place of Birth: Angul, Orissa

Nationality: India

Email: mpradhan@ice.mpg.de, maitreepradhan28@gmail.com

Education

2016-2019: **Ph. D studies (Molecular biology)**

Max-Planck-Institute for Chemical Ecology, Jena, Germany, and Friedrich Schiller University Jena, Germany

Dissertation topic: Understanding the regulatory basis of defense signaling in plants: The role of Argonautes in modulating defense responses in *Nicotiana attenuata*

2008-2010: **Master of Science (Biotechnology)**

Siksha O' Anusandhan University, Orissa, India

2005-2008: **Bachelor of Science (Botany)**

Utkal University, Orissa, India

Professional and Scientific career

2015-2019 Ph. D. student at Max Max Planck Institute for Chemical Ecology, Department of Molecular Ecology, Jena, Germany

2014-2015 Junior research fellow, Indian Institute of Science Education and Research, Kolkata, India

Project- Understanding the regulatory basis of defense signaling in plants

2013-2014 Project Fellow, National Institute of Science Education and Research, Bhubaneswar, India

Project- Exploring the role of splice variant of CONSTANS, the key regulator of photoperiodic flowering time control in Arabidopsis

2012-2013 Project Fellow, National Institute of Science Education and Research, Bhubaneswar, India

Project- Plant derived mammalian immune responsive proteins to induce host protective immunity and its implication in translational research

2009-2010 Master thesis, National Metallurgical Laboratory (CSIR), MEF Division, Jamshedpur, India
Project- Isolation of acidophiles from mine water and their adaptation studies for application in bioleaching

Publication

1. Pradhan M, Gase K^+, Chuang L^+, Baldwin IT, Groten K, Pandey SP. Argonaute7 (AGO7) moderates plant fitness and arbuscular mycorrhizal fungal associations under competitive and resource limited conditions in *Nicotiana attenuate*. (Manuscript under preparation for Plant Physiology)

2. Pradhan M, Priyanka Pandey, Ian T. Baldwin, Shree P. Pandey. Argonaute 4 modulates resistance against hemibiotrophic fungal infection by regulating jasmonic acid signaling in *Nicotiana attenuata* plants. (Under revision)

3. Pradhan M, Pandey P, Gase K, Shraff M, Singh RK, Sethi A, Baldwin IT and Pandey SP (2017). Argonaute 8 (AGO8) mediates the elicitation of primary defense against herbivory. *Plant Physiology*, **175**:927-946

4. Sahu R, Sharaff M, Pradhan M, Sethi A, Bandyopadhyay T, Mishra VK, Chand R, Chowdhury AK, Joshi AK, Pandey SP (2016) Elucidation of defense-related signaling responses to spot blotch infection in bread wheat (*Triticum aestivum* L.). Plant J **86**: 35-49

5. Sahu R, Kundu P, Sharaff M, Pradhan M, Sethi A, Mishra VK, Chand R, Joshi AK, Kumar A, Pandey SP (2016).. Understanding the defense-related mechanism during the wheat's interaction with fungal pathogens. Indian Phytopathology. **69**. 260-265.

Presentations

- Pradhan M., Pandey P., Singh R.K., Gase K., Baldwin I.T., Pandey S.P. (2018). Functional diversity of Argonautes in modulating ecological interactions in *Nicotiana attenuata*. Poster presented at Institute Symposium, MPI for Chemical Ecology, Jena, DE
- Brütting C., Schäfer M., Li J., Heiling S., Zhou W., Adam N., Meza Canales I.D., Pradhan M., Baldwin I.T. (2016). From small molecules to multispecies interactions – different layers of plant-herbivore interactions. Poster presented at SAB Meeting 2016, MPI for Chemical Ecology, Jena, DE
- Gase K., Brockmöller T., Ling Z., Pradhan M., Sethi A., Xu S. (2016). The genome of Nicotiana attenuata and the genome-enabled approaches to ecology that it empowers. Poster presented at SAB Meeting 2016, MPI for Chemical Ecology, Jena, DE
- Maitree Pradhan, Murali Sharaff, Ravi K Singh, Ian T. Baldwin, Shree P. Pandey (2016) Engineering a small RNA pathway that regulates plant defenses against insect attack. Poster presentation at BITS Conference on Gene & Genome Regulation, Pilani, India.

10. APPENDIX

The following supplementary data for manuscripts I-III are provided in the attached CD-ROM.

10.1 Supporting materials for Manuscript I

Supplemental Figure S1. MSA of NaAGOs corresponding to Figure 1A, and phylogenetic tree of Arabidopsis AGOs.

Supplemental Figure S2. Transcript abundance of NaAGOs in roots in a time-course experiment.

Supplemental Figure S3. Complete southern blots of all the transgenic genotypes.

Supplemental Figure S4. Silencing of AGO8 expression does not affect the development and growth of *N. attenuata*.

Supplemental Figure S5. Evaluation of the silencing efficiency of nine NaAGOs and XCP1 in irAGO8 samples.

Supplemental Figure S6. Validation of the susceptibility of irAGO8 plants to herbivore attack.

Supplemental Figure S7. DEMs in the wild type and irAGO8.

Supplemental Figure S8. Chromatograms of the standards used for targeted analysis of nicotine, DTGs, and rutin.

Supplemental Figure S9. Evaluation of phytohormones in the wild type and irAGO8 upon herbivory attack.

Supplemental Figure S10. Dynamics of transcript accumulation in phytohormone signaling genes in response to herbivory.

Supplemental Figure S11. Simplified scheme for the synthesis of major components of defense-related metabolites in *N. attenuata*.

Supplemental Table S1. Conserved and predicted novel miRNAs identified in the wild type and irAGO8 across the three time points: 0, 0.75, and 18 h.

Supplemental Table S2. Mature miRNAs conserved to other species when mapped against 72 plant species in miRBase.

Supplemental Table S3. Accumulation of miRNAs at each time point (0, 0.75, and 18 h) for irAGO8 and the wild type.

Supplemental Table S4. DEMs for irAGO8 and the wild type.

Supplemental Table S5. Differentially accumulated metabolites on silencing NaAGO8.

Supplemental Table S6. DEMs showed binding sites in defense-signaling pathway genes.

Supplemental Table S7. List of primers used in this study.

10.2 Supporting materials for Manuscript II

Supplemental Figure S1. No abnormalities in development and growth were evident in plants silenced in AGO4 expression.

Supplemental Figure S2. Microscopic observations of *F. brachygibbosum* reveal infection structures on plant surface.

Supplemental Figure S3. Study of 24 nt smRNAs in AGO4 and WT plants at various stages of infection.

Supplemental Figure S4. Principal component analysis (PCA) of the accumulation of conserved (A) and novel (B) miRNAs during infection of irAGO4 and WT.

Supplemental Figure S5. Dynamics of transcript accumulation in genes of Jasmonic acid (JA) pathway during pathogen infection.

Supplemental Figure S6. Three transcription factors, known to regulate JA signaling, show similar patterns of transcript accumulation in irAGO4 and WT plants during infection.

Supplemental Figure S7. Phenotypes of 12 dpi (days post inoculation) symptoms on wild type (WT) and AGO4-silenced plants (irAGO4) and when irAGO4 were complemented with jasmonic acid (JA) and methyl jasmonate (MeJA).

Supplemental Figure S8. Phenotypic representation of disease at 12 dpi (days post inoculation) on the WT, irAGO4, irAOC and irOPR3 plants that were not complemented (buffer treated mock, left panel) or complemented with OPDA.

Supplemental Figure S9. Characterization of plants silenced in expression of the three Dicer like genes (DCL's; A) and RNA-directed RNA polymerase genes (RdR's; B) against 12 days infection of F. *brachygibbosum*.

Supplemental Figure S10. Evaluation of salicylic acid (SA) and abscisic acid (ABA) levels after 48 hpi of F. brachygibbosum in irDCL3, irRdR1, and irRdR2 as compared to WT.

Supplemental Figure S11. Characterization of lines silenced in expression of AGO4, DCL3, RdR1 and RdR2 under field condition.

Supplemental Figure S12. A simplified model of the action of AGO4, DCL3 and RdR1/2 sector of the smRNA machinery during modulation of immune response of *N. attenuata* against *F. brachygibbosum* infection.

Supplemental Table S1. miRNA reads sequenced in 24 samples.

Supplemental Table S2. Conserved and predicted novel miRNAs identified in this study.

Supplemental Table S3. Mature miRNAs conserved to other species when mapped against 72 plant species in miRBase.

Supplemental Table S4. Differentially accumulated miRNAs for irAGO4 and WT. p-value <0.05. RPM=Reads Per Million.

Supplemental Table S5. List of primers used in the study.

10.3 Supporting materials for Manuscript III

Figure S1. Silencing AGOs 1, 2, 4, and 10 does not affect competitive fitness of *N. attenauta* plants under resource limited conditions. Rosette diameter (c), stalk length (b) as well as total number of seed capsules produced by irAGOs and WT plants were similar.

Table S1. miRNA and their putative target genes tested in Nicotiana-AMF interaction

Table S2. List of primers (a, of genes, and b, of miRNAs) used in this study.